PERFORMANCE OPTIMIZATION OF THERMOELECTRIC COOLERS USING THE DIMENSIONAL PARAMETERS IN RESTRICTED SPACE BY STOCHASTIC ALGORITHMS

A Thesis Submitted

IN PARTIAL FULFILLMENT OF THE REQUIREMENTS
FOR THE DEGREE OF

DOCTOR OF PHILOSOPHY

IN

MECHANICAL ENGINEERING

By

JITENDRA MOHAN GIRI
Regd. No. –11SETPH104001

Supervisor
Prof. (Dr.) Pawan Kumar Singh Nain

DEPARTMENT OF MECHANICAL & CHEMICAL ENGINEERING
SCHOOL OF ENGINEERING
GALGOTIAS UNIVERSITY
UTTAR PRADESH

2021

CANDIDATE'S DECLARATION

I hereby certify that the work which is being presented in the thesis, entitled "Performance Optimization of Thermoelectric Coolers using the Dimensional Parameters in Restricted Space by Stochastic Algorithms" in fulfillment of the requirements for the award of the degree of Doctor of Philosophy in Mechanical Engineering and submitted to the Galgotias University, Greater Noida is an authentic record of my own work carried out during a period from 2012-21 under the supervision of Dr. Pawan Kumar Singh Nain.

The matter embodied in this thesis has not been submitted by me for the award of any other degree of this or any other University/Institute.

(Jitendra Mohan Giri)

This is to certify that the above statement made by the candidate is correct to the best of our knowledge.

(Dr. Pawan Kumar Singh Nain)
Supervisor
Department of Mechanical & Chemical Engineering

The Ph.D. Viva-Voice examination of Mr. Jitendra Mohan Giri, Research Scholar, has been held on_____.

Sign. of Supervisor Sign. of External Examiner

ABSTRACT

A thermoelectric cooler (TEC) is a solid-state eco-friendly cooling device that operates virtually silently. The performances of thermoelectric coolers have so far been inferior to that of competing vapour compression refrigeration technique. In the present thesis, work on the performance enhancement of thermoelectric cooler is presented. The dimensional geometric and operating parameters of the TEC system have been efficaciously incorporated into the performance optimization and analysis. This study takes into account a number of minor effects, including thermal contact resistance, electrical contact resistance, and heat sink resistance. Not all of these factors were considered simultaneously by previous studies, which distinguishes this work. The length of the thermoelectric elements, their cross-sectional area, and the electric current were selected as design variables for this study. There had been no research in which a combination of these design variables was used simultaneously. The optimum design parameters have been used to improve the cooling capacity (Q_c), coefficient of performance (*COP*) and exergetic efficiency of the thermoelectric cooler. This study used precise temperatures at interfaces, which resulted in a more accurate analysis using a more advanced model than previous ones. A thermal resistance model by employing the electrical analogy to the heat flow has been developed. It effectively demonstrates its incorporation in an insightful and illustrative manner, from model generation to results acquisition.

Genetic algorithm and simulated annealing are popular stochastic algorithms and have been used in this study. It was observed through a pilot study in the current research work that genetic algorithm is a suitable optimization technique for handling such design problems. During cooling capacity optimization, it was found that the typical TE element length is considerably less than the optimal length to maximize *COP*. The *COP* optimization result shows that the length of the thermoelectric element has to be more with respect to the area of cross-section. The electric current, cross-sectional area, and the number of thermoelectric elements are unique for the best performance and have to identify according to the objective function. The optimum values of performance parameters are obtained at

different sets of design parameters. A mathematical model for calculating first and second law efficiencies with interface temperatures was also developed, which has not been previously reported. The results demonstrated that at the same current, both first law and second law efficiency are maximized. Further, this study has established that the maximum values of first law and second law efficiencies are obtained not only at the same current but the length and cross-sectional area of thermoelectric elements are also the same. It is an important bearing that by maximizing second law efficiency rather than both, we ensure that we have achieved optimized first law efficiency.

The optimization results were validated with the finite-element method. The numerical simulation abilities of finite-element ANSYS® software were successfully used to validate GA results. Finite-element simulation results confirmed the GA results. The results of the three-dimensional finite element numerical simulations for Q_c, *COP* and exergy efficiency were very close to GA results. The temperatures were varying within 2%. The heat rejection rate and the input electric power were varied by less than 1%. It is therefore concluded that three-dimensional analysis performed with ANSYS® validates all of the mathematical GA results obtained using a one-dimensional heat transfer model.

Dedicated to my Father (Late) Sh. K. G. Giri

ACKNOWLEDGEMENTS

First, I am beholden to **Lord Shiva** for his blessings to help me to raise my academic level to this stage.

I wish to convey my deep gratitude and sincere thanks to my PhD supervisor **Dr. Pawan Kumar Singh Nain** who trusted me and provided me with an opportunity to work under his guidance. Without his guidance, inspiration, constant encouragement, and constructive criticism, the completion of this thesis would not have been possible. No amount of words would suffice in return for his favour and cooperation. I am grateful to him in all respects.

I would like to thank my doctoral committee members whose periodic assessment and review of my work helped in going forward in the right direction. I express my deep sense of gratitude to Prof. (Dr.) P.M. Pandey (IIT Delhi) for being part of my research committee and thankful for his valuable suggestions and positive comments during my research work.

I gratefully acknowledge the fee waiver support during my academic break provided by the Honourable Chancellor of Galgotias University Shri Suneel Galgotia. This greatly helped me to manage financial and medical difficulties during the critical period.

I profusely thank Vice-Chancellor Prof. (Dr.) Preeti Bajaj Ma'am for allowing me to do my research in this prestigious university. She herself is academically active and sets a powerful example to research students. I extend my sincere thanks to Prof. (Dr.) Naresh Kumar (Dean PG & PhD) for his support, constant support, and valuable guidance. I would like to express sincere appreciation to Galgotias University for providing an excellent academic environment.

I am also thankful to former Pro-Vice-Chancellor Prof. Renu Luthra for her kind support and help. My special thanks go to Registrar Dr. Nitin Gaur for his cooperation during my research work.

My special thanks go to Dr. Arvind Kumar Jain, Dr. Sudhir Kumar Singh, Dr. Kaushalendra Kumar Dubey, Mr Brahma Nand Agrawal and Mr K.S. Srikanth for their

kind help and valuable time that is given for my research discussions. I am deeply grateful to all the faculty members of the mechanical engineering department at Galgotias University whose constant support made my study meaningful and knowledgeable.

I express my sincere thanks to Shri S.L. Vaswani (Honourable Chairman) and Shri Anil Kumar Vaswani (Honourable Vice-Chairman) of Skyline Group of Institutions for permitting me to carry out my PhD work. I am very thankful for their support and help. I will forever cherish my close association with Skyline Group. I acknowledge with gratitude the support received from the former directors and current director of Skyline Institute of Engineering & Technology, Dr. I.K.Sharma, Dr. S.S.Chauhan and Dr. R.K.Yadav during different stages of my study.

No words of gratitude can justify the support, help, care, and love I have received from my well-wishers, friends, and colleagues. I am grateful to my friends Dr Navneet Kumar Pandey, Dr Sudhanshu Sharma, Dr Akant Kumar Singh, Dr Amit Kumar Sharma, Mr Rajeev Saini, Mr Yogesh Kumar Yadav, Mr Pradeep Kumar Chandra, Mr Abhishek Kaushik and Mr Sunil Kumar Yadav who were always there to lend a helping hand when it mattered most.

Finally, I deeply thank my mother Smt. Vimlesh Giri, my wife Mrs Deepti Goswami, my daughter Harshita, and my son Pallav for their endless love, unconditional trust, moral support, and constant encouragement. I feel privileged and lucky to have you all in my life.

I would also like to thank all those who helped me directly or indirectly during my research work if I have missed their names to acknowledge here.

Jitendra Mohan Giri

TABLE OF CONTENTS

LIST OF FIGURES

LIST OF TABLES

LIST OF PUBLICATIONS

Paper I J. M. Giri and P. K. S. Nain, "Performance Optimization of Thermoelectric Cooler using Genetic Algorithm," *Mathematical Modelling of Engineering Problems*, Vol. 7, No. 3, pp. 427–435, Sep. 2020, https://doi.org/10.18280/mmep.070313
[Scopus Indexed]

Paper II J. M. Giri and P. K. S. Nain, "Maximization of Energy and Exergy Efficiencies for a Sustainable Thermoelectric Cooling System by applying Genetic Algorithm," *International Journal of Exergy* [Accepted, In publication].
[SCIE and Scopus Indexed]

Paper III J. M. Giri and P. K. S. Nain, "Optimization of Refrigeration Rate for a Thermoelectric Cooler in Restricted Space using Stochastic Algorithms," *International Journal of Recent Technology and Engineering*, Vol. 8, No. 2, pp. 2306–2311, Jul. 2019, https://doi.org/10.35940/ijrte.b2701.078219
[Scopus Indexed]

Paper IV J. M. Giri and P. K. S. Nain, "Review of Recent Progresses in Thermoelectric Materials," *Advances in Engineering Materials, Lecture Notes in Mechanical Engineering*, Springer Nature, Singapore, pp. 269-280, April 2021, https://doi.org/10.1007/978-981-33-6029-7_26
[Scopus Indexed]

NOMENCLATURE

Symbol	Description	Unit
A	Cross-sectional area of TE elements	mm^2
c	Temperature reduction factor	-
COP	Coefficient of Performance	-
f	Objective function	-
i	Iteration number	-
I	Electric current	A
k_B	Boltzmann constant	J/K
K	Thermal conductance	W/K
L	Length of thermoelectric elements	mm
n	Number of iterations	-
N	Number of thermoelectric couples	-
P	Input electric power	W
Q	Rate of heat rejection or absorption	W
Q_c	Cooling capacity	W
r_c	Electrical contact resistance	Ω-m^2
R	Electrical resistance	Ω
R_{th}	Thermal resistance	$^0C/W$
ROR	Rate of refrigeration	W
S	Cross-sectional area of TEC device	mm^2
S_{gen}	Rate of entropy generation	W/K
T	Temperature	K
ΔT	Temperature difference	K
U	Overall heat transfer coefficient	W/m^2K
ΔV	Voltage difference	V
X	Design Point	-
Z	Figure of merit	1/K

ZT	Dimensionless figure of merit	-

Greek Symbol	**Description**	**Unit**
α	Seebeck coefficient	V/K
Π	Peltier coefficient	W/A
σ	Thomson coefficient	V/K
ρ	Electrical resistivity	Ω-m
κ	Thermal conductivity	W/m-K
γ	Electrical conductivity	S/m
η_I	First law efficiency or energy efficiency	-
η_{II}	Second law efficiency or exergy efficiency	-

Subscripts	**Description**
a	Ambient
ave	Average
c, cold	Cold side
co	Cold surface
conduction	Conduction
cr	Ceramic
h, hot	Hot side
ho	Hot surface
hs	Heat Sink
o	Outside
joule	Joule
peltier	Peltier
p	p-type element
n	n-type element

Acronym	**Description**
CFC	Chlorofluorocarbons
DC	Direct Current

FEM	Finite Element Method
FOM	Figure of Merit
GA	Genetic Algorithm
HCFC	Hydro chlorofluorocarbons
HFC	Hydrofluorocarbons
PD	Packaging Density
SA	Simulated Annealing
TE	Thermoelectric
TEC	Thermoelectric Cooler

CHAPTER 1

INTRODUCTION

CHAPTER 1

INTRODUCTION

1.1 General Background

The Peltier effect of thermoelectrics is the direct method to pump heat using electricity. The potential of thermoelectrics is now generally acknowledged to be limitless. Despite the rapid growth of electronic devices, still there are some concerns. The temperature control of electronic systems is one of the most significant considerations. The traditional cooling systems are no longer capable of removing heat fluxes at a sufficient pace for heat-intensive electronic devices. One potential way to resolve the heat dissipation issue is to use a thermoelectric cooler (TEC). Solid-state thermoelectric coolers are attractive and promising and do not use refrigerants. These devices are environment-friendly, noiseless, scalable, and reliable. They are without vibration, without mechanical movements, and almost maintenance-free.

However, the low performances of TEC have become the limitation of its applications. According to published research, bismuth telluride is considered the best thermoelectric material and used to have a *ZT* around 1.0 at 300 K [1]. With a *ZT* of 1.0, thermoelectric coolers are reported to work at just 10% of Carnot efficiency [2]. A TEC system with a *ZT* value of 4.0 could achieve 30 percent of Carnot efficiency (competitive with compressor-based refrigerators) but achieving the 4.0 value of *ZT* and commercialization can take a long time. A high value of the figure of merit (*ZT*) of thermoelectric materials is required to increase the device's efficiency. Also, to build high-performance thermoelectric cooling devices, it is necessary to have good contacts, mechanical properties, thermal interfaces, and packaging techniques. The thermoelectric (TE) material properties, system design, and assembly are crucial factors. In recent years, comprehensive research has been carried for the development

of efficient thermoelectric materials. With the development of advanced thermoelectric materials, the design and assembly of the TEC system have become highly significant. The research on TEC devices is lagging behind the advancement of thermoelectric materials [3]. The cost of TE materials is also high. Hence, the future of TEC depends greatly on its high performance at a low cost. As a result, advances in TEC performance are attracting more interest, and research on the subject is becoming more noticeable.

Thermoelectric cooling devices are capable of dissipating limited heat flux. Besides that, such devices have a low *COP*. Exergy efficiency is also an important concern. The performance parameters such as cooling capacity, coefficient of performance, and exergy efficiency are of special interest among researchers. The performance of a TEC device is based on a number of factors, including the input electric current, ambient temperature, architecture of the device, contact resistance, and thermal conductance of the heat sink. These are crucial factors in designing the optimum TEC for a particular need. A haphazard implementation of TE technology would almost certainly be more expensive and unsuccessful than a well-thought-out technique. To get the best out of these devices, it's vital to study them. There is a lot of scope for improvement with thermoelectric coolers.

Optimization of TEC is an important research objective for enhancing its uses. The methods taken by researchers to this problem are extremely diverse. These methods can be categorized into two broad groups. The first method is to optimize the TEC system by using dimensional structural parameters as design variables in order to obtain the feasible best performance with given materials. The second method is to optimize the TEC system by using the operating parameters as design variables to get the highest possible output for a given materials set. There had not been a study by simultaneously using a combined set of geometric characteristics and operating parameters. The combined effect of length and cross-sectional area of p-type and n-type thermoelectric elements, and the electric current needs to be investigated.

Stochastic optimization methods have been rapidly increasing in popularity over the past decade or two, with a variety of techniques. These techniques are becoming “industry standard” methods for solving complex optimization problems. Genetic

algorithm and simulated annealing have recently gained popularity as optimization tools, and they have been widely used to solve a variety of complex problems.

1.2 Research Objectives

Thermoelectric coolers are extremely sensitive to their operating and boundary conditions. The selection of appropriate materials, geometry, and operating conditions are all important factors in developing the best technologies for a given application. The objective for this optimization search is the maximum of the cooling capacity or rate of refrigeration, maximum of coefficient of performance, and best exergetic performance at a given cold side temperature by the acceptable design. Dimensional structural and operational variables such as thermoelectric element length, the cross-sectional area of elements, number of elements, and electric current are used as design variables in the models. There had not been a study by simultaneously using a combined set of these design variables. The models of this study take into account complications like electric contact resistance, thermal resistance, ambient temperature, and packaging density. The significant restriction in this work is the device's limited space.

The aim of this research work is to learn about the TEC system and to maximize the TEC performance within the restricted space of the device by using the stochastic algorithm. This goal has been achieved with:

(1) TEC mathematical modelling
(2) Pilot study to select a suitable stochastic algorithm for this class of optimization problems
(2) Optimization of the cooling capacity of TEC
(3) Optimization of coefficient of performance of TEC
(4) Optimization of energy and exergy efficiency of TEC
(5) Finite-element simulation of TEC with ANSYS@ to validate results.

1.3 Thesis Structure

This thesis consists of eight chapters, which are briefly discussed below.

Chapter-1 is devoted to the general background of the thermoelectric cooling system. The research objectives and thesis structure are also discussed.

Chapter-2 deals with the basic concepts of thermoelectrics, the construction of TEC, working principles, applications, and advantages of thermoelectric coolers. The literature review on the thermoelectric materials as well as existing design and methods of TEC for enhancing performances have been discussed.

Chapter-3 explains the methodology and assumptions. The theoretical description of the model and an overview of optimization methodologies are discussed. The basic procedures of two different stochastic algorithms, namely, genetic algorithm and simulated annealing are presented. A simplified TEC model has been prepared for a pilot study on the basis of essential performance parameter, i.e., cooling capacity. The comparative results have been investigated and a stochastic optimization technique is selected to proceed for further research in this work.

Chapter-4 provides the thermodynamic modeling of the TEC system. For cooling capacity maximization, genetic algorithm is used. The optimal length, the cross-sectional area of TE elements, and input electric current are estimated.

Chapter-5 provides the optimization of the coefficient of performance of TEC. GA implementation, results, and discussion are presented.

Chapter-6 describes the thermodynamic formulations for the first and second law efficiencies of the TEC system. GA is used to find optimal solutions considering maximization of first and second law efficiencies.

Chapter-7 describes the basic concepts of the finite-element method and basic procedure to use ANSYS® workbench. To validate GA results (for each optimization problem), finite-element simulations are done. A comparison of GA and finite-element simulation results are presented.

Chapter-8 presents the conclusions of the work reported in this thesis and recommendations for future work are presented.

1.4 Summary

In Chapter 1, the general background of thermoelectric coolers is summarized. The potential use of thermoelectric coolers and the performance limitations are briefly introduced. The research objectives and the thesis structure are also presented. In the next chapter, the literature review is presented.

CHAPTER 2

LITERATURE REVIEW

CHAPTER 2

LITERATURE REVIEW

2.1 Introduction to Thermoelectrics

A thermoelectric (TE) system can operate in one of two modes: to pump heat or to generate power. The heat pumping process begins when electrical current is supplied to the terminals. The pumped heat can be used for cooling or heating applications. In second mode, when a temperature differential is maintained through the TE device, heat passing through it is converted into electrical current.

The fundamental scientific phenomena needed to comprehend the TE system behaviour is given in 'CRC Handbook of Thermoelectrics by Rowe [4]. The recent advances and design methods for thermoelectric materials as well as devices are described in 'Thermoelectrics: design and materials' by Lee [5].

Thermoelectrics primarily emerged during two phases of activities. The fundamental effects were discovered between 1821 and 1851 [6]. It was macroscopically realized that they could be used in generating power, and refrigeration purposes. In 1910, Edmund Altenkirch evaluated the potential efficiency of TE generators and described the materials parameters required to construct practical TE devices. Then, starting in the late 1930s, a 20-year journey led to a microscopic comprehension of thermoelectricity.

2.1.1 Seebeck effect

Hans Christian Oersted, a Danish scientist, discovered in 1820 that an electric current flowing in a wire parallel to and near to a magnetic needle might deflect it [7]. Electromagnetism was established as a result of his observation that an electric current

induces a magnetic field. When Thomas Johann Seebeck heard of Oersted's findings, he decided to focus on studying electromagnetism. In 1821, he observed that if the junctions of two dissimilar metal conductors were held at different temperatures, a compass needle deflected [8]. He also noticed that the magnitude of the deflection was proportional to temperature difference. He observed that the deflection was material (conducting) dependent and the temperature difference across the conductors had no effect on the deflection. He discovered that if one junction was heated to a high temperature while the other remained at a lower temperature, a magnetic field formed around the circuit of different temperatures. He had investigated the effects of heating and cooling one of the junctions using a variety of metal combinations. He named the phenomenon "thermo-magnetism" after describing the observation as "the magnetic polarization of metals".

Later confirmed, that the temperature difference between the two junctions of a closed bi-metallic circuit does generate an electric current. The electromotive force that drives this current is referred to as a "thermoelectric electromotive force" and the phenomenon is called as the "Seebeck effect". The voltage produced per kelvin difference is on the order of several microvolts. The electromotive force or voltage driving this electric current can be determined, if we break the closed loop and measure the open circuit voltage difference (ΔV). The Seebeck effect can be described how ΔV forms in a semiconductor (or conductor) when its load carriers diffuse over a temperature difference (ΔT). The relationship between ΔV and ΔT is given by:

$$\Delta V = \alpha \Delta T \tag{2.1}$$

Where, α = Factor of proportionality, known as Seebeck coefficient (V/K)

$\Delta T = T_{hot} - T_{cold}$ (difference of hot & cold junction temperatures)

2.1.2 Peltier effect

An electrical current can heat or cool the junction of two dissimilar metals. It had been discovered by J. C. A. Peltier. Peltier effect was the name given to this phenomenon discovered in 1834 [9]. Lenz demonstrated in 1838 that heat produced by current that

flows in one direction could be absorbed when the current was reversed [10]. The heat absorbed or emitted at the junction is directly proportional to the electrical current. Thermoelectric cooling is based on this basis. The rate at which Peltier heat ($Q_{peltier}$) is absorbed or released from the junction can be estimated using the following equation:

$$Q_{Peltier} = \Pi I \tag{2.2}$$

Where, I = Electric current (A),

Π = Proportionality constant, known as Peltier coefficient (Watts/Ampere)

The Peltier effect's main advantage is that it enables the design of cooling and heating devices without the use of moving parts. In comparison to conventional coolers and heaters, such devices are much less likely to malfunction and therefore do not require maintenance. However, the Peltier effect's efficiency is limited, which is a drawback. Another disadvantage is that the circulating current tends to generate considerable heat, adding to the heat dissipation process. The Peltier effect is usually useful at the microscopic level, where conventional cooling methods are ineffective. The Peltier effect and Seebeck effect are depicted in Figure 2.1.

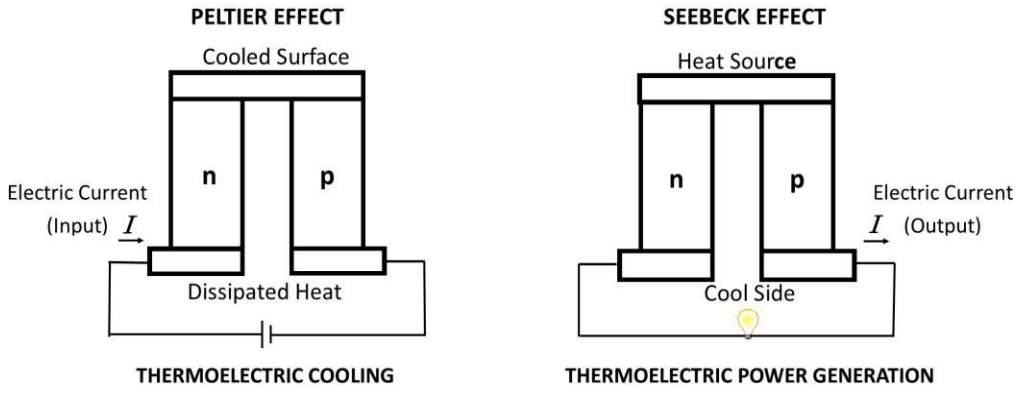

Figure 2.1 Peltier effect and Seebeck effect

2.1.3 Thomson effect

There is also the Thomson effect, which is the third facet of thermoelectrics. When the current flow, as well as temperature gradient, are present at the same time, the Thomson effect refers to heat dissipation and absorption in a single substance. According to the

Thomson effect, which was predicted by W. Thomson (later Lord Kelvin) in 1855, a material with current may absorb or dissipate heat along a temperature gradient [11]. The Thomson effect explains the heat loss of a material when a current flows through it, and this heat transfer is noticeable instantly. The Thomson heat is in proportion to the product of electric current and the thermal gradient [4]:

$$\frac{Q}{dx} = \sigma\, I\, \frac{dT}{dx} \tag{2.3}$$

Where, Q/dx = Rate of heating or cooling per unit length (W/m),
dT/dx = Temperature gradient (K/m),
I = Electric current (A),
σ = Proportionality constant, known as Thomson coefficient (V/K)

2.1.4 Kelvin relations in thermoelectrics

William Thomson (later Lord Kelvin) discovered two thermoelectric coefficient relationships in 1854, which are now known as Kelvin thermoelectricity relations [12]. The first Kelvin relation gives the direct relationship between the Seebeck and Peltier coefficients:

$$\Pi = \alpha\, T \tag{2.4}$$

Where, T represents the temperature of the junction

The change in the Seebeck coefficient per change in temperature is equal to the change in the Thomson coefficient. The expression is:

$$\sigma = T\, \frac{\Delta\alpha}{\Delta T} \tag{2.5}$$

2.1.5 Joule effect

James Prescott Joule, about the year 1840, was the first to study and classify the heating effect [13].

This refers to the irreversible conversion of electrical energy into heat as a result of resistance to an electric current flowing through a conductor. James Prescott Joule discovered and revealed a quantitative relationship between the amount of heat emitted in a conductor and an electric current flowing through it in 1840. When a current of voltaic electricity is propagated through a metallic conductor, the heat produced in a given time is proportional to the conductor's resistance multiplied by the square of the electric intensity, according to this rule. The following equation is established for Joulean heat generation due to current flow:

$$Q_j = I^2 R \tag{2.6}$$

Where, Q_j = Rate of heat (Joulean) generation (W),
I = Electric current (A),
R= Electrical resistance (Ω)

2.1.6 Altenkirch's theory

By 1911, Edmund Altenkirch proposed a satisfactory theory of thermoelectricity generation and refrigeration, demonstrating that good thermoelectric materials should have certain properties [14]. According to the theory, a good TE material should have high Seebeck coefficient, low thermal conductivity to retain the heat at the junction and sustain a large temperature gradient and low electrical resistance to keep Joule heating to a minimum. A so-called thermoelectric material property Figure of Merit or FOM (Z) encapsulated these desirable properties.

$$Z = \frac{\alpha^2}{RK} \tag{2.7}$$

Where, α= Seebeck coefficient (V/K),
R= Electrical resistance (Ω),
K= Thermal conductance (W/K)

Using the dimensionless figure of merit, ZT, where T is the absolute temperature of interest, is a more useful way of representing the thermoelectric efficiency of a material

system. Thermoelectric materials have thus been characterized using *ZT*. The higher the value, the better for thermoelectric refrigeration.

2.1.7 Thermoelectric materials

Because of their low Seebeck coefficient and significant electronic contribution to thermal conductivity, metals are poor thermoelectric materials. Insulators have a low electronic contribution to thermal conductivity and a high Seebeck coefficient. Their electrical conductivity is poor due to their low charge density, resulting in a low thermoelectric effect. Semiconductors are the next type of material to be considered, as they can have extremely high Seebeck coefficients. However, semiconductors with high Seebeck coefficients have low electrical conductivity, making finding a suitable thermoelectric material more difficult. Using doped semiconductors, on the other hand, improves the performance of *ZT*. Furthermore, studies have shown that a strong thermoelectric material is likely to be made up of high-atomic-weight elements or heavy-element compounds [15].

The compound bismuth telluride Bi_2Te_3, which is most widely used in thermoelectric coolers, is a good example of thermoelectric material made from high atomic weight materials [16]. Bi_2Te_3 has a FOM (*ZT*) around 1 at room temperature. Other thermoelectric materials that may be used in specific situations include Lead Telluride (PbTe), Silion Germanium (SiGe), and Bismuth-Antimony (Bi-Sb) alloys. Several techniques have been used in recent years to increase the *ZT* values of TE materials, including optimizing carrier concentration, controlling the band structure, nanostructure engineering, and defect manipulation. Semiconductor materials are classified as n-type or p-type depending on if they have sufficient electrons for a perfect molecular grid structure (n-type) or not sufficient electrons for a grinding structure (p-type). The extra electrons in the n-type TE material and the hole in the p-type TE material are known as "carriers". They are the agents that transfer heat energy from one side to the other. If an electron in the n-type element is added to a high-current DC power supply, it will travel in the opposite direction to the current flow, while hole in

a p-type element will move in the same direction, both of which are removing heat energy [17].

2.2 Thermoelectric Cooling System

A thermoelectric cooler (TEC) is a solid-state cooling system that uses the Peltier effect to work. Heat would be absorbed into one junction and removed from the other in proportion to the current if a potential is applied between two junctions. When temperature stabilization or cooling below ambient is needed, thermoelectric coolers are used. Thermoelectric coolers are solid-state machines that do not have any moving parts, fluids, or gases. The basic laws of thermodynamics refer to TEC in the same way as they do to traditional heat pumps, absorption refrigerators, and other heat-transfer instruments. A TEC, on the other hand, is built and structured differently than a standard refrigerator, necessitating knowledge of materials and semiconductor technology in addition to heat transfer.

2.2.1 Working Principle of thermoelectric coolers

Thermoelectric cooling is a method of transferring heat from one side of a system to another. It is accomplished by applying voltage between two electrodes that are attached to a semiconductor material. The Peltier Effect, which causes a temperature difference, can be used for cooling, heating, and precise temperature control in many applications. TE coolers, also referred as Peltier coolers, are solid-state heat pumps that use the Peltier effect to dissipate heat and require DC voltage. An array of n-and p-type semiconductor materials soldered between two ceramic plates makes up a thermoelectric cooler. Electric current passes through the system during operation, causing heat transfer as well as temperature difference through the ceramic plates, resulting in one hot and one cold side of TEC. The performance of the thermoelectric cooler is influenced by one factor, heat conduction. Conventional heat conduction can transport heat from the hot to the cold side of TE materials. Heat will be created as a result of the current flow in the materials due to the Joule effect. Each junction will receive a portion of the Joulean heat. It is common to consider that each junction receives half of the Joulean heat. The Thomson effect is also present. The net Thomson

coefficient (σ_p-σ_n) for a pair of n-and p-type TE elements becomes zero as current flows through the material with a constant Seebeck coefficient. As a result, the Thomson Effect is ignored.

2.2.2 Applications of thermoelectric coolers

Thermoelectric coolers are suitable for applications requiring heat removal from milliwatts to hundreds of watts. In thermoelectrics, however, there is a standard axiom: the smaller the better. Thermoelectric cooling systems come in a variety of shapes and sizes, as well as various levels of heat pumping capability, so they can meet a wide range of industry needs. Industrial, military, aerospace, defense, radio-electronics, telecommunication, medical and scientific/laboratory organizations use these devices. A thermoelectric cooler, unlike a basic heat sink, can lower an object's temperature under ambient while still stabilizing the temperature of structures that are exposed to greatly varied ambient conditions. Thermoelectric cooling modules are typically used in the following applications: microprocessor cooling, night vision equipment, parametric amplifiers, refrigerators, wine cabinets, precision device cooling (microprocessors and laser), microtome stage coolers, wet process temperature controller, infrared detectors, dewpoint hygrometers, blood analyzers, cooled personal garments, integrated circuit coolers, hypothermia blankets, automobile seat cooler etc.

The performance of the TEC system is currently not comparable to the performance of compressor-type systems. The gap between the two types of coolers is likely to close over time, but until then, TEC will be limited to applications where it has clear advantages. A TE device's performance is apparently independent of capacity, which is one of its most distinguishing features. As a consequence, it has a distinct advantage when it comes to cooling small enclosures. The use of the thermoelectric cooling device for portable boxes has been considered beneficial by manufacturers. Absorption refrigerators compete in this area, and although they have the benefit of being refrigerant-operated, they are not effective as TEC when using electricity. The TE devices are also unaffected by inclination or movement, making them suitable to use on ships.

The Peltier effect has the advantage of being able to heat as well as cool. Thus, foodstuffs can be kept refrigerated until they are ready to be consumed, at which point they can be heated to the proper temperature. Air conditioning or heat pumps are two of the most promising areas of application. As compared to the limit that can be achieved, the necessary temperature difference in source and sink is often small. Compressor units respond to this condition by turning on for short durations, while TEC systems may run at the optimal current continuously. This enables them to quickly adjust to temperature changes in the sink if heating or cooling is needed.

2.2.3 Advantages of thermoelectric coolers

Thermoelectric coolers, unlike mechanical refrigeration systems, have no moving parts. Perhaps, the most significant advantage of TECs over other cooling systems is the easiness to control.

They offer various advantages as mentioned below:

- No working fluids and gases
- Operation in any orientation and zero gravity
- No moving elements
- Reduced size and weight
- No electrical or acoustical noise
- No friction
- High resistance to vibration or shock
- Environment friendly
- Ability to cool below the ambient temperature
- Precise temperature control (+/- 0.1°C)
- Convenient power supply
- High reliability (Greater than 200000 hours)
- Low maintenance
- Less expensive (20% to 40%) than compressor or absorption systems
- Ability to use the same module for cooling and heating
- Flexible control

2.2.4 Drawbacks of thermoelectric coolers

Thermoelectric cooling devices have the following significant drawbacks:

- Efficiency at dismal level
- Consumes a significant amount of electricity, making it costly to use in large-scale applications
- Current flow itself generates considerable heat, which contributes to the total heat dissipation
- Higher temperature differentials necessitate complex, multistage TEC systems.
- Condensation may occur resulting in a short circuit, if device components are excessively cooled

2.3 Current Research Works on Thermoelectric Coolers

The thermoelectric cooler modules are electronic components that work on the principle of the Peltier effect. It functions as a heat pump moving heat from one side of the device to the other. Based on type, thermoelectric cooler modules are categorized as bulk thermoelectric modules, micro thermoelectric modules, and thin-film thermoelectric modules. The growing adoption of electric vehicles, growing inclination toward renewable energy sources, and increase in demand for energy-efficient consumer electronics are the key factors driving the thermoelectric coolers market. However, the high cost of thermoelectric modules, design complexity, and heat dissipation issues restrain market growth. The reduced size of the TE elements is one goal for TE module manufacturers. Various benefits can be achieved if TEC are made lighter and smaller. When the size of a TEC is reduced, however, we run into issues with heat transfer. It is difficult to transfer heat (source to sink) when end plates are small in cross-section. Increasing the gap between the TE elements would almost certainly solve the issue. But conduction, convection, and radiation heat losses increase substantially. The best compromise between unnecessary thermal resistance and undesirable heat losses can be found by placing the TE elements at the appropriate spacing.

2.3.1 Performance improvisation of thermoelectric cooling systems

Thermoelectric cooling systems could have different architectures based on the shapes of heat source and heat sink, such as the traditional flat plate and annular structure. In addition, for high temperature applications, segmented structure may be implemented, and cascaded structure has been suggested. In addition, various thermoelectric leg geometries, including standard rectangular and asymmetric geometric shapes, have been tested. Thermoelectric element's height/length, cross-sectional area of TE elements, number of TE elements and shape of elements are the four major parameters which are paid much attention to during geometry optimization.

The thermoelectric element length is a significant parameter that can be optimized to improve the thermoelectric cooler's performance. Cheng et al. [18] reported that the benefit of optimizing the dimensions of the thermoelectric cooler elements is that it increases the rate of cooling. Shen et al. [19] investigated the efficiency of a segmented thermoelectric cooler. The segment number appeared to be more susceptible to the thermal conductivity of the thermoelectric material, according to the study. The two segmented thermoelectric element using distinct thermoelectric materials of almost similar Seebeck coefficient value, with a significant difference of figure of merit, could get the better performance of cooling without enhancing the overall figure of merit of thermoelectric cooler. They observed that as element length increases, maximum temperature difference, maximum coefficient of performance, maximum cooling power, and all lowers. Three separate double-stage TECs were optimized by Wang et al. [20]. To improve the cooling capacity and coefficient of performance, they discovered that the number of thermoelectric elements on the hot side should be higher than the number of thermoelectric elements on the cold side. Besides this, the authors believed that the only way to reliably predict double-stage TEC output is to use temperature dependent TE materials properties. Lamba et al. [21] used a thermodynamic model to study a thermoelectric cooler and discovered that the Thomson effect improved the cooling rate of TEC. Lin et al. [22] improved a trapezoid-shaped thermoelectric cooler with two stages. To improve performance of device and reduce thermal resistance (inter-stage), ceramic plates (intermediate) were removed.

The trapezoid leg shape ratio on the hot-stage had an effect on the maximum *COP* and maximum rate of cooling, they discovered.

A variety of publications have published on studies on the experimental calculation and generalization of physical parameters of TEC systems. Fraisse et al. [23] have compared various modeling methods and measured the accuracy of certain simplified models, while preserving the invariance of other parameters. Riffat et al. [24] used a small prototype device to build a computer model for simulating the efficiency of a novel TE heat pump. The thermoelectric parameters were determined using a quadratic empirical equation based on the hot side temperature and cold side temperature. In his classic textbook, Rowe [4] discussed temperature dependent properties of physical parameters. These parameters were validated by using them to solve a thermal resistance issue in TEC device [25]. The results showed that the errors remained below 5%. To define their module criteria, Chen et al.[26], Lineykin et al. [27], and Luo et al.[28] used curves for performances and many range values from TEC vendor datasheets. The key benefit of this approach is that the solutions can be found without having to use p-n type pellet data. Huang et al.[29] and Mitrani et al.[30] looked at how a TEC's output changed as the cold and hot side temperatures changed, and how TEC performed under such thermoelectric conditions. The electrical resistance had been obtained from the voltage and current curves. The effective value of Seebeck coefficient was calculated by dividing the open circuit (measured) by the temperature difference (external).

Significant attempts have been made to boost device efficiency thereby lowering energy consumption. Cai et al. [31] built an air source TE heat pump device that can deliver cold air and hot water at the same time. The thermal conductance as well as specific heat allocations in heat exchangers (cold and hot side), they found, could have a significant impact on *COP* and cooling capacity. Zhou et al. [32] proposed a TE supported evaporative cooling device (indirect). The TEC units are located between many channels of the evaporative cooling device (cross-flow flat plate) to improve heat transfer capacity at the hot side of TEC. The performance of a heat sink assisted TEC within a square duct was investigated numerically and experimentally by Seo et al.[33].

It was observed that the heat sink's various parameters affect the TEC system's efficiency. Theoretical study of a thermoelectric device fitted with an office space in Morocco was suggested by Allouhi et al. [34]. The number of TE modules needed to obtain a maximum *COP* of 2.0 was determined to be 12 in this study. Liu et al. [35] developed a conceptual model for a PV-thermally-compound TE ventilator framework that generates electric power in the winter while also preheating the fresh air, allowing for full solar energy utilization.

To simplify TEC system with totally temperature-dependent thermoelectric material properties, McCarty [36] reported a numerical technique of one-dimensional result. The precision of the numerical TEC model was further verified by experimental results. Finned arrangement of heat pipes could reach greater than 200 W/K values of UA (overall heat conductance × area) for gas flow systems, according to existing technologies, since they have larger efficient areas for heat transfer.

A novel TEC architecture was proposed by Owoyele et al. [37]. The effects of different geometry parameters were investigated, and it was discovered that the corrugated thermoelectric cooler worked better. It was more cost-effective for applications requiring low value of cooling power density. In a corrugated TEC, proper thickness selection was suggested for minimizing losses. Using simulated annealing, Khanh et al. [38] optimized the geometry of thermoelectric coolers. To increase the rate of refrigeration, the dimensions of thermoelectric coolers were optimized using simulated annealing. Lamba et al. [39] optimized the geometric parameters of a trapezoidal-shaped heat pump using a genetic algorithm. After 20 runs, the population of the GA converged rapidly, demonstrating that it is a cost and time-effective method. They noticed that the Thomson effect had a negative impact on the system's heating load, and that contact resistance had a negative impact on the system's performance. Soprani et al. [40] used topology optimization to improve TEC efficiency. Also, a three-dimensional finite-element method was used. The experimental outcome and the model predictions were very similar to each other. Electronic devices that were actively cooled were designed using the optimization process.

Saifizi et al. [41] designed and tested a hybrid device that used a direct air to air heat pump to hold vaccine packages at a low temperature. Lal and Kumari [42] investigated the performance of a cost-oriented TEC in an experimental environment. With a minimum attainable temperature of 2.3°C, the optimum amount of the *COP* was recorded to be 0.26. Dongareet al. [43] designed and updated a real-world TEC device with 18 litre volume. From 33°C to 22°C, it took one hour to maintain this temperature with coefficient of performance of 0.2-0.6. Ebrahimi et al. [44] developed a model with micro-combination of heating, cooling and power generation features. They used a thermoelectric cooler as the cooling system. Shafee et al. [45] designed and tested a thermoelectric heating as well as cooling system that was cascaded and incorporated. For this cascading and integration configuration, the coefficient of performance were 0.02 and 0.294, respectively. Adeyanju et al. [46] investigated a fast drink cooler relying on TEC in attempt to chilling a glass of water. The volumetric size of glass was 0.5 litre and the time taken to chill was 2 minutes. It was done both experimentally and theoretically. Chiba et al. [47] investigated the Peltier and Seebeck effects in multistage thermoelectric cooler depending on hydrogen liquefier.

The finite element approach was used to perform three-dimensional numerical simulation by Qiu et al. [48]. A sandwiched construction of thermoelectric cooler using uniform cross-section as well as non-uniform cross-section was used. To illustrate the working mechanism of the factors at play, a detailed mathematical model was built. For an input of smaller portion of thermoelectric element, non-uniform section type TEC is beneficial with more cooling capacity with 6%-12% improvement. However, the coefficient of performance was identical. A modest element height (1.5 mm) will greatly boost the cooling rate of the thermoelectric cooler as compared to 3.0 mm height of TE element, with a 52.96 percent increase in peak cooling rate. A -20.66 percent change in peak *COP* was evaluated. For the *COP* and cooling rate of the thermoelectric cooler, the contact layers provided different effect patterns and sensitivities. The TEC's output deteriorated as the solder thickness increased. The thickness of copper layer, on the other hand, had the opposite effect. The maximum *COP* and maximum cooling capacity were taken into consideration for a Pareto-optimal front with the help of

NSGA-II by Lu et al. [49]. The effect of design variables like electric current and element structure on the performance of thermoelectric cooler has been demonstrated.

An electrically disconnected double-stage TEC's exergy as well as exergoeconomic analysis is reported by Nemati et al. [50]. The effects of electrode length, applied current, cross-sectional area ratio and stage-wise number of electrodes were studied. At first stage, the optimum current is lower as compared to the current at second stage. The maximum second law efficiency is achieved at small values of current. The exergy efficiency improves with an increment in electrode numbers (both stages). Smaller optimal values of the cross-sectional area ratio and greater applied currents have better economic efficiency. The effects of electrical current, air flow rate, air inlet temperature, water flow rate and water inlet temperature, were investigated using a Peltier air cooler by Dizaji et al. [51]. The exergetic performance has a minimum value when the DC voltage reaches an extreme. The exergetic performance was high for warmer temperature of air inlet. The rate of air flow was also high. A theoretical evaluation of the optimum performance of a TE cooler was done by Tan et al. [52]. The optimization objectives were chosen to be cold exergy and second law efficiency. The effects of several main parameters on cooling performance, such as thermal conductance allocation ratio, electric current, and cooling temperature, were theoretically investigated. This was realized that there is an optimum cooling temperature that leads to maximum cooling rate and second law efficiency. A heat sink design optimization model for a TEC device was proposed by Zhu et al. [53]. The TEC system was optimized using an entropy generation minimization process. The cooling fluid’s heat capacity rate is sensitive parameter and must be chosen appropriately to minimize entropy generation.

Maximum rate of refrigeration, maximum electric current and voltage at different hot side temperatures were calculated using COMSOL® multiphysics by Panigrahi et al. [54]. At a given hot side temperature, the low cold side temperature attracted low rate of cooling. At a given cold side temperature, the rate of cooling increased with an increment in current followed by hot side temperature. The results have also shown that, regardless of cold side temperature, the COP for a given relative current value is

higher in a higher hot side temperature. Analytically, the partial differential equations that control the function of a TEC were solved by Fong et al. [55]. It was carried out in order to calculate the temperature profile within the TE element and system's *COP* and cooling capacity. The thermoelectric cooler's transient behavior could be used as an optimization method for different design setups in order to satisfy particular packaging requirements. Using CFD, a TEC model with a heat sink was developed by Seo et al. [33]. As a result of the time-dependent characteristics revealed by the numerical solutions, the cooling capacity of TEC differ over time. Teixeira et al. [56] showed that a TEC can be made using cylindrical or cubic geometry of elements and performs equally. According to simulations, increasing the cross-sectional area of the TE elements increases the power output of a TE device. Çağlar et al. [57] designed and fabricated a portable thermoelectric refrigerator. This refrigerator was tested at various ambient temperatures and for *COP*, a method for determining optimal operating conditions was defined. It was also observed that when the cooled space temperature drops from 293 K to 254.8 K, the system's *COP* drops from 0.351 to 0.011.

2.3.2 Improvements in figure of merits of thermoelectric materials

The figure of merit (Z) is a measurement of a thermoelectric material's performance. Z is determined by three critical material parameters: the Seebeck coefficient (α), the thermal conductivity (κ), and the electrical conductivity (γ). At absolute temperature (T), Z is expressed in dimensionless form. $ZT=\alpha^2\gamma T/\kappa$ is used to define the dimensionless figure of merit. Alternatively, ZT is also defined as $(\alpha^2/\rho\kappa)\ T$, where ρ is the electrical resistivity. A large power factor (α^2/ρ) is required to enhance thermoelectric performance. A good thermoelectric material should possess a large Seebeck coefficient (α), low thermal conductivity (κ), and high electrical conductivity (γ). The conversion efficiency of TE devices is directly related to the dimensionless figure of merit of their constituting materials. Thus a high value of the figure of merit is highly desirable.

In recent years, researchers applied new approaches and techniques in maximizing the ZT values of various thermoelectric materials. The available thermoelectric materials

exhibit varying performance in the different temperature ranges. Improvement in each available thermoelectric material is a focused goal of researchers for a sustainable alternative of conventional energy converters. Earlier, the performance of the semiconductors used in TE applications was dependent on the available pure and perfect single crystals. However, these materials can be doped by adding small quantities of impurities. These impurities act as the electron donor for the parent materials. Most traditional semiconductors have cubic structures, whereas anisotropic crystals are used for TE applications. The task of designing high-performance thermoelectric materials is to adjust the physical parameters of interconnected α, σ, and κ for a crystalline structure. Thermoelectric transport includes the flow of thermal energy and charge. The energy of phonons (vibrational waves of atoms) represents the thermal energy. Electrons scattering on phonons creates electrical resistance. Through incorporating some new scattering mechanisms, nanostructures provide an opportunity to sever the connection between electric and thermal transport. The lattice thermal conductivity needs to be reduced for improvement in TE performance. Mass fluctuations increment through vacancies, and interstitial atoms result in higher phonon scattering that can lead to better TE performance. Sintering of bulk materials and melting production are the techniques used for research efforts to get improved TE materials. This review summarizes recent approaches to enhance the *ZT* of various thermoelectric materials. There is a wide variety of elements as well as compounds which may be categorized as TE materials. It is to be noted that every thermoelectric material exhibits different performance at different temperatures. Hence, it is not possible to recommend a single TE material that is suitable for all practical ranges of temperature in real-world applications. In the present review, TE materials are classified based on their suitability for low, medium, and high-temperature applications.

Low-temperature thermoelectric materials (<500 K)

Bi_2Te_3 and its alloys with *ZT* values of around 0.9–1.0 are considered prominent TE materials at room temperature and widely used for practical thermoelectric applications [58], [59]. Hu et al. [60] demonstrated that the porous structure affects thermoelectric

performance. As porosity increased, electrical and thermal conductivity decreased significantly. Reducing thermal conductivity compensates for the deterioration in electrical conductivity and improves the *ZT* value. A sample premixed with five wt percent NH_4HCO_3 was reported with 1.1 value of maximum *ZT* at temperature 343 K. This was around 20 percent better than that of the entirely dense sample with 0.92 value of *ZT*. Bi-containing Sb_2Te_3 and the related alloys with a high thermoelectric FOM can be futuristic options to use in thermoelectric devices. $Sb_{2-x}Bi_xTe_3$ samples were milled, pressed, and annealed under vacuum for 3 hours at 250°C by Adam et al. [61]. Bi was added to the binary Sb_2Te_3 system. An increased Seebeck coefficient and power factor were obtained for $Sb_{1.65}Bi_{0.35}Te_3$ with the reduced value of thermal conductivity. Subsequently, a high *ZT* of 1.14 at 400 K was attained. The sample composition of $(Bi_2Te_3)_{0.15}+(Sb_2Te_3)_{0.85}$ was prepared to shift maximum *ZT* to the high-temperature zone by Madavali et al. [62]. The maximum *ZT* values of 1.3 and 1.07 were reported at 400 K and 300 K, respectively.

Tellurium is the prevailing thermoelectric material utilized in low to medium range of temperature. However, it contains an inferior thermoelectric efficiency with a low value of *ZT*. An enhancement in the performance of amorphous silicon has been reported by Banerjee et al. [63]. The magneto-TE *ZT* in 3-D Dirac semimetal Cd_3As_2 crystal was reported by Wang et al. [64]. The magnetic field very effectively reduces thermal conductivity and electric conductivity. The maximum *ZT* value of 1.1 was obtained at 350 K temperature under 7 T of the magnetic field.

A hypothesis of thermoelectric transport properties in 2-D semiconducting quantum well structures is built up by Yelgel et al. [65]. It is discovered that diminishing the well thickness pronouncedly affects upgrading the *ZT* value. At 350 K temperature, the maximum *ZT* value of 0.97 is obtained for $Bi_2Se_3/Bi_2Te_3/Bi_2Se_3$. At 440 K temperature, the maximum *ZT* value of 1.945 is obtained for $Sb_2Te_3/Bi_2Te_3/Sb_2Te_3$. $CaMnO_3$ has a generally high Seebeck coefficient; however, the electrical conductivity (γ) is quite low (within the temperature range 300–1000 K). Hence, an un-doped material brings a low power factor ($\alpha^2\sigma$). The bismuth doping of $Ca_{1-x}Bi_xMnO_3$ has been reported by Paengson et al. [66]. With x range of 0-0.05, TE materials were setup. The solid-state

reaction and hot pressing techniques were used. Bi doping increased carrier concentration for all samples with different x. The electrical resistivity diminished with expanding bismuth content. The maximum *ZT* value of 0.065 at 473 K was found for $Ca_{0.97}Bi_{0.03}MnO_3$. It is worth mentioning that the *ZT* value was increased by 95% at the same temperature compared to $CaMnO_3$. Bi_2Te_3 and the family of similar compounds potentially satisfy the thermoelectric efficiency levels at low temperatures. However, the dimensionless figure of merit values decreases severely at a temperature over 450 K.

The bulk $Bi_{1.9}Lu_{0.1}Te_3$ samples with diverse micro-grained particles were fabricated using cold isolated pressing (CIP) with annealing at high temperature and secondly by spark plasma sintering (at 653 and 683 K) by Yaprintsev et al. [67]. The maximum *ZT* ~0.9 for 450–500 K range of temperature range is obtained. The summary of recent *ZT* improvements of thermoelectric materials at low temperatures discussed in this study is presented below in Table 2.1.

Table 2.1 Summary of recent *ZT* improvements of TE materials at low temperatures

Researchers	Year	Thermoelectric Material	Method for properties enhancement	Impact on *ZT* Performance
Hu et al. [60]	2020	$Bi_{0.4}Sb_{1.6}Te_3$	Pre-mixing with NH_4HCO_3	• Max. Dimensionless figure of merit (ZT_{max}) of 1.11 at 343 K • 20% increment in ZT_{max} as compared with fully dense material
Adam et al. [61]	2020	Sb_2Te_3	Bi-containing	ZT_{max} value of 1.14 at 400 K for Sb_2Te_3

Madavali et al. [62]	2018	$(Bi_2Te_3)_x$ + $(Sb_2Te_3)_{1-x}$	Increasing Sb_2Te_3 content	• ZT_{max} value of 1.3 at 400 K • ZT_{max} value of 1.07 at 300 K
Banerjee et al. [63]	2018	Amorphous Silicon	Arsenic doping	ZT around ~0.64±0.13 at room temperature
Wang et al. [64]	2018	Cd_3As_2	Enhancement by the magnetic field	ZT_{max} value of 1.1 at 350 K
Yelgel and Srivastava [65]	2014	$Bi_2Se_3/Bi_2Te_3/Bi_2Se_3$ and $Sb_2Te_3/Bi_2Te_3/Sb_2Te_3$	By varying the well thickness.	ZT_{max}=0.97 at 350 K for $Bi_2Se_3/Bi_2Te_3/Bi_2Se_3$ and ZT_{max} =1.945 at 440 K for $Sb_2Te_3/Bi_2Te_3/Sb_2Te_3$
Paengson et al. [66]	2017	$CaMnO_3$	Bi doping and hot pressing of $CaMnO_3$	• ZT_{max} value of 0.065 at 473 K for $Ca_{0.97}Bi_{0.03}MnO_3$ • 95% increment in ZT_{max} as compared with un-doped material
Yaprintsev et al. [67]	2017	$Bi_{1.9}Lu_{0.1}Te_3$	Fabrication by cold isostatic pressing and SPS	ZT_{max} value ~ 0.9 for 450-500 K

Medium-temperature thermoelectric materials (500–900 K)

CuAgSe exhibits excellent potential due to its fantastic carrier mobility. It also has low thermal conductivity. To prepare monodisperse CuAgSe nanocrystals, a scalable colloidal synthesis has been reported by Zuo et al. [68]. The gathered powder test was

cleaned by a non-sulfur substance of $NaNH_2$. It was done to expel the organic ligands from the surface. After that, annealing process was also done. A 0.68 value of maximum *ZT* at 566 K was obtained. The obtained material shows the potential of TE applications for mid-range temperatures. The material before annealing exhibits a temperature- controlled transition from n-type toward p-type. This makes it suitable for thermal control transistor applications. $CoSb_3$ skutterudite is considered potential TE material for power generation. La Filler atoms are used to minimize lattice thermal conductivity for the skutterudite to get better TE performance [69], [70]. Bashir et al. [71] reported a high *ZT* value of 1.15 at 692 K with La and In as the $In_{0.3}La_{0.5}Co_4Sb_{12}$ skutterudite. BiCuSeO contains low thermal conductivity and an average power factor. BiCuSO was doped with Pb and effectively synthesized by high pressure by Zhu et al. [72]. BiCuSeO doped with Pb increases the carrier concentration. This Pb doping improves the power factor. The thermal conductivity is smothered by Pb doping. At 700 K temperature, the maximum *ZT* of 0.14 is achieved. Synthetisation with feasible high temperature and pressure techniques can increase the TE performance of Cu_2Se bulk materials. At 723 K, a high *ZT* value of 1.19 was reported for Cu_2Se synthesized at 3 GPa by Xue et al. [73]. Recently, GeTe and its derivatives have gained considerable attention as promising thermoelectric materials. Perumal et al. [74] reported a maximum *ZT* value of 2.1 for In and Bi co-doped GeTe at 723 K.

The synthesization of a group of TiNiSn-based alloys has been performed by Chen et al. [75]. It was done by way of an easy solid-state reaction followed by the SPS method. The amount and mixture of the heterogeneous phase were precisely managed, which results in a successful decrement of thermal conductivity (up to 2.3–3.0 $Wm^{-1}K^{-1}$). Besides, TE figure-of-merit was enhanced up to 0.49 at 750 K temperature. Silicon-Germanium based alloys are appealing. For radioisotope thermoelectric power generation at an excessive temperature (more than 1000°C), they offer a good choice of TE material. On the other side, Mesostructured $In_{0.25}Co_4Sb_{12}$ and $In_{0.25}Yb_{0.05}Co_4Sb_{12}$ samples have been synthesized by Benyahia et al. [76]. The samples were fabricated through melting and annealing. Then, the ball-milling procedure was applied to minimize size and sintered through the SPS method. With a mean grain size of 400 nm, a maximum dimensionless FOM of 1.4 at 750 K temperature is obtained. It was

achieved in the BM $In_{0.25}Co_4Sb_{12}$+0% CeO_2. TiNiSn-based half-Heusler (HH) alloys are widely studied. These TE materials show a high-temperature stabilization. However, the thermal conductivity is constantly enormously high, and hence, further *ZT* enhancement is difficult. SiC nanoparticles were brought into the matrix of $Pb_{0.98}Na_{0.02}Te$ doped with SrTe by Ai et al. [77]. The increased Seebeck coefficient and decreased electrical conductivity resulted in a remarkable peak *ZT* of 1.73 at 750 K.

Copper selenide is a promising TE material because of its fantastic electrical properties. A hydrothermal technique to incorporate astounding β-$Cu_2Se_{1-x}I_x$ nanopowder with a cost-effective minimum consumption of energy is reported by Wang et al. [78]. The nanopowder with different levels of doped iodine was used. Utilizing this straightforward and modest methodology, an improved *ZT* of 1.13 is obtained at a temperature of 773 K in iodine-doped Cu_2Se (x = 0.03) pellets after hot squeezing. Recently, the synthesis of p-type SiGe with Boron using varied proportion is reported by Murugasami et al.[79]. The material was sintered through the spark plasma sintering technique. Doped with $B_{1.5}$ at % synthesized SiGe alloy exhibit the enhanced *ZT* of 0.525 at 800°C temperature. A considerable improvement of approximately 9.38 % is obtained. Recently, the enhancement of Skutterudite performance is reported by Yang et al. [80]. Tellurium doped skutterudite has been shown to have promising TE properties using nano-micro level pores. Cobalt, antimony, and tellurium powders were utterly blended with a nominal composition of $Co_4Sb_{11.5}Te_{0.5}$. Then the material was stacked into carbon cauldrons and kept inside quartz tubes below vacuum for heating. The acquired ingots were ground into powders utilizing two successive methods, first by a mortar and then by ball milling below vacuum. The two powders (without ball milling and with ball milling) with different proportions were blended, and after that, sintered using spark plasma sintering technique. The annealing process below vacuum was also done on the obtained bulk material. The authors reported that annealed nano-particles carry some randomly allotted nano-pores with a range of sizes from 200 nm to 2 μm. The development of these nano-sized pores is due to strain during sintering. The thermal conductivity drops drastically which is a desired effect. A 1.2 value of the maximum dimensionless FOM is obtained for the annealed material at a temperature of 800 K. A significant increment of approx. 35% was reported. The thermoelectric

properties of n-type doped Mg_2 $(Si_{0.4}Sn_{0.6})_{1-y}$ Bi_y solid solutions solid solutions is investigated theoretically by Yelgel et al. [81]. From 300 K to 800 K temperature range, the selected y range is 0.005-0.06 for doping Bi with available experimental data. It was found that an appropriate y can increase *ZT*. The maximum *ZT* is obtained with y = 0.03 at 800 K and values 1.82.

The graphene nanoplate incorporated into Cu_2Se samples has been fabricated by Li et al. [82]. The ball milling technique was applied. Then, sintering through the SPS method was done. The homogeneous dispersion of the carbon phase reduced the Cu_2Se particles to form an excellent dense construction. Maximum *ZT* reached a high 1.7 value at 873 K. This gives an appropriate technique to use carbon engineering to maximize TE performance for Cu_2Se and family compounds.

The deliberate actuated dislocations and vacancies are compelling in diminishing the thermal conductivity of polycrystalline SnS, as reported by Asfandiyar et al. [83]. Low thermal conductivity and high electrical conductivity $Sn_{0.99}Ag_{0.005}S$ sample were obtained at 877 K. Ag doping bring high power factor, and an enhanced *ZT* of 1.1 at 877 K was recorded for $Sn_{0.99}Ag_{0.005}S$. N-type half-Heusler NbCoSn performs well in TE performance, but p-type performs poorly. Yan et al. [84] showed that by changing the Fermi level indicates that Sc is a suitable dopant. ZT_{max} value of 0.13 at 879 K has been reported.

The summary of recent *ZT* improvements of thermoelectric materials at medium temperatures discussed in present study is given below in Table 2.2.

Table 2.2 Summary of recent *ZT* improvements of TE materials at medium temperatures

Researchers	Year	Thermoelectric Material	Method for properties enhancement	Impact on *ZT* Performance
Zuo et al. [68]	2018	CuAgSe	Colloidal synthesis of monodisperse CuAgSe NCs	ZT_{max} value of 0.68 at 566 K

Bashir et al. [71]	2018	$CoSb_3$	La and In filling	ZT_{max} value of 1.15 at 692 K
Zhu et al. [72]	2018	BiCuSO	Doping with Pb	ZT_{max} value of 0.14 at 700 K
Xue et al. [73]	2019	Cu_2Se	Synthesis with High pressure	ZT_{max} value of 1.1 at 723 K
Perumal et al. [74]	2019	GeTe	In and Bi-doping	ZT_{max} value of 2.1 at 723 K
Chen et al. [75]	2017	TiNiSn-based half-Heusler (HH) alloys	Synthesis with solid-state reaction	ZT_{max} value of 0.49 at 750 K
Benyahia et al. [76]	2018	$In_{0.25}Co_4Sb_{12}$	Synthesis by a melting-annealing - ball-milling – SPS method	ZT_{max} value of 1.4 at 750 K
Ai et al. [77]	2020	PbTe	SiC dispersing and SrTe doping	ZT_{max} value of 1.73 at 750 K for $Pb_{0.98}Na_{0.02}Te$/ 4mol%SrTe composite
Wang et al. [78]	2019	Cu_2Se	Synthesis of Cu_2Se alloys doped with iodine	ZT_{max} value of 1.13 at 773 K for $Cu_2Se_{1-x}I_x$ (x=0.03)
Murugasami et al. [79]	2019	SiGe	Synthesis of SiGe alloys doped with Boron	ZT_{max} value of 0.525 at 800°C for doped with $B_{1.5}$
Yang et al. [80]	2019	Te-doped skutterudite ($Co_4Sb_{11.5}Te_{0.5}$)	Nano-microporous structure in $Co_4Sb_{11.5}Te_{0.5}$ materials via annealing the nano-$Co_4Sb_{11.5}Te_{0.5}$ / $Co_4Sb_{11.5}Te_{0.5}$ composites	• Max. Dimensionless figure of merit (ZT_{max}) of 1.2 at 800 K for annealed sample (N10-A100) • 33.7% increment in ZT_{max} as compared with dense material (N0)
Yelgel [81]	2016	$Mg_2Si_{0.4}Sn_{0.6}$	$Mg_2(Si_{0.4}Sn_{0.6})_{1-y}$ Bi solid solutions	ZT_{max} value of 1.82 at 800 K

Li et al. [82]	2018	Cu_2Se	By graphene nanoplate incorporation	ZT_{max} value of 1.7 at 873 K
Asfandiyar et al. [83]	2020	SnS	Intentional-induced dislocations and vacancies and Ag doping	ZT_{max} value of 1.1 at 877 K for $Sn_{0.99}Ag_{0.005}S$
Yan et al. [84]	2020	NbCoSn	Sc substitution at the Nb site	ZT_{max} value of 0.13 at 879 K

High-temperature thermoelectric materials (>900 K)

Lead selenide (PbSe) displays a temperature-dependent Seebeck coefficient, low thermal conductivity, and low electrical resistivity. Further, it has resolved the issue that emerges to get both n and p-type legs. A simultaneous advancement of thermal and electrical properties of p-type PbSe has been reported by Zhao et al.[85]. The density hypothesis for estimations of valence band energy levels was used. Between Lead selenide and nanostructures of $CdS_{1-x}Se_x/ZnS_{1-x}Se_x$, appropriate valence band alignments were introduced. A highly enhanced dimensionless figure of merit of 1.6 at 923 K was attained at $Pb_{0.98}Na_{0.02}Se$+3%Cds. Due to its high TE efficiency, Si-Ge alloys are considered valuable TE materials operating at high temperatures. The influence on TE properties of B-doped Si-Ge-Au nanocomposites was examined, taken as $Si_{65-x}Ge_{31}Au_4B_x$ by Muthusamy et al. [86]. At 973 K, a maximum *ZT* value of 1.63 was reported at x=3. The phonon-liquid electron-crystal concept for copper sulfide with reduced thermal conductivity and higher thermoelectric performance has been proposed by He et al. [87]. A high *ZT* value of 1.7 was reported at 1000 K by using copper deficiency as $Cu_{2-x}S$ with x=0.03.

Half-Heusler compounds are increasingly attracting attention because of their strong mechanical and electrical properties at high temperatures. At 1200 K, through heavier Hf doping the p-type FeNbSb heavy-band half-Heusler alloys with 1.5 value of high *ZT* was reported by Fu et al. [88]. $Yb_{14}ZnSb_{11}$ is considered for intermediate valence

interest. With rare earth (RE) solution as $Yb_{14-x}RE_xZnSb_{11}$ was investigated by Wille et al. [89]. The dimensionless FOM was reported as high as 0.7 at 1275 K with x=0.5.

The summary of recent *ZT* improvements of thermoelectric materials at high temperatures discussed in present study is given below in Table 2.3.

Table 2.3 Summary of recent *ZT* improvements of TE materials at high temperatures

Researchers	Year	Thermoelectric Material	Method for properties enhancement	Impact on *ZT* Performance
Zhao et al. [85]	2013	PbSe	Integration of band structure with hierarchical structuring	ZT_{max} value of 1.6 at 923 K
Muthusamy et al. [86]	2020	Si-Ge-Au	Boron Doping	ZT_{max} value of 1.63 at 973 K
He et al. [87]	2014	Cu_2S	Cu deficiency	ZT_{max} value of 1.7 at 1000 K
Fu et al. [88]	2015	FeNbSb	Hf doping	ZT_{max} value of 1.5 at 1200 K
Wille et al. [89]	2019	$Yb_{14}ZnSb_{11}$	Containing RE	ZT_{max} value of 0.7 at 1275 K

From this review, it can be highlighted that in the recent past, material researchers are successfully applying new approaches to upgrade the performance of available materials for a particular temperature range. A promising new approach is to create nano-level and macro-level pores in tellurium doped skutterudite to enhance *ZT* by approximately 35%. Another interesting approach is introducing a facile method for colloidal synthesis of copper-silver selenide. With ZT_{max} value of 0.68 at temperature 566 K, this resulted as a promising candidate for TE research in the intermediate temperature range. For greater commercialization of thermoelectric applications, improved materials with high values of *ZT* are required at prevailing operating temperatures. This will boost the manufacture of better performing TE modules.

2.4 Conclusion of the Literature Review

In recent years, thermoelectric coolers have been used extensively because of its light weight, environment friendly and solid state structure and other benefits. Despite the benefits of thermoelectric cooling devices, their low performance and high material costs have inhibited widespread adoption of the technology. As a result, rigorous research is being conducted on geometry, operating parameters and material optimization in order to improve the performance of thermoelectric coolers. Thermoelectric cooler performance optimization is a primary research goal. Various strategies are being used to improve the efficiency of thermoelectric materials. These advancements in *ZT* values could close the gap in performance between conventional bismuth-tellurium based materials and newer materials. However, the costs of candidate materials, costs to process those materials into TE elements, and cost to compensate the material loss are significant for the real commercial applications of newly invented materials. The non-availability of the requisite raw materials might result in holding the production of TE devices. Furthermore, TE materials have only been studied in terms of their efficiency to date, with no study into their lifecycle results. More extensive work on that would be useful. On the other side, for various applications of thermoelectric cooling technology, system level design optimization has been shown to be beneficial and significant. The study and understanding of the interaction within thermal, electric, and structural parameters is critical for revealing various physical characteristics and important to achieve performance enhancement.

2.4.1 Motivation of the work

It was apparent from the preceding sections that thermoelectric cooler is an important cooling device for a variety of applications. However, thermoelectric coolers have certain performance limitations. Such devices have a low cooling capacity, coefficient of performance and exergetic efficiency. There is a lot of scope for improvement with thermoelectric coolers. Many researchers are currently working to widen the demand for TEC devices' applicability. The most notable approach is to enhance TE material properties, since TE output is profoundly limited by the materials used. The second

method involves optimizing the device by using dimensional structural parameters as variables to obtain the best possible device performance for a given variety of materials. The third method is to optimize the device using operating parameters as variables in order to obtain the best possible performance. The key benefit of geometry and structure optimization is that the amount of material required for optimal performance can be minimized, resulting in increased efficiency and lower material costs. The optimization of input electric current is also an effective and feasible approach to enhance TEC performance. A simultaneous consideration of geometric and operating parameters can also be used to enhance TEC performance. It may assist in the precise design of a realistic TEC device.

2.5 Summary

In Chapter 2, thermoelectric concepts such as Seebeck effect, Peltier effect, Thomson effect and Joule effect are discussed. The relationship among various thermoelectric coefficients is presented. The basic information about thermoelectric coolers, their applications, advantages and drawbacks are also discussed. A state of art literature review to provide a summary of the base of knowledge already available involving thermoelectric coolers is presented. Numerous design and performance improvement of prior TEC systems, and significant works done in the context of numerous thermoelectric materials are also discussed.

CHAPTER 3

METHODOLOGY AND PILOT STUDY

CHAPTER 3

METHODOLOGY AND PILOT STUDY

3.1 Introduction

As described in the previous chapter, a lot of researches has been done to improve the performance of thermoelectric cooling system setups with different working solutions. In some studies, the performance of the TEC was investigated on the basis of geometry configurations while in some other studies, the research was carried out on the basis of operating parameters. Some analyses, available in the literature, also report about the usefulness of various thermoelectric materials as working solutions for application in cooling.

The study of thermoelectric cooling systems incorporating optimum values of design variables is timely in view of the demand for clean energy converters. To effectively simulate and design complicated thermoelectric cooling systems, examining the behavior of parameters is significant. It was pointed out in the previous chapter that a combination of geometric and operating parameters also has the potential to be used as performance optimization of thermoelectric coolers. A feasible approach to the problem of optimal design of TECs for cooling electronic/telecommunication components with both the geometric and operating variables is the basis of this work. The maximized cooling capacity and maximized *COP* are the important findings of the first part of this research work. In the second part, optimized TEC performance is obtained with energy and exergy point of view based on the first law and second law of thermodynamics. Modeling is often considered to be the definitive guide for gaining an insight into the device's principle of operation. The proper methodology is crucial to the success of any research aimed at finding the best design.

3.2 Methodology

The inferences are obtained from the analysis of published literature. From the inferences, the objectives are determined. Finally, from the objectives, a methodology is decided. The purpose of the research in this thesis is to analyze thermoelectric cooling system and model it for better performance optimization goals. The methodology adopted and followed in the implementation of this research work is as follows:

1) The theoretical model of a single-stage thermoelectric cooling system has been designed.
2) The geometric and operating parameters to be used as design variables have been identified.
3) Two different stochastic algorithms, namely genetic algorithm, and simulated annealing have been used for a pilot study on cooling capacity or rate of refrigeration based on a simplified model. The optimization results using these two algorithms have been compared and a suitable technique has been selected to proceed further.
4) The next objective was to use detailed mathematical models for performance optimization of TEC based on two criteria: General Cooling Performance Parameters (Cooling capacity and Coefficient of performance) and Energy based Performance Parameters (Energy Efficiency and Exergy efficiency). With the help of a suitable stochastic method, these parameters have been optimized. The optimization results have been analyzed.
5) A method for validation of optimization results was required. Three-dimensional finite-element models have been developed and the performances have been predicted using ANSYS@.

The investigation scheme for this research work is given in the flowchart as shown in Figure 3.1.

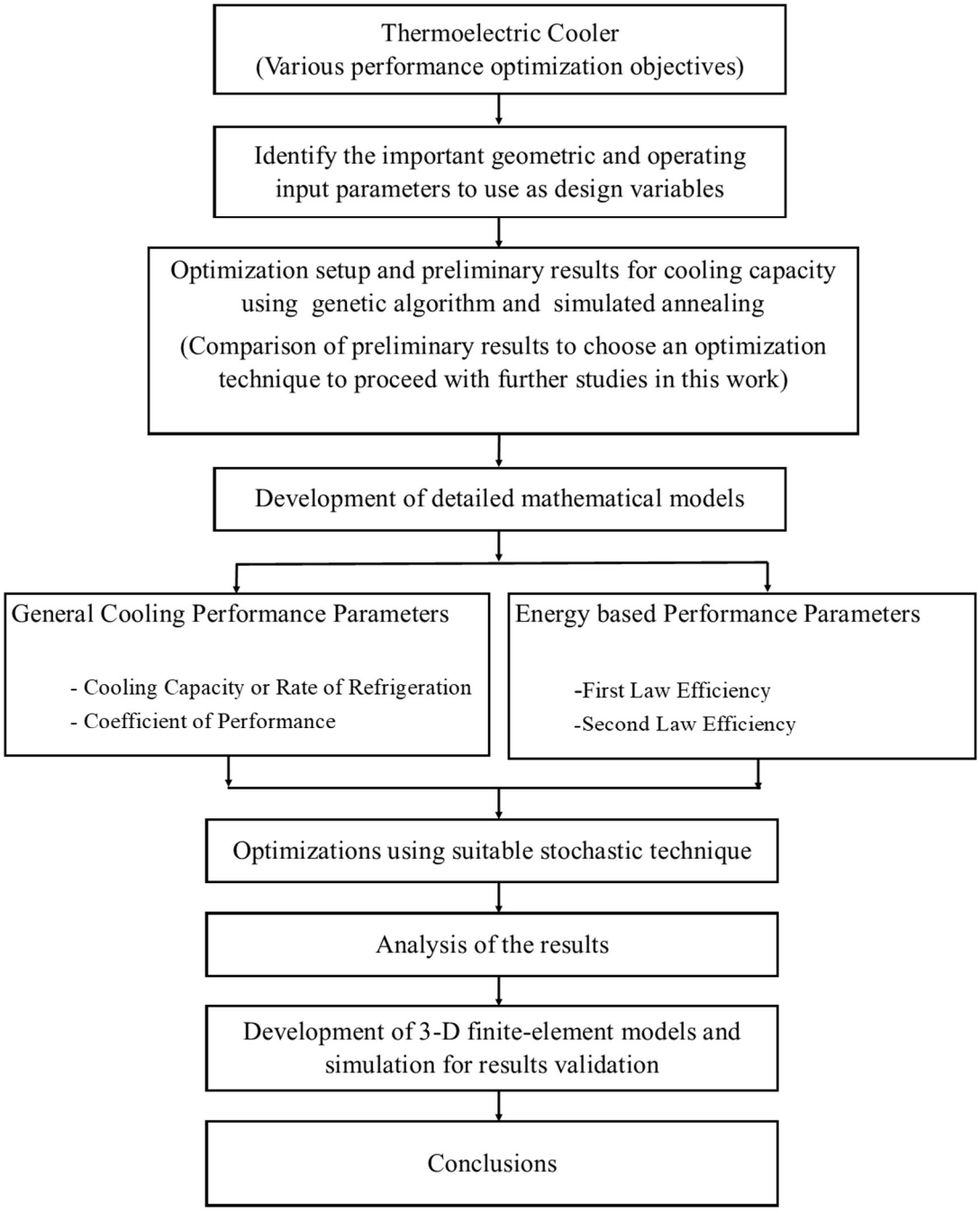

Figure 3.1 Scheme of investigation

3.3 Assumptions

To simplify the thermoelectric cooling system, the below-mentioned assumptions are made:

(i) The thermoelectric cooler is a single-stage module made of *N* thermoelectric couples that are identical and connected electrically in series and thermally parallel.
(ii) The n-type and p-type TE elements possess the same length and area of cross-section.
(iii) The electrical contact resistance is present.
(iv) Thomson effect is ignored.
(v) The numerical model of the thermoelectric cooler is for a steady-state system.
(vi) The basic assumption is that heat transfer occurs along the length of TE elements.
(vii) In the thermoelectric cooling system, heat transfer occurs at a finite rate. The electrical resistive losses are essentially irreversible and inevitable in nature.
(viii) In the three-dimensional finite-element simulations, the convection losses from the exposed surfaces are considered.

3.4 Description of TEC Model

Figure 3.2 depicts a single-stage thermoelectric cooler schematic. The TEC system comprises the following major parts:

(1) One thermoelectric cooling module
(2) Cold and hot side material
(3) External hot side heat sink

On the cold side of the junctions, an electrically shielded and thermally conductive ceramic material is in thermal contact with a heat source. On the hot side of the junctions, it is connected with a heat sink. To form an electrical circuit inside the thermoelectric module, an electrically conductive material is alternately connected to

the cold and hot sides. Copper is a strong conductor of both electricity and heat. Heat is dissipated to the ambient atmosphere via the external hot side heat exchanger.

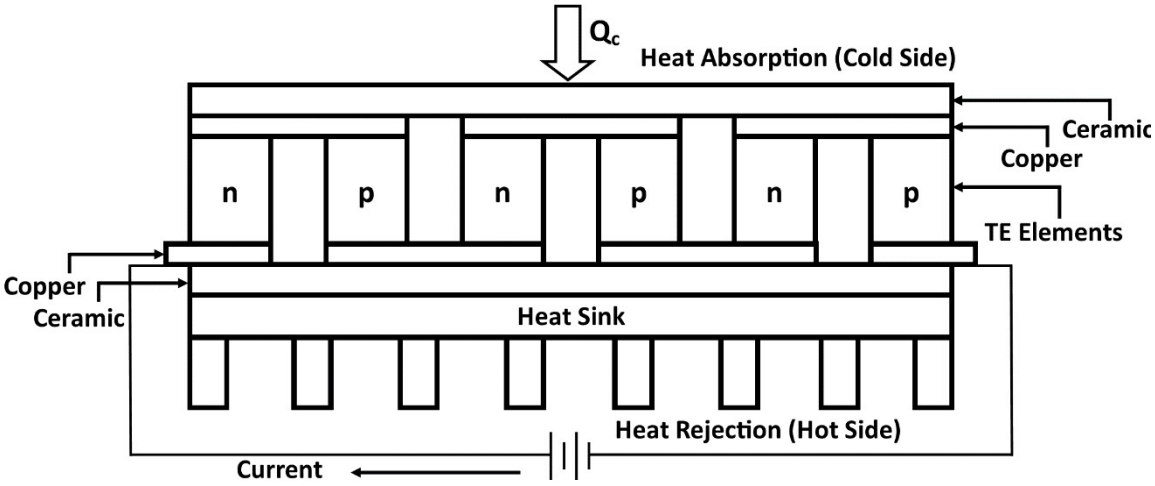

Figure 3.2 Schematic of the single-stage TEC

Optimized performance management of a thermoelectric cooler can be challenging. Over the past few years, thermoelectric cooling technology has been a major interest among researchers. TEC is bringing significant advantages with outstanding potential. We aim to work on ameliorating the performance of the thermoelectric cooler by considering a practical or realistic model approach. Many of the approaches have not been able to incorporate various realistic issues so far and are only correct if a variety of assumptions are made. As the assumptions made in such models are not realistic, they often give erroneous results. In this presented work, various effects and issues are taken into consideration that have not been paid attention to in the previous work.

3.4.1 Electrical contact resistance

The numerous losses such as electrical contact resistance, thermal resistance, and heat losses are not included in the modelling equations. The issue is that the multiple losses, which are generally unexplained, are very difficult to account for. The electrical contact resistance can cause the extreme reduction in the performance of a thermoelectric cooler among all adverse factors. At the interfaces of n-type and p-type thermoelectric materials and metal connecting layers, the electrical contact resistance (r_c) is considered

in this work for practical consideration. Engineering experts reveal the fact that when manufacturing defects occur, electrical contact resistance can increase significantly. With a reduction in the value of thermoelectric elements' length, the effect of electrical contact resistance gradually increases. The effect of electrical contact resistance on the performance of thermoelectric coolers becomes significant when the TE elements-metal connecting layer is comparable with the height of TE elements.

Owing to a limited calculated value, direct measurement of electrical contact electrical resistance experiences significant difficulties. The literature data for electrical contact resistance shows its variation from 1×10^{-8} Ω m^2 to 1×10^{-12} Ω m^2 [90], [91]. In addition to energy losses and the increase in TEC dimensions, the existence of electrical contact resistance can also contribute to a substantial reduction in an obtainable temperature drop. The greater value of electrical contact resistance leads to a significant increase in the input power. The electric contact resistance should be considered to obtain the realistic model equations of TEC.

3.4.2 Thermal resistance

In several practical applications, a key factor in the deterioration of the TEC performance is thermal resistance. It is worth noticing that practically all the heat flow does not take place within the TE elements only. The thermal resistance may be divided into three major categories: thermal resistance in between the thermoelectric module and the actual heat source, the thermoelectric module itself, and between the thermoelectric module and sink.

Ceramic substrates that serve as the thermoelectric module's electrical insulators induce some thermal resistance. Conducting strips also cause certain thermal resistance. An increment in the thermal resistance will result caused due to the processing technology and the connection mode between the heat/cold source and the thermoelectric module. When the electric power is supplied to a thermoelectric cooling module, one side becomes cold and the other side is heated.

The heat flows from the cold side to the hot side according to thermodynamics laws. There can be a significant temperature change over their length, even though solid

copper conductors are being used to disperse the heat flux. The use of a heat sink offers a solution to this problem. The hot side of the thermoelectric cooler must be connected to a proper heat sink. The heat sink dissipates the heat pumped by the system and the heat created due to the Joule effect. The heat sink is the essential element of a TEC system. TEC operating characteristics are related to the temperature of the heat sink and hence, its importance to the system performance should be emphasized. The efficiency of the heat sink is generally characterized in terms of thermal resistance.

3.4.3 Packaging density

Packaging density refers to the occupied area (in percentage) of n-type and p-type TE elements with reference to the total area of the thermoelectric cooler. One of the remarkable characteristics of the thermoelectric cooling module is the high packaging density of thermocouples. Many advances in the performance of thermoelectric cooling technology are possible by improving the packaging density of TE elements.

The packaging density of TE legs can vary from 25% to 90% [92]–[94]. The conventional method of manufacturing limits the shape, size, and packaging density of thermoelectric elements. Advanced manufacturing techniques such as lithographic patterning and laser additive manufacturing enable high packaging density. The packaging density is also related to the ability of effective transfer of heat.

3.4.4 Space restriction

Thermoelectric coolers are available in a range of sizes and for numerous applications. However, thermoelectric coolers are suitable for applications with tight constraints of geometric space. A custom assembly can also be specified to meet unique space constraints or requirements for the environment. Thermoelectric coolers are widely used in telecommunications, medical, space, optoelectronics, aerospace, military equipment for cooling, being light in weight and small in size.

Practically, in general, thermoelectric coolers are available from 3.0 mm × 3.0 mm in size. However, the smallest size as per manufacturer's catalogue is 1.0 mm × 1.0 mm.

In order to maximize efficiency and performance for the application area, TEC embedded into the assembly can be customized.

3.4.5 Interface temperatures

The important task of the numerical optimization for better performance of thermoelectric cooling is to know exact values of the hot side, cold side, and intermediate temperatures of the device. Knowing temperature precisely is always preferred for design efforts. It is important to note that designing an appropriate TEC for any application depends on getting their critical values.

It is important that the relevant electrical and thermal parameters be incorporated into design process. Parameters such as space restriction and packaging density deserve to be included as well.

3.5 Optimization Methodologies

3.5.1 Introduction

Optimization is a technique that aims at finding the best alternatives available. The alternatives available are termed feasible solutions. The procedure for determining their quality involves a numerical function. This numerical function is called the objective function. An optimal solution is a viable solution that yields the best (maximum or minimum) value of the objective function. To define the objective function, the heuristic is to include only elements that can be reasonably calculated and controlled via design decisions.

The word heuristic implies that it utilizes human experience that is intuitive or proven. The design variables may be an integer or real or a combination of both. It depends on the nature of the problem. The problem can either be unconstrained or constrained. The objective function and constraints can be linear or non-linear. Based on the function properties, the optimization problems could also be convex or non-convex, differentiable or non-differentiable.

In an optimization process, there are some fundamental steps involved:

1. To specify the objective function.
2. To indicate whether we want to maximize or minimize.
3. To specify the design variable set.
4. To relate the design variables to the objective function.
5. To define constraint equations.
6. To specify the method of solution for the optimization problem. This is termed as optimization approach or algorithm.
7. To execute the procedure and converge to solution(s).

3.5.2 Classification of optimization problems

It is difficult to furnish the taxonomy of optimization. However, it may be understood in these important manners.

Continuous Optimization and Discrete Optimization

Some models make sense only if the variables start taking values from some kind of a discrete set, often a subgroup of integers, while other models have variables that can accept any real value. Discrete optimization problems are models with discrete variables; continuous optimization problems are models with continuous variables. The objective of a discrete optimization problem is to find an object from a countable set that is an integer, permutation, or graph. However, upgradation in algorithms combined with advancements in computational technology have significantly increased the size and scope of discrete optimization problems that can be efficiently solved. In discrete optimization, continuous optimization algorithms are significant since a sequence of continuous sub problems is generated by many discrete optimization algorithms.

Unconstrained Optimization and Constrained Optimization

Another major distinction is between optimization problems in which the variables have no limit constraints and optimization problems in which variables have lower and upper limit constraints. Constraints that impose lower or upper limits on design

variables are inequality constraints by nature. Sometimes we provide equality constraints. In several practical applications, unconstrained optimization problems appear directly. They often appear in the reformulation of problems of constrained optimization. The constraints are removed in the objective function by applying a penalty term in the reformulated problems. Problems of constrained optimization emerge from applications in which the variables are explicitly constrained. The constraints on the design variables can differ widely. The constraints can be simple limits or bounds. The constraints can also be a set of equalities and inequalities which make the more complex relationship of the variables. It is possible to further classify constrained optimization problems based on the nature of the constraints (such as non-linear, linear, convex) and also based on the class of the functions (such as differentiable or non-differentiable).

Single or Multi-Objective Optimization

Most problems in optimization are having a single objective function. In the single objective optimization problem, the main goal is to determine the best possible solution corresponding to the maximum or minimum value of a single objective function. There are also cases of optimization problems having multiple objective functions. These problems involve two or more objective functions which are to be maximized or minimized. Multi-objective optimization problems are found in many areas, such as engineering, logistics, and economics. The aim of multi-objective optimization problems is to find a set of optimal solutions. This set of optimal solutions defines the best trade-off between two or more competing or conflicting objectives. For example, designing a new component might require weight minimization while maximizing strength. As another example, maximizing the expected rate of return and minimizing the risk could be involved in selecting a portfolio. In practice, multi-objective problems are often restructured as single-objective problems. This can be done by creating a weighted combination of various objectives. This can also be done by replacing a few of the objectives with constraints.

3.5.3 Optimization methods

The optimization problem can be solved by an approximate method or an exact method, depending on the complexity of the optimization problem. Exact methods produce optimal solutions and ensure their optimality. However, they are considered to be time-consuming and are not used for large problems. Approximate (or heuristic) techniques produce high-quality solutions for practical use in a reasonable period of time. However, there is no guarantee of determining an optimum global solution. There are two sub-categories of algorithms in the category of approximate methods: approximation and heuristic. Approximation algorithms give provable solution quality. They give provable run-time bounds. To determine worst-case bounds is the goal of designing the approximation algorithm. The analysis of approximation algorithms offers more understanding of the complexity of the problem and can assist in the design of effective heuristics. The approximation algorithms, however, are problem-dependent. Their applicability is limited by this feature. Besides, achievable approximations are too far from the optimal global solution in practice. This makes these algorithms not very practical for many real applications. Heuristic algorithms provide good solutions in large-scale cases of problems. They allow achieving satisfactory performance at affordable costs for a wide variety of problems. In general, there is no approximation guarantee for heuristics on the solutions obtained.

Most real-world problems in search and optimization include complexities such as nonlinearities, non-convexity, discontinuities, multiple disciplines, mixed types of variables, and large dimensionality. A combination of such complexities makes classical algorithms inefficient, inapplicable, or impractical. There are no established mathematically inspired algorithms to find the optimal solution within a limited computational time for all such problems. Thus, search and optimization algorithms are typically developed by using certain heuristics to solve such problems for practicality. The term heuristic, which originated in Greek, means ‘to discover’. A heuristic approach is a rule-of-thumb technique that does not guarantee optimality and convergence. However, they work well in most cases and deliver solutions with acceptable quality. In optimization, the use of a heuristic approach is not new.

Heuristics, however, have been developed in the past based on the principle of either conventional optimization methods or traditional techniques of artificial intelligence. Nowadays, genetics, neuroscience, physics, and other sciences also inspire heuristics.

Heuristic algorithms may be categorized into two families: metaheuristics and specific heuristics. Specific heuristics are customized and built to solve a particular problem and/or case. Metaheuristics are algorithms for general purposes that can be used to solve almost any problem of optimization. The term Meta means 'higher level'. In the context of resolving search and optimization kinds of problems, a metaheuristic approach is especially important and relevant. It defines a technique that utilizes one or more than one heuristics. It inherits all the necessary properties.

A metaheuristic technique:-

(a) instead of specifically attempting to determine the exact optimum solution, attempts to determine a near-optimal solution
(b) normally has no rigorous evidence of convergence to the optimum solution
(c) is generally computationally quick than exhaustive search.

These techniques are iterative in nature. In their search method, these techniques often use stochastic operations to modify initial candidate solutions (one or more). Usually, the random sampling of the design search space is used to generate the initial candidate solutions. Several real-world problems are complicated due to inherent practicalities. Algorithms for classical optimization can not always be applicable. They may not be fairly good in pragmatically resolving such problems. Researchers and practitioners have pursued metaheuristic methods without disregarding the significance of classical algorithms in the progress of the search and optimization field. Instead of awaiting for a provable technique to be established, a near-optimal solution can be attained for such problems. In the recent past, the key reason for the success of metaheuristic techniques is the ability to deal with different complexities of the problems and to provide a fairly acceptable solution.

3.5.4 Deterministic and stochastic algorithms

The methods for optimization can differ significantly from one to another. For varied categories of optimization problems, we often use different optimization methods. There can be no unified approach. In general, algorithms for optimization are divided into two broad categories:

(i) Deterministic algorithms

(ii) Stochastic algorithms

The deterministic algorithm is the algorithm in which output is uniquely defined. A deterministic algorithm is the algorithm that follows a fixed set of steps. The deterministic algorithm would always achieves the same result. A rigorous method is followed by deterministic algorithms. The path and values are repeatable. This repeatability exists for both design variables and the functions. During reruns, the algorithm operates in precisely the same way. In deterministic optimization, the data for the given problem is presumed to be accurately known. However, for many real problems, for a number of reasons, the data cannot be precisely known. Deterministic algorithms could have some poor inputs and computing could go to the worst-case runtime. The deterministic algorithm obtains solution with reasonable computation time. However, these algorithms often struggle to have any solution for complicated problems and their usefulness declines as discontinuities or non-convexity exist. Few examples of deterministic algorithms are Simplex method, Newton-Raphson method, Hooke-Jeeves pattern search method and Nelder-Mead downhill simplex method. A stochastic algorithm is the algorithm that is non-deterministic and depends on probabilistic practices. The algorithm's behaviour is not completely determined by the input. In stochastic algorithm, randomness is inherent to maximize or minimize an objective function. A stochastic algorithm is a random search, alongwith hints by a selected heuristics (or meta-heuristics) to direct the next potential solution to evaluate. During reruns, the algorithm can operate differently. The convexity in unimodal functions ensures that the final solution is also the global optimum. However, a local optimum is possible in case of multimodal functions. Randomness with certain variations can help to avoid local optima and improve the possibility of reaching a

global optimum. Few popular examples of stochastic algorithms are genetic algorithm, simulated annealing, particle swarm optimization and ant colony optimization.

3.6 Genetic Algorithm

The Genetic algorithm (GA), introduced by John Holland and his team at the University of Michigan, is a population based search and optimization technique [95]. GA is a stochastic method and applies the evolutionary concepts found in nature. The development of this approach was inspired by the two main principles of natural evolution: natural selection and genetic dynamics. In natural genetics, the basic objective is the preservation of the fit genes and remove of the redundant. New generations are created by changing the genetic code. Genetic algorithm mimics the evolutionary processes such as selection, crossover and mutation. GA is able to deal with many complex optimization problems.

3.6.1 Basic procedure of the genetic algorithm

The genetic algorithm is a stochastic global search technique. GA begins with a population of potential solutions [96], [97]. Each individual in the population is referred to as a chromosome. A randomly selected assortment of chromosomes serves as the initial population. The term chromosome corresponds to a numerical value or values that indicate a candidate solution to the problem. In a chromosome, each setting is called a gene. The representations used in the genetic algorithm are binary alphabets, integers or real numbers. In the population, each chromosome is evaluated and a fitness value is assigned to indicate how good the solution is. The term' fitness' is taken from the theory of evolution. Fitness evaluation is performed by an objective function. The objective function characterizes the performance of individual in the problem domain. As the algorithm advances, it is expected that the individual fitness and total fitness (population) will increase.

After the total population has been tested, the following steps are used to create a new population:-

(i) Selection

From the current population, we need to choose two parent chromosomes based on their fitness. The objective function serves the basis to choose pairs of individuals. The better the fitness value, the more likely the particular chromosome will be chosen. Selection methods, such as roulette wheel selection, rank-based selection, tournament selection, elitism selection, niching selection, steady state selection and Boltzmann selection have been considered as operators. Elitism, in particular, ensures that the best chromosomes from each generation would pass to the next generation without change.

(ii) Crossover

If a pair of chromosomes has been chosen, crossover to produce offspring will take place. Crossover combines the elements of the two parent chromosomes to produce two offspring. The two offspring replace the parents chromosomes. With a certain crossover probability cross-over the parents. This is done by exchanging their encodings to form offspring with characteristics taken from both parent chromosomes. A crossover probability of 1.0 implies that all the chromosomes selected for reproduction are used. This means that there are no survivors. Empirical studies, however, have shown that better outcomes are obtained with a crossover probability in between 0.65 and 0.85.

(iii) Mutation

Another genetic operator, mutation introduces variability into the gene pool by randomly modifying genes. With no mutation, offspring chromosomes will be restricted to genes present within the initial population. With a probability of mutation, mutate new offspring at every locus which represents position in chromosome.

All the above-mentioned steps must be repeated till a new population of chromosomes (of the same size as that of previous population) has been created. Each new population is termed a generation. A further iteration of the algorithm uses the new generated population. In the current population, each of the chromosomes is evaluated by using fitness function. This evaluation is done in the same manner as the initial population

was done. As all possible settings are not being tried, to decide when to stop, termination criteria need to be defined. Typically, these criteria take the form of a maximum number of generations. At the end, the chromosomes having best fitness is retained and applied to return the best settings. When the termination criterion is met, the single best program of the population generated during the run is harvested. This is considered as the result of the run. If the run is successful, the result could be a solution (or approximate solution) to the problem. A flow chart of simple genetic algorithm is shown in Figure 3.3.

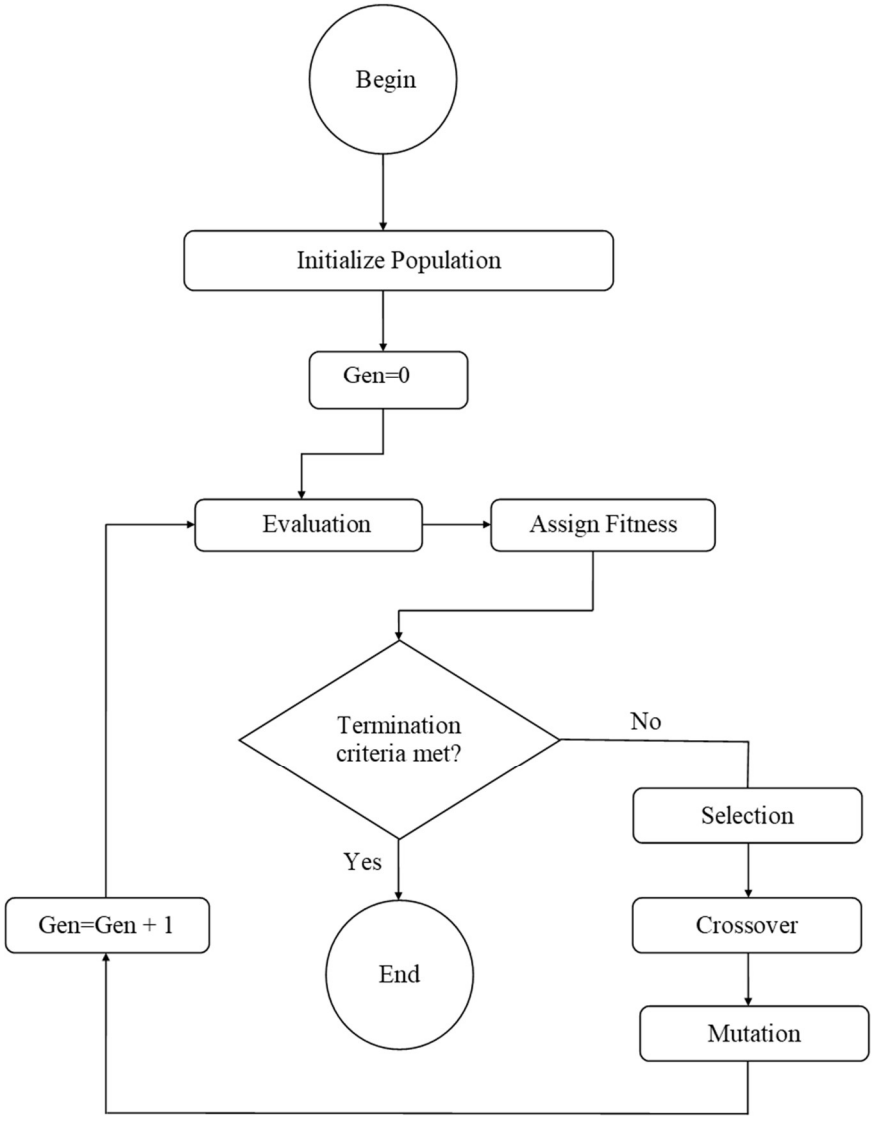

Figure 3.3 Flow Chart of a simple genetic algorithm

3.6.2 Encoding of chromosomes

The chromosome should contain information about the solution which it serves in some way. The first step in solving the problem is encoding of chromosomes, which is highly dependent on the problem. Binary encoding, value encoding, permutation encoding, and tree encoding are examples of encoding methods. In binary encoding chromosomes are a string of bits, 0 or 1. In the chromosome, each position represents a specific characteristics of the problem. Each chromosome is a string of values when value encoding is used. Value encoding is used when complex values, such as real numbers, are present and binary encoding is inadequate. Every chromosome in permutation encoding is a string of numbers that represents the number in a sequence. Any chromosome is a tree of certain objects in tree encoding, such as functions or commands in programming language.

3.7 Simulated Annealing

Simulated annealing (SA) is a heuristic-based algorithm that allows for the search for a solution to a given problem. Annealing is a well-known thermal process of heating up a solid and then cooling it slowly until it crystallizes. At high temperatures, atoms of the material possess high energies. In the molten state at high temperature, atoms are able to move freely. As cooling proceeds, the atoms begins to get ordered. The annealing process improve the quality of a solid and obtains low energy state of the solid. If the initial temperature is too low or cooling process is insufficiently slow, the system can become quenched, forming defects or stuck in a state of local minimum energy (metastable states). Simulated annealing is based on the same principle. The idea of SA is based on a paper by Metropolis et al. [98] and developed by Kirkpatrick, Gelatt and Vecchi [99]. Simulated annealing starts at a very high temperature, with the input values being given a broad range of variation. Temperature is permitted to fall as the algorithm progresses. This limits the degree that can be allowed in the inputs to vary. This often leads to a better solution for the algorithm in a similar manner as the annealing process improves the crystal structure of a metal. As the temperature decreases, changes occur at the inputs, leading to successively better solutions. With a certain probability, this algorithm also allows to accept worse solutions to avoid chance

of being stuck in a local minimum. However, the control parameters (e.g. initial temperature, rate of cooling etc.) of the algorithm should be defined from empirical basis to maximize the performance.

3.7.1 Basic procedure of the simulated annealing

Simulated annealing is a stochastic search and optimization technique. SA may be used to determine the objective function's minimum value. In general, SA starts with an initial state and a high temperature. The state of the system is considered at energy E. By the analogy of thermodynamic system, energy E is the function which is to be minimized. At a state i, the energy level is considered as E_i. At a fixed temperature T, by small perturbation, a subsequent state j is generated randomly. Assume E_j as the energy level at state j.

If $E_j \leq E_i$: State j will be accepted right away

In other words, supposing minimization problem, if the new solution has smaller value of the objective function compared to that of old solution, the new solution is accepted.

If $E_j > E_i$: State j will be accepted with the probability using Boltzmann distribution factor, i.e. $e^{-\frac{E_j - E_i}{k_B T}}$ (k_B= Boltzmann constant, T= Temperature)

At temperature T, the system gradually achieves thermal equilibrium. When equilibrium is achieved, temperature T can be decreased. This process is repeated several times until the termination criteria is met. In the algorithm, temperature, T is the control parameter and it must be defined carefully.

The initial temperature, the iterations to be performed at each temperature and at each step, how much does the temperature drop as the cooling proceeds are important considerations for this algorithm. Each solution is associated with a particular state of the system and optimal solution is associated with ground state. A flow chart of simulated annealing process is shown in Figure 3.4.

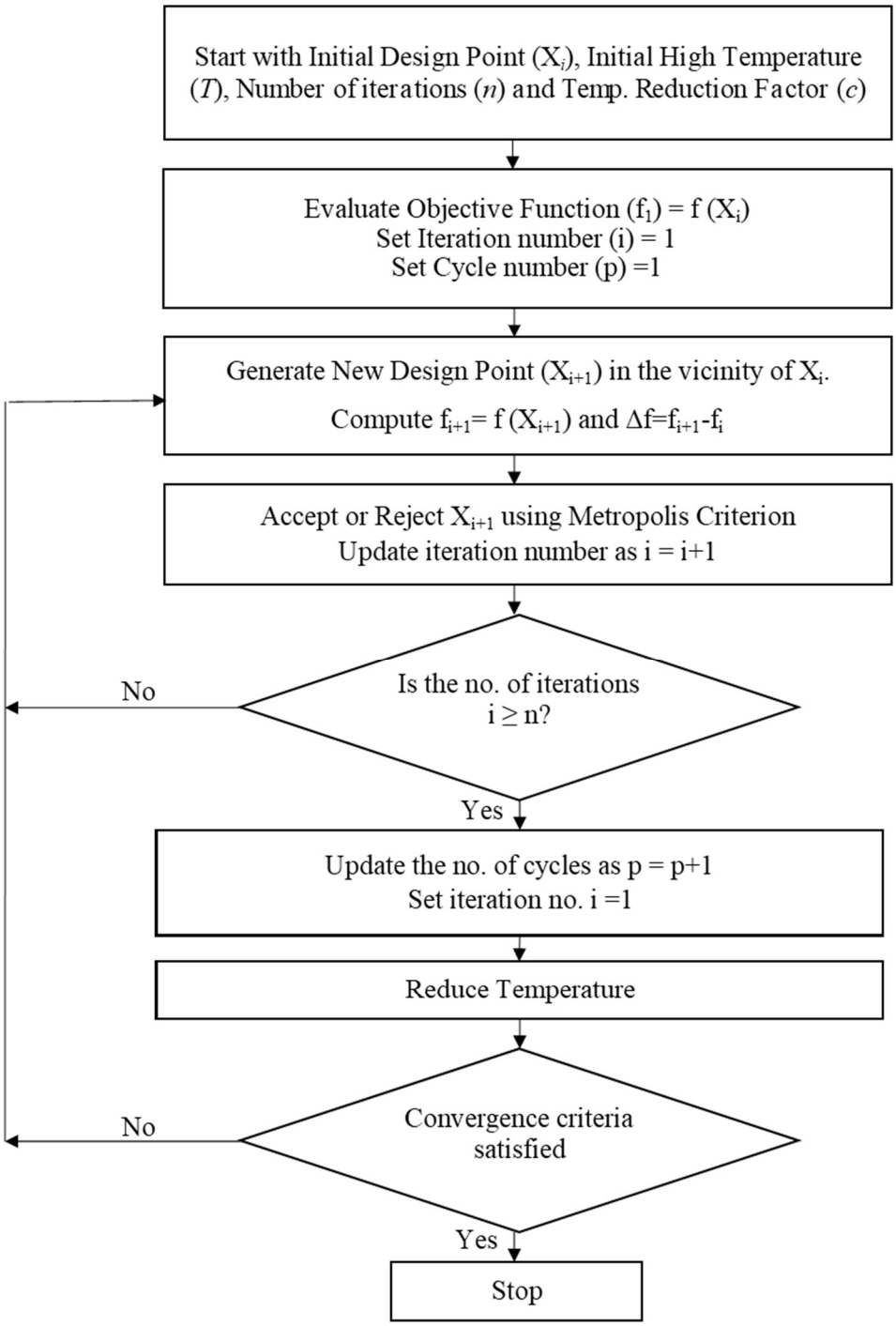

Figure 3.4 Flow Chart of a simulated annealing

3.7.2 Important SA parameters

The terms in simulated annealing have a relationship with that of physical annealing as described in Table 3.1.

Table 3.1 Relationship between simulated annealing and physical annealing

Simulated Annealing	Physical Annealing
Objective function	Energy
Feasible Solutions	System States
Neighbouring Solutions	Change of State
Optimal Solution	Frozen State
Control parameter	Temperature

The choice of certain parameters are important in simulated annealing. The initial temperature is important parameter. Initial temperature must be sufficiently high to allow easy exchange of solutions in the neighbourhood. Otherwise, the final solution may be close or same to the starting solution. However, if the initial temperature is quite high, almost all changes will be accepted. On the other side if initial temperature is too low, acceptance will be rare and will lead to limited diversity of the solution.

Another important parameter in SA is the maximum iterations (n) to be performed at each temperature. Iterations may be fixed or varied in number. The number of iterations is increased at lower temperatures to explore local minima. Final temperature is also crucial. It is normal to allow the temperature to drop to zero. However, it is not necessary because the chances of accepting a worse step will be the same as the temperature approaches zero. A suitable low temperature or the system being "frozen" at the current temperature may also be used as stopping conditions. The temperature reduction factor (c) is also important parameter. Naturally, the higher the value of temperature reduction factor, the longer it will take to get the temperature down to the stopping point.

3.8 Pilot Optimization Study

There are many complexities to perform real-world optimization. It is well recognized that no single method or algorithm works best on all or even a wide range of optimization problems. Some techniques work only for discrete or continuous variables

but not for both kinds. Some methods work for a very small number of design variables. Some techniques require a reasonably significant number of evaluations to be carried out in order to determine an optimal solution. . In order to select the best technique for a given optimization problem, one should first know the nature of the design space being searched. The vastness of the design search space is governed by the number and bounds of the design variables.

Stochastic optimization methods have been rapidly increasing in popularity over the past decade or two, with a variety of techniques. These techniques are becoming "industry standard" methods for solving complex optimization problems. There are lots of stochastic algorithms available to choose from. Understanding any specific algorithm requires some time. After formulating an appropriate mathematical model of a specific type of problem, we try out a solver and observe whether the optimized solutions are satisfactory. Stochastic algorithms are the specialized algorithms whose designs are capable of exploiting the specific structure of the problem.

The pilot study step of this work has specific purpose that is to select a stochastic optimization technique to proceed for further research in this work. Genetic algorithm and simulated annealing are popular stochastic algorithms for global optimization problems. They are popular and commonly used in actually solving engineering optimization problems due to their good ability to solve problems. The global optimized solution to the problem can be found by randomly searching in GA and SA. However, there are some limitations in every algorithm which is in practice. In this pilot study, GA and SA results for the same performance optimization of TEC problem are compared and checked for their relative performances.

3.8.1 Description of the TEC system and constituents of the methodology

Figure 3.5 depicts the physical model of a single-stage thermoelectric cooler. One thermoelectric module, cold and hot side material, and an external hot side heat sink are included. The investigation starts with the established phenomenological relationships in the literature. The Peltier effect allows thermoelectric cooling to take place. A temperature difference is generated when DC current flows through a number

of pairs of p-type and n-type thermoelectric elements connected electrically in series and thermally in parallel [4], [100].

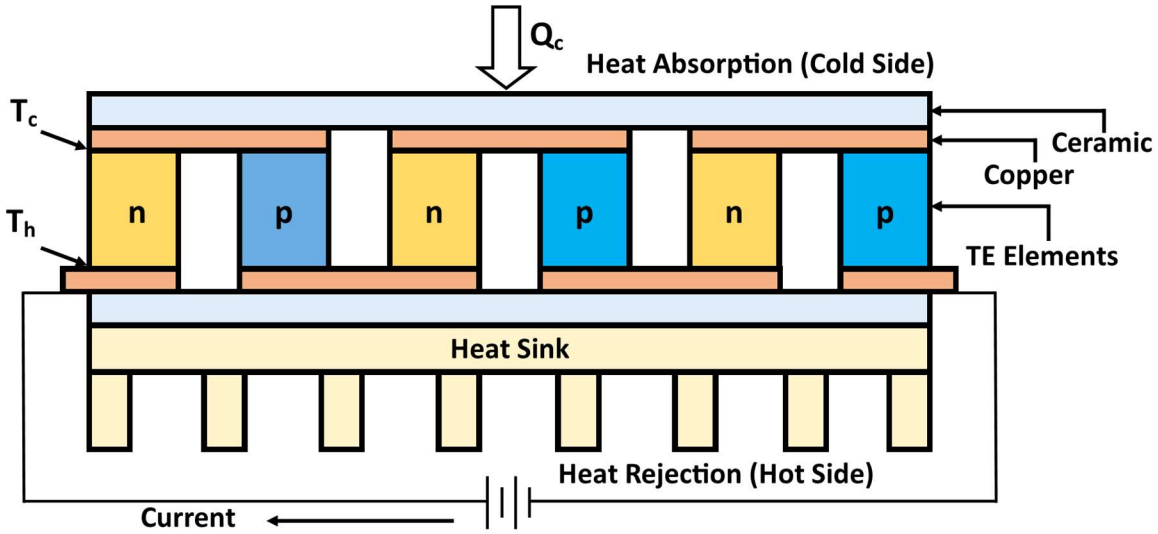

Figure 3.5 Single-stage TEC

Thermal conduction is taking place from the hot side of the TEC to the cold side. Current flow in thermoelectric materials produces Joule heat, which will be produced as well. Half of the Joule heat emitted will be distributed to each side of the module. The heat source on the cold side of the junctions and the heat sink on the hot side of the junctions are in thermal contact with a thermally conductive and electrically insulated substance. As shown in Figure 3.5, the electrically conductive material is alternately connected to the hot and cold sides of the thermoelectric cooling module to establish an electrical circuit. Heat is dissipated to the ambient environment via the external hot side heat exchanger.

The heat balance equations at the TEC module's two junctions are as follows:-

$$Q_c = 2N\left[I\alpha T_c - \frac{kA(T_h - T_c)}{L} - \frac{1}{2}I^2\left(\frac{\rho L}{A} + 2\frac{r_c}{A}\right)\right] \qquad (3.1)$$

$$Q_h = 2N\left[I\alpha T_h - \frac{kA(T_h - T_c)}{L} + \frac{1}{2}I^2\left(\frac{\rho L}{A} + 2\frac{r_c}{A}\right)\right] \quad (3.2)$$

Where Q_h is the rate of heat rejection from the hot junction. Q_c is the rate of heat absorption at the cold junction, which is generally referred to as the cooling power or rate of refrigeration (*ROR*). The Seebeck coefficient (α), electrical resistivity (ρ), thermal conductivity (k), and electrical contact resistance (r_c) are all thermoelectric material properties. The cold and hot junction temperatures, respectively, are T_c and T_h, and the length and cross-sectional area of p-type and n-type TE elements are L and A. The electric current in the TEC module is I, and the total number of thermoelectric couples is N. Heat flows $\frac{1}{2} I^2 (\rho L/A + 2r_c/A)$ and $kA(T_h - T_c)/L$ describes to Joule heat and thermal conduction, respectively. At the hot junction, $I\alpha T_h$ is the Peltier heat. Similarly, at the cold junction, $I\alpha T_c$ shows the Peltier heat.

Bismuth telluride is the material for the thermoelectric elements used in this study. The average of the hot and cold side temperatures (T_{ave}) is used to determine the properties of thermoelectric material. Melcor Corporation provided the equations for this temperature range as specified by Fraisse et al. [23] and described as follows:

$$\alpha = (22224 + 930.6\,T_{ave} - 0.9905\,T_{ave}^2) \times 10^{-9} \quad (3.3)$$

$$\rho = (5112 + 163.4\,T_{ave} + 0.6279\,T_{ave}^2) \times 10^{-10} \quad (3.4)$$

$$k = (62605 - 277.7\,T_{ave} + 0.4131\,T_{ave}^2) \times 10^{-4} \quad (3.5)$$

The thermal resistance of the hot side heat sink is considered in this study in order to address its effect on the estimation of temperature at the hot junction. The system's performance will satisfy the equation below.

$$T_h = Q_h \times R_{th} + T_a \quad (3.6)$$

Where R_{th} refers to the thermal resistance of heat exchanger (at hot side) and T_a refers to the ambient temperature.

3.8.2 Description of the pilot optimization problem

The cooling capacity or rate of refrigeration of a single stage TEC is examined in order to evaluate device's performance. Since space in electronic devices is limited, the TEC must be designed as compacted as feasible. The area of cross-section of the restricted space (*S*) is set to 25 mm^2 in this study. Additionally, the maximum length of TE elements is restricted, limiting the total amount of space available. The design variables for the optimization process are the length of p-type and n-type elements (*L*), area of cross-section of TE elements (*A*), number of thermoelectric couples (*N*) in TEC, and input electric current (*I*). The objective now is to determine the values of *L*, *A*, *N*, and *I* in order to obtain the best output, i.e., maximum cooling capacity or *ROR* for the thermoelectric cooling system in restricted space.

The optimization of cooling capacity or *ROR* of TEC is presented as the single objective constrained optimization problem as described in equation (3.7).

$$\left.\begin{array}{ll} Maximize & ROR \\ subject\ to & \\ & I_{min} \le I \le I_{max} \\ & L_{min} \le L \le L_{max} \\ & A_{min} \le A \le A_{max} \\ & N_{min} \le N \le N_{max} \end{array}\right\} \quad (3.7)$$

At hot side heat exchanger, the thermal resistance is set as 0.1°C/W. The *ROR* is reduced and the hot-side temperature is raised as the thermal resistance of the hot side heat exchanger increases. The electrical contact resistance of $1x10^{-8}$ Ω-m^2 is another fixed design parameter. The temperature at the cold junction is set as 293.15 K. The ambient temperature is assumed as 298.15 K. Because of realistic manufacturing constraints, the packaging density is set at 80%. According to real-world applications, the four design variables may vary within some ranges. The length of TE elements may vary from 0.5 mm to 1.5 mm. The cross-sectional area of TE elements may vary within a range of 0.25-1.0 mm^2. The total space is limited to 25 mm^2 x 1.5 mm = 37.5 mm^3 due to the available area of cross-section (*S*) and the upper limit of length. The number of thermocouples (*N*) is a dependent variable, as its value is determined by the

thermoelectric cooler's available cross-sectional area and the cross-sectional area of the TE components. The number of thermocouples is rounded down to the nearest integer using equation (3.8).

$$N = \frac{S \times packaging\ density}{2 \times A} \tag{3.8}$$

With 25 mm^2 of the available cross-sectional area of the restricted space and a packaging density of 0.8, the number of thermocouples in this work will range from 10 to 40. The electric current can vary from 0.1 A to 3.0 A. The hot side temperature (T_h) is initially set to a guessed value in order to measure material properties using equations (3.3), (3.4), and (3.5). (3.5). The new value of T_h is calculated using equations (3.1), (3.2), and (3.6). This difference between the guessed and new value of T_h is used to iteratively change the guess value of T_h until the difference is negligible. To solve this optimization problem, we used genetic algorithm and simulated annealing as optimization techniques in this analysis.

3.8.3 Optimization and results using GA

For this single objective optimization, Deb and Agarwal's real-variable genetic algorithm with the SBX operator is used [101]. The algorithm is developed in the C programming language [102]. Genetic algorithm needs a population of data points to be analyzed over several generations to reach at an optimum solution. Table 3.2 shows genetic algorithm parameters, used in the single-objective optimization of cooling capacity or rate of refrigeration. Since GA is stochastic, the simulation was run five times and the best one is reported.

Table 3.2 Parameters Settings for GA

Population size	20
Termination Criteria	1000 generations
Mutation probability	0.25
Crossover probability	0.80
Number of runs	5

With genetic algorithm, the search process is completed rapidly. Figure 3.6 shows the best run's optimization history in terms of the optimized average *ROR* for the entire population by generation number. The optimal values of *I*, *L,* and *A* are found as 2.360 A, 0.542 mm, and 1.0 mm^2 respectively. The optimal number of thermoelectric couples is 10. With these optimal values of design variables, the genetic algorithm achieved the best *ROR* of 1.144869 W. The optimal length of TE elements is found as 0.542 mm. It establishes that it is specific while maximizing *ROR*. It does not meet any of the permitted range's variable bounds of 0.5-1.5 mm. The optimum cross-sectional area of TE elements was 1.0 mm^2, which was the upper variable bound. Therefore, it emphasizes the importance of exploring the upper bound of the TE element's permissible cross-sectional area range.

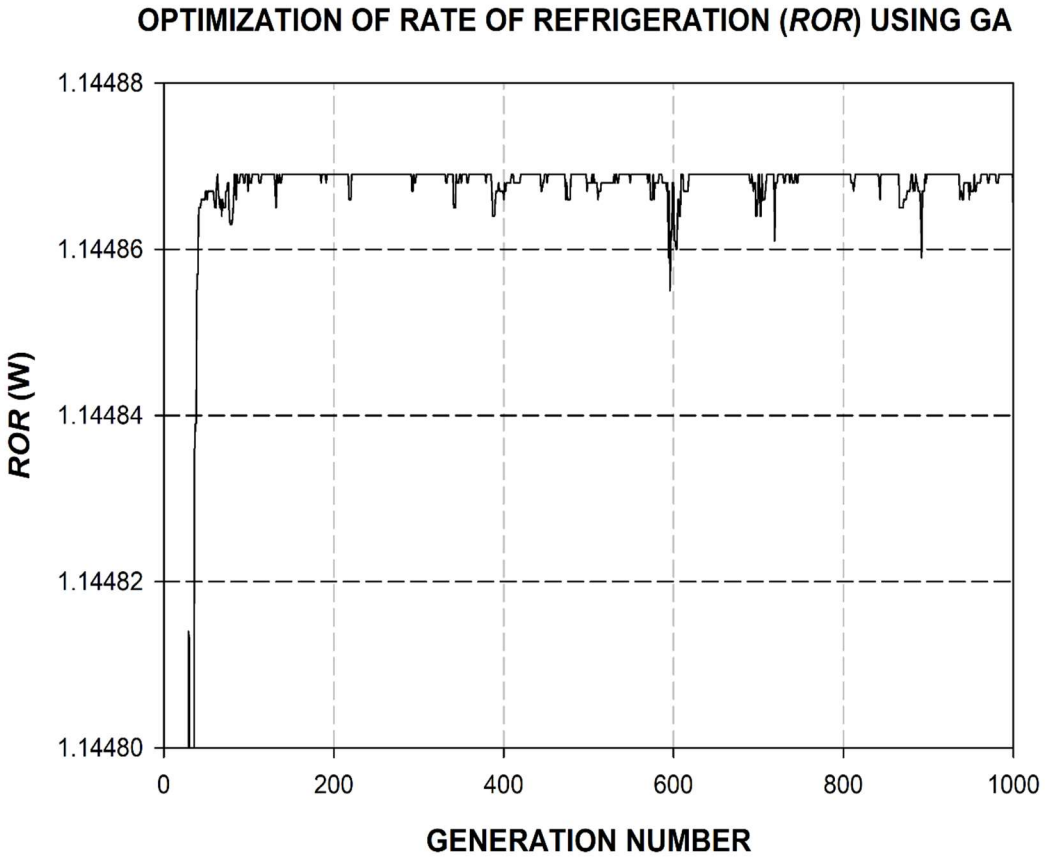

Figure 3.6 GA convergence curve of optimized *ROR*

This simulation was run several times with different settings to see whether multiple optima in the search space were possible. The current optimization problem has three distinct optima with the same *ROR* values, as discovered. As a result, this is a multimodal function optimization problem.

Table 3.3 shows the optimum parameters for these captured peaks. Optima-1, Optima-2, and Optima-3 are the three captured peaks of the objective function. If these optimum solution vectors as mentioned in Table 3.3 are focused, in all three cases, the optimum length of thermoelectric elements '*L*' is found to be 0.542 mm.

Table 3.3 GA optimization results

S. No.	*I* (A)	*L* (mm)	*A* (mm^2)	*N*	Optimized *ROR* (Watts)	Label
1	2.360	0.542	1.0	10	1.144869	Optima -1
2	1.180	0.542	0.5	20	1.144869	Optima-2
3	0.944	0.542	0.4	25	1.144869	Optima-3

3.8.4 Optimization and results using SA

Another robust stochastic algorithm, simulated annealing, is used to check these optimization results and the searchability of genetic algorithm. Simulated annealing is a global optimization technique that uses a random search procedure. It is similar to the annealing process and use for solving a problem related to optimization. This process practices the careful control of cooling rate and temperature that controls the search. Initially, the temperature parameter is set to a high value. Before reducing the temperature at each instance until the convergence conditions are met, a number of iterations are conducted. Xin-She Yang [103] developed the simulated annealing source code, which is robust for MATLAB® and can handle non-linear constraints. It was used in this research. The simulation was performed using a range of different SA settings. Table 3.4 lists SA parameters with best-obtained performance, applied to maximize *ROR*.

Table 3.4 Parameters Settings for SA

Number of iterations per temperature level	500
Initial Temperature	1.0
Final Temperature	$1e^{-10}$
Boltzmann Constant	1
Cooling Factor	0.8

SA captured the maximum *ROR* as 1.144869 watts. The Optimum *ROR* captured by SA is 1.144869 watts. The solution vector is identical to Optima-1 of GA results. This simulation was run multiple times with various settings, but SA was only able to capture one best peak, as mentioned in Table 3.5. The optimized value of *ROR* and corresponding optimal design parameters are doubly ensured by these identical GA and SA performance.

Table 3.5 SA optimization results

S. No.	*I* (A)	*L* (mm)	*A* (mm^2)	*N*	Optimized *ROR* (Watts)	Label
1	2.360	0.542	1.0	10	1.144869	Optima -1

In the mathematical model used in this analysis, *ROR* is defined as a function of *I*, *L*, *A*, and *N*. The independent design variables are *I*, *L*, and *A*, while *N* is a dependent design variable since it is defined by the value of *A* and the equation (3.8). The optimal value of *L* in all results of GA and SA simulations is found as 0.542 mm. Though *ROR* has three different variables, i.e. *I*, *L,* and *A*. If *L* is fixed at 0.542 mm as found in all solutions for this problem, *ROR* can be represented with *I* and *A* in a 3D plot. Hence, a three-dimensional plot is created using equation (3.1) and *L* is set to 0.542 mm, as illustrated in Figure 3.7. The X-axis, Y-axis, and Z-axis are used to represent the parameters *I*, *A*, and *ROR*, respectively. Following that, three GA-discovered optima

are superimposed, as listed in Table 3.3. In the same order as reported in Table 3.3, these are labeled as Optima-1, Optima-2, and Optima-3. According to Table 3.3 and Table 3.5, Optima-1 is discovered by GA and SA, but Optima-2 and Optima-3 are discovered only by GA. The combined selection of the geometric structural parameters and electric current used as design variables in this study provides a guide to future research. Designers can handle space restriction for the case at hand and improve *ROR*.

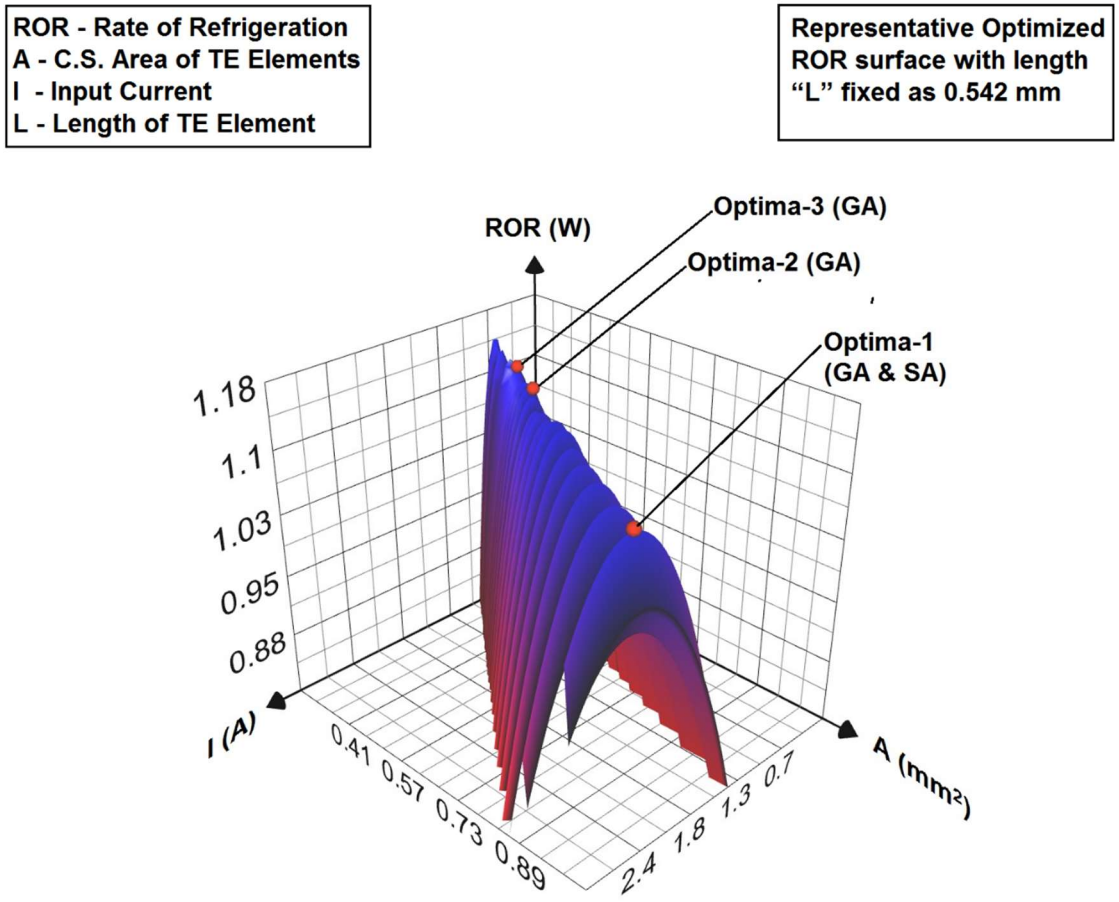

Figure 3.7 Multiple optima labelled at the *ROR* surface with thermoelectric element length L = 0.542 mm

3.8.5 Comparison of the pilot optimization results

Using genetic algorithm and simulated annealing, this work attempted to determine the optimum design parameters for improving a critical performance indicator (*ROR*) of a thermoelectric cooler. This study has shown that the geometric structural parameters of the TE elements and the input current affect the *ROR* of TEC. These parameters can be adjusted to improve the performance of thermoelectric cooler. The *ROR* of a TEC was successfully optimized in this work within the restricted space of 37.5 mm^3.

The optimum *ROR* in all solution vectors is 1.144869 W. Genetic algorithm has discovered each of the three possible optima. Thus, it can handle this multimodal optimization problem. Though the simulation was performed several times with different settings, simulated annealing was unable to locate multiple optima. Thus, the conspicuous observation of genetic algorithm and simulated annealing findings in the present multimodal optimization problem is that GA search outperformed SA and discovered multiple optima.

3.9 Summary

In this chapter, the description of the thermoelectric cooling system model is presented. The important characteristics are discussed which are crucial to understand the practical TEC system. The standard equations are far away from that of real thermoelectric cooling systems. The described effects are used to predict the optimized performance in the later part of this study. Recognizing the theoretical boundaries of any area of research involves clear analysis of continuously applied assumptions. The major assumptions are highlighted which are used later according to the need of the objective. The methodology used to perform this research is described. An overview of optimization methodologies is presented. The basic descriptions of two stochastic algorithms, namely genetic algorithm and simulated annealing are given which are used for this study. There are many complexities to perform real-world optimization. It is well recognized that no single method and checked for steady and satisfactory optimization performance. A pilot study was conducted to find a suitable algorithm for this type of optimization problem from a set of two stochastic algorithms. This pilot

study was conducted for the optimization of rate of refrigeration and a certain configuration of TEC system was used. Using GA and SA, this pilot optimization study attempted to determine the best design parameters for improving a critical performance measure (*ROR*) of TEC. In the said analysis, the GA outperformed the SA search. On the basis of pilot study, GA has been selected to proceed for the performance optimization of TEC system for further research in this work.

CHAPTER 4

OPTIMIZATION OF THE COOLING CAPACITY OF THERMOELECTRIC COOLER

CHAPTER 4

OPTIMIZATION OF THE COOLING CAPACITY OF THERMOELECTRIC COOLER

4.1 Introduction

Thermoelectric energy conversion technique has tried to be a pioneer in green technologies. J.Peltier discovered the Peltier effect, which is a well-known term and is at the core of a thermoelectric cooler (TEC). Thermoelectric cooler is a low-maintenance solid-state system that do not need any moving parts or refrigerants. Unlike conventional refrigerator or cooler systems, TEC does not contain unfavourable chlorofluorocarbons (CFCs). An input current of electricity flows through n-type and p-type TE elements in thermoelectric coolers, generating a temperature gradient. Thermoelectric coolers of small size have applications in laser, optical, and radio-electronic instruments. Noiseless operation, Modular design, low maintenance, and high reliability open up new thermoelectric cooling application possibilities [2], [104]–[106].

Thermoelectric cooling is environmentally friendly, making it a viable option for future cooling. However, compared to compressor-based systems, thermoelectric coolers have a restricted range of applications. The reasons are their low cooling power or rate of refrigeration (*ROR*). Some researchers have previously devoted to the development of newer semiconductor materials with a high value of figure of merit. However, a comparable refrigeration rate has yet to be reached. Hence, achieving the maximum possible cooling power or *ROR* with the available semiconductor materials is a challenge. Furthermore, the key challenge in increasing thermoelectric cooler market penetration is to increase cooling capacity within available space.

4.1.1 Description of the main TEC model

The schematic diagram in Figure 4.1 illustrates a basic single-stage TEC design. Multiple thermoelectric (TE) elements are used to construct a thermoelectric cooling device. Electrically, these TE elements are connected in series. Interconnecting p-type and n-type TE elements is achieved with copper tabs. Between two ceramic substrates (thermally conducting), this array arrangement is sandwiched. The exploded view of a practical TEC device is depicted in Figure 4.2. A thermocouple is the basic physical unit of a thermoelectric cooler's physical model. A thermocouple is the pair of semiconductor p-type and n-type dissimilar elements. The TE elements pair count can be from few to hundreds, depending on the design. On the one side, TEC has a high manufacturing cost, and on the other side, many TE products are expensive. In addition, predicting the temperatures at interfaces are very difficult. Hence, the performance prediction of the thermoelectric cooling system (with heat sink) is also complicated. Furthermore, the thermal resistances in the ceramic substrates, copper conductors, and heat sink contribute to the overall heat flow resistance in the thermoelectric cooling system. The performance optimization problem is difficult to solve because of these challenges. The effects of thermal resistance as well as electrical contact resistance are considered in this research. The effects of Joule heating and thermal conduction are also taken into account. A thermal-resistance model has been created for this research study to make the analysis of thermal resistances easier. To develop more realistic thermoelectric cooler model, this model contains thermal resistances of ceramic substrates, copper parts, and hot side heat sink. Figure 4.3 illustrates a pair of semiconductor p-type and n-type TE elements. The model of thermal resistance developed for this study is also demonstrated.

Using heat flow as an electrical analogy to the model of thermal resistance as shown in Figure 4.3 (b), the temperatures at the TEC's hot and cold surfaces can be expressed as:

$$T_h = Q_h(R_{hs} + R_{cr} + R_{cu}) + T_a \tag{4.1}$$

$$T_c = T_{co} - Q_c(R_{cr} + R_{cu}) \tag{4.2}$$

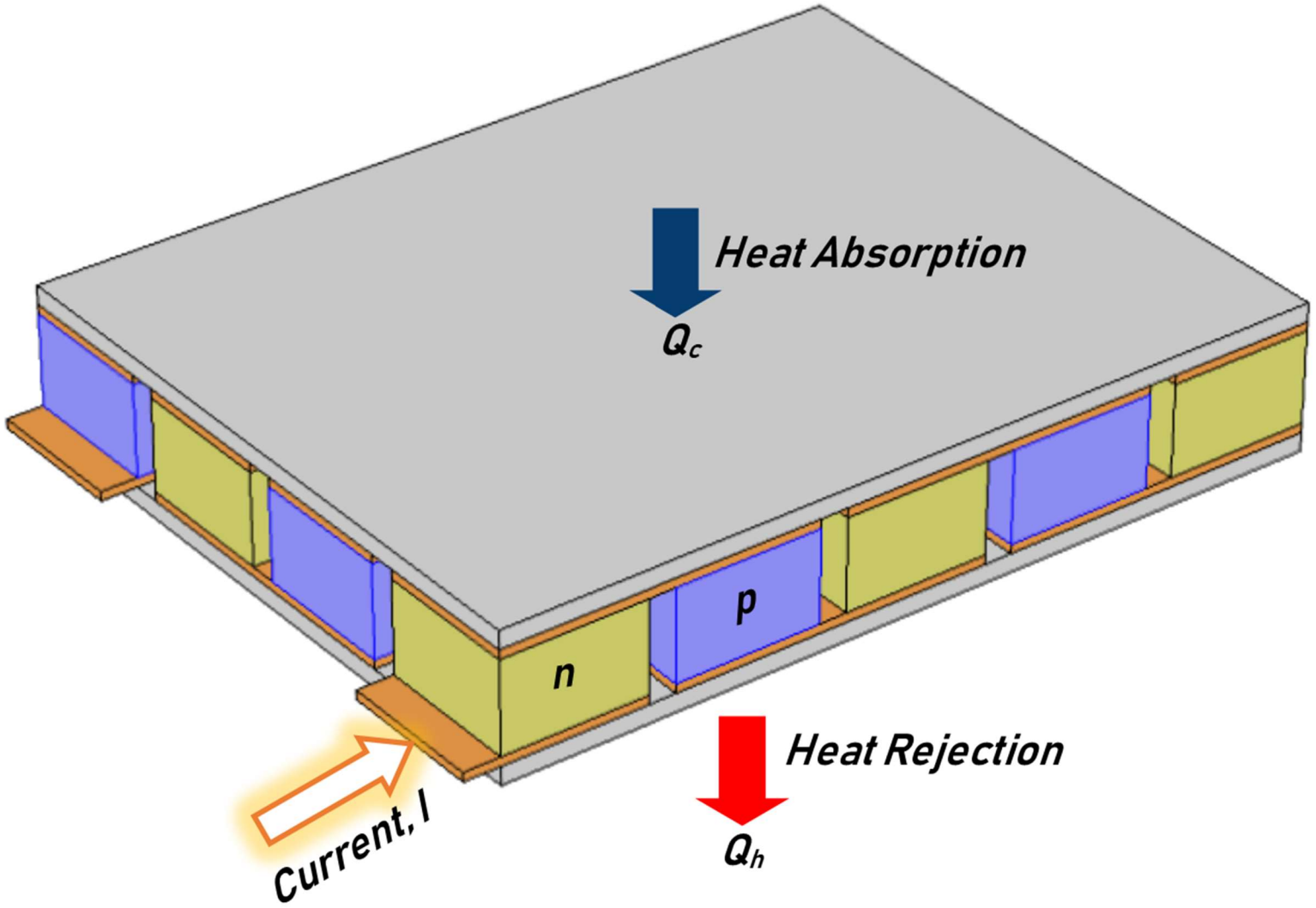

Figure 4.1 Single-stage thermoelectric cooler [107]

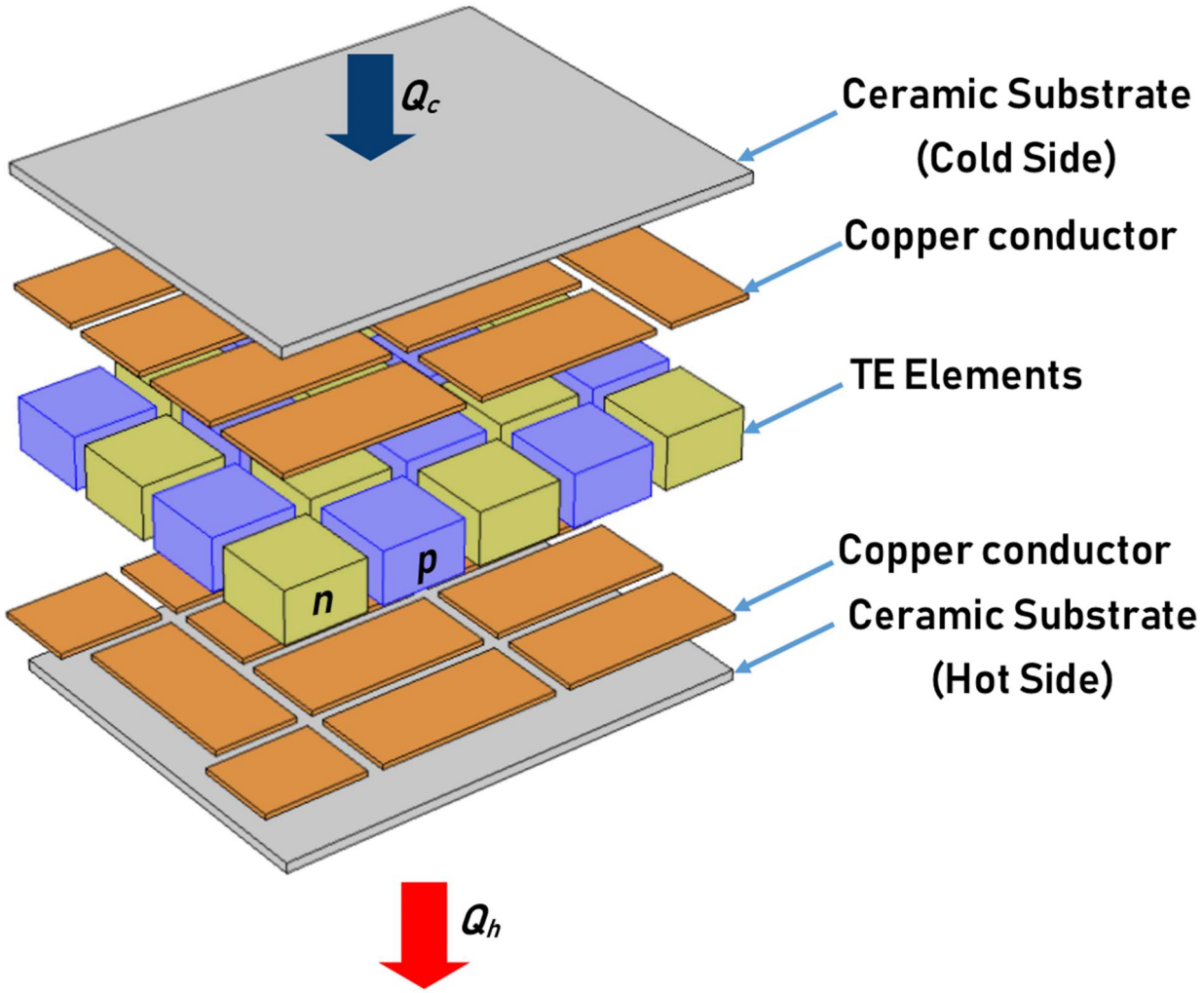

Figure 4.2 Exploded view of thermoelectric cooler [107]

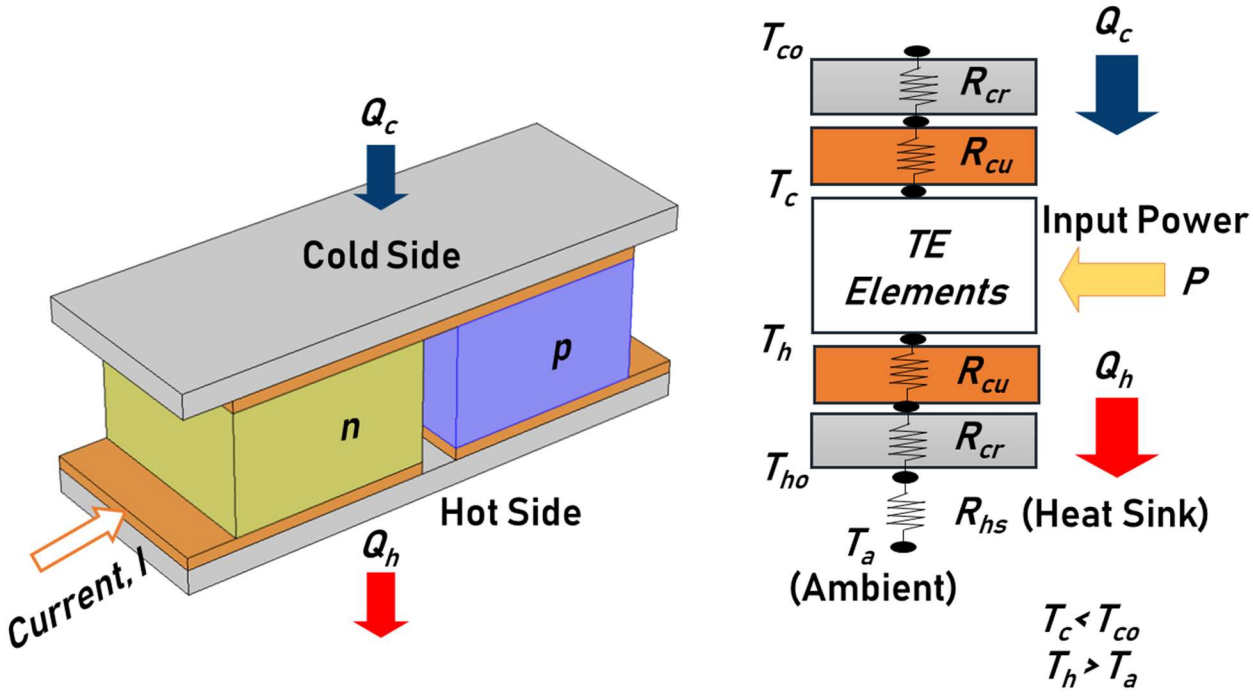

(a) (b)

Figure 4.3 (a) Thermoelectric couple (b) Thermal resistance model [107]

Where T_c and T_h denote the temperatures on the cold and hot sides of semiconductor p-type and n-type dissimilar elements, respectively. Q_h denotes the rate at which heat is rejected from the hot side. Q_c is the rate at which heat is absorbed on the cold side, which is commonly known as the cooling capacity. T_{ho} and T_{co} denote the temperatures at the thermoelectric cooler's hot and cold surfaces, respectively. R_{hs} denotes the thermal resistance of the hot side heat sink in thermoelectric cooling system, R_{cr} denotes the thermal resistance of the ceramics, and R_{cu} denotes the thermal resistance of the copper parts. T_a denotes the ambient temperature.

A few reasonable assumptions are taken into account in this study.

(a) Heat transfer is taking place along the length of TE elements.

(b) The cross-section and length of the thermoelectric elements are similar.

(c) Thomson effect is not taken into account.

(d) Steady-state condition is prevailing.

The circuit of dissimilar semiconductors has a constant electric current flowing through it. Heat is moved to one of TEC's two sides. As a result, one side becomes cool while the other becomes

hot. Heat is dissipated to the ambient environment by a heat sink connected to the hot side ceramic substrate. Depending on which way the electric current flows, a thermoelectric couple provides cooling or heating. Equation (3.1) and equation (3.2) represent the heat energy balance on the cold and hot sides of the thermoelectric cooler. T_c and T_h denotes the temperature at the interface of TE elements and copper tabs at the cold and hot sides, respectively, and are used for the same relation in each of the work's referred equations.

The choice of thermoelectric materials has a direct impact on TEC performance. The TE element's material properties are temperature-dependent. The thermoelectric material bismuth telluride (Bi_2Te_3) is a commonly used thermoelectric material in thermoelectric coolers. The material properties of Bi_2Te_3 that were used in this work, according to Fraisse et al. [23] are described in equations (3.3), (3.4) and (3.5).

4.2 Optimization Problem

Researchers have been exploring the possibility of using solid-state thermoelectric (TE) technology as a potential green energy conversion system. A thermoelectric cooler is used to cool various electronic devices where space constraints are very common. Hence, it is vital to think about TEC performance optimization with space constraints. The mathematical formulation of the single-objective optimization problem for maximizing the cooling power of TEC is as follows:

$$\begin{cases} Maximize\ Q_c \\ Subject\ to \\ \quad I_{\min} \le I \le I_{\max} \\ \quad L_{\min} \le L \le L_{\max} \\ \quad A_{\min} \le A \le A_{\max} \\ \quad \left(\dfrac{2A \times N}{PD}\right) \le S \end{cases} \tag{4.3}$$

The number of thermoelectric couples (N) is an integer design variable. The value of N is calculated using equation (3.8) and is rounded down to the nearest integer. S is the available cross-sectional area of the restricted space wherein the TEC is placed. PD denotes the packaging density and A is the cross-sectional area of thermoelectric elements.

The optimization problem, as stated in equation (4.3), was solved by employing some unique parameter values. The values for the properties and parameters used in this work are mentioned in Table 4.1.

Table 4.1 Values of parameters and properties

Description	Parameter	Value
Ambient temperature	T_a	298.15 K or 25℃
Cold surface temperature	T_{co}	293.15 K or 20℃
Heat sink thermal resistance	R_{hs}	0.10 ^{0}C/W
Electrical contact resistance	r_c	1 x 10^{-8} Ω m^2
Available cross-sectional area of the restricted space	S	225 mm^2
Packaging density	PD	80%
Ceramic thermal conductivity	k_{cr}	35.3 W/ m-°C
Copper thermal conductivity	k_{cu}	386 W/ m-°C

Lower and upper bounds constrain the design variables in the current analysis. From a practical standpoint, the length and cross-sectional area of p-type and n-type TE elements have been set to 1.0-2.0 mm and 1.0-2.0 mm^2, respectively. 0.1-3.0 A has been chosen as the input electric current range. The dependent variable N will range between 45 and 90 as equation (3.8) governs its value. The design variables used in this optimization process have lower and upper bounds, as shown in Table 4.2.

Table 4.2 Bounds of the design variables

Variable	Lower limit	Upper limit
Length of TE elements, mm	1.0	2.0
C.S. area of TE elements, mm^2	1.0	2.0
Electric current, A	0.1	3.0
Number of thermoelectric couples (dependent variable)	45	90

Copper tabs and ceramic substrates have thicknesses of 0.1 mm and 0.2 mm, respectively. The surface area of the ceramic substrates on both the cold and hot sides is equal to the size of the thermoelectric cooler. The copper tab's total surface area is 90% of the size of the thermoelectric cooler on either side. R_{cu} and R_{cr} are calculated as 0.001279345 °C/W and 0.025181 °C/W, respectively. All such values are based on catalogues from thermoelectric coolers manufacturing firms.

The word "genetic algorithm" refers to an evolutionary algorithm that is based on natural genetics. The first step in the genetic algorithm is the establishment of a population of possible solutions (individuals). Every member of the population shall be assigned a fitness value based on the value of the objective function. In order to produce better solutions, new generations are created through the selection, recombination and mutation of solutions. The new generation's fitness is determined. This cycle is repeated indefinitely until the stopping criterion is met. The aim of a genetic algorithm is to find an optimal solution to design problems. This entails the objective function being minimized or maximized. Genetic algorithms are a type of population-based optimization technique used to find optimal or nearly optimal solutions. GA's capability has been widely recognized for its ability to produce excellent results on both classic discrete and continuous optimization problems in terms of robustness and solution consistency. The performance of a genetic algorithm is dependent on a number of genetic parameters, including population size, crossover rate, and mutation rate. Genetic algorithm parameters are critical, and a different combination of parameters can result in a major change in GA output. The various genetic algorithm parameters and operators are usually chosen based on recommendations from experts in the field of genetic algorithms. In this work, Deb and Agarwal's real-variable GA with the SBX operator is used [101]. Table 4.3 shows the values of the GA parameters used in this analysis, such as population size, crossover, mutation, and number of generations. The findings are published after several runs of the genetic algorithm converged on the same optimal solution.

Table 4.3 Parameters Settings for GA

Number of runs	5
Population size	50
Probability of crossover	0.80
Probability of mutation	0.25
Termination Criteria	1000 generations

4.2 Implementation of GA

To apply GA to the optimization problem mentioned in equation (4.3), solution vectors must be evaluated for fitness. However, the procedure for determining the fitness function is tricky in this situation. For the initial calculation of Q_h and Q_c, the uncertain values of T_c and T_h are guessed. The unknown values of T_c and T_h are initially guessed for approximately estimate Q_h and Q_c. The initial guess for T_c and T_h is consistent with the temperature conditions observed at TEC, i.e., $T_h > T_a$ and $T_c < T_{co}$. In practice, these requirements must be met. The initial values will be updated iteratively until the exact value is found. Equation (4.1) and equation (4.2) are used to compute new values of T_h and T_c that are termed as T_{hn} and T_{cn}. These are updated repeatedly to corresponding new values until there is no difference between the old values and new values. The Q_c and Q_h values are then accepted.

A flowchart for genetic algorithm implementation for this optimization problem is given in Figure 4.4.

The brief steps of the fitness evaluation procedure for a population individual (solution vector) followed in this work are described below.

(a) The hot side and cold side temperatures of TE elements (T_h and T_c) are initially assigned to a guessed value.
(b) The material properties are calculated using equations (3.3), (3.4) and (3.5).
(c) The expected values of Q_c and Q_h are calculated using equations (3.1) and (3.2).
(d) Using equations (4.1) and (4.2) the new values of T_h and T_c are calculated. These are termed as T_{hn} and T_{cn}, respectively.
(e) If the difference of guessed values and new values is considerable, then guessed value is updated as $T_h = T_{hn}$ and $T_c = T_{cn}$. Go to step (b) and repeat the iteration.
(f) If the difference of guessed values and new values is small, then accept the solution. Take the next individual in the GA population to evaluate until all individuals of the current generation are evaluated.

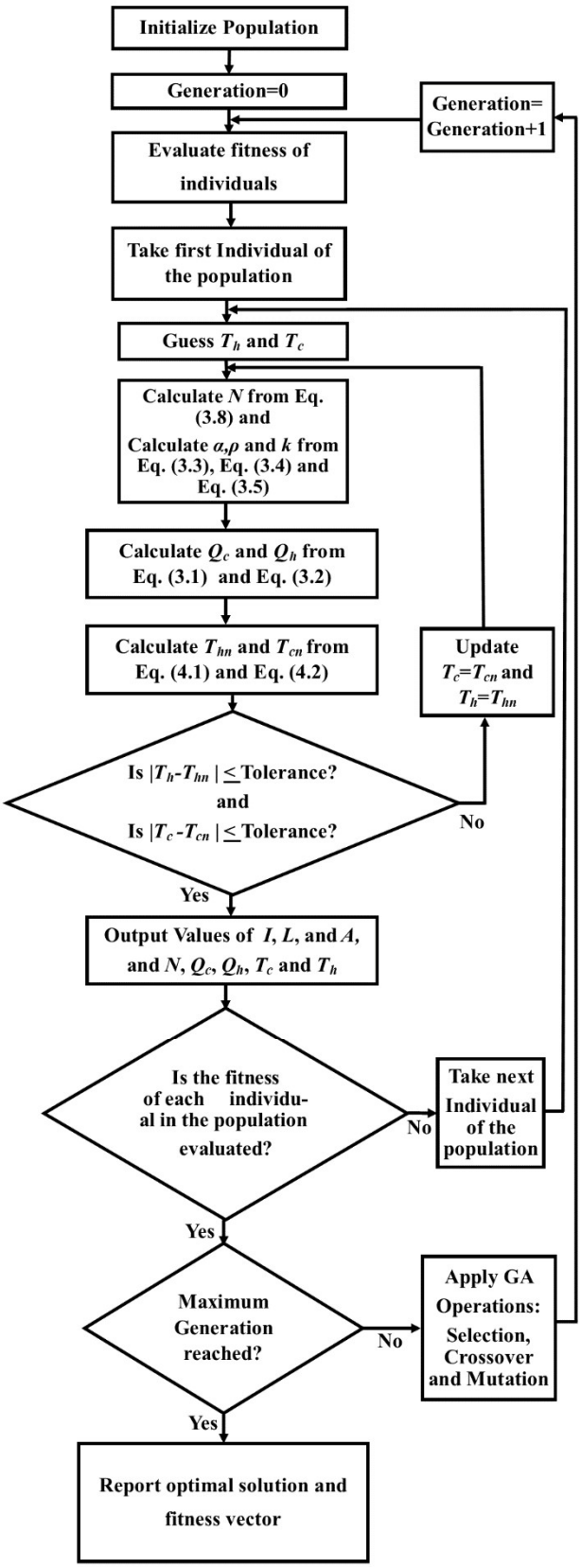

Figure 4.4 Flowchart for calculation of T_h, T_c, Q_c and Q_h for any solution vector [107]

4.2 Results and Discussion

In this segment of present work, cooling capacity Q_c, the first performance index of TEC is maximized. The algorithm of this study is coded in C language. The GA source code is developed by Deb and used in this work [102]. Multiple runs of 1000 generations have been repeated, and the best run is reported in Table 4.4 on which algorithm converged several times during various runs.

Table 4.4 Result of GA based optimization for maximum Q_c

Optimized Q_c	Optimal Values of Design Variables			
	I	L	A	N (Dependent)
8.476807 W	2.993 A	1.0 mm	1.607 mm^2	56

The corresponding values of T_h and T_c at optimum values of design variables are 28.59°C and 19.78°C, respectively. The hot surface temperature (T_{ho}) of TEC is 27.84°C. The heat rejection rate (Q_h) at the hot side is 28.401 W. The obtained COP value for the maximized Q_c is 0.425. It can be shown that L is approaching the lower bound of the permitted range, while the other parameters have optimum values without approaching any of the permitted range's bounds. The maximization of Q_c at a different set of design parameters is well established as a result of this result. The findings of this study show that by adjusting these design variables, thermoelectric coolers can increase their cooling ability and compete with compressor-based cooling devices. The TEC's performance is affected by the complex effects of electrical contact resistance and thermal resistance. For optimization and analysis, these variables must always be included in the model.

4.5 Summary

This section of the study explains how to increase the cooling power of a thermoelectric cooler for a specific need using a new analytical model. The current and geometric parameters of the thermoelectric cooler were set to be variables in order to evaluate more than one factor at the

same time. The aim of the study was to investigate the optimum current, length of n-type and p-type TE elements, and cross-sectional area of TE elements while staying within space constraints. The length of the thermoelectric components, their cross-sectional area, and the input electric current all had a significant impact on the TEC output. The genetic algorithm was successful in solving the problem of performance optimization to optimize cooling capacity. This stochastic optimization algorithm based on natural genetics theory turned out to be the right choice. Over many runs, the genetic algorithm successfully converged to the same optimal performance. Any space constraint can be solved by achieving the best possible results. This research will support TEC designers who are working on specific cooling goals.

CHAPTER 5

OPTIMIZATION OF THE COEFFICIENT OF PERFORMANCE OF THERMOELECTRIC COOLER

CHAPTER 5

OPTIMIZATION OF THE COEFFICIENT OF PERFORMANCE OF THERMOELECTRIC COOLER

5.1 Introduction

Technically, the term efficiency refers to the ratio of work output to power input in a system. This term is rarely used in heat pumping applications since it is possible to extract more heat than the power required to transfer the heat. The term 'Coefficient of Performance' (*COP*) is used instead of efficiency when referring to such applications. In general, *COP* is described as the ratio of the desired effect of heat transfer to the cost of achieving that effect in terms of work. Another important performance indicator for thermoelectric coolers is the coefficient of performance.

For a thermoelectric cooler, *COP* is the ratio of heat absorbed (from the cold side) to the electric power consumption and described by the following equation:-

$$Coefficient\ of\ Performance, \qquad COP = \frac{Q_c}{P} \tag{5.1}$$

The input electric power (P) can be evaluated by the following relationship:-

$$Input\ Electric\ Power, \qquad P = Q_h - Q_c \tag{5.2}$$

It is important to note that the performance of the heat exchange processes on the hot and cold sides of the TEC has a direct effect on the system's *COP*. The system's efficiency increases as the coefficient of performance increases. From an economic perspective, the best cooling

performance is one that pumps the heat in greatest amount with minimum expenditure of electrical energy. It's also worth noting that by maintaining the temperature difference in between the cold side and hot side of the system as small as possible, higher *COP* values can be obtained. The *COP* performance of TEC has improved only marginally over the last two decades. The major focus of effort has been on improving the thermocouple materials' figure of merit. Bismuth telluride (Bi_2Te_3) is the finest low-temperature thermoelectric material currently available, and it is commonly used in thermoelectric coolers. There have also been other new approaches to the TEC design of improved *COP* proposed. The effect of the size of the thermoelectric elements on the *COP* has also been demonstrated in studies. However, a combination of geometric and operating parameters are yet to be dealt with. The new method of design and analysis for the high *COP* performance of TEC used in this study include structural parameteres and electric current.

5.2 Optimization Problem

The single-objective optimization problem for maximization of the Coefficient of Performance (*COP*) of TEC is formulated mathematically as:

$$\begin{cases} Maximize\ COP \\ Subject\ to \\ \quad I_{\min} \le I \le I_{\max} \\ \quad L_{\min} \le L \le L_{\max} \\ \quad A_{\min} \le A \le A_{\max} \\ \quad \left(\dfrac{2A \times N}{PD}\right) \le S \end{cases} \tag{5.3}$$

Different parameters influence this objective function, but only three are chosen as decision variables because they can easily adjust in real-world situations. The aim of the optimization problem is to determine *I*, *L*, and *A*, as well as the number of thermocouples, in order to maximize *COP*. In this problem, the total number of thermoelectric couples (*N*) is an integer design variable. As explained in the previous chapter, its value is calculated using equation (3.8) and is rounded down to the nearest integer. *S* is the available cross-sectional area of the restricted space wherein the TEC is placed. *PD* denotes the packaging density.

The decision variables are identical to those used in the main problem of single-objective optimization of cooling capacity. Table 4.2 showed the lower and upper bounds of variables. The goal of this optimization problem is to find the design variables within the variable bounds that result in the maximum coefficient of performance of the device. The optimization problem, as presented in equation (5.3) has been solved using some specific values of parameters. The values of the parameters and properties that were used in this *COP* maximization research are identical to that of the optimization problem of the cooling capacity and described in the Table 4.1.

5.3 Implementation of GA

The problem is solved using the genetic algorithm, which optimizes the values of each parameter to increase coefficient of performance. The fitness evaluation of solution vectors is necessary to apply the genetic algorithm to the optimization problem defined in the equation (5.3). The similar approach has been used as used in the maximization of cooling capacity of the main problem and described in the previous chapter with the help of a flowchart in Figure 4.4. The procedure that was used was as follows:

(1) Firstly, the cold side and hot side temperatures of TE elements (T_h and T_c) are initially assigned to a guessed value.
(2) Equations (3.3), (3.4), and (3.5) are used to estimate material properties.
(3) Equations (3.1) and (3.2) are used to measure the expected value of Q_c and Q_h.
(4) The new values of T_h and T_c are determined using equations (4.1) and (4.2). These are termed as T_{hn} and T_{cn}, respectively.
(5) If the difference between the guessed and new values is relevant, the guessed value is changed to $T_h = T_{hn}$ and $T_c = T_{cn}$. Return to step (b) and iterate again.
(6) Accept the solution if the difference between the guessed and new values is minimal. Take the next individual in the GA population to evaluate until all individuals of the current generation are evaluated.

Table 5.1 shows the values of the GA parameters used in this analysis, such as population size, crossover, mutation, and generation number. Multiple GA runs converged to the same best solution, and the results are reported.

Table 5.1 Parameters Settings for GA

Population size	20
Crossover probability	0.80
Mutation probability	0.25
Termination Criteria	1000 generations
Number of runs	5

5.4 Results & Discussion

To optimize the second performance index of thermoelectric cooler, the coefficient of performance (*COP*) is maximized. The assumptions and boundary conditions are the same as those used in the optimization of Q_c. The parameters of GA are used to solve this optimization problem, as mentioned in Table 5.1. Implementing genetic algorithm in this problem follows the same steps as those for optimizing cooling capacity and are depicted in Figure 4.4 with the aid of a flowchart. To achieve the highest-quality solutions, several 1000-generation runs were performed, with the best GA run being reported in Table 5.2. GA converged to the same results in different runs, which is worth noting.

Table 5.2 Result of GA based optimization for maximum *COP*

Optimized *COP*	Optimal Values of Design Variables			
	I	*L*	*A*	*N* (Dependent)
4.11	0.283 A	2.0 mm	1.956 mm^2	45

With this value of maximum *COP*, the corresponding Q_c is obtained as 0.745992 W. The corresponding values of T_h and T_c are 25.11°C and 19.97°C, respectively. The thermoelectric cooler's hot surface temperature (T_{ho}) is 25.09°C. The heat rejection rate (Q_h) at the hot side of TEC is 0.927 W. The optimal values of *I* and *A* design variables are unique, while the optimal value of *L* is hitting the upper boundary. As can be seen, COP has significantly increased, and

cooling capacity is just 8.8% of Max. Q_c obtained, as mentioned in Table 5.2. A design variable L is found to reach its lower bound for high Q_c thus hitting its upper bound for high COP.

From these two results (single-objective optimization of Q_c and single-objective optimization of COP), it is well established that maximization of cooling capacity and maximization of coefficient of performance are obtained at a different set of design parameters. Also, maximum Q_c does not mean maximum COP, and vice versa. As a result, these goals are at conflicts with one another. If there is no specific objective interest, Pareto solutions by multi-objective optimization can be used to resolve these conflicting performance objectives. It would be beneficial to identify a range of solutions from which the decision-maker can choose depending on the specifications of the application.

The results of the two single-objective optimization problems (Cooling capacity, Q_c and COP) show that with these design variables, thermoelectric coolers may enhance their cooling capacity or coefficient of performance to compete with traditional compressor-based systems. The complex impacts of electrical contact resistance and thermal resistance deteriorate the TEC performance. For optimization and analysis, these factors must always be included in the model.

5.5 Summary

This chapter reports the maximized COP value of a taken case of thermoelectric cooler. It is clearly shown how these design variables (I, L, A) in a thermoelectric cooling system can be suitably selected to maximize the COP of the TEC system. A similarity in the GA procedure has been shown in the optimization attempts for Q_c and COP but the optimal design variables are not identical. It is concluded that the COP is maximum i.e. 4.11 at the optimized value of parameters when the input electric current (I), length of TE elements (L), cross-sectional area of TE elements (A) are 0.283 A, 2.0 mm and 1.956 mm^2 respectively.

Results reported in previous and this chapter revealed that the coefficient of performance (COP) and cooling capacity have an inverse relationship. Maximum cooling capacity does not always correspond to the best COP, and vice versa. The maximum cooling capacity is

facilitated by smaller length of thermoelectric elements, while the maximum coefficient of performance is obtained by greater length of TE elements. Specific values of cross-sectional area of p-type and n-type TE elements and electric current as per the objective requirements are needed for the best performance. Any space constraint can be tackled to produce the best possible results. A high *COP* is beneficial in order to reduce electricity consumption and waste heat production.

CHAPTER 6

ANALYSIS AND OPTIMIZATION OF FIRST AND SECOND LAW EFFICIENCY OF THERMOELECTRIC COOLER

CHAPTER 6

ANALYSIS AND OPTIMIZATION OF FIRST AND SECOND LAW EFFICIENCY OF THERMOELECTRIC COOLER

6.1 Introduction

Each system or process conserves energy. However, the concept of energy conservation alone is insufficient to represent certain key aspects of resource use. At present, more than three-fourths of refrigeration systems work on vapour compression and use refrigerants. These systems are one of the most important factors of stratospheric ozone depletion. The adverse environmental impacts of chloro-fluoro-carbons (CFCs), hydro-chloro-fluoro-carbons (HCFCs), and hydro-fluoro-carbons (HFCs) used in vapour compression-based cooling systems have forced the energy researchers to strongly explore renewable alternatives. A promising eco-friendly replacement for the cooling systems using refrigerants is thermoelectric cooler (TEC). A thermoelectric cooler is a solid-state and practically silent device. TEC is powered by the Peltier effect and achieved by supplying electric current through n-type and p-type thermoelectric material. TEC does not have moving components. Thermoelectric coolers are significant because of the need for steady, small size and environmental sustainability for many applications. Thermoelectric coolers are prominently used for cooling requirements of small volumes. These are preferred in various high technology applications such as electronics, space, medicine, telecommunications, and others. TECs are best suited to areas that are not accessible to compressors.

Notwithstanding, currently, thermoelectric coolers have low rate of cooling and energy conversion efficiency compared to other traditional cooling technologies that impeded their wide-spread usage [108]. Various models and hypotheses have been presented in the literature on this problem, and several solutions have been suggested [18], [109], [118]–[127], [110],

[128], [129], [111]–[117]. A significant number of papers are concerned with the design and simulation of thermoelectric cooling or heat pumping systems. However, it is important to note that most of these optimization attempts were primarily made to improve rate of cooling or coefficient of performance (*COP*) of TEC. Energy has two faces: Exergy and Anergy. The expression "exergy" derives from the Greek terms ex and ergon, representing from and work [130]. Exergy represents available part of energy. Anergy shows dispersed part of energy source or lost potential. Very few articles appear to deal with the exergy aspects of the thermoelectric cooling or heat pumping devices, two of such articles which are prominent Kaushik et al. [131] and Nami et al. [132]. Kaushik et al. [131] performed exergy analysis of reversible, endoreversible, exoreversible, and irreversible heat pump. Analytical expressions of thermodynamic models were derived. Exergy output for the different temperature difference between hot and cold sides was observed. It was found that exergy output increases at a higher temperature difference. The increment in contact resistance reduces exergy output. Nami et al. [132] reported a comparison of single-stage and two-stage thermoelectric devices for *COP* and exergetic efficiencies. It was established that a higher current is needed in a single-stage device for maximum values of energy efficiency and exergy efficiency. The research on exergy is focused on the quality of energy used to assess the energy process in compliance with ideal thermodynamic equality [133], [134]. The exergy study is used to recognize exergy losses. It is used to understand irreversible energy conversion losses in the design of the system. To provide effective efficiency and meet several design requirements, computer-aided design, optimization, and analysis have been important parts for the design of thermoelectric cooling systems.

A focussed effort on optimization of TEC to achieve maximum energy and exergy efficiencies is presented now. The TEC geometry and current can change the efficiencies, and optimum values can be obtained under given circumstances. In this study, an optimization method for the TEC design for improved results has been attempted by considering three of the main parameters: namely electric current, length of thermoelectric elements, and cross-sectional area of thermoelectric elements.

6.2 Thermodynamics Formulations

A thermoelectric cooler consists of several couples made out of n-type and p-type thermoelectric elements. These thermoelectric (TE) elements are tied together electrically by using highly conductive copper tabs. These elements are connected thermally parallel. Between two ceramic layers, this structure is sandwiched.

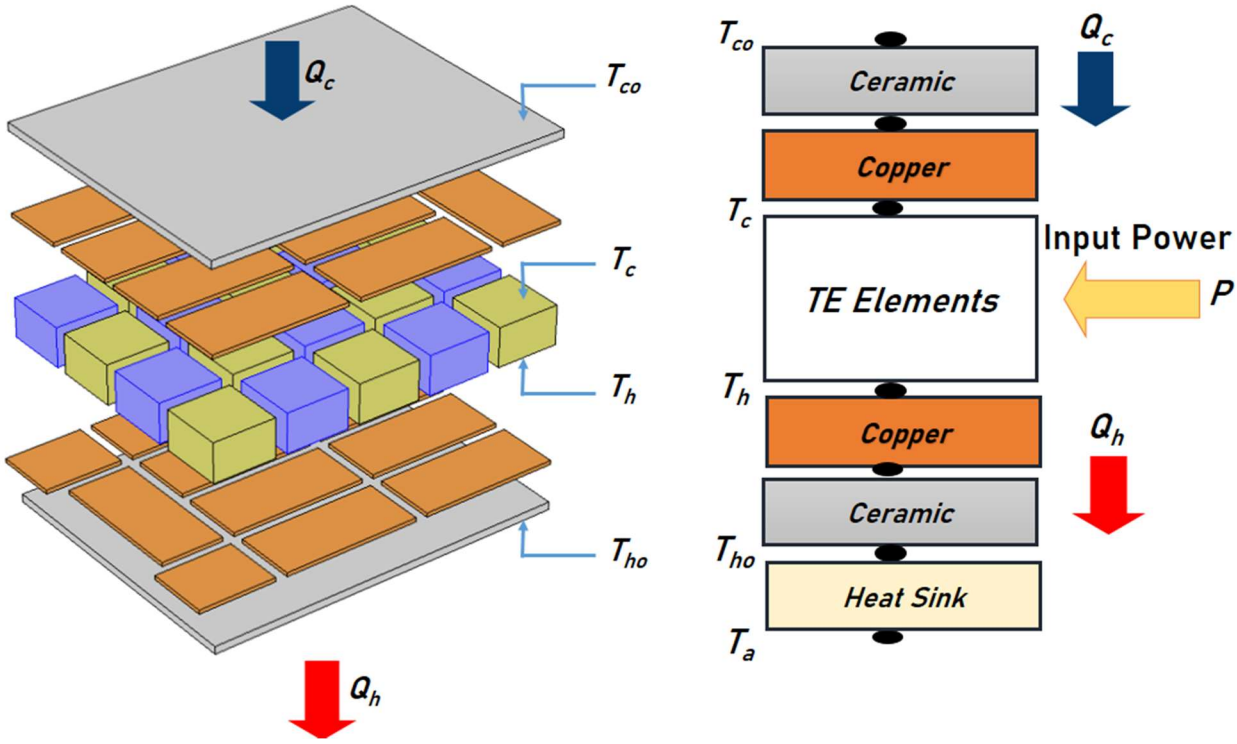

Figure 6.1 (a) Exploded view of TEC (b) Various parts for thermal resistances

For simplifying the complexity of calculation, some assumptions are made for this study.

- Heat transfer takes place along the length of thermoelectric elements.
- The cross-section and length of the thermoelectric elements are similar.
- Thomson effect is not considered.
- Steady-state condition is prevailing.

A thermoelectric cooling system is configured to transfer thermal energy from the source at temperature T_{co} to a sink at a higher temperature T_{ho}. The basic units of a TEC are

thermocouples that possess temperatures T_c and T_h at cold and hot junctions respectively. The material properties and heat balance equations are fundamentally established for thermocouple portions of TEC. In the present work, we have modelled TEC realistically considering copper and ceramic effects with cold and hot side temperatures of T_{co} and T_{ho} for GA based optimization and finite-element simulations. An exploded view of the TEC and various parts for thermal resistances in TEC are shown in Figure 6.1. Electric power is provided as input to the TEC system, and the Peltier effect is at work according to the direction of electric current. Thermoelectric coolers are inherently irreversible because the flow of heat and current is necessary during operation. These irreversibilities are the reason for the requirement of the performance optimization of thermoelectric coolers.

The reversible cycle concept as explained by Sadi Carnot is well established and significant. Thermodynamically, a practical thermoelectric cooler can be modelled as an irreversible reversed heat engine. An irreversible thermoelectric cooler possesses both types of the irreversibilities, i.e., internal and external. The internal irreversibility is generated as TEC operates between cold and hot junctions of p-type and n-type thermoelectric elements at temperatures T_c and T_h, respectively. The external irreversibility is generated due to the finite temperature gap (T_{co}-T_c) responsible for heat absorption rate, Q_c at the cold side of the TEC system. On the hot side, it is due to the temperature gap (T_h-T_{ho}) responsible for heat rejection rate, Q_h. So far in all reported research, the authors have taken T_c=T_{co} and T_h=T_{ho} which leads to modelling error. In the present work, a more realistic model has been used and T_c is separately computed and not taken equal to T_{co}. T_h and T_{ho} are also separately calculated.

At the cold side of the thermoelectric cooler, the heat energy balance may be expressed as:-

$$Q_c = Q_{Peltier} - Q_{conduction} - Q_{Joule} \tag{6.2}$$

At the hot side of the thermoelectric cooler, the heat energy balance may be expressed as:-

$$Q_h = Q_{Peltier} - Q_{conduction} + Q_{Joule} \tag{6.2}$$

The Peltier heat ($Q_{Peltier}$) at the cold and hot sides corresponds to $I\alpha T_c$ and $I\alpha T_h$ respectively. The irreversible heat transfer due to conduction ($Q_{conducion}$) at the cold side and hot side corresponds to $K(T_h\text{-}T_c)$. The irreversible Joule heat generation (Q_{Joule}) corresponds to ½ I^2R. In these expressions, I refers to supplied electric current (A), α is the Seebeck coefficient (V/K) and R represents the electrical resistance. T_c and T_h are the cold side and hot side temperatures (K) of n-type and p-type elements. If N represents the total number of thermoelectric couples used in the thermoelectric cooler, the heat energy balance equations become:

$$Q_c = 2N\left[I\,\alpha\,T_c - K(T_h - T_c) - \frac{1}{2}I^2(R)\right] \tag{6.3}$$

$$Q_h = 2N\left[I\,\alpha\,T_c - K(T_h - T_c) + \frac{1}{2}I^2(R)\right] \tag{6.4}$$

If k and r_c represent the thermal conductivity (W/mK) and the electrical contact resistance (Ωm^2), respectively. L and A represent the length (m) and cross-sectional area (m^2) of n-type and p-type thermoelectric elements, respectively. Equations (6.3) and (6.4) can be rearranged as:

$$Q_c = 2N\left[I\,\alpha\,T_c - \frac{k\,A\,(T_h - T_c)}{L} - \frac{1}{2}I^2\left(\frac{\rho L}{A} + 2\frac{r_c}{A}\right)\right] \tag{6.5}$$

.

$$Q_h = 2N\left[I\,\alpha\,T_h - \frac{k\,A\,(T_h - T_c)}{L} + \frac{1}{2}I^2\left(\frac{\rho L}{A} + 2\frac{r_c}{A}\right)\right] \tag{6.6}$$

The choice of the thermoelectric element's material directly affects TEC performance. Bismuth telluride (Bi_2Te_3) is considered as the most popular material and used in practical thermoelectric coolers. The temperature-dependent properties of Bismuth telluride used in this study are calculated from the below-mentioned expressions as specified [135].

$$\alpha = (22224 + 930.6\,T_{ave} - 0.9905\,T_{ave}^2) \times 10^{-9} \tag{6.7}$$

$$\rho = (5112 + 163.4\,T_{ave} + 0.6279\,T_{ave}^2) \times 10^{-10} \quad (6.8)$$

$$k = (62605 - 277.7\,T_{ave} + 0.4131\,T_{ave}^2) \times 10^{-4} \quad (6.9)$$

Where,

$$Average\ Temperature, T_{ave} = 0.5 \times (T_c + T_h)$$

The irreversible heat flow rate with the heat source or TEC cold surface temperature (T_{co}) to the cold side temperature of n-type and p-type elements (T_c) is given by:

$$Q_c = U_c\,A_c(T_{co} - T_c) \quad (6.10)$$

Similarly, the irreversible heat flow rate with the hot side temperature of n-type and p-type elements (T_h) to the heat sink or TEC hot surface temperature (T_{ho}) is given by:

$$Q_h = U_h\,A_h(T_h - T_{ho}) \quad (6.11)$$

In the above expressions, U_c and U_h represent the overall heat transfer coefficients (W/m^{2}K) while A_c and A_h represent heat transfer surface areas (m^2) at the cold and hot surfaces of TEC.

Thermal conductance is reciprocal thermal resistance. We have used a thermal resistance model and have incorporated thermal resistances of ceramic substrates, copper conductors, and heat sink at the hot side for realistic TEC model consideration. By using thermal resistance models, equations (6.10) and (6.11) are restructured as:

$$T_h = Q_h(R_{hs} + R_{cr} + R_{cu}) + T_o \quad (6.12)$$

$$T_c = T_{co} - Q_c(R_{cr} + R_{cu}) \quad (6.13)$$

Where, R_{hs}, $R_{cr,}$ and R_{cu} are the thermal resistances (^{0}C/W) of the ceramic substrates, copper conductors and heat sink.

From the ‘available work’ or ‘exergy’ point of view, it is well established by the researchers

that the exergy input to the thermoelectric cooling system is equal to the input electric power (P), and it is 100% exergy. The concept of exergy needs the first law of thermodynamics as well as the second law of thermodynamics. In the thermoelectric cooling system, the temperature of the cold side of TEC (T_{co}) is less than the environment temperature (T_o). The temperature difference (T_o-T_{co}) leads to the absorption of heat from the refrigerated space.

The first law of thermodynamics can be applied to obtain:

$$Exergy\ Input = Input\ Electric\ Power\ (P) = Q_h - Q_c \tag{6.14}$$

Applying the second law of thermodynamics for irreversible TEC, we can write:

$$\frac{Q_c}{T_{co}} - \frac{Q_h}{T_{ho}} < 0 \tag{6.15}$$

The second law of thermodynamics can also be applied to obtain rate of entropy generation as:

$$Rate\ of\ Entropy\ Generation, S_{gen} = \left(\frac{Q_h}{T_{ho}} - \frac{Q_c}{T_{co}}\right) > 0 \tag{6.16}$$

If we combine the first law and second law of thermodynamics used for conservation of energy and non-conservation of entropy, exergy balance for a thermodynamic system can be obtained as:

$$Exergy\ Input = Exergy\ Output + Exergy\ Losses \tag{6.17}$$

$$\begin{aligned} &Exergy\ Input \\ &\quad = Exergy\ Output + (Exergy\ Waste\ Emission \\ &\quad + Exergy\ Destruction) \end{aligned} \tag{6.18}$$

The exergy output refers to the thermal exergy deposited at the cold side of the thermoelectric cooler. This exergy transfer accompanying heat transfer Q_c can be calculated by [136]–[138]:

$$Exergy\ Output = Q_c \left(\frac{T_o}{T_{co}} - 1\right) \tag{6.19}$$

Where T_o represents a typical environment or outside temperature.

Exergy Waste Emission or Exergy lost represents the exergy rejected at the hot side of the thermoelectric cooler (If present) and can be written as [116]:

$$Exergy\ Lost = Q_h \left(1 - \frac{T_o}{T_{ho}}\right) \tag{6.20}$$

Substituting equations (6.14), (6.19), and (6.20) into equation (6.18), Irreversibility or exergy destruction in the process can be obtained as:

$$Irreversibility\ or\ Exergy\ Destruction = T_o \left(\frac{Q_h}{T_{ho}} - \frac{Q_c}{T_{co}}\right) = T_o\, S_{gen} \tag{6.21}$$

First law efficiency or energy efficiency of a thermoelectric cooler is obtained as:

$$First\ Law\ Efficiency\ or\ Energy\ Efficiency\ (\eta_I) = \frac{Energy\ Output}{Energy\ Input} = \frac{Q_c}{Q_h - Q_c} \tag{6.22}$$

The second law efficiency or exergy efficiency is a measure of approach to reversibility or ideality. A key goal of exergy analysis is to identify this significant efficiency and actual values of exergy losses with the identification of possible reasons [139].

$$Second\ Law\ Efficiency\ or\ Exergy\ Efficiency\ (\eta_{II}) = \frac{Exergy\ Output}{Exergy\ Input} \tag{6.23}$$

Alternatively, this can be expressed as:

$$\eta_{II} = 1 - \frac{Exergy\ Losses}{Exergy\ Input} \tag{6.24}$$

The purpose of the thermoelectric cooler is to absorb heat from the space to be cooled. Thus, it helps in increasing exergy output while this heat absorption takes place. The exergy efficiency of a thermoelectric cooler can be understood as the ratio of minimum exergy or work requirement to the actual exergy input. For simplicity, the thermal reservoir at hot surface temperature T_{ho} is set to be the typical environment. Hence, T_{ho} is the outside temperature (T_o) for the thermoelectric cooler.

Hence,

$$Exergy\ Output = Q_c \left(\frac{T_{ho}}{T_{co}} - 1\right) \tag{6.25}$$

Second law efficiency or exergy efficiency of an irreversible thermoelectric cooler is obtained as:

$$\eta_{II} = \frac{Q_c \left(\frac{T_{ho}}{T_{co}} - 1\right)}{P} = 1 - \frac{T_{ho} S_{gen}}{P} \tag{6.26}$$

This establishes a relationship between first law efficiency (η_I) and second law efficiency (η_{II}) of the thermoelectric cooler:

$$\eta_{II} = \frac{\eta_I}{\frac{1}{\left(\frac{T_{ho}}{T_{co}} - 1\right)}} \tag{6.27}$$

The *COP* of the thermoelectric cooler is the ratio of useful energy to the required energy and is equal to energy efficiency as described in equation (6.22). According to the reversed Carnot cycle phenomenon, $\frac{1}{\left(\frac{T_{ho}}{T_{co}} - 1\right)}$ represents the Carnot or reversible Coefficient of performance (*COP*), the highest theoretical *COP* of thermoelectric cooler working within temperature bounds T_{co} and T_{ho}. Hence, the second law efficiency of TEC can also be expressed as:

$$\eta_{II} = \frac{Actual\ COP}{Reversible\ COP}\ or\ \frac{Actual\ COP}{Maximum\ COP} \tag{6.28}$$

It is clear that second law efficiency indicates the irreversibilities associated with the thermoelectric cooling system and can vary from 0 to 1.

6.3 Optimization Problem

In this part of work, two objectives are optimized separately. The first optimization problem's objective is the first law efficiency (η_I), which is of significance to obtain higher energy efficiency in a restricted space. The second optimization problem's objective is the second law efficiency (η_{II}), which is important to achieve a higher exergy efficiency. After modelling, we select the design variables to achieve optimum engineering goals. The geometry, material and operating conditions play a vital role in designing a TEC with higher performances. The restriction of space in designing TEC is a major constraint. At present, thermoelectric coolers are widely used in the high technology fields such as electronics, telecommunications, space, and others. Space restrictions are very prevalent in these fields and hence there are practical limits to the size of the thermoelectric cooler. Therefore, the space constraints of the thermoelectric elements are very relevant assumptions to consider. This study uses the approach to select three design variables, i.e., length of n-type and p-type TE elements, the cross-sectional area of n-type and p-type TE elements, and the input electric current.

6.3.1 Maximization of first law efficiency

The first single-objective optimization problem for maximization of the energy efficiency or first law efficiency (η_I) of the thermoelectric cooler is formulated mathematically as:

$$\begin{cases} Maximize\ \eta_I \\ Subject\ to \\ \quad I_{\min} \le I \le I_{\max} \\ \quad L_{\min} \le L \le L_{\max} \\ \quad A_{\min} \le A \le A_{\max} \\ \quad \left(\frac{2A \times N}{PD}\right) \le S \end{cases} \tag{6.29}$$

Where, (I_{min}, I_{max}), (L_{min}, L_{max}) and (A_{min}, A_{max}) are the bounds of design variables I, L and

A, respectively. *N* is an integer design variable and computed using equation (3.8) and is rounded down to the nearest integer. *S* is the available cross-sectional area for TEC. *PD* is the packaging density.

The bounds of the design variables of this optimization study are listed in Table 6.1.

Table 6.1 Lower and upper bounds of design variables

Variable	Description	Lower limit	Upper limit
I	Input electric current, A	1.0	2.0
L	Length of n-type and p-type TE elements, mm	1.0	2.0
A	Cross-sectional area of n-type and p-type TE elements, mm^2	0.1	3.0

Besides, the total number of thermoelectric couples (*N*) depends on the cross-sectional area of TE elements and packaging density. Its value can be evaluated using this equation:

$$N = \frac{Available\ area\ (S)\ for\ TEC\ \times\ packaging\ density\ (PD)}{2 \times A} \qquad (6.30)$$

The detailed specifications of the thermoelectric cooling system considered for this work are presented in Table 6.2.

Table 6.2 Specifications of the thermoelectric cooling system

Description	Parameter	Value
Available cross-sectional area of the restricted space	S	225 mm^2
Packaging density	PD	80%
Ambient temperature	T_o	25°C or 298.15 K
Cold surface temperature	T_{co}	20°C or 293.15 K
Electrical contact resistance	r_c	1 x 10^{-8} Ω m^2
Thermal resistance of heat sink	R_{hs}	0.10 °C/W
Ceramic thermal conductivity	k_{cr}	35.3 W/m°C
Copper thermal conductivity	k_{cu}	386 W/m-°C

The lower bound and upper bound of the number of thermoelectric couples is the dependent variable and become 45 and 90, respectively for the present work. The cold side and hot side ceramic substrates are 0.2 mm in thickness. The cold side and hot side copper tabs are considered 90% of the available cross-sectional area of TEC and 0.1 mm in thickness.

6.3.2 Maximization of second law efficiency

The second single-objective optimization problem for maximization of the exergy efficiency or second law efficiency (η_{II}) of the thermoelectric cooler is formulated mathematically as:

$$\begin{cases} Maximize\ \eta_{II} \\ Subject\ to \\ I_{\min} \le I \le I_{\max} \\ L_{\min} \le L \le L_{\max} \\ A_{\min} \le A \le A_{\max} \\ \left(\frac{2A \times N}{PD}\right) \le S \end{cases} \tag{6.31}$$

The bounds of design variables and specifications of thermoelectric cooling system resulting in variations of output are identical to previous optimization problem of maximization of energy efficiency.

6.4 Implementation of GA

In complex engineering applications, the implementation of stochastic algorithms has become popular and common. The stochastic algorithm, like genetic algorithm attempts to perform a global search within the search space of design variables. Because of the promising potential researchers are using stochastic methods to evaluate, predict, and optimize different systems. Genetic algorithm (GA), which is used for this study, uses a population of individuals to search the design space. In the literature, many coding schemes are available for genetic algorithm such as binary-coded GA, gray coded GA, integer genes, and real-coded GA (RGA). RGA is more popular than others because of its inherent potential to directly provide numeric value solutions with no need to code and decode the solutions. Many real-world applications have shown the advantage of RGA compared to others. The simulated binary crossover (SBX) operator performs excellently in optimization problems with continuous search space. The real-variable GA is implemented in this paper as created by Deb and Agarwal (1995). GA parameters settings used for this work are given in Table 6.3.

Table 6.3 Parameters settings for GA

Population size	50
Crossover probability	0.80
Mutation probability	0.25
Termination Criteria	1000 generations
Number of runs	5

The GA solution procedure adopted for this work has major steps similar to previous problems. The population is initialized. Then T_h and T_c values are guessed to compute TE material properties and subsequently Q_c and Q_h. After that new values of T_h and T_c are computed and old values are replaced with new values. This process is repeated until the difference in new and old values of T_h and T_c becomes negligible. If the conditions are satisfied, the individual (solution) of the population is accepted. The individual of the population is evaluated for fitness value. The next individual of the current population is taken and the process discussed above is repeated. After the entire population is evaluated, a new population is formed by using selection, crossover, and mutation operators of genetic algorithm. Then, the entire process is repeated for a stipulated number of maximum generations. Finally, the important statistics of generations are reported.

6.5 Results & Discussion

In two single-objective optimization problems, the energy efficiency and the exergy efficiency of the irreversible thermoelectric cooler are maximized using genetic algorithm. Genetic algorithm based optimizations are coded in C language. In this study, the GA source code developed by Deb [102] was employed. Multiple independent runs were performed for each optimization problem. Table 6.4 contains the best optimization results after 1000 generations for multiple runs of energy efficiency maximization and exergy efficiency maximization. These best results are repeatedly found over various runs.

Table 6.4 Results of GA based optimization for maximization of energy and exergy efficiencies

Case	η_I	η_{II}	Optimal Values of Design Variables			
			I	*L*	*A*	*N (Dependent)*
Optimization of energy efficiency	4.116	0.0715	0.28 A	2.0 mm	1.956 mm^2	45
Optimization of exergy efficiency	4.116	0.0715	0.28 A	2.0 mm	1.956 mm^2	45

The optimal values of design variables are identical for both the optimization problems as per simulation results. The optimum input current to obtain maximum energy and exergy efficiency are with the same values of 0.28A. This finding of results is a reliable match as reported by researchers [116], [131]. This study found that besides input current, the length and cross-sectional area of TE elements to obtain maximum energy and exergy efficiencies are also the same.

In the optimized solutions, the length of TE element is found as 2.0 mm which is the upper limit of the range. The other design variables (*I* and *A*) are unique and well between the bounds of given ranges. Depending on the optimal design values of three different variables, the corresponding temperature T_h is obtained as 25.11℃, and T_c is found as 19.97℃. The corresponding hot surface temperature (T_{ho}) is estimated as 25.09℃. The rate of cooling (Q_c) and the rate of heat rejection (Q_h) are achieved as 0.746 W and 0.927 W, respectively. Exergy parameters for optimized exergy efficiency are given in Table 6.5.

Table 6.5 Exergy parameters for maximized exergy efficiency (η_{II})

Maximized Exergy Efficiency	Exergy Input	Exergy Output	Exergy Destructed	Entropy Generation Rate
7.15%	0.1874 W	0.0134 W	0.1740 W	0.5835×10^{-3} W/K

The heat rejection increases the rate of entropy generation (S_{gen}) and exergy destruction in the TEC system. The work provided to the TEC system includes exergy transfer towards the cold side and loss of available work due to the irreversibility of the system. Hence, the required work exceeds the threshold value. S_{gen} is minimized for maximum exergy efficiency. The exergy efficiency or second law efficiency is maximized and achieved as 7.15%.

6.6 Summary

In this chapter, the energy and exergy efficiencies of TEC are discussed. Designers have been looking for better ways to improve energetic and exergetic performance for energy converters. The objective of the first and second laws of thermodynamic analysis of this research is to determine the maximized energy efficiency (η_I) and exergy efficiency (η_{II}) of a thermoelectric cooler. This work introduced a new approach by selecting three design variables, i.e., length of n-type and p-type TE elements, the cross-sectional area of n-type and p-type TE elements, and the input electric current. A thermal resistance model has been used in the analytical model. The thermal resistances of ceramic substrates, copper conductors, and heat sink at the hot side have been incorporated for realistic TEC model consideration. Unlike previous research, the cold side and hot side junction temperatures were taken different from TEC's surface temperatures.

Previous studies [116], [131] indicate that η_I and η_{II} are maximum at the same current. This study has shown that the maximum values of η_I and η_{II} are obtained not only at the same current but also at the same values of length and cross-sectional area of thermoelectric elements. If we consider three performance indicators for thermoelectric coolers, i.e., cooling capacity, energy efficiency (η_I) and exergy efficiency (η_{II}), through this work it is clear that maximum η_{II} automatically assures maximum η_I.

For environmental consideration, it is recommended that the maximization of exergy efficiency should be the basis of TEC design. The improvement in exergy efficiency is a reflection of the thermodynamic improvement of the thermoelectric cooling operation and high sustainable score. Exergy analysis includes all losses (irreversibilities) in the parts and complete thermoelectric cooling system. Irreversibilities can be minimized to get maximum

exergy efficiency, which makes the TEC system more sustainable.

The *ZT* value of thermoelectric materials plays an important role in characterizing the performance of TEC. It is important to develop more efficient thermoelectric materials with a focus on maximizing *ZT* value. When significant advances in the peak value of the dimensionless figure of merit of thermoelectric materials will be found, the exergy efficiency of TEC can be higher than the vapour compression refrigeration systems.

CHAPTER 7

VALIDATION OF RESULTS BY FINITE ELEMENT METHOD

CHAPTER 7

VALIDATION OF RESULTS BY FINITE ELEMENT METHOD

7.1 Introduction

In present times, the computational models that are capable of accurately capturing the geometric, as well as physical phenomena, are used for complex designs. In today's computational times, the importance of physical modeling and computer algorithms and methodologies can not be overstated. The finite element method (FEM) is a popular numerical technique. The FEM is a numerical technique used in science and engineering to find approximated solutions to problems. These problems are controlled by the components such as mathematical (differential) equations, boundary conditions, and the geometries. In FEM, the problems specified in geometric space (domain) are split into small regions or elements (mesh) to find the local solutions within the elements' boundaries. A global solution can be achieved by stitching these local solutions on these elements back together. The elements are linked by nodes, which are where the unknowns would be calculated. The governing differential equations explaining physics are used to derive the finite element equations to every element. These equations (finite element) are combined to form a large number of algebraic equations and the boundary conditions are imposed in order to solve for solutions (at each nodes).

In general, the FEM method procedure consists of certain steps:

(a) Construct the geometry of the problem. Then, a finite element mesh is generated on the geometry. A mesh may have elements of different forms (such as line, brick, and triangle). These elements are linked at nodes that contain the problem unknowns.
(b) Choose the element types. The number of unknowns and, as a result, the computational

time will increase if an element is selected having more nodes. If a more complex interpolation function is used, the solution accuracy also can improve.

(c) To derive the finite element equations (from governing equations) is the important step. The derived equations are algebraic equations that can be numerically computed.

(d) All of the finite element equations are then put together to form a broad set of equations (algebraic equations).

(e) The boundary conditions are imposed on the algebraic equations before the nodal unknowns are solved. The displacements in a structural problem and the temperatures in a heat transfer problem are the nodal unknowns.

(f) The solution of many other quantities of interest is then possible. For heat transfer problem, once the nodal temperatures are known, heat fluxes can be determined.

7.2 Advantages of ANSYS®

To verify GA results, a finite-element simulation tool was required, and ANSYS® workbench was chosen for this work. ANSYS® is a finite element analysis software. It is widely used for analyzing and optimizing a large class of complex engineering problems. The workbench feature in ANSYS® simplifies the software's use via a graphical user interface (GUI). ANSYS® workbench is used to solve a wide range of problems in many fields such as thermal, structural, electrical, fluid flow, electromagnetics etc. There are several advantages to using ANSYS®. The geometric shapes (two-dimensional and three-dimensional) can be created and also can be imported from different CAD software. ANSYS® can integrate several formulae into an unified platform, making the analysis process easier and quicker. For example, thermal and structural analysis can be integrated. It has collection of engineering materials and corresponding properties. New materials can also be created. It has robust foundation and capability for multi-physics and enables the user to solve complicated analyses. It has a strong simulation capability that allows it to demonstrate perfect results.

7.3 Procedure involved in Finite Element Simulation Using ANSYS®

The basic simulation procedure with ANSYS® workbench involved the three major phases, pre-processing, solution and post-processing [140]. Each phase of the simulation analysis

is designed to address the related functional requirements. Figure 7.1 illustrates the general procedure of ANSYS® workbench simulation study.

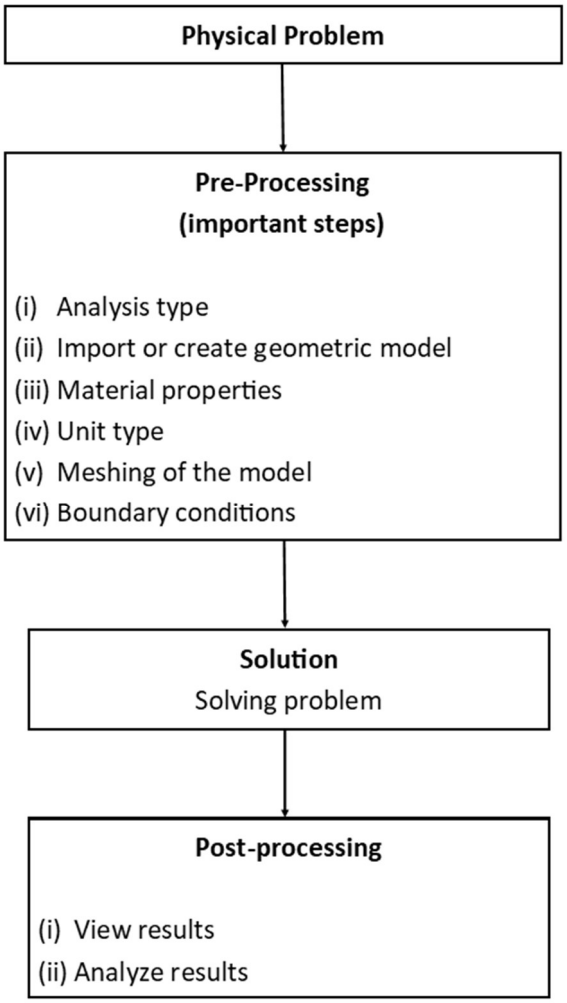

Figure 7.1 General procedure of simulation analysis using ANSYS® workbench

7.3.1 Pre-processing

The usual key steps involved in the pre-processing stage are selection of analysis type (tool for solving class of problem), creating or importing 3D geometric model, specifying materials properties, unit type, assigning appropriate materials, and meshing of the model. In this work, Thermal-Electric tool was used for the analysis as it was suitable for this class of engineering problem. The toolbox region is shown in Figure 7.2.

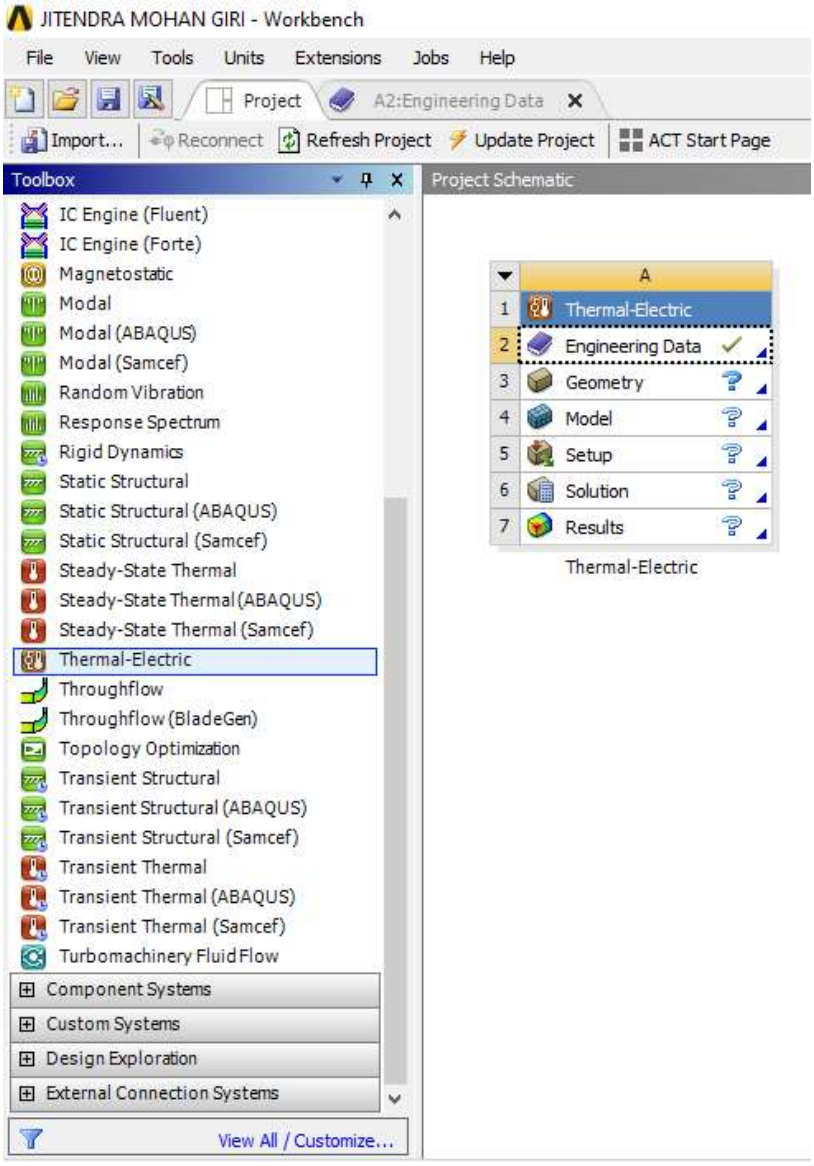

Figure 7.2 Toolbox region of ANSYS®

The problem related engineering data (such as density of a material, specific heat capacity of a material etc.) is provided during this stage. The geometric model can be either created or imported. In this work, the 3D models are created using DesignModeler which is a parametric solid modelling feature of the ANSYS® software and shown in Figure 7.3. The desired unit system for the work can be selected. The appropriate materials are assigned to the model. The model is discretized into small elements and the mesh is generated. The boundary conditions are specified, initial and other settings are provided.

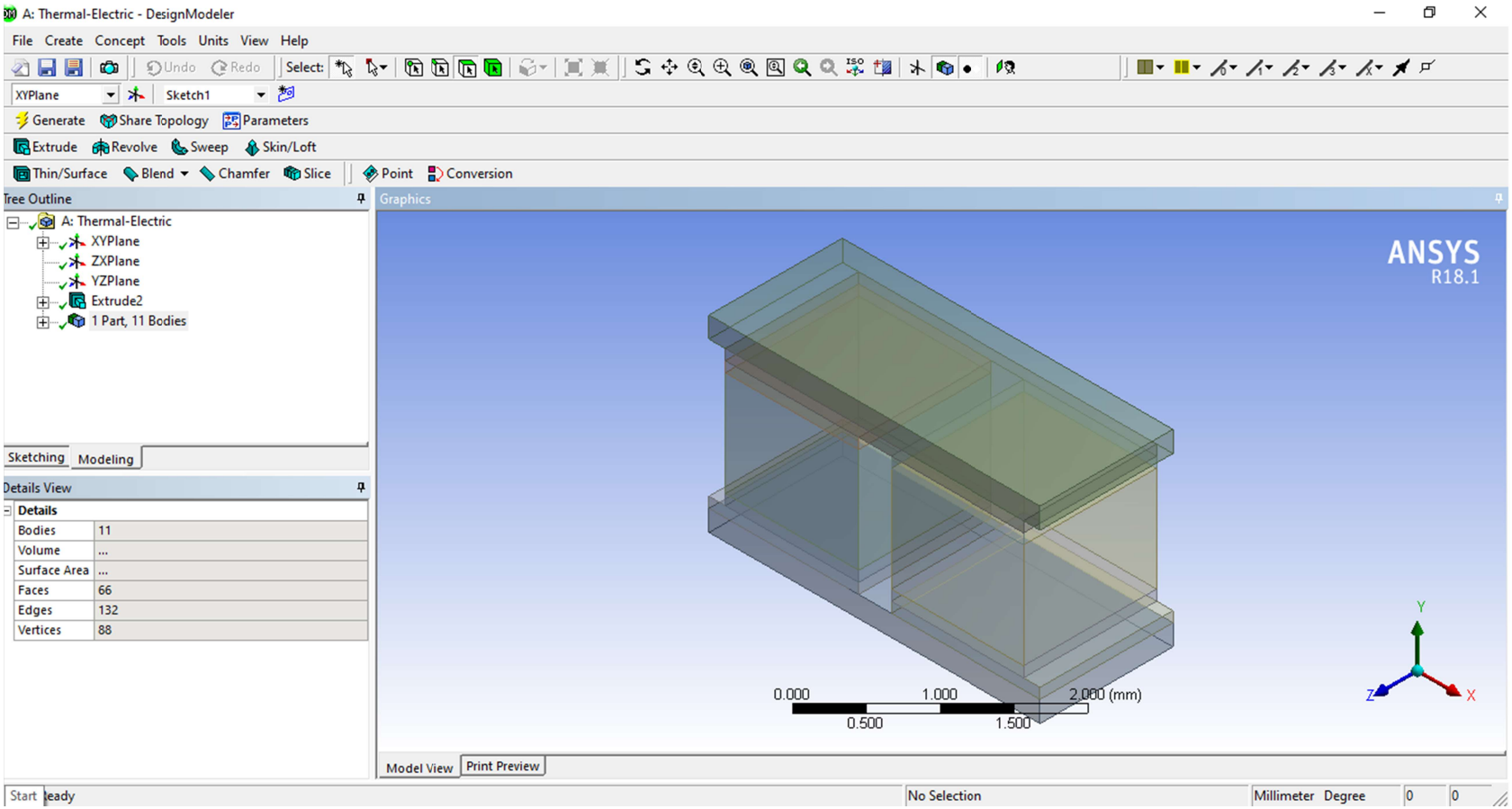

Figure 7.3 DesignModeler application of ANSYS®

7.3.2 Solution

In this phase, the problem is solved for the solutions. If the information given in the previous steps is complete, this step is performed by the ANSYS® solver. At last, the set of equations that results are solved.

7.3.3 Post-processing

The user will check and analyze the results after obtaining a solution in a session. In this phase of post-processing, the solutions are displayed in various forms (such as surface plots, colour contours etc.). The results are reviewed according to the choice (graphical display or the listing of various findings).

7.4 Simulations for Results Validation

Finite-element simulation is a computational tool for resolving real-world complex engineering problems. The genetic algorithm optimization results are validated using finite element simulations. ANSYS® is a very useful, common purpose finite-element simulation tool. It is used to numerically solve a broad range of engineering problems. Hence, ANSYS® is used in this work. The ANSYS® Thermal-Electric module can solve the thermal and electrical couple-field of TEC.

7.4.1 Simulation for result validation of optimized cooling capacity

For the steady-state analysis of the TEC model, the thermal-electric module is used in this study. The model is set up as a non-linear three-dimensional finite-element model. According to the GA result for optimization of cooling capacity (as reported in chapter 4), the model in this work is developed using a single pair of n-type and p-type components. This study employs a novel approach to account for the effect of electric contact resistance on the TEC performance. The finite-element simulation incorporates four additional geometrical parts labelled as ‘Contact’ that are used to model the effect of the electric contact resistance. The material properties of these parts are based on the thermo-electric behavior of electrical contact resistance. At each end of the TE elements, ‘Contact’ geometries are formed. Figure 7.4 displays the full schematic of the TEC model for Finite-element simulation to verify GA performance.

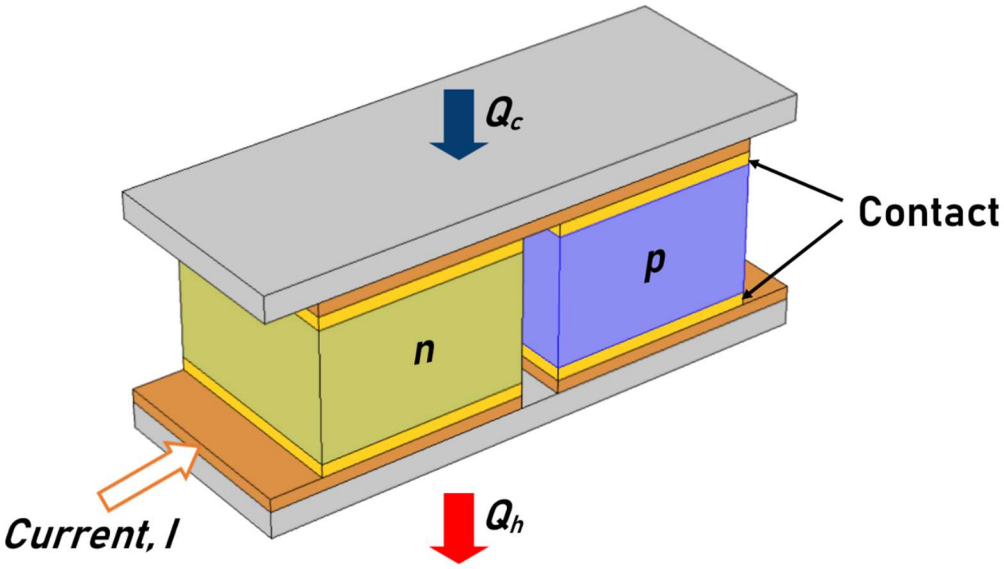

Figure 7.4 Schematic of thermoelectric cooler for finite-element simulation to validate GA results

The length of n-type and p-type elements is considered as 1.0 mm to validate GA predictions for maximum Q_c, as can be seen in Table 4.4. The thermoelectric elements have a 1.27 mm square cross-section. The distance between elements of the p-and n-types is 0.31 mm. The material properties for this simulation are computed at average temperature (T_{ave}) of T_h and T_c values obtained during the GA-based optimization of Q_c. Table 7.1 displays the modelled TEC's finite-element simulation input parameters.

Table 7.1 Finite-element simulation input parameters for maximum Q_c

Description	Parameter	Value per pair of TE Elements
Cooling Capacity	Q_c	0.1514 W
Electric current	I	2.993 A
Temperature (At the hot side of TEC)	T_{ho}	27.84 °C

To model adiabatic heat transfer from the exposed surfaces of thermoelectric cooler, a slight convection loss of 0.000001 W/mK was applied on all surfaces except the ones on which boundary conditions mentioned in Table 7.1 are specified. The computationally generated mesh, electrical voltage, and temperature distribution across the finite-element model of the thermoelectric cooler are illustrated in Figure 7.5.

In Table 7.2, the parameters obtained from the finite-element simulation are compared to the genetic algorithm results. The results obtained from genetic algorithm-based optimization and those obtained from finite-element simulation for a single pair of thermoelectric elements are found to be very similar. The finite-element simulation result represents a three-dimensional solution based on a numerical technique, while the genetic algorithm results are based on one-dimensional analytical equations. Hence, the optimization result obtained by genetic algorithm is verified through the solutions of the thermal-electric module of ANSYS®.

Table 7.2 Comparison of GA and ANSYS® results for maximum cooling capacity (Q_c)

Description	Parameter	GA	ANSYS®	Remarks
Cold surface temperature	T_{co}	20 ℃	20.25 ℃	Value per pair of TE elements
Rate of heat rejection	Q_h	0.507 W	0.508 W	
Input Electric Power	P	0.356 W	0.357 W	

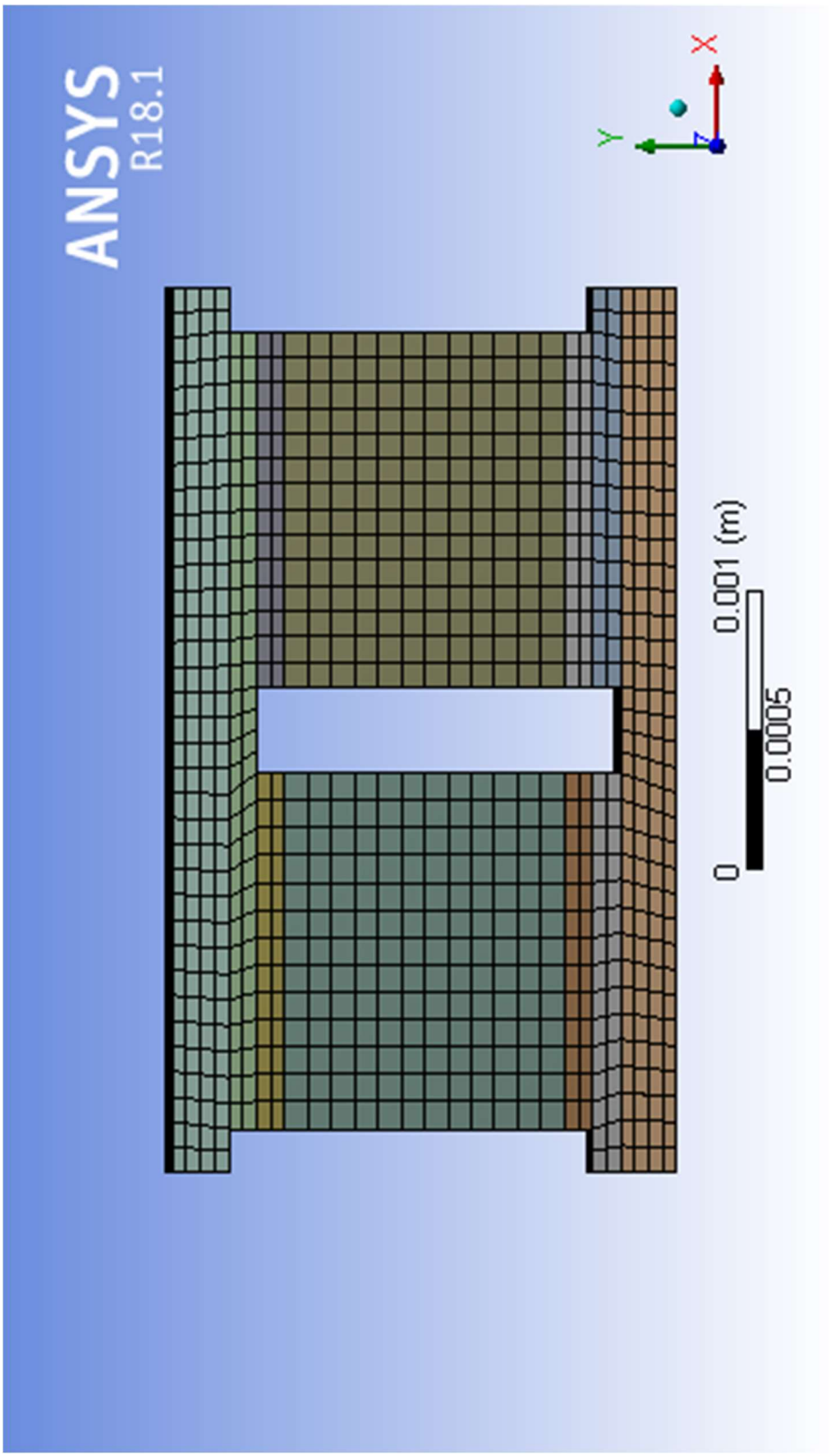

(a)

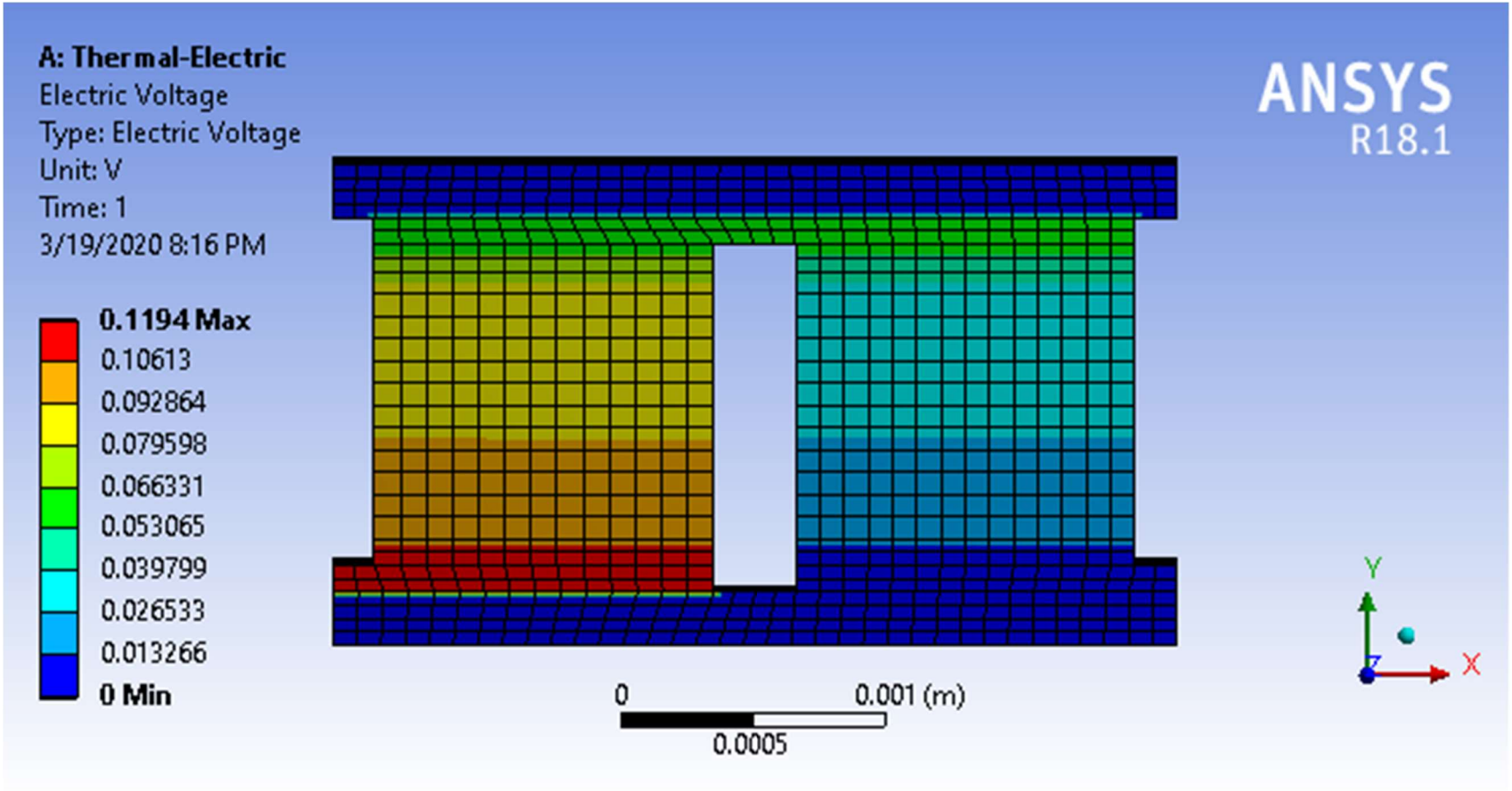
A: Thermal-Electric
Electric Voltage
Type: Electric Voltage
Unit: V
Time: 1
3/19/2020 8:16 PM
0.1194 Max
0.10613
0.092864
0.079598
0.066331
0.053065
0.039799
0.026533
0.013266
0 Min
ANSYS
R18.1
0
0.001 (m)
0.0005
Y
X

(b)

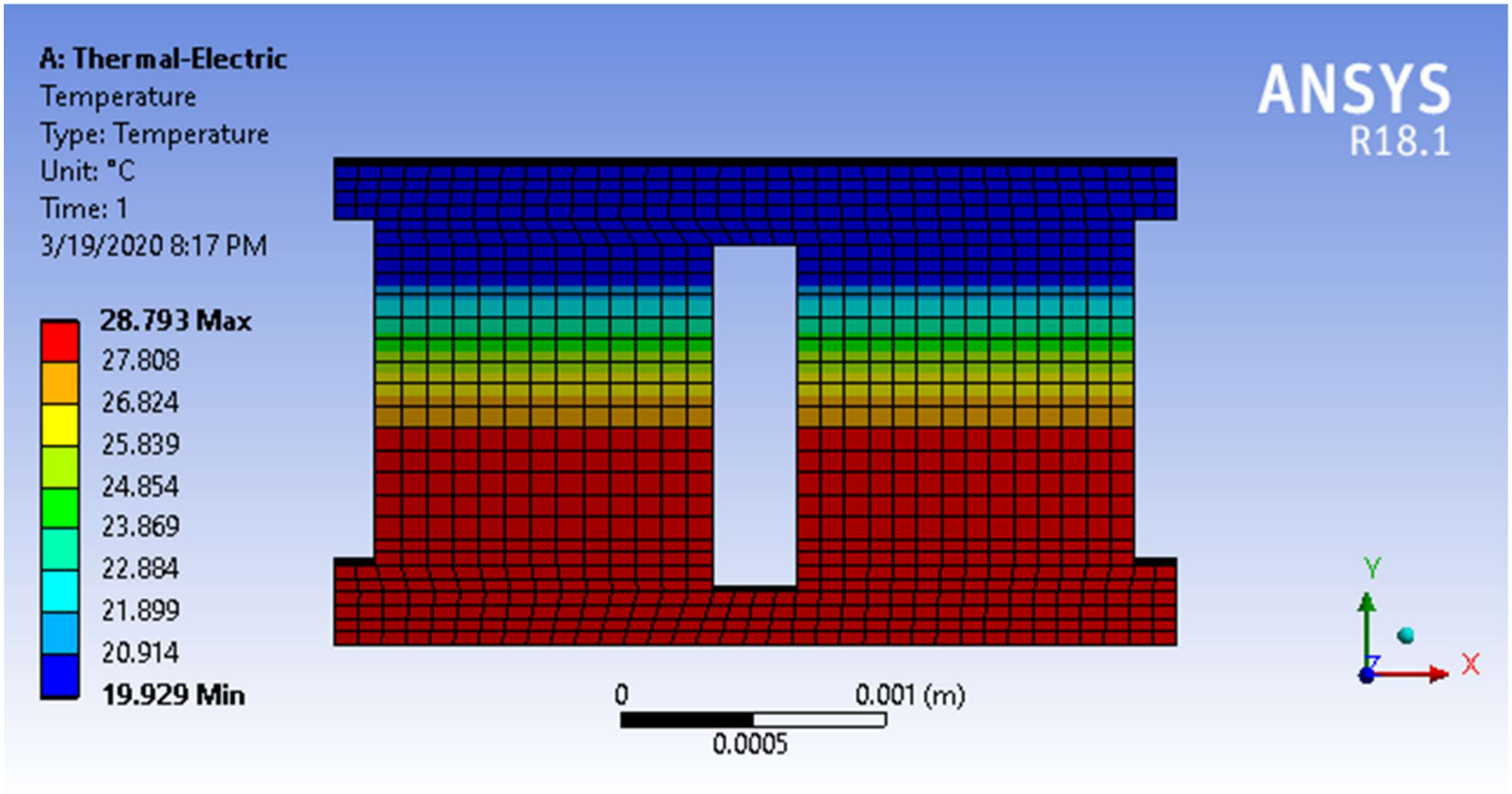

(c)

Figure 7.5 (a) Mesh (b) Voltage distribution (c) Temperature distribution in the finite-element TEC model for maximum Q_C

7.4.2 Simulation for result validation of optimized *COP*

ANSYS® software is used to perform a finite-element simulation for maximum coefficient of performance in this section. The steady-state thermoelectric cooler model is made up of thermoelectric elements with a length of 2.0 mm, as mentioned in Table 5.2. The thermoelectric elements have a 1.4 mm square cross-section. The n-type and p-type thermoelectric elements are 0.38 mm apart. The temperature-dependent material properties are computed on the basis of average of $T_{h,}$ and T_c observed during genetic algorithm based optimization of coefficient of performance. Table 7.3 displays the thermoelectric cooler model's input parameters for finite element simulation.

Table 7.3 Finite-element simulation input parameters for maximum coefficient of performance (*COP*)

Description	Parameter	Value per pair of TE Elements
Cooling Capacity	Q_c	0.0165 W
Electric current	I	0.283 A
Temperature (At the hot side of TEC)	T_{ho}	25.09 ℃

The proposed genetic algorithm based *COP* optimization is validated using three-dimensional finite element analysis. The three-dimensional steady-state thermoelectric cooler model is created, and for maximum coefficient of performance, genetic algorithm based optimization predictions are tested.

For this finite-element simulation, the mesh, electric voltage, and temperature distribution are shown in Figure 7.6.

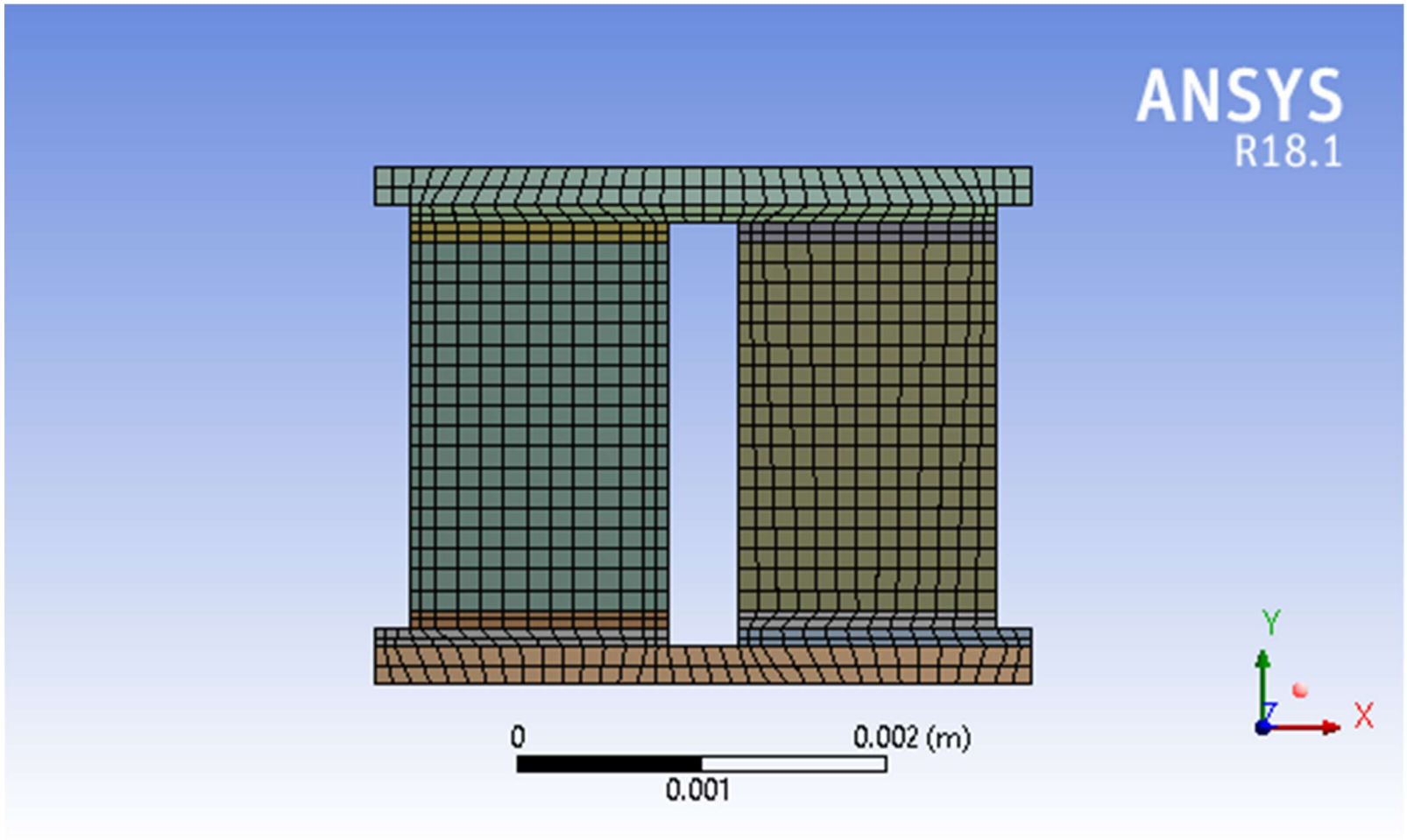

(a)

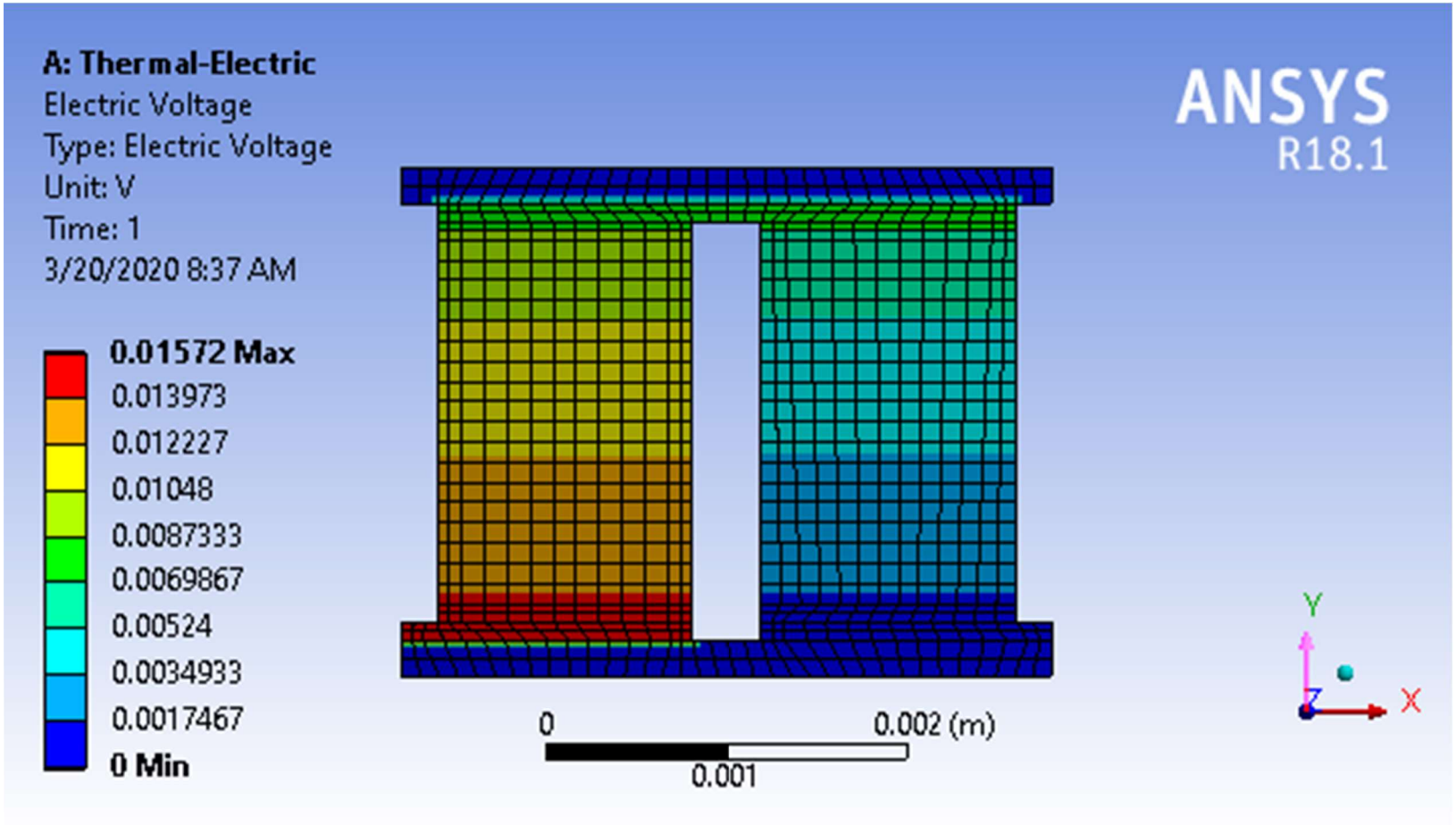
A: Thermal-Electric
Electric Voltage
Type: Electric Voltage
Unit: V
Time: 1
3/20/2020 8:37 AM
0.01572 Max
0.013973
0.012227
0.01048
0.0087333
0.0069867
0.00524
0.0034933
0.0017467
0 Min
ANSYS
R18.1
0
0.002 (m)
0.001
Y
X

(b)

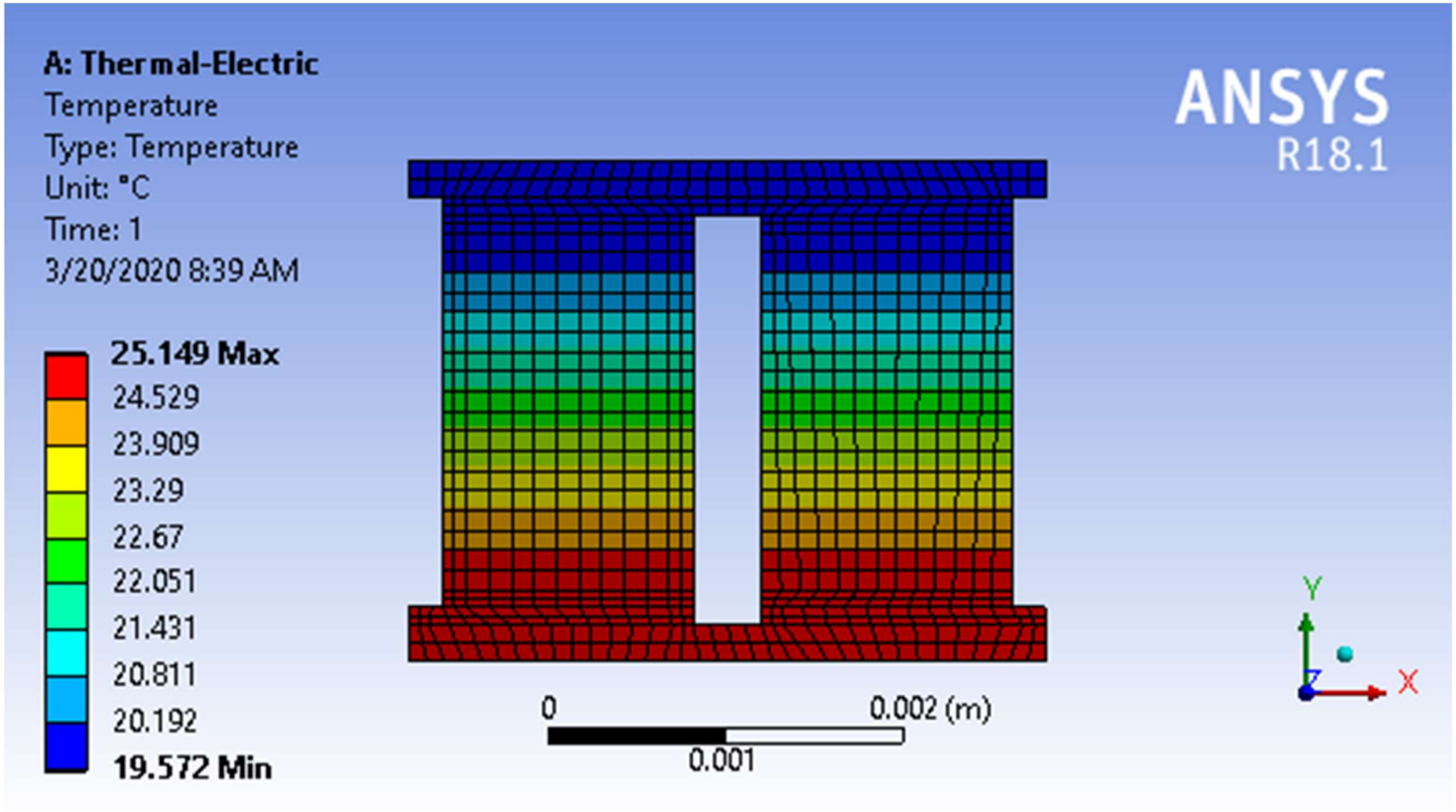

(c)

Figure 7.6 (a) Mesh (b) Voltage distribution (c) Temperature distribution in the finite-element TEC model for maximum *COP*

The GA results and the results from the finite-element simulation agree well. Table 7.4 compares and reports the parameters for GA and finite-element simulation performance.

Table 7.4 Comparison of GA and ANSYS® results for maximum coefficient of performance (*COP*)

Description	Parameter	GA	ANSYS®	Remarks
Cold surface temperature	T_{co}	20 ℃	19.61 ℃	Value per pair of TE elements
Rate of heat rejection	Q_h	0.021 W	0.021 W	
Input Electric Power	P	0.004 W	0.004 W	

The ANSYS® result is consistent with GA-based optimization results for the maximization of *COP*. With Q_c and P values from finite-element simulation, *COP* is very nearly matched. Hence, the optimization result is verified through the solutions of the thermal-electric module of ANSYS®.

Validated finite-element numerical simulation are beneficial as experimental methods are normally costly and time-consuming, even impossible sometimes. The strong agreement between these findings and optimization results obtained using the genetic algorithm demonstrates the efficacy of our method in this study. In the next part of this study, a similar approach will be applied to validate other results.

7.4.3 Simulation for result validation of optimized first law and second law efficiency

Finite-element simulation is a powerful computational tool for approximate solutions to various complex real-world engineering problems with given boundary conditions. It has become an important software application for the assessment of real-world engineering problems. In this segment, finite-element simulation is performed to validate GA results for

maximization of energy and exergy efficiencies. Since the maximum energy and exergy efficiency are achieved with the same amount of I, L, and A, either of the two maximization results can be evaluated. The maximum exergy efficiency has been selected to be verified. Because of environmental considerations, it may be the recommended basis for TEC design. A three-dimensional non-linear finite-element model has been set up. Following the genetic algorithm result, this finite-element model consists of a thermoelectric cooler structure with one pair of n-type and p-type thermoelectric elements.

The input parameters for finite-element simulations to validate the genetic algorithm result of maximum exergy efficiency of thermoelectric cooler are given in Table 7.5. A small convection loss of 0.000001 W/mK is applied to all surfaces of the adiabatic heat transfer models from the exposed surfaces of the thermoelectric cooling device, except for those for which the boundary conditions are defined in Table 7.5.

Table 7.5 Finite-element simulation input parameters for maximum exergy efficiency (η_I)

Description	Parameter	Value per pair of TE Elements
Cooling Capacity	Q_c	0.0165 W
Electric current	I	0.28 A
Temperature (At the hot side of TEC)	T_{ho}	25.09 ℃

The steady-state finite-element TEC model for validating GA results has thermoelectric elements of length and cross-sectional area as reported in Table 6.4. The material properties of thermoelectric elements are temperature-dependent and computed using T_c and T_h values. The GA predictions for maximum exergy efficiency (η_{II}) were tested. The mesh generated for this simulation, electric voltage distribution, and temperature distribution are shown in Figure 7.7.

The result of the finite-element simulation is in strong alignment with those predicted by

genetic algorithm. Table 7.6 shows the comparison of the findings.

Table 7.6 Comparison of GA and ANSYS® results for maximum exergy efficiency (η_{II})

Description	Parameter	GA	ANSYS®	Remarks
Input Electric Power	P	0.004 W	0.004 W	Value per pair of TE elements
Rate of heat rejection	Q_h	0.021 W	0.021 W	
Cold surface temperature	T_{co}	20 ℃	19.61 ℃	

As can be seen from the comparison presented in Table 7.6, the values of P and Q_h are nearly identical, while T_{co} differs slightly which is quite acceptable. The ANSYS® result strongly matches the genetic algorithm result. With the values of Q_c, Q_h, T_{ho}, T_{co}, and I from finite-element simulation, the maximum value of exergy efficiency is very closely matched to GA result. The ANSYS® thermal-electric module solutions validate the GA optimization result.

Over the last few decades, the finite-element analysis has evolved into a critical technology for modeling and simulation of a wide range of engineering systems. As techniques for rapid and efficient modeling and simulation become more important in the development of advanced engineering devices, the use of finite-element analsyis has increased significantly. In this work, the finite-element numerical simulations display excellent concordance with GA solutions.

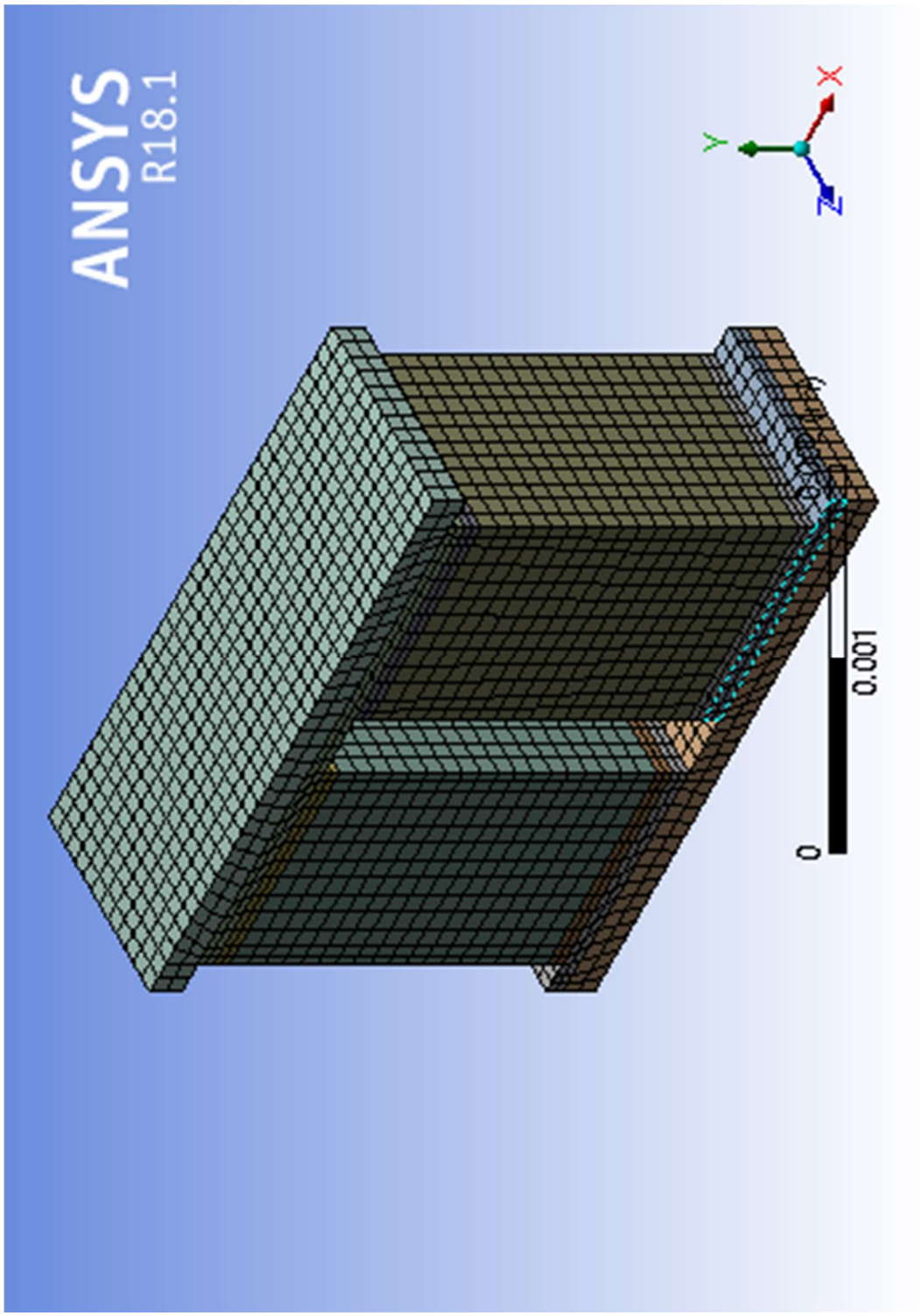

(a)

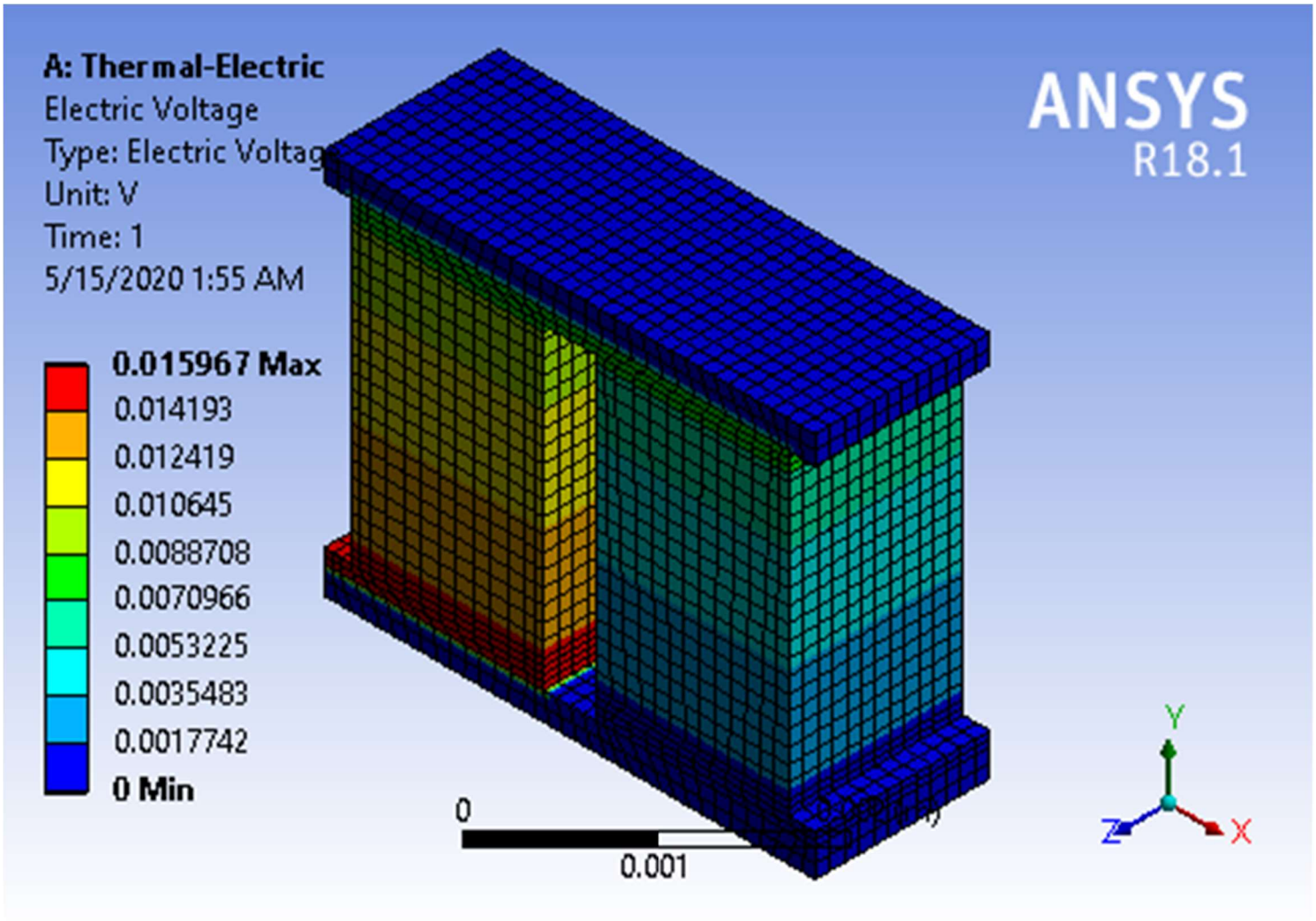
A: Thermal-Electric
Electric Voltage
Type: Electric Voltag
Unit: V
Time: 1
5/15/2020 1:55 AM
0.015967 Max
0.014193
0.012419
0.010645
0.0088708
0.0070966
0.0053225
0.0035483
0.0017742
0 Min
ANSYS
R18.1
0
0.001
Y
Z
X

(b)

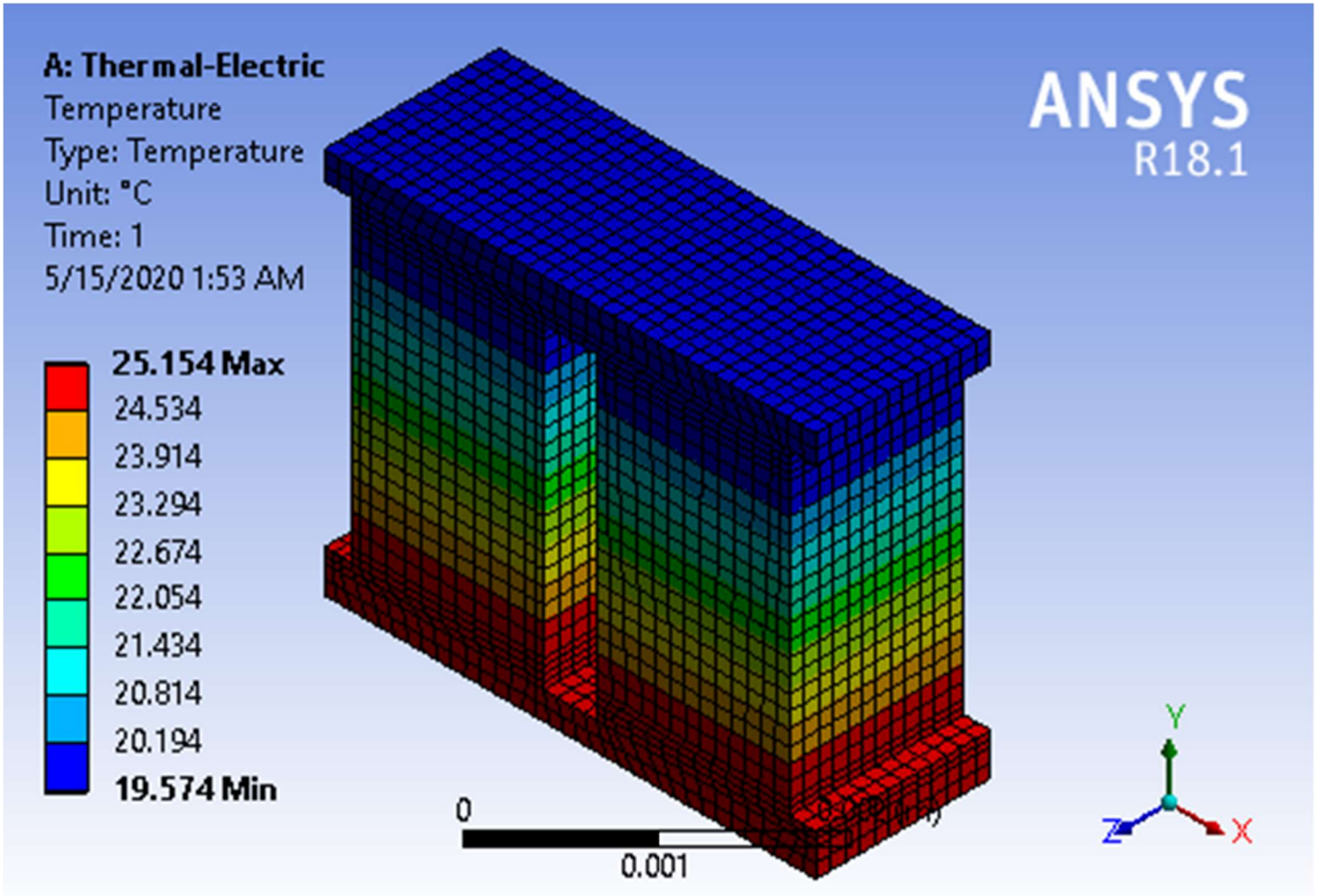

(c)

Figure 7.7 (a) Mesh (b) Voltage distribution (c) Temperature distribution in the finite-element TEC model for maximum η_{II}

7.5 Summary

In this chapter, the finite element simulations are performed to validate GA based optimization results as reported in chapter 4-6. The three dimensional finite-element models are prepared as well as finite-element simulations are conducted using ANSYS® software. By using material library tool, the material properties (such as thermal conductivity, Seebeck coefficient, electrical conductivity etc.) were applied. The boundary conditions were applied before obtaining simulation results. In this study, the performances of finite-element simulations are compared with GA results. The below-mentioned significant points are made from this work.

- The engineering problem could be solved successfully when the simulation setup allows for the physical effect to be added to the model.
- The genetic algorithm solutions are examined using finite-element simulation with the ANSYS® thermal-electric module. The GA results are based on 1-D analytical equations, while the finite-element simulation result provides a 3-D solution based on a numerical technique.
- The optimal configurations obtained through genetic algorithm based optimization aimed for maximization of cooling capacity, maximization of coefficient of performance and maximization of exergy efficiency were compared with the finite-element simulation results.
- The GA results and finite-element simulation results for a single pair of thermoelectric elements are found to be nearly identical. They are in close agreement. As an outcome, the GA optimization results are validated using ANSYS® thermal-electric module solutions.

CHAPTER 8

CONCLUSIONS AND RECOMMENDATIONS FOR FUTURE WORK

CHAPTER 8

CONCLUSIONS AND RECOMMENDATIONS FOR FUTURE WORK

8.1 Conclusions

The solid-state energy conversion technology of thermoelectrics is of significant relevance. A thermoelectric cooler has the capability to convert electrical energy into a heat flux. The potential application for temperature control and the recent improvements in the performance of thermoelectric coolers have attracted great interest among researchers. Thermoelectric coolers are widely used in many application domains such as electronics, medicine, space, telecommunications, and several others. Thermoelectric cooling systems are needed for modern laser, radio-electronic, and optical systems to operate efficiently. Thermoelectric coolers have some significant benefits such as:

- No moving parts
- No refrigerants
- Ecologically clean energy conversion
- Reduced weight and size
- Low-noise mode of operation
- Capable to operate in every spatial position
- High reliability

All of these benefits make thermoelectric coolers a potential alternate. However, the TEC performance has remained inferior as compared to the conventional compressor based cooling devices. In order to compete with traditional cooling devices, thermoelectric coolers need improvements in various performance parameters such as cooling capacity, coefficient of performance, and exergetic efficiency. A TEC system is affected by contact

resistances. Hence, the overall modelling of the system is quite critical. This research provides novel optimization strategies to the field of thermoelectric cooling systems. With its original work, this research adds to the existing knowledge about thermoelectric cooling systems. The intent to provide optimized solutions for TEC with maximization objectives of important performance parameters with a new set of design variables has been accomplished.

The following are the main characteristics of the current work:

- This study contributes with a unique modeling and optimization strategy for thermoelectric cooling systems. The dimensional structural and operating variables of the TEC system are efficaciously incorporated for the performance optimization within the space restrictions. The length (L) and cross-sectional area (A) of p-type and n-type thermoelectric elements, and input electric current (I) have have been set as design variables. No study has reported the simultaneous use of these variables.
- This research also considers the various kinds of significant effects such as thermal contact resistance, electrical contact resistance, and heat sink resistance. Not all these aspects were taken simultaneously by previous researchers, which makes the work distinct.
- The two popular stochastic algorithms namely genetic algorithm (GA) and simulated annealing (SA) are considered to find out the optimum results with the design variables. By integrating suitable heuristics in the optimization algorithm, the task of determining interface temperatures is incorporated to find accurate feasible solutions. In previous studies, end temperatures have been used to calculate performance parameters instead of interface temperatures. The exact temperatures at interfaces are used in this research. It makes the current analysis more precise due to the accurate model.

Based on the present work, the following conclusions are drawn.

1. When genetic algorithm and simulated annealing are used for a pilot optimization study, it has been observed that both GA and SA converged to the same optimal value of the objective function. SA has obtained a single optimal solution. However, GA has

discovered three optimal solutions having the same objective function value at different sets of design variables. GA has been able to capture the multimodality of the pilot problem. Hence considering the performance, GA is found as a suitable choice in this class of optimization problem.

2. Taking L, A, and I as independent design variables, 8.476 W value of the maximum cooling capacity (Q_c) is obtained. At the maximized Q_c condition, the COP is 0.425. Within the permitted range of 1.0-2.0 mm, the optimal value of L is 1.0 mm. The optimal I, A, and N for maximum Q_c are found as 2.993 A, 1.607 $mm^{2,}$ and 56 respectively. It is then concluded that the length of thermoelectric elements is best to be on the lower side to achieve maximum Q_c.
3. From second optimization study, the maximum COP is found as 4.11. The optimal I, L, A, and N are 0.283 A, 2.0 mm, 1.956 $mm^{2,}$ and 45. The maximized COP is obtained with a corresponding 0.745992 W value of Q_c. In this case, L hits the upper limit of the range. It is observed that a higher value of L is desired for maximizing COP. The optimization results for Q_c and COP indicate that both objectives conflict. An optimum Q_c does not ensure an optimum COP and vice versa. Under these circumstances, only one performance parameter can be maximized according to the need. It has been noticed that during Q_c optimization, the typical TE element length is considerably less than the optimal length to maximize COP.
4. An optimal current of 2.993 A for maximum Q_c and 0.283 A for maximum COP is found. It is observed that a higher value of current is desired for increasing heat transfer due to the Peltier effect. However, it also increases Joule heating and affects the TEC performance. With a high current, a low value of L/A ratio is required to reduce the Joule effect and optimize Q_c. The electrical power and Joule heating is a quadratic function of current. Hence, to maximize COP, a lower value of current is needed.
5. Based on the present analysis, it has been observed that a lower L/A for optimum Q_c and higher L/A for optimum COP are required. At optimized conditions of Q_c and COP, L/A ratios are 0.622 and 1.022 respectively. A trade-off between two objectives may be used to play a balanced TEC performance. A suitable L/A within the range 0.622 - 1.022 may be selected for this decision in combination with the current value ranging from 2.993 - 0.283 A.

6. The single objective optimization results for energy efficiency (η_I) and the exergy efficiency (η_{II}) demonstrate that at the same current, both the efficiencies are maximized. This aspect is supported by the previously reported work [131]. Further, this study has established that the maximum η_I and η_{II} (4.116 and 0.0715 respectively) are obtained not only at the same current but also at the same value of the length and cross-sectional area of thermoelectric elements. It is an important bearing that by maximizing second law efficiency rather than both, we ensure that we have achieved optimized first law efficiency.
7. The numerical simulation abilities of finite-element ANSYS® software have been successfully used to validate GA results. The simulation results for Q_c, *COP,* and exergy efficiency are very close to GA results. The temperatures are varying within 2%. The heat rejection rate and the input electric power are varied by less than 1%. Finite-element simulation results confirmed the GA results. Hence, it is concluded that all of the mathematical GA results obtained using a 1-D heat transfer model are validated by a 3-D analysis performed using ANSYS®. With the values of Q_h, T_{ho}, T_{co}, and I from finite-element simulation the maximum values of Q_c, *COP,* and exergy efficiency are very closely matched to GA predictions.

8.2 Recommendations for Future Work

In this study, significant work has been done for the performance optimization of thermoelectric coolers. There is still potential for future investigations. The following future research directions are recommended.

- The approach of this work can be considered for the investigation of multi-stage TEC systems in future research.
- It is recommended that researchers continue to use the models described here to optimize the performance of thermoelectric coolers with non-constant elements' area.
- It may be worthwhile to investigate the performance of annular TEC as well.
- Experiments in conjunction with numerical optimization can be performed.

REFERENCES

REFERENCES

[1] Z. Ma *et al.*, "Review of experimental approaches for improving zT of thermoelectric materials," *Materials Science in Semiconductor Processing*, vol. 121. Elsevier Ltd, p. 105303, Jan. 01, 2021, doi: 10.1016/j.mssp.2020.105303.

[2] D. Zhao and G. Tan, "A review of thermoelectric cooling: Materials, modeling and applications," *Applied Thermal Engineering*, vol. 66, no. 1–2. Pergamon, pp. 15–24, May 01, 2014, doi: 10.1016/j.applthermaleng.2014.01.074.

[3] R. He, G. Schierning, and K. Nielsch, "Thermoelectric Devices: A Review of Devices, Architectures, and Contact Optimization," Advanced Materials Technologies, vol. 3, no. 4, p. 1700256, Apr. 2018, doi: 10.1002/admt.201700256.

[4] D. M. Rowe, *CRC Handbook of Thermoelectrics*. 1995.

[5] H. S. Lee, *Thermoelectrics: Design and materials*. wiley, 2016.

[6] D. Beretta *et al.*, "Thermoelectrics: From history, a window to the future," *Materials Science and Engineering R: Reports*, vol. 138. Elsevier Ltd, p. 100501, Oct. 01, 2019, doi: 10.1016/j.mser.2018.09.001.

[7] D. K. C. MacDonald, *Thermoelectricity: An Introduction to the Principles*. 2006.

[8] N. M. Ravindra, B. Jariwala, A. Bañobre, and A. Maske, *Thermoelectrics : Fundamentals, Materials Selection, Properties, and Performance*. Cham: Springer International Publishing, 2019.

[9] C. Goupil, *Continuum Theory and Modeling of Thermoelectric Elements*. Wiley, 2016.

[10] A. F. Joffe, "The Revival of Thermoelectricity on JSTOR," Scientific American, vol. 199, no. 5, pp. 31–37, 1958, Accessed: Apr. 07, 2021. [Online]. Available: https://www.jstor.org/stable/24944818?seq=1.

[11] B. S. Finn, "Thomson's dilemma," Physics Today, vol. 20, no. 9, pp. 54–59, Sep. 1967, doi: 10.1063/1.3034483.

[12] Y. Apertet and C. Goupil, "On the fundamental aspect of the first Kelvin's relation in thermoelectricity," International Journal of Thermal Sciences, vol. 104, pp. 225–227, Jun. 2016, doi: 10.1016/j.ijthermalsci.2016.01.009.

[13] R. de A. Martins, "Joule's 1840 manuscript on the production of heat by voltaic electricity,"

Notes and Records: the Royal Society Journal of the History of Science, Sep. 2020, doi: 10.1098/rsnr.2020.0027.

[14] "Thermoelectrics - Basic Principles and New Materials Developments | G.S. Nolas | Springer." https://www.springer.com/gp/book/9783540412458 (accessed Apr. 08, 2021).

[15] K. Kurosaki, Y. Takagiwa, and X. Shi, *Thermoelectric Materials-Principles and Concepts for Enhanced Properties*. De Gruyter, 2020.

[16] I. T. Witting *et al.*, "The Thermoelectric Properties of Bismuth Telluride," Advanced Electronic Materials, vol. 5, no. 6, p. 1800904, Jun. 2019, doi: 10.1002/aelm.201800904.

[17] L. Chen, R. Liu, and X. Shi, *Thermoelectric Materials and Devices - 1st Edition*. Elsevier Science Ltd, 2020.

[18] Y. H. Cheng and W. K. Lin, "Geometric optimization of thermoelectric coolers in a confined volume using genetic algorithms," Applied Thermal Engineering, vol. 25, no. 17–18, pp. 2983–2997, Dec. 2005, doi: 10.1016/j.applthermaleng.2005.03.007.

[19] L. Shen *et al.*, "Performance enhancement investigation of thermoelectric cooler with segmented configuration," Applied Thermal Engineering, vol. 168, p. 114852, Mar. 2020, doi: 10.1016/j.applthermaleng.2019.114852.

[20] X. D. Wang, Q. H. Wang, and J. L. Xu, "Performance analysis of two-stage TECs (thermoelectric coolers) using a three-dimensional heat-electricity coupled model," Energy, vol. 65, pp. 419–429, Feb. 2014, doi: 10.1016/j.energy.2013.10.047.

[21] R. Lamba, S. Manikandan, S. C. Kaushik, and S. K. Tyagi, "Thermodynamic modelling and performance optimization of trapezoidal thermoelectric cooler using genetic algorithm," Thermal Science and Engineering Progress, vol. 6, pp. 236–250, Jun. 2018, doi: 10.1016/j.tsep.2018.04.010.

[22] S. Lin and J. Yu, "Optimization of a trapezoid-type two-stage Peltier couples for thermoelectric cooling applications," International Journal of Refrigeration, vol. 65, pp. 103–110, May 2016, doi: 10.1016/j.ijrefrig.2015.12.007.

[23] G. Fraisse, J. Ramousse, D. Sgorlon, and C. Goupil, "Comparison of different modeling approaches for thermoelectric elements," Energy Conversion and Management, 2013, doi: 10.1016/j.enconman.2012.08.022.

[24] S. B. Riffat, X. Ma, and R. Wilson, "Performance simulation and experimental testing of a novel thermoelectric heat pump system," Applied Thermal Engineering, vol. 26, no. 5–6,

pp. 494–501, Apr. 2006, doi: 10.1016/j.applthermaleng.2005.07.016.

[25] D. Astrain, J. G. Vián, A. Martínez, and A. Rodríguez, “Study of the influence of heat exchangers’ thermal resistances on a thermoelectric generation system,” Energy, vol. 35, no. 2, pp. 602–610, Feb. 2010, doi: 10.1016/j.energy.2009.10.031.

[26] M. Chen and G. J. Snyder, “Analytical and numerical parameter extraction for compact modeling of thermoelectric coolers,” International Journal of Heat and Mass Transfer, vol. 60, no. 1, pp. 689–699, May 2013, doi: 10.1016/j.ijheatmasstransfer.2013.01.020.

[27] S. Lineykin and S. Ben-Yaakov, “Analysis of thermoelectric coolers by a spice-compatible equivalent-circuit model,” IEEE Power Electronics Letters, vol. 3, no. 2, pp. 63–66, 2005, doi: 10.1109/LPEL.2005.846822.

[28] Zhaoxia Luo, “A Simple Method to Estimate the Physical Characteristics of a Thermoelectric Cooler from Vendor Datasheets | Electronics Cooling,” 2008. https://www.electronics-cooling.com/2008/08/a-simple-method-to-estimate-the-physical-characteristics-of-a-thermoelectric-cooler-from-vendor-datasheets/ (accessed Mar. 31, 2021).

[29] B. J. Huang, C. J. Chin, and C. L. Duang, “Design method of thermoelectric cooler,” International Journal of Refrigeration, vol. 23, no. 3, pp. 208–218, May 2000, doi: 10.1016/S0140-7007(99)00046-8.

[30] D. Mitrani, J. A. Tomé, J. Salazar, A. Turó, M. J. García, and J. A. Chávez, “Methodology for extracting thermoelectric module parameters,” IEEE Transactions on Instrumentation and Measurement, vol. 54, no. 4, pp. 1548–1552, Aug. 2005, doi: 10.1109/TIM.2005.851473.

[31] Y. Cai, D. D. Zhang, D. Liu, F. Y. Zhao, and H. Q. Wang, “Air source thermoelectric heat pump for simultaneous cold air delivery and hot water supply: Full modeling and performance evaluation,” Renewable Energy, vol. 130, pp. 968–981, Jan. 2019, doi: 10.1016/j.renene.2018.07.007.

[32] Y. Zhou, T. Zhang, F. Wang, and Y. Yu, “Performance analysis of a novel thermoelectric assisted indirect evaporative cooling system,” Energy, vol. 162, pp. 299–308, Nov. 2018, doi: 10.1016/j.energy.2018.08.013.

[33] Y. M. Seo, M. Y. Ha, S. H. Park, G. H. Lee, Y. S. Kim, and Y. G. Park, “A numerical study on the performance of the thermoelectric module with different heat sink shapes,” Applied

Thermal Engineering, vol. 128, pp. 1082–1094, Jan. 2018, doi: 10.1016/j.applthermaleng.2017.09.097.

[34] A. Allouhi *et al.*, "Dynamic analysis of a thermoelectric heating system for space heating in a continuous-occupancy office room," Applied Thermal Engineering, vol. 113, pp. 150–159, Feb. 2017, doi: 10.1016/j.applthermaleng.2016.11.001.

[35] Z. Liu *et al.*, "Modeling and simulation of a photovoltaic thermal-compound thermoelectric ventilator system," Applied Energy, vol. 228, pp. 1887–1900, Oct. 2018, doi: 10.1016/j.apenergy.2018.07.006.

[36] R. McCarty, "A comparison between numerical and simplified thermoelectric cooler models," Journal of Electronic Materials, vol. 39, no. 9, pp. 1842–1847, Sep. 2010, doi: 10.1007/s11664-010-1075-x.

[37] O. Owoyele, S. Ferguson, and B. T. O'Connor, "Performance analysis of a thermoelectric cooler with a corrugated architecture," Applied Energy, vol. 147, pp. 184–191, Jun. 2015, doi: 10.1016/j.apenergy.2015.01.132.

[38] D. V. K. Khanh, P. M. Vasant, I. Elamvazuthi, and V. N. Dieu, "Geometric optimisation of thermo-electric coolers using simulated annealing," International Journal of Computational Science and Engineering, vol. 14, no. 3, pp. 279–289, 2017, doi: 10.1504/IJCSE.2017.084164.

[39] R. Lamba, S. C. Kaushik, and S. K. Tyagi, "Geometric optimization of trapezoidal thermoelectric heat pump considering contact resistances through genetic algorithm," International Journal of Energy Research, vol. 42, no. 2, pp. 633–647, Feb. 2018, doi: 10.1002/er.3845.

[40] S. Soprani, J. H. K. Haertel, B. S. Lazarov, O. Sigmund, and K. Engelbrecht, "A design approach for integrating thermoelectric devices using topology optimization," Applied Energy, vol. 176, pp. 49–64, Aug. 2016, doi: 10.1016/j.apenergy.2016.05.024.

[41] M. Saifizi, M. S. Zakaria, S. Yaacob, and K. Wan, "Development and Analysis of Hybrid Thermoelectric Refrigerator Systems," in *IOP Conference Series: Materials Science and Engineering*, Mar. 2018, vol. 318, no. 1, p. 012036, doi: 10.1088/1757-899X/318/1/012036.

[42] S. Lal and E. Kumari, "Performance Analysis of a Low Price Thermoelectric Cooler: An Experimental Approach," International Conference & Expo on Advances in Power Generation from Renewable Energy Sources, no. Apgres, pp. 76–82, 2017.

[43] V. . Dongare and R. . Kinare, “Design and Development of Thermoelectric Refrigerator,” International Research Journal of Engineering and Technology, vol. 5, no. 4, pp. 2970–2974, 2018, Accessed: Mar. 31, 2021. [Online]. Available: www.irjet.net.

[44] M. Ebrahimi and E. Derakhshan, “Design and evaluation of a micro combined cooling, heating, and power system based on polymer exchange membrane fuel cell and thermoelectric cooler,” Energy Conversion and Management, vol. 171, pp. 507–517, Sep. 2018, doi: 10.1016/j.enconman.2018.06.007.

[45] S. Sm *et al.*, “Performance study on thermoelectric cooling and heating system with cascaded and integrated approach,” ~ 1348 ~ International Journal of Chemical Studies, vol. 6, no. 1, pp. 1348–1354, 2018, Accessed: Mar. 31, 2021. [Online]. Available: https://www.chemijournal.com/archives/?year=2018&vol=6&issue=1&ArticleId=1777&si=false.

[46] A. A. Adeyanju, E. Ekwue, and W. Compton, “Experimental and theoretical analysis of a beverage chiller,” Research Journal of Applied Sciences, vol. 5, no. 3, pp. 195–203, 2010, doi: 10.3923/rjasci.2010.195.203.

[47] Y. Chiba, Y. Marif, A. Boukaoud, K. Brahim, A. Tlemcani, and N. Henini, “A Multi Stage Study of Thermoelectric Device Based on Semi-conductor Materials,” in *Lecture Notes in Networks and Systems*, vol. 62, Springer, 2019, pp. 560–565.

[48] C. Qiu and W. Shi, “Comprehensive modeling for optimized design of a thermoelectric cooler with non-constant cross-section: Theoretical considerations,” Applied Thermal Engineering, vol. 176, p. 115384, Jul. 2020, doi: 10.1016/j.applthermaleng.2020.115384.

[49] T. Lu, X. Zhang, J. Zhang, P. Ning, Y. Li, and P. Niu, “Multi-objective optimization of thermoelectric cooler using genetic algorithms,” AIP Advances, vol. 9, no. 9, p. 095105, Sep. 2019, doi: 10.1063/1.5119022.

[50] A. Nemati, H. Nami, M. Yari, and F. Ranjbar, “Effect of geometry and applied currents on the exergy and exergoeconomic performance of a two-stage cascaded thermoelectric cooler,” International Journal of Refrigeration, vol. 85, pp. 1–12, Jan. 2018, doi: 10.1016/j.ijrefrig.2017.09.006.

[51] H. Sadighi Dizaji, S. Jafarmadar, S. Khalilarya, and S. Pourhedayat, “A comprehensive exergy analysis of a prototype Peltier air-cooler; experimental investigation,” Renewable Energy, vol. 131, pp. 308–317, Feb. 2019, doi: 10.1016/j.renene.2018.07.056.

[52] H. Tan, H. Fu, and J. Yu, “Evaluating optimal cooling temperature of a single-stage thermoelectric cooler using thermodynamic second law,” Applied Thermal Engineering, vol. 123, pp. 845–851, Aug. 2017, doi: 10.1016/j.applthermaleng.2017.05.182.

[53] L. Zhu and J. Yu, “Optimization of heat sink of thermoelectric cooler using entropy generation analysis,” International Journal of Thermal Sciences, vol. 118, pp. 168–175, Aug. 2017, doi: 10.1016/j.ijthermalsci.2017.04.015.

[54] N. Panigrahi, K. Venkatesan, and M. Venkata Ramanan, “Performance study of thermoelectric cooler using multiphysics simulation and numerical modelling,” International Journal of Ambient Energy, 2019, doi: 10.1080/01430750.2019.1611655.

[55] E. Fong, T. T. Lam, W. D. Fischer, and S. W. K. Yuan, “Analytical approach for study of transient performance of thermoelectric coolers,” Journal of Thermophysics and Heat Transfer, vol. 33, no. 1, pp. 96–105, Jun. 2019, doi: 10.2514/1.T5452.

[56] S. Ferreira-Teixeira and A. M. Pereira, “Geometrical optimization of a thermoelectric device: Numerical simulations,” Energy Conversion and Management, vol. 169, pp. 217–227, Aug. 2018, doi: 10.1016/j.enconman.2018.05.030.

[57] A. Çağlar, “Optimization of operational conditions for a thermoelectric refrigerator and its performance analysis at optimum conditions,” International Journal of Refrigeration, vol. 96, pp. 70–77, Dec. 2018, doi: 10.1016/j.ijrefrig.2018.09.014.

[58] I. T. Witting *et al.*, “The Thermoelectric Properties of Bismuth Telluride,” Advanced Electronic Materials, vol. 5, no. 6, p. 1800904, Jun. 2019, doi: 10.1002/aelm.201800904.

[59] H. J. Goldsmid, “Bismuth telluride and its alloys as materials for thermoelectric generation,” *Materials*, vol. 7, no. 4. MDPI AG, pp. 2577–2592, 2014, doi: 10.3390/ma7042577.

[60] X. Hu *et al.*, “Artificial porous structure: An effective method to improve thermoelectric performance of Bi2Te3 based alloys,” Journal of Solid State Chemistry, vol. 282, 2020, doi: 10.1016/j.jssc.2019.121060.

[61] A. M. Adam *et al.*, “Enhanced thermoelectric figure of merit in Bi-containing Sb2Te3 bulk crystalline alloys,” Journal of Physics and Chemistry of Solids, vol. 138, p. 109262, 2020, doi: 10.1016/j.jpcs.2019.109262.

[62] B. Madavali, H. S. Kim, C. H. Lee, D. soo Kim, and S. J. Hong, “High Thermoelectric Figure of Merit in p-Type (Bi2Te3)x − (Sb2Te3)1−x Alloys Made from Element-

Mechanical Alloying and Spark Plasma Sintering," Journal of Electronic Materials, vol. 48, no. 1, pp. 416–424, Jan. 2019, doi: 10.1007/s11664-018-6706-7.

[63] D. Banerjee *et al.*, "Elevated thermoelectric figure of merit of n-type amorphous silicon by efficient electrical doping process," Nano Energy, vol. 44, pp. 89–94, 2018, doi: 10.1016/j.nanoen.2017.11.060.

[64] H. Wang *et al.*, "Magnetic-field enhanced high-thermoelectric performance in topological Dirac semimetal Cd3As2 crystal," Science Bulletin, vol. 63, no. 7, pp. 411–418, 2018, doi: 10.1016/j.scib.2018.03.010.

[65] Ö. C. Yelgel and G. P. Srivastava, "Thermoelectric properties of Bi2Se3/Bi 2Te3/Bi2Se3 and Sb 2Te3/Bi2Te3/Sb2Te 3 quantum well systems," Philosophical Magazine, vol. 94, no. 18, pp. 2072–2099, 2014, doi: 10.1080/14786435.2014.903340.

[66] S. Paengson, P. Pilasuta, K. Singsoog, W. Namhongsa, W. Impho, and T. Seetawan, "Improvement in thermoelectric properties of CaMnO3 by Bi doping and hot pressing," in *Materials Today: Proceedings*, 2017, vol. 4, no. 5, pp. 6289–6295, doi: 10.1016/j.matpr.2017.06.129.

[67] M. Yaprintsev, R. Lyubushkin, O. Soklakova, and O. Ivanov, "Microstructure and thermoelectric properties of Bi1.9Lu0.1Te3 compound," Rare Metals, vol. 37, no. 8, pp. 642–649, 2018, doi: 10.1007/s12598-017-0926-5.

[68] Y. Zuo, Y. Liu, Q. P. He, J. M. Song, H. L. Niu, and C. J. Mao, "CuAgSe nanocrystals: colloidal synthesis, characterization and their thermoelectric performance," Journal of Materials Science, vol. 53, no. 21, pp. 14998–15008, 2018, doi: 10.1007/s10853-018-2676-7.

[69] S. Bao, J. Yang, W. Zhu, X. Fan, X. Duan, and J. Peng, "Preparation and thermoelectric properties of La filled skutterudites by mechanical alloying and hot pressing," Materials Letters, vol. 60, no. 16, pp. 2029–2032, Jul. 2006, doi: 10.1016/j.matlet.2005.12.074.

[70] K. Liu, X. Dong, and Z. Jiuxing, "The effects of La on thermoelectric properties of LaxCo 4Sb12 prepared by MA-SPS," Materials Chemistry and Physics, vol. 96, no. 2–3, pp. 371–375, Apr. 2006, doi: 10.1016/j.matchemphys.2005.07.068.

[71] M. B. A. Bashir *et al.*, "In-Filled La0.5Co4Sb12 Skutterudite System with High Thermoelectric Figure of Merit," Journal of Electronic Materials, vol. 47, no. 4, pp. 2429–2438, Apr. 2018, doi: 10.1007/s11664-018-6074-3.

[72] H. Zhu, T. Su, H. Li, Q. Hu, S. Li, and M. Hu, “Thermoelectric properties of BiCuSO doped with Pb,” Solid State Communications, 2018, doi: 10.1016/j.ssc.2018.04.013.

[73] L. Xue *et al.*, “Thermoelectric performance of Cu2Se bulk materials by high-temperature and high-pressure synthesis,” Journal of Materiomics, vol. 5, no. 1, pp. 103–110, Mar. 2019, doi: 10.1016/j.jmat.2018.12.002.

[74] S. Perumal *et al.*, “Realization of High Thermoelectric Figure of Merit in GeTe by Complementary Co-doping of Bi and In,” Joule, vol. 3, no. 10, pp. 2565–2580, Oct. 2019, doi: 10.1016/j.joule.2019.08.017.

[75] J. L. Chen *et al.*, “Improved Thermoelectric Performance Achieved by Regulating Heterogeneous Phase in Half-Heusler TiNiSn-Based Materials,” Journal of Electronic Materials, 2018, doi: 10.1007/s11664-017-6013-8.

[76] M. Benyahia, V. Ohorodniichuk, E. Leroy, A. Dauscher, B. Lenoir, and E. Alleno, “High thermoelectric figure of merit in mesostructured In0.25Co4Sb12 n-type skutterudite,” Journal of Alloys and Compounds, 2018, doi: 10.1016/j.jallcom.2017.11.195.

[77] X. Ai, D. Hou, X. Liu, S. Gu, L. Wang, and W. Jiang, “Enhanced thermoelectric performance of PbTe-based nanocomposites through element doping and SiC nanoparticles dispersion,” Scripta Materialia, vol. 179, pp. 86–91, 2020, doi: 10.1016/j.scriptamat.2020.01.014.

[78] J. Wang, B. Liu, N. Miao, J. Zhou, and Z. Sun, “I-doped Cu2Se nanocrystals for high-performance thermoelectric applications,” Journal of Alloys and Compounds, 2019, doi: 10.1016/j.jallcom.2018.08.291.

[79] R. Murugasami, P. Vivekanandhan, S. Kumaran, R. Suresh Kumar, and T. John Tharakan, “Simultaneous enhancement in thermoelectric performance and mechanical stability of p-type SiGe alloy doped with Boron prepared by mechanical alloying and spark plasma sintering,” Journal of Alloys and Compounds, 2019, doi: 10.1016/j.jallcom.2018.09.029.

[80] H. Yang *et al.*, “Enhanced thermoelectric performance of Te-doped skutterudite with nano-micro-porous architecture,” Scripta Materialia, 2019, doi: 10.1016/j.scriptamat.2018.09.015.

[81] Ö. C. Yelgel, “Theoretical study of thermoelectric properties of n-type doped Mg2Si0.4Sn0.6 solid solutions,” Philosophical Magazine, 2016, doi: 10.1080/14786435.2016.1143128.

[82] M. Li, S. M. Kazi Nazrul Islam, S. Dou, and X. Wang, “Significantly enhanced figure-of-merit in graphene nanoplate incorporated Cu 2 Se fabricated by spark plasma sintering,” Journal of Alloys and Compounds, 2018, doi: 10.1016/j.jallcom.2018.07.353.

[83] Asfandiyar, B. Cai, L. D. Zhao, and J. F. Li, “High thermoelectric figure of merit ZT > 1 in SnS polycrystals,” Journal of Materiomics, vol. 6, no. 1, pp. 77–85, 2020, doi: 10.1016/j.jmat.2019.12.003.

[84] R. Yan, W. Xie, B. Balke, G. Chen, and A. Weidenkaff, “Realizing p-type NbCoSn half-Heusler compounds with enhanced thermoelectric performance via Sc substitution,” Science and Technology of Advanced Materials, vol. 21, no. 1, pp. 122–130, Jan. 2020, doi: 10.1080/14686996.2020.1726715.

[85] L. D. Zhao *et al.*, “High thermoelectric performance via hierarchical compositionally alloyed nanostructures,” Journal of the American Chemical Society, 2013, doi: 10.1021/ja403134b.

[86] O. Muthusamy *et al.*, “Enhancement of the Thermoelectric Performance of Si-Ge Nanocomposites Containing a Small Amount of Au and Optimization of Boron Doping,” Journal of Electronic Materials, vol. 49, pp. 2813–2824, 2020, doi: 10.1007/s11664-019-07857-5.

[87] Y. He *et al.*, “High Thermoelectric Performance in Non-Toxic Earth-Abundant Copper Sulfide,” Advanced Materials, vol. 26, no. 23, pp. 3974–3978, Jun. 2014, doi: 10.1002/adma.201400515.

[88] C. Fu *et al.*, “Realizing high figure of merit in heavy-band p-type half-Heusler thermoelectric materials,” Nature Communications, vol. 6, no. 1, pp. 1–7, Sep. 2015, doi: 10.1038/ncomms9144.

[89] E. Kunz Wille, N. Grewal, S. Bux, and S. Kauzlarich, “Seebeck and Figure of Merit Enhancement by Rare Earth Doping in Yb14-xRExZnSb11 (x = 0.5),” Materials, vol. 12, no. 5, p. 731, Mar. 2019, doi: 10.3390/ma12050731.

[90] L. W. Da Silva and M. Kaviany, “Miniaturized thermoelectric cooler,” in *ASME International Mechanical Engineering Congress and Exposition, Proceedings*, 2002, vol. 1, pp. 249–263, doi: 10.1115/IMECE2002-32437.

[91] L. M. Vikhor, L. I. Anatychuk, and P. V. Gorskyi, “Electrical resistance of metal contact to Bi2Te3 based thermoelectric legs,” Journal of Applied Physics, vol. 126, no. 16, 2019, doi:

10.1063/1.5117183.

[92] S. Ramanathan and G. M. Chrysler, “Solid-state refrigeration for cooling microprocessors,” IEEE Transactions on Components and Packaging Technologies, vol. 29, no. 1, pp. 179–183, Mar. 2006, doi: 10.1109/TCAPT.2006.870392.

[93] K. Wang, R. Baskaran, and K. F. Böhringer, “Template based high packing density assembly for microchip solid state cooling application,” Dec. 2006, Accessed: Feb. 24, 2021. [Online]. Available: https://pure.ncue.edu.tw/en/publications/template-based-high-packing-density-assembly-for-microchip-solid-.

[94] P. Y. Hou, R. Baskaran, and K. F. Böhringer, “Optimization of microscale thermoelectric cooling (TEC) element dimensions for hotspot cooling applications,” in *Journal of Electronic Materials*, Jul. 2009, vol. 38, no. 7, pp. 950–953, doi: 10.1007/s11664-009-0694-6.

[95] J. H. Holland, “Genetic Algorithms and Adaptation,” in *Adaptive Control of Ill-Defined Systems*, Springer US, 1984, pp. 317–333.

[96] K. Deb, *OPTIMIZATION FOR ENGINEERING DESIGN: Algorithms and Examples*. PHI Learning Pvt. Ltd., 2012.

[97] X.-S. Yang, *Engineering Optimization: An Introduction with Metaheuristic Applications | Wiley*. John Wiley & Sons, New Jersey.

[98] N. Metropolis, A. W. Rosenbluth, M. N. Rosenbluth, A. H. Teller, and E. Teller, “Equation of State Calculations by Fast Computing Machines,” Citation: J. Chem. Phys, vol. 21, no. 6, p. 1087, 1953, doi: 10.1063/1.1699114.

[99] S. Kirkpatrick, C. D. Gelatt, and M. P. Vecchi, “Optimization by simulated annealing,” Science, vol. 220, no. 4598, pp. 671–680, May 1983, doi: 10.1126/science.220.4598.671.

[100] H. J. Goldsmid, *Introduction to Thermoelectricity*, vol. 121. Berlin, Heidelberg: Springer Berlin Heidelberg, 2010.

[101] K. Deb and R. B. Agrawal, “Simulated Binary Crossover for Continuous Search Space,” Complex Systems, vol. 9, no. 2, pp. 115–148, 1995, doi: 10.1.1.26.8485Cached.

[102] K. Deb, “Single-objective GA code in C.” 2001, [Online]. Available: https://www.iitk.ac.in/kangal/codes.shtml.

[103] X.-S. Yang, “Simulated Annealing for Constrained Optimization - File Exchange - MATLAB Central.” https://www.mathworks.com/matlabcentral/fileexchange/29739-

simulated-annealing-for-constrained-optimization.

[104] F. J. Disalvo, “Thermoelectric cooling and power generation,” *Science*, vol. 285, no. 5428. American Association for the Advancement of Science, pp. 703–706, Jul. 30, 1999, doi: 10.1126/science.285.5428.703.

[105] M. Sajid, I. Hassan, and A. Rahman, “An overview of cooling of thermoelectric devices,” *Renewable and Sustainable Energy Reviews*, vol. 78. Elsevier Ltd, pp. 15–22, Oct. 01, 2017, doi: 10.1016/j.rser.2017.04.098.

[106] C. B. Vining, “Semiconductors are cool,” *Nature*, vol. 413, no. 6856. Nature Publishing Group, pp. 577–578, Oct. 11, 2001, doi: 10.1038/35098159.

[107] J. M. Giri and P. K. S. Nain, “Performance Optimization of Thermoelectric Cooler Using Genetic Algorithm,” Mathematical Modelling of Engineering Problems, vol. 7, no. 3, pp. 427–435, Sep. 2020, doi: 10.18280/mmep.070313.

[108] C. J. L. Hermes and J. R. Barbosa, “Thermodynamic comparison of Peltier, Stirling, and vapor compression portable coolers,” Applied Energy, vol. 91, no. 1, pp. 51–58, Mar. 2012, doi: 10.1016/j.apenergy.2011.08.043.

[109] L. Shen *et al.*, “Performance enhancement investigation of thermoelectric cooler with segmented configuration,” Applied Thermal Engineering, vol. 168, 2020, doi: 10.1016/j.applthermaleng.2019.114852.

[110] H. Y. Zhang, “A general approach in evaluating and optimizing thermoelectric coolers,” International Journal of Refrigeration, vol. 33, no. 6, pp. 1187–1196, Sep. 2010, doi: 10.1016/j.ijrefrig.2010.04.007.

[111] D. Astrain, J. G. Vián, and M. Domínguez, “Increase of COP in the thermoelectric refrigeration by the optimization of heat dissipation,” Applied Thermal Engineering, vol. 23, no. 17, pp. 2183–2200, Dec. 2003, doi: 10.1016/S1359-4311(03)00202-3.

[112] H. S. Lee, “Optimal design of thermoelectric devices with dimensional analysis,” Applied Energy, vol. 106, pp. 79–88, 2013, doi: 10.1016/j.apenergy.2013.01.052.

[113] A. Miner, A. Majumdar, and U. Ghoshal, “Thermo-electro-mechanical refrigeration based on transient thermoelectric effects,” in *International Conference on Thermoelectrics, ICT, Proceedings*, 1999, pp. 27–30, doi: 10.1109/ict.1999.843327.

[114] J. Yu and B. Wang, “Enhancing the maximum coefficient of performance of thermoelectric cooling modules using internally cascaded thermoelectric couples,” International Journal of

Refrigeration, vol. 32, no. 1, pp. 32–39, 2009, doi: 10.1016/j.ijrefrig.2008.08.006.

[115] W. Seifert and V. Pluschke, “Maximum cooling power of a graded thermoelectric cooler,” Physica Status Solidi (B) Basic Research, 2014, doi: 10.1002/pssb.201451038.

[116] S. Manikandan, S. C. Kaushik, and K. Anusuya, “Thermodynamic modelling and analysis of thermoelectric cooling system,” in *2016 International Conference on Energy Efficient Technologies for Sustainability, ICEETS 2016*, Oct. 2016, pp. 685–693, doi: 10.1109/ICEETS.2016.7583838.

[117] E. S. Jeong, “A new approach to optimize thermoelectric cooling modules,” Cryogenics, vol. 59, pp. 38–43, 2014, doi: 10.1016/j.cryogenics.2013.12.003.

[118] P. K. S. Nain, S. Sharma, and J. M. Giri, “Non-dimensional multi-objective performance optimization of single stage thermoelectric cooler,” in *Lecture Notes in Computer Science (including subseries Lecture Notes in Artificial Intelligence and Lecture Notes in Bioinformatics)*, 2010, vol. 6457 LNCS, pp. 404–413, doi: 10.1007/978-3-642-17298-4_44.

[119] E. Thiébaut, C. Goupil, F. Pesty, Y. D’Angelo, G. Guegan, and P. Lecoeur, “Maximization of the Thermoelectric Cooling of a Graded Peltier Device by Analytical Heat-Equation Resolution,” Physical Review Applied, 2017, doi: 10.1103/PhysRevApplied.8.064003.

[120] K. H. Lee and O. J. Kim, “Analysis on the cooling performance of the thermoelectric micro-cooler,” International Journal of Heat and Mass Transfer, vol. 50, no. 9–10, pp. 1982–1992, May 2007, doi: 10.1016/j.ijheatmasstransfer.2006.09.037.

[121] S. Ferreira-Teixeira and A. M. Pereira, “Geometrical optimization of a thermoelectric device: Numerical simulations,” Energy Conversion and Management, 2018, doi: 10.1016/j.enconman.2018.05.030.

[122] J. M. Giri and P. K. S. Nain, “Optimization of Refrigeration Rate for a Thermoelectric Cooler in Restricted Space using Stochastic Algorithms,” International Journal of Recent Technology and Engineering, vol. 8, no. 2, pp. 2306–2311, Jul. 2019, doi: 10.35940/ijrte.b2701.078219.

[123] M. Yamanashi, “A new approach to optimum design in thermoelectric cooling systems,” Journal of Applied Physics, vol. 80, no. 9, pp. 5494–5502, Nov. 1996, doi: 10.1063/1.362740.

[124] F. Völklein, G. Min, and D. M. Rowe, “Modelling of a microelectromechanical thermoelectric cooler,” Sensors and Actuators, A: Physical, vol. 75, no. 2, pp. 95–101, 1999,

doi: 10.1016/S0924-4247(99)00002-3.

[125] Y. Pan, B. Lin, and J. Chen, “Performance analysis and parametric optimal design of an irreversible multi-couple thermoelectric refrigerator under various operating conditions,” Applied Energy, vol. 84, no. 9, pp. 882–892, 2007, doi: 10.1016/j.apenergy.2007.02.008.

[126] A. Fabián-Mijangos, G. Min, and J. Alvarez-Quintana, “Enhanced performance thermoelectric module having asymmetrical legs,” Energy Conversion and Management, vol. 148, pp. 1372–1381, 2017, doi: 10.1016/j.enconman.2017.06.087.

[127] Y. X. Huang, X. D. Wang, C. H. Cheng, and D. T. W. Lin, “Geometry optimization of thermoelectric coolers using simplified conjugate-gradient method,” Energy, vol. 59, pp. 689–697, 2013, doi: 10.1016/j.energy.2013.06.069.

[128] B. Abramzon, “Numerical optimization of the thermoelectric cooling devices,” Journal of Electronic Packaging, Transactions of the ASME, vol. 129, no. 3, pp. 339–347, 2007, doi: 10.1115/1.2753959.

[129] U. Ghoshal, S. Ghoshal, C. McDowell, L. Shi, S. Cordes, and M. Farinelli, “Enhanced thermoelectric cooling at cold junction interfaces,” Applied Physics Letters, vol. 80, no. 16, pp. 3006–3008, Apr. 2002, doi: 10.1063/1.1473233.

[130] I. Dincer and M. A. Rosen, *Exergy*. Elsevier Ltd, 2013.

[131] S. C. Kaushik, S. Manikandan, and R. Hans, “Energy and exergy analysis of thermoelectric heat pump system,” International Journal of Heat and Mass Transfer, vol. 86, pp. 843–852, Jul. 2015, doi: 10.1016/j.ijheatmasstransfer.2015.03.069.

[132] H. Nami, A. Nemati, M. Yari, and F. Ranjbar, “A comprehensive thermodynamic and exergoeconomic comparison between single- and two-stage thermoelectric cooler and heater,” Applied Thermal Engineering, vol. 124, pp. 756–766, Sep. 2017, doi: 10.1016/j.applthermaleng.2017.06.100.

[133] I. Dincer and M. Kanoglu, *Refrigeration Systems and Applications, 3rd Edition*. 2017.

[134] A. Bejan, “Fundamentals of exergy analysis, entropy generation minimization, and the generation of flow architecture,” International Journal of Energy Research, vol. 26, no. 7, pp. 0–43, Jun. 2002, doi: 10.1002/er.804.

[135] G. Fraisse, J. Ramousse, D. Sgorlon, and C. Goupil, “Comparison of different modeling approaches for thermoelectric elements,” Energy Conversion and Management, vol. 65, pp. 351–356, Jan. 2013, doi: 10.1016/j.enconman.2012.08.022.

[136] M. J. Moran, M. J. Moran, H. N. Shapiro, D. D. Boettner, and M. B. Bailey, *Fundamentals of Engineering Thermodynamics*, 9th Editio. Wiley, 2018.

[137] A. Bejan, *Advanced Engineering Thermodynamics*. Wiley, 2016.

[138] M. Çengel, Yunus A. Boles, Michael A. Kanoğlu, *Thermodynamics: An Engineering Approach*, Ninth Edit. McGraw Hill, 2019.

[139] I. Dincer, "Exergization," International Journal of Energy Research, vol. 40, no. 14, pp. 1887–1889, Nov. 2016, doi: 10.1002/er.3606.

[140] S. Tickoo, *ANSYS Workbench : A Tutorial Approach* , 3rd ed. CADCIM Technologies, Schererville, 2019.

MANUSCRIPTS OF PUBLICATION

IIETA International Information and Engineering Technology Association
Advancing the World of Information and Engineering

Mathematical Modelling of Engineering Problems
Vol. 7, No. 3, September, 2020, pp. 427-435
Journal homepage: http://iieta.org/journals/mmep

Performance Optimization of Thermoelectric Cooler Using Genetic Algorithm

Jitendra Mohan Giri*, Pawan Kumar Singh Nain

School of Mechanical Engineering, Galgotias University, Greater Noida 201312, India

Corresponding Author Email: jitendra.giri@galgotiasuniversity.edu.in

https://doi.org/10.18280/mmep.070313

Received: 1 April 2020
Accepted: 12 August 2020

Keywords:
thermoelectric cooler, optimization, genetic algorithm, finite-element method, ANSYS workbench, cooling capacity, COP

ABSTRACT

Thermoelectric coolers (TECs) use the Peltier effect for thermal management of electronic devices. They offer high reliability and low noise operation but limited in use due to low performance. In the present work, through the use of a genetic algorithm (GA), two single-objective optimizations associated with two separate objectives are carried out, aiming maximization of cooling capacity and maximization of the coefficient of performance (*COP*) of TEC with space restrictions. Interfacial thermal resistance and electrical contact resistance are taken into consideration to obtain a more realistic model. This paper presents a new approach to finding appropriate solutions by optimally arranging the length of n-type and p-type thermoelectric (TE) elements, the cross-sectional area of TE elements, and input electric current. To validate the GA predictions, three-dimensional steady-state TEC models are prepared, and finite-element simulations are carried out using ANSYS®. Close agreement between the GA and ANSYS® has been observed. This study provides a new mathematical optimization model that is more realistic and is quite close to the physical construction of TEC modules manufactured by industry.

1. INTRODUCTION

The solid-state thermoelectric (TE) technology attract great attention of the researchers because of its potential use as green energy conversion devices. The Peltier effect of thermoelectric technology offers direct conversion of electrical energy into temperature difference. Conversely, the Seebeck effect of TE technology provides the conversion of thermal energy of temperature differential into electric power [1]. A thermoelectric cooler (TEC) dissipates the heat and removes the hotspots of the electronic devices in an environment-friendly manner using the Peltier effect. A TEC could be installed easily within a restricted space due to its practical manufacturing possibility in small sizes. Thermoelectric coolers must be appropriately designed and manufactured to meet the necessary performance requirements. Two essential performance parameters of a TEC are the cooling capacity and the coefficient of performance. The cooling capacity of thermoelectric coolers ranges from milliwatts to watts depending on the requirements. The maximum cooling effect or higher *COP* for a thermoelectric cooler can be achieved through upgraded TE materials and improved device design.

The efficiency of TE materials increases with a material property known as figure of merit (Z). The term Z is defined as α^2/RK, where α is the Seebeck coefficient, R is the electrical resistance, K is the thermal conductance. With absolute temperature (T), the dimensionless figure of merit (ZT) is used to characterize TE materials. A higher value of ZT corresponds to better cooling performance. Hicks et al. described that the value of ZT could be enhanced by reducing the dimensions of thermoelectric materials [2, 3]. At room temperature, Venkatasubramanian et al. [4] reported a $ZT\sim2.4$ for p-type Bi_2Te_3/Sb_2Te_3 superlattice devices. Peak ZT values of different TE materials are attainable at different temperatures. Over the past two decades, significant progress in maximizing ZT has been made in developing thermoelectric materials [5-10].

With the significant ongoing efforts to improve TE materials, the researchers also focus on designing and assembling the TECs. The investigations established that the geometric structure of thermoelectric elements affects the performance of thermoelectric coolers [11-15]. Huang et al. [16] combined a three dimensional TEC model with a simplified conjugate-gradient technique. They reported that at a fixed temperature difference and fixed current, a substantial value of the total area of TE elements with small element length can maximize cooling capacity. Yang et al. [17] reported that micro-thermoelectric coolers operating in a transient regime could provide a better cooling effect. Nain et al. [18] reported that a suitable value of dimensionless current can enhance the performance of TEC. Pareto-optimal solutions were obtained for different settings of temperature ratio. Shen et al. [19] reported that a two-segmented TE element structure can reduce the joule heating effect from 50% to 35% on the cold side. The results showed a remarkable 118.1% improvement in maximum cooling capacity. Nain et al. [20] optimized cooling capacity and *COP* performance of TEC using dimensional structural parameters as design variables. The geometrical parameters were optimized to find Pareto-optimal solutions. Jeong [21] reported that the *COP* of TEC can be increased by optimal values of current and length of thermoelements. Lee [22] proposed a dimensional analysis approach to find out the optimal design of TE devices with feasible mechanical constraints. Mijangos et al. [23] reported a novel design of asymmetrical legs to enhance the performance of TE devices.

Literature reports several studies on performance optimization of TEC [13, 15, 24-29]. However, in the current study, the two performance parameters, namely, cooling capacity and coefficient of performance, are optimized as two single-objective optimization problems. So far, the standard approach has been to choose either a set of geometric design variables or operating design variables. In this paper, a combined set of three design variables, electric current, length of n-type and p-type TE elements and cross-sectional area of TE elements is chosen in both optimization problems. The optimization algorithm mathematical model is customized to handle the presence of ceramic substrate, copper contacts, electric contact resistances at the interface, and heat sink, which are essential parts in the fabrication of a TEC module in industrial applications. It is a new aspect of modelling TEC. The geometry of the thermoelectric element plays a vital role in the performance of the thermoelectric cooler. However, tight geometric space constraints are found in many telecommunications and other scientific applications. The TEC is used for cooling electronic devices where space restrictions are quite prevalent. Hence, consideration of performance optimization of TEC with space restrictions is a very valid assumption. The genetic algorithm is used to maximize the cooling capacity and *COP* of a TEC with space restrictions in two different optimization problems. The optimization results are validated through finite-element simulations using ANSYS®.

2. DESCRIPTION OF A THERMOELECTRIC COOLER MODEL

The general schematic diagram of a practical single-stage thermoelectric cooler is shown in Figure 1 (a). A thermoelectric cooler (TEC) consists of many thermoelectric (TE) elements. These thermoelectric elements are assembled electrically in series. Copper tabs are used to interconnect n-type and p-type elements. This array configuration is sandwiched between two thermally conducting ceramic substrates. Figure 1 (b) is an exploded view diagram of a practical TEC system.

The basic unit of the physical model of a TEC is a thermocouple (pair of n-type and p-type semiconductor thermoelectric elements). The number of pairs of thermoelectric elements may vary from several to hundreds. On the one hand, the manufacturing cost of TEC is high, and on the other hand, many TE materials are high-priced. Further, to predict the performance of a TEC with a heat sink, knowing the temperature at important points is quite difficult. Also, the thermal resistances in the heat sink, copper conductors, and ceramic substrates play a significant role in the total resistance to heat flow in the TEC system. These issues make the performance optimization problem challenging to solve. In this work, the effects of electrical contact resistance and thermal resistance are included. The impact of Joule heat and thermal conduction are included as well.

In this work, to simplify the investigation considering thermal resistances, a thermal-resistance model has been developed. This model includes thermal resistance of copper tabs, ceramic substrates, and cold side heat sink for developing a more realistic TEC model. A thermocouple and the developed thermal resistance model for this work is shown in Figure 2.

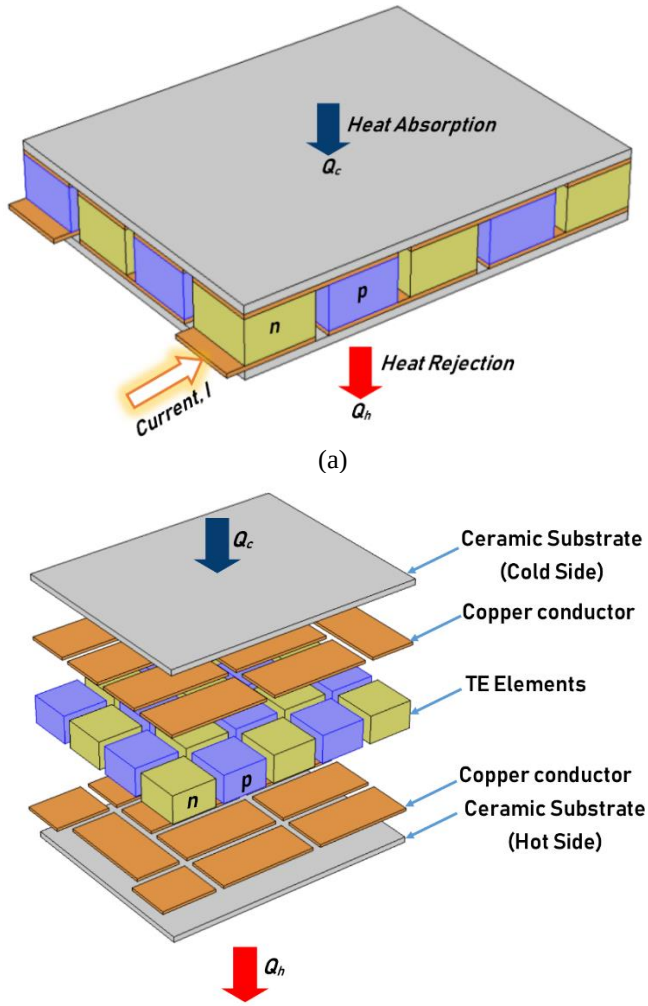

Figure 1. (a) Single-stage TEC (b) Exploded view of TEC

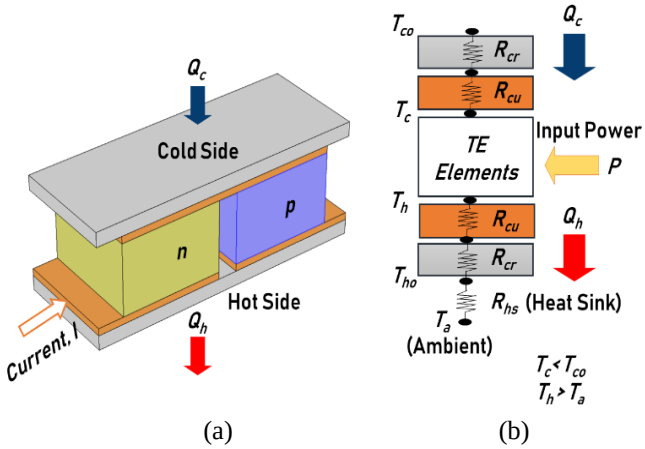

Figure 2. (a) Thermoelectric couple (b) Thermal resistance model

By applying the electrical analogy of the heat flow to the thermal resistance model shown in Figure 2(b), the temperatures at the TEC hot surface and the cold surface can be expressed as

$$T_h = Q_h(R_{hs} + R_{cr} + R_{cu}) + T_a \quad (1)$$

$$T_c = T_{co} - Q_c\left(R_{cr} + R_{cu}\right) \quad (2)$$

where, T_h and T_c are the hot and cold side temperatures (K) of n-type and p-type elements. Q_h is the heat rejection rate (W) from the hot side. Q_c is the heat absorption rate at the cold side (W), which is referred to as the cooling capacity in common usage. T_{co} and T_{ho} are the temperatures (K) at the cold surface and hot surface of TEC, respectively. R_{hs} is the thermal resistance (°C/W) of the heat sink attached to the hot side of TEC, R_{cr} is the thermal resistance (°C/W) of the ceramic substrates, and R_{cu} is the thermal resistance (°C/W) of the copper tabs. T_a is the ambient temperature (K).

In the current study, some reasonable assumptions are considered.

(a) Heat transfer is assumed to take place along the length of TE elements.
(b) The thermoelectric elements have the same cross-section and length.
(c) Thomson effect is not considered.
(d) Steady-state condition is prevailing.

A constant electric current pass through the circuit of dissimilar semiconductors. The heat is pumped to one of the two sides. It results in making one side cool and another side hot. A heat sink attached externally to the hot side ceramic substrate dissipates heat to the ambient environment. A thermoelectric couple produces cooling or heating effect depending on the direction of the electric current. Eq. (3) and Eq. (4) shows the heat energy balance at the cold and the hot side of the thermoelectric cooler. T_c and T_h correspond to the temperature at TE element-copper conductor interface at the cold side and hot side, respectively, and used with the same reference in each referred equation of this paper.

$$Q_c = 2N\left[I\alpha T_c - \frac{k\,A\left(T_h - T_c\right)}{L} - \frac{1}{2}I^2\left(\frac{\rho L}{A} + 2\frac{r_c}{A}\right)\right] \quad (3)$$

$$Q_h = 2N\left[I\alpha T_h - \frac{k\,A\left(T_h - T_c\right)}{L} + \frac{1}{2}I^2\left(\frac{\rho L}{A} + 2\frac{r_c}{A}\right)\right] \quad (4)$$

where, thermoelectric material properties α, ρ, k are the Seebeck coefficient (V/K), electrical resistivity (Ωm) and thermal conductivity (W/mK), respectively. r_c is the electrical contact resistance (Ωm^2). L and A are the length (m) and cross-sectional area (m^2) of n-type and p-type thermoelectric elements, respectively. I is the supplied electric current (A), and N is the total number of thermoelectric couples. There are three essential terms on the right side of Eq. (3) and Eq. (4). The first terms, $I\alpha T_c$ and $I\alpha T_h$, represent the Peltier heat at the cold junction and hot junction, respectively. The second heat transfer term $kA\,(T_h - T_c)/L$ is due to thermal conduction. The third term ½ I^2 ($\rho L/A + 2r_c/A$) represents the Joule heat generation.

The selection of thermoelectric materials directly affects the performance of TEC. The material properties of thermoelectric elements are temperature dependent. Bismuth telluride (Bi_2Te_3) is the popular thermoelectric material used in thermoelectric coolers. The material properties of Bi_2Te_3 used in this work are given below, as specified by Fraisse et al. [30]. T_{ave} is the average of T_c and T_h.

$$\alpha = \left(22224 + 930.6T_{ave} - 0.9905T_{ave}^2\right)\times 10^{-9} \quad (5)$$

$$\rho = \left(5112 + 163.4T_{ave} + 0.6279T_{ave}^2\right)\times 10^{-10} \quad (6)$$

$$k = \left(62605 - 277.7T_{ave} + 0.4131T_{ave}^2\right)\times 10^{-4} \quad (7)$$

Cooling capacity (Q_c) is one of the significant performance indexes of TEC, which is used in this study. The Coefficient of Performance (*COP*) is another crucial performance index of thermoelectric coolers. Both performance indexes are considered in the current study. *COP* is the ratio of cooling capacity to power consumption and defined by the following equation.

$$Coefficient\ of\ Performance, COP = \frac{Q_c}{P} \quad (8)$$

The input electric power (P), as shown in Figure 2(b), can be calculated by the following relationship.

$$Input\ Electric\ Power, P = Q_h - Q_c \quad (9)$$

The cost-competitive and high-performance TEC system will pave the way for a promising future of such green devices.

3. METHODOLOGY

The various geometrical, material and operational parameters affect the cooling performance of the thermoelectric cooler. Besides, the restricted maximum area of cooling devices, which depends on its application in electronic devices, is a significant constraint for TEC design. Performance optimization is vital to enhance the use of thermoelectric coolers in real-world applications. In this study, the objective is to maximize the cooling capacity of TEC with space restrictions. This paper presents a new approach by selecting electric current, length of n-type and p-type TE elements and cross-sectional area of TE elements as design variables.

3.1 Optimization of cooling capacity of TEC

The single-objective optimization problem for maximization of the cooling capacity of TEC is formulated mathematically as:

$$\begin{cases} Maximize\ Q_c \\ Subject\ to \\ \quad I_{\min} \le I \le I_{\max} \\ \quad L_{\min} \le L \le L_{\max} \\ \quad A_{\min} \le A \le A_{\max} \end{cases} \quad (10)$$

Further, the total number of thermoelectric couples (N) is a dependent design variable. Its value depends on the cross-sectional area of n-type and p-type thermoelectric elements and computed using Eq. (11).

$$N = \frac{Available\,area(S)of\ \ TEC \times packaging\ \ density}{2 \times A} \quad (11)$$

The optimization problem, as mentioned in Eq. (10) has been solved using some specific values of parameters. Table 1 lists the values of the parameters and properties used in this work.

Table 1. Values of parameters and properties

Description	Parameter	Value
Cold surface temperature	T_{co}	293.15 K or 20°C
Ambient temperature	T_a	298.15 K or 25°C
Heat sink thermal resistance	R_{hs}	0.10 °C /W
Electrical contact resistance	r_c	1 x 10^{-8} Ω m^2
Available C.S. area of TEC	S	15 mm x 15 mm
Packaging density	PD	80%
Ceramic thermal conductivity	k_{cr}	35.3 W/m°C
Copper thermal conductivity	k_{cu}	386 W/m-°C

The design variables in the present study are constrained by lower and upper bounds. From a practical viewpoint, the range for length and cross-sectional area of n-type and p-type TE elements is taken as 1.0-2.0 mm and 1.0-2.0 mm^2, respectively. The range for input electric current is taken as 0.1-3.0 A. The dependent design variable N will vary from 45 to 90 as it is governed by Eq. (11). The thicknesses of ceramic substrates and copper tabs are taken as 0.2 mm and 0.1 mm, respectively. The surface area of the ceramic substrate on each side is considered identical to the size of TEC. The total surface area of the copper tab on each side is considered 90% of the size of TEC. R_{cr} and R_{cu} are computed as 0.025181 °C/W and 0.001279345 °C/W, respectively. All these values are taken with the help of TEC manufacturing companies' catalogues.

Genetic algorithm (GA) is an evolutionary algorithm based on natural genetics. The genetic algorithm begins with the creation of a population of possible solutions (called individuals). Based on the value of the objective function, each member of the population is assigned a fitness value. To evolve better solutions, new generations are created by undergoing selection, recombination, and mutation of solutions. The fitness of the new generation is evaluated. This cycle is repeated over generations until the stopping criterion is met. The objective of GA is to search for an appropriate solution for the design problems. This involves maximization or minimization of the objective function.

Genetic algorithm is a population-based optimization approach to find optimal or near-optimal solutions. In terms of quality and robustness of solutions, GA's capability has been widely recognized for providing excellent results on classic discrete and continuous optimization problems. The genetic algorithm's performance depends on many genetic parameters such as population size, crossover, and mutation rate. GA parameters play an important role, and a different combination of parameters may lead to a significant GA performance change. The smaller population size helps faster convergence than larger population sizes. The decision on various GA parameters and operators are usually selected based on recommendations made by GA researchers.

The real-variable GA employing SBX operator created by Deb and Agarwal is used in this study [31]. Table 2 lists the values of the GA parameters like population size, crossover, mutation & number of generations that are used in the present study. The results are reported after multiple runs of GA converged to the same best solution.

Table 2. Values of GA parameters

Parameter	Value
Population size	50
Crossover probability	0.80
Mutation probability	0.25
Number of generations	1000

3.2 Optimization of Coefficient of Performance (*COP*) of TEC

The objective of the second optimization problem is the maximization of the coefficient of performance of TEC. The design variables are the same as those selected in the previous problem. The fixed values of the parameters and properties are identical to the values used in the previous problem and described in Table 1. The thicknesses of ceramic substrates and copper tabs have the same values of 0.2 mm and 0.1 mm, respectively. This new problem is mathematically expressed as:

$$\begin{cases} Maximize\,COP \\ Subject\,to \\ \quad I_{min} \le I \le I_{max} \\ \quad L_{min} \le L \le L_{max} \\ \quad A_{min} \le A \le A_{max} \end{cases} \quad (12)$$

The goal of this optimization problem is to find the design variables within the variable bounds that result in the maximum *COP* of the device.

3.3 Optimization procedure

To apply the genetic algorithm to the optimization problems described in Eq. (10) and Eq. (12), the fitness evaluation of solution vectors is required. However, the procedure for evaluating fitness function is slightly tricky for this problem. The unknown values of T_h and T_c are initially guessed for approximately estimate Q_c and Q_h. The initial guess for T_h and T_c satisfies TEC's prevailing temperature conditions, i.e., $T_h > T_a$ and $T_c < T_{co}$. In principle, these conditions must be satisfied. The initial guess will be iteratively modified and reach the exact value. Eq. (1) and Eq. (2) are used to calculate new values of T_h and T_c that are termed as T_{hn} and T_{cn}. These are updated repeatedly to corresponding new values until the difference in old values and new values are negligible. Then the values of Q_c and Q_h are accepted.

A flowchart for GA implementation for these two optimization problems are given in Figure 3.

The brief steps of the fitness evaluation procedure for a population individual (solution vector) followed in this work are described below.

(a) The hot side and cold side temperatures of TE elements (T_h and T_c) are initially assigned to a guessed value.
(b) The material properties are estimated using Eq. (5), (6) and (7).
(c) The expected values of Q_c and Q_h are calculated using Eq. (3) and (4).
(d) Using Eq. (1) and (2) the new values of T_h and T_c are calculated. These are termed as T_{hn} and T_{cn}, respectively.
(e) If the difference of guessed values and new values is considerable, then guessed value is updated as $T_h = T_{hn}$

and $T_c = T_{cn}$. Go to step (b) and repeat the iteration.

(f) If the difference of guessed values and new values is small, then accept the solution. Take the next individual in the GA population to evaluate until all individuals of the current generation are evaluated.

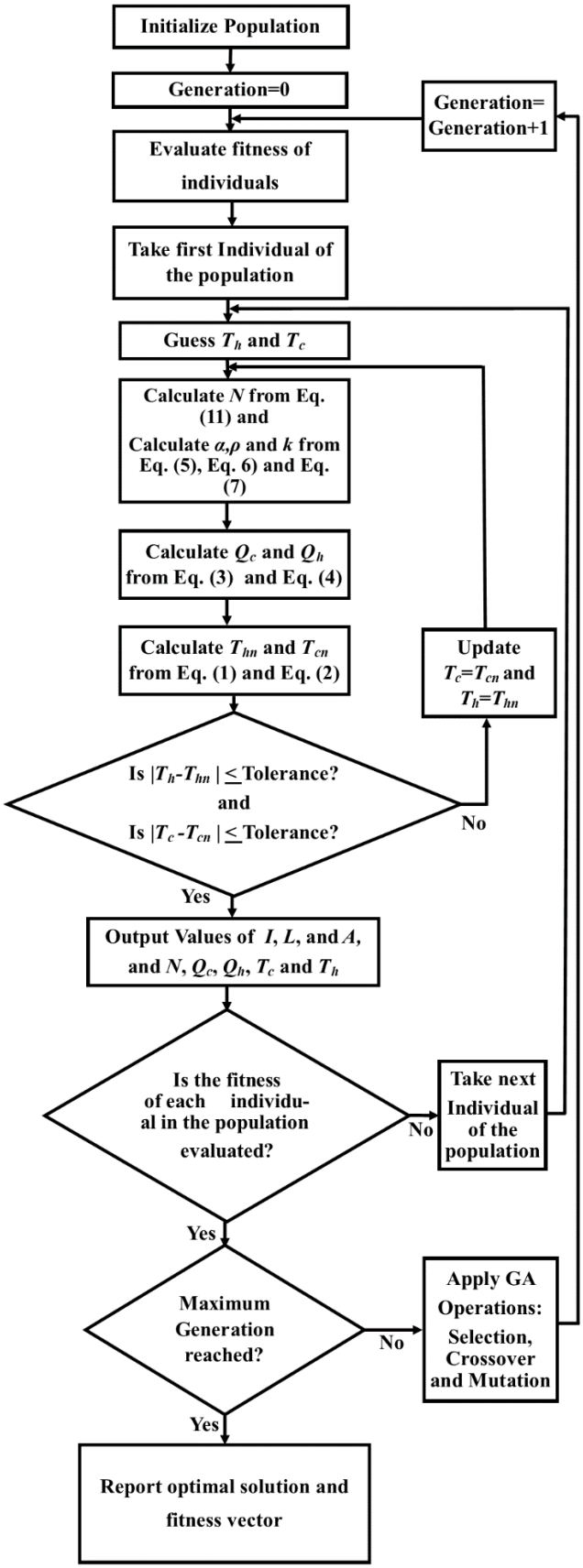

Figure 3. Flowchart for GA implementation

4. RESULTS AND DISCUSSIONS

In the first segment of present work, cooling capacity Q_c, the first performance index of TEC is maximized. The algorithm of this study is coded in C language. The GA source code is developed by Deb and used in this work [32]. Multiple runs of 1000 generations have been repeated, and the best run is reported in Table 3 on which algorithm converged several times during various runs.

Table 3. Result of GA based optimization for maximum Q_c

Optimized Q_c	Optimal Values of Design Variables			
	I	L	A	N (Dependent)
8.476807 W	2.993 A	1.0 mm	1.607 mm^2	56

At optimal values of design variables, the corresponding values of T_h and T_c are found at 28.59℃ and 19.78℃, respectively. The hot surface temperature (T_{ho}) of TEC is 27.84℃. The heat rejection rate (Q_h) at the hot side is 28.401 W. For the maximized Q_c, the value of *COP* obtained is 0.425. It can be observed that L is hitting lower bound while other parameters have optimal values without hitting any bound of the permitted range.

To optimize the second performance index of TEC, the coefficient of performance (*COP*) is maximized. The boundary conditions and assumptions are similar to those considered during the optimization of Q_c. This optimization problem is solved using the same parameters of GA, as mentioned in Table 2. The steps to implement GA in this problem are similar to those used in the optimization of cooling capacity and shown with the help of a flowchart in Figure 3. Several runs of 1000 generations have been performed to reach solutions with the highest quality, and the best run is reported in Table 4. It is worth mentioning that GA converged to the same results in various runs.

Table 4. Result of GA optimization for maximum *COP*

Optimized *COP*	Optimal Values of Design Variables			
	I	L	A	N (Dependent)
4.11	0.283 A	2.0 mm	1.956 mm^2	45

With this maximum *COP*, the corresponding Q_c is obtained as 0.745992 W. The corresponding values of T_h and T_c are 25.11℃ and 19.97℃, respectively. The hot surface temperature (T_{ho}) of the thermoelectric cooler is 25.09℃. The heat rejection rate (Q_h) at the hot side is 0.927 W. The optimal values of I and A design variables are unique, while the optimal value of L is hitting the upper boundary. It can be seen that *COP* increased significantly, and cooling capacity is just 8.8% of Max. Q_c obtained, as mentioned in Table 4. It is found that a design variable L hits its lower bound for high Q_c while for high *COP*, L hits its upper bound.

From these two results, it is well established that maximization of Q_c and maximization of *COP* are obtained at a different set of design parameters. Also, maximum Q_c does not ensure providing optimal *COP* and vice-versa. This means that these objectives are conflicting. The resolution of these conflicting design objectives will be Pareto solutions through multi-objective optimization if there is no specific objective interest. It will be useful to determine a set of solutions that will allow the decision-maker to choose among them

according to the application's requirement.

The results of this study show that it is possible to improve the cooling capacity or *COP* of the thermoelectric coolers with these design variables to be competitive with compressor-based cooling devices. The complex impacts of electrical contact resistance and thermal resistance deteriorate the TEC performance. These factors always need to be included in the model for optimization and analysis.

5. FINITE-ELEMENT SIMULATION FOR RESULT VALIDATION

Finite-element simulation is a computational method for solving complex engineering problems of the real-world. The finite element simulations are performed to validate the optimization results of GA. ANSYS® is a useful, common-purpose finite-element method tool. It is used to solve a broad range of engineering problems numerically. Hence ANSYS® is used in the current study. The Thermal-electric module of ANSYS® is capable of providing simultaneous solutions of thermal and electrical fields. The present work makes use of the thermal-electric module for the steady-state analysis of the TEC model. A three-dimensional non-linear finite-element model is setup. The model in this work is set up with one pair of n-type and p-type elements as per the GA result. A new approach to incorporate the effect of electric contact resistance on the performance of TEC is used in the present study. The finite-element simulation includes four additional geometric parts termed as 'Contact' and used for modelling of the electric contact resistance effect. These parts have material properties as per the thermo-electric behaviour of electrical contact resistance. The contact geometries are created at each end of the TE elements. The complete schematic of the TEC model for Finite-element simulation to validate GA results is shown in Figure 4.

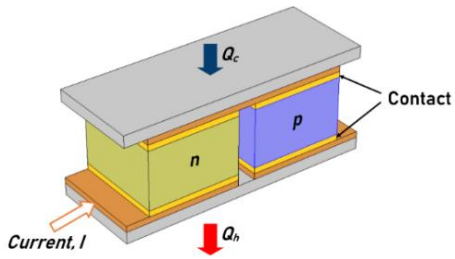

Figure 4. Schematic of TEC for finite-element simulation to validate GA results

5.1 Finite-element simulation for maximum Q_c

To validate GA predictions for maximum Q_c, the length of n-type and p-type elements is taken as 1.0 mm, as reported in Table 3. The TE elements are of the square cross-section of 1.27 mm. The distance between n-type and p-type elements is 0.31 mm. The material properties for the simulation are computed at average (T_{ave}) of T_h and T_c values obtained during the GA based optimization of Q_c. The finite-element simulation input parameters of the modelled TEC are given in Table 5.

To model adiabatic heat transfer from the exposed surfaces of TEC, a small convection loss of 0.000001 W/mK was applied on all surfaces except the ones on which boundary conditions mentioned in Table 5 are specified. The computationally generated mesh, electric voltage, and temperature distribution across the finite-element model of the thermoelectric cooler are shown in Figure 5.

Table 5. Finite-element simulation input parameters for maximum Q_c

Description	Parameter	Value per pair of TE Elements
Cooling Capacity	Q_c	0.1514 W
Current	I	2.993 A
Temperature (hot side of TEC)	T_{ho}	27.84°C

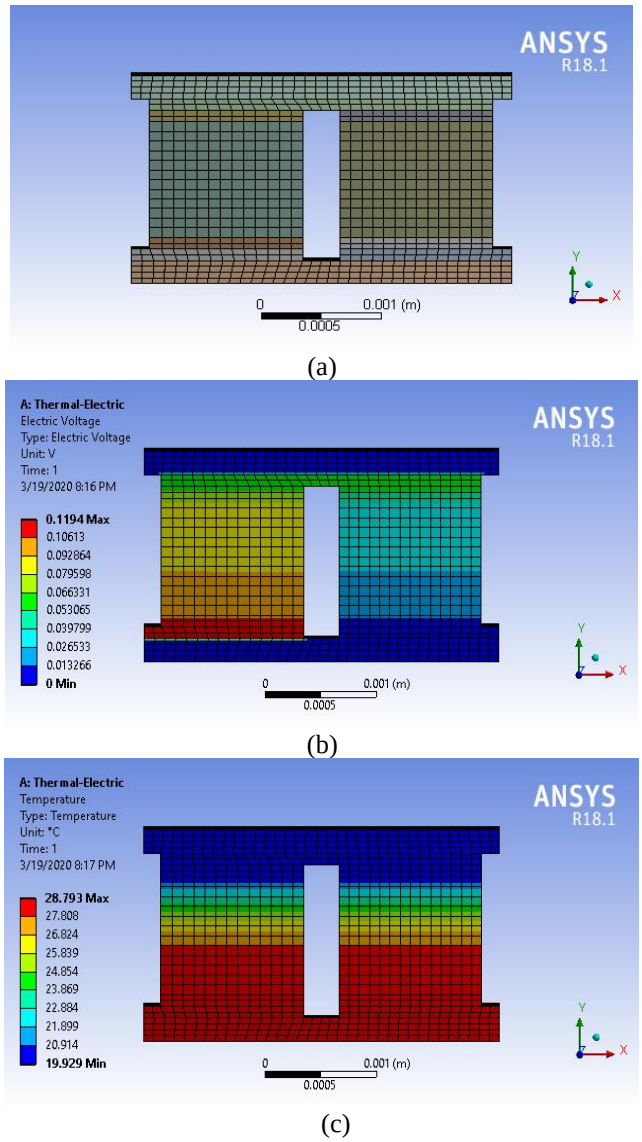

Figure 5. (a) Mesh (b) Voltage distribution (c) Temperature distribution in the finite-element model for maximum Q_C

The parameters obtained from finite-element simulation are compared with the GA results and reported in Table 6. It is observed that the results for a single pair of TE elements from GA simulation and those obtained from finite-element simulation are in close agreement. The finite-element simulation result represents a 3-D solution based on a numerical technique, while GA results are based on 1-D analytical equations. Hence, the optimization result obtained by GA is verified through the solutions of the thermal-electric module of ANSYS®.

Table 6. Comparison of results for maximum Q_c

Parameter	GA	ANSYS®	Remarks
T_{co}	20°C	20.25°C	Value per pair of TE elements
Q_h	0.507 W	0.508 W	
P	0.356 W	0.357 W	

5.2 Finite-element simulation for maximum *COP*

In this segment, the finite-element simulation for maximum *COP* is performed with ANSYS® software. The steady-state TEC model consists of TE elements with 2.0 mm length, as reported in Table 4. The TE elements are of the square cross-section of 1.4 mm. The distance between n-type and p-type elements is 0.38 mm. The temperature-dependent material properties are calculated based on the average of T_h, and T_c found during GA based optimization of *COP*. The input parameters of the TEC model for finite-element simulation are given in Table 7.

Table 7. Finite-element simulation input parameters for maximum *COP*

Description	Parameter	Value per pair of TE Elements
Cooling Capacity	Q_c	0.0165 W
Current	I	0.283 A
Temperature (hot side of TEC)	T_{ho}	25.09°C

The three-dimensional steady-state TEC model is created, and predictions of GA based optimization are tested for maximum *COP*. For this simulation, the mesh, electric voltage, and temperature distribution are shown in Figure 6. The finite-element simulation results agree well with the GA results. The parameters for GA and finite-element simulation results have been compared and reported in Table 8.

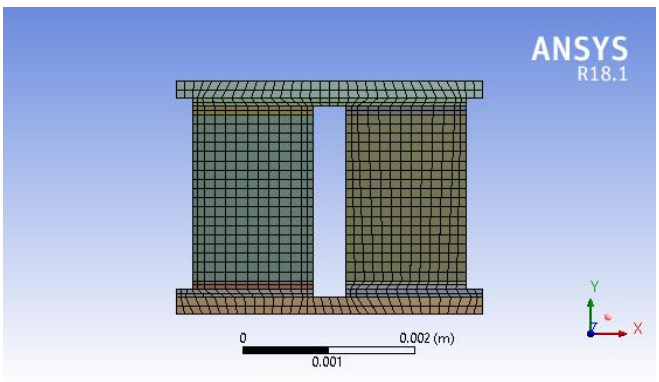

(a)

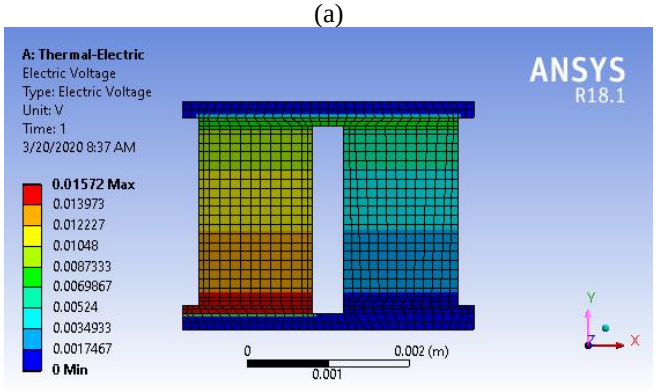

(b)

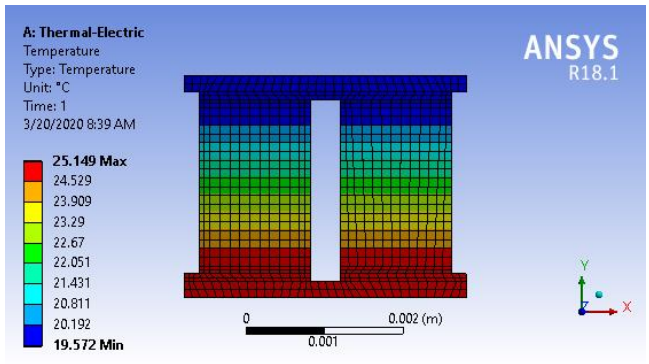

(c)

Figure 6. (a) Mesh (b) Voltage distribution (c) Temperature distribution in the finite-element model for maximum *COP*

The ANSYS® result is consistent with GA based optimization results for the maximization of *COP*. Hence, the optimization result is verified through the solutions of the thermal-electric module of ANSYS®.

Table 8. Comparison of results for maximum *COP*

Parameter	GA	ANSYS®	Remarks
T_{co}	20°C	19.61°C	Value per pair of TE elements
Q_h	0.021 W	0.021 W	
P	0.004 W	0.004 W	

6. CONCLUSIONS

This paper presents an effective method with a new analytical model to improve cooling capacity and coefficient of performance of thermoelectric cooler for a specific need. In order to analyze more than one factor simultaneously, the thermoelectric cooler's current and geometric parameters were set to be variables. The described study emphasized to find out the optimal values of current, length of n-type and p-type TE elements and cross-sectional area of TE elements within size restrictions on space. It was found that length, the cross-sectional area of thermoelectric elements, and input electric current had a great influence on the TEC performance. Performance optimizations to maximize cooling capacity and to maximize *COP* were successfully performed by the genetic algorithm. The use of this stochastic optimization algorithm based on natural genetics theory proved to be the right option. The genetic algorithm successfully converged to the same optimal results over several runs. The finite-element simulations through ANSYS® validated the GA result.

The work suggests that these design variables should be appropriately selected in practical application. Results revealed that the relationship between the coefficient of performance and cooling capacity is inverse. The maximum cooling capacity does not provide optimum *COP* and vice-versa. The smaller length of thermoelectric elements facilitates maximum cooling capacity whereas greater length of elements obtains maximum coefficient of performance. The best performance requires specific values of electric current and cross-sectional area of TE elements as per the objective requirements. The appropriate optimum results can be achieved for any space restriction. This study can guide the TEC designers working for some specific cooling targets. The use of microprocessor-based control of input power

parameters to get an optimal cooling with the best possible COP under dynamic conditions needs to be explored.

REFERENCES

[1] Rowe, D.M. (1995). CRC Handbook of Thermoelectrics. CRC Press. https://doi.org/10.1201/9781420049718

[2] Hicks, L.D., Dresselhaus, M.S. (1993). Effect of quantum-well structures on the thermoelectric figure of merit. Physical Review B, 47: 12727. https://doi.org/10.1103/PhysRevB.47.12727

[3] Hicks, L.D., Dresselhaus, M.S. (1993). Thermoelectric figure of merit of a one-dimensional conductor. Physical Review B, 47: 16631. https://doi.org/10.1103/PhysRevB.47.16631

[4] Venkatasubramanian, R., Siivola, E., Colpitts, T., O'Quinn, B. (2001). Thin-film thermoelectric devices with high room-temperature figures of merit. Nature, 413: 597-602. https://doi.org/10.1038/35098012

[5] Su, C.H. (2019). Design, growth and characterization of PbTe-based thermoelectric materials. Progress in Crystal Growth and Characterization of Materials, 65(2): 47-94. https://doi.org/10.1016/j.pcrysgrow.2019.04.001

[6] Tan, G., Zhao, L.D., Kanatzidis, M.G. (2016). Rationally designing high-performance bulk thermoelectric materials. Chemical Reviews, 116(19): 12123-12149. https://doi.org/10.1021/acs.chemrev.6b00255

[7] Poudel, B., Hao, Q., Ma, Y., Lan, Y., Minnich, A., Yu, B., Yan, X., Wang, D.Z., Muto, A. (2008). High-thermoelectric performance of nanostructured bismuth antimony telluride bulk alloys. Science, 320(5876): 634-8. https://doi.org/10.1126/science.1156446

[8] Chen, G., Dresselhaus, M.S., Dresselhaus, G., Fleurial, J.P., Caillat, T. (2003). Recent developments in thermoelectric materials. International Materials Reviews, 48(1): 45-66. https://doi.org/10.1179/095066003225010182

[9] Sootsman, J.R., Chung, D.Y., Kanatzidis, M.G. (2009). New and old concepts in thermoelectric materials. Angewandte Chemie - International Edition, 48(46): 8616-8639. https://doi.org/10.1002/anie.200900598

[10] Alam, H., Ramakrishna, S. (2013). A review on the enhancement of figure of merit from bulk to nano-thermoelectric materials. Nano Energy, 2(2): 190-212. https://doi.org/10.1016/j.nanoen.2012.10.005

[11] Völklein, F., Min, G., Rowe, D.M. (1999). Modelling of a microelectromechanical thermoelectric cooler. Sensors and Actuators, A: Physical, 75(2): 95-101. https://doi.org/10.1016/S0924-4247(99)00002-3

[12] Yu, J., Wang, B. (2009). Enhancing the maximum coefficient of performance of thermoelectric cooling modules using internally cascaded thermoelectric couples. International Journal of Refrigeration, 32(1): 32-39. https://doi.org/10.1016/j.ijrefrig.2008.08.006

[13] Abramzon, B. (2007). Numerical optimization of the thermoelectric cooling devices. Journal of Electronic Packaging, 129(3): 339-347. https://doi.org/10.1115/1.2753959

[14] Pan, Y., Lin, B., Chen, J. (2007). Performance analysis and parametric optimal design of an irreversible multi-couple thermoelectric refrigerator under various operating conditions. Applied Energy, 84(9): 882-892. https://doi.org/10.1016/j.apenergy.2007.02.008

[15] Cheng, Y.H., Lin, W.K. (2005). Geometric optimization of thermoelectric coolers in a confined volume using genetic algorithms. Applied Thermal Engineering, 25(17-18): 2983-2997. https://doi.org/10.1016/j.applthermaleng.2005.03.007

[16] Huang, Y.X., Wang, X.D., Cheng, C.H., Lin, D.T.W. (2013). Geometry optimization of thermoelectric coolers using simplified conjugate-gradient method. Energy, 59: 689-697. https://doi.org/10.1016/j.energy.2013.06.069

[17] Yang, R., Chen, G., Kumar, A.R., Snyder, G.J., Fleurial, J.P. (2005). Transient cooling of thermoelectric coolers and its applications for microdevices. Energy Conversion and Management, 46(9-10): 1407-1421. https://doi.org/10.1016/j.enconman.2004.07.004

[18] Nain, P.K.S., Sharma, S., Giri, J.M. (2010). Non-dimensional multi-objective performance optimization of single stage thermoelectric cooler. Lecture Notes in Computer Science, 404-413. https://doi.org/10.1007/978-3-642-17298-4_44

[19] Shen, L., Zhang, W., Liu, G., Tu, Z., Lu, Q., Chen, H., Huang, J.Q. (2020). Performance enhancement investigation of thermoelectric cooler with segmented configuration. Applied Thermal Engineering, 168: 114852. http://doi.org/10.1016/j.applthermaleng.2019.114852

[20] Nain, P.K.S., Giri, J.M., Sharma, S., Deb, K. (2010). Multi-objective performance optimization of thermo-electric coolers using dimensional structural parameters. Lecture Notes in Computer Science, pp. 607-614. https://doi.org/10.1007/978-3-642-17563-3_71

[21] Jeong, E.S. (2014). A new approach to optimize thermoelectric cooling modules. Cryogenics, 59: 38-43. https://doi.org/10.1016/j.cryogenics.2013.12.003

[22] Lee, H.S. (2013). Optimal design of thermoelectric devices with dimensional analysis. Applied Energy, 106: 79-88. https://doi.org/10.1016/j.apenergy.2013.01.052

[23] Fabián-Mijangos, A., Min, G., Alvarez-Quintana, J. (2017). Enhanced performance thermoelectric module having asymmetrical legs. Energy Conversion and Management, 148: 1372-1381. https://doi.org/10.1016/j.enconman.2017.06.087

[24] Göktun, S. (1996). Optimal performance of a thermoelectric refrigerator. Energy Sources, 18(5): 531-536. https://doi.org/10.1080/00908319608908788

[25] Cheng, Y.H., Shih, C. (2005). Application of genetic algorithm to maximizing the cooling capacity in a thermoelectric cooling system. Proceedings of the IEEE International Conference on Industrial Technology, Hong Kong, China. https://doi.org/10.1109/ICIT.2005.1600648

[26] Thiébaut, E., Goupil, C., Pesty, F., D'Angelo, Y., Guegan, G., Lecoeur, P. (2017). Maximization of the thermoelectric cooling of a graded Peltier device by analytical heat-equation resolution. Physical Review Applied, 8(6). http://doi.org/10.1103/PhysRevApplied.8.064003

[27] Seifert, W., Pluschke, V. (2014). Maximum cooling power of a graded thermoelectric cooler. Physica Status Solidi (B) Basic Research, 251(7): 1416-1425. https://doi.org/10.1002/pssb.201451038

[28] Erturun, U., Erermis, K., Mossi, K. (2014). Effect of various leg geometries on thermo-mechanical and power generation performance of thermoelectric devices. Applied Thermal Engineering, 73(1): 128-141.

https://doi.org/10.1016/j.applthermaleng.2014.07.027
[29] Chen, L., Li, J., Sun, F., Wu, C. (2007). Optimum allocation of heat transfer surface area for heating load and COP optimisation of a thermoelectric heat pump. International Journal of Ambient Energy, 28(4): 189-196. https://doi.org/10.1080/01430750.2007.9675043
[30] Fraisse, G., Ramousse, J., Sgorlon, D., Goupil, C. (2013). Comparison of different modeling approaches for thermoelectric elements. Energy Conversion and Management, 65: 351-356. https://doi.org/10.1016/j.enconman.2012.08.022
[31] Deb, K., Agrawal, R.B. (1994). Simulated binary crossover for continuous search space. Complex Systems, 9(2).
[32] Deb, K. (2001). Single-objective GA code in C. https://www.iitk.ac.in/kangal.

NOMENCLATURE

A	cross-sectional area of TE elements, m^2
COP	coefficient of performance
I	electric current, A
k	thermal conductivity, W/m K
L	length of thermoelectric element, m
N	number of thermoelectric couples
P	power input, W
PD	packaging density
Q_c	heat absorption rate at the cold side, W
Q_h	heat rejection rate from the hot side, W
R_{hs}	thermal resistance of heat sink, ℃/W
R_{cr}	thermal resistance of ceramic, ℃/W
R_{cu}	thermal resistance of copper, ℃/W
S	available cross-sectional area of TEC, m^2
T_c	temperature at the cold side of elements, K
T_h	temperature at the hot side of elements, K
T_{co}	temperature at the cold surface of TEC, K
T_{ho}	temperature at the hot surface of TEC, K
T_a	ambient temperature, K
T_{ave}	average of T_c and T_h, K
Z	figure of merit, 1/K

Greek symbols

α	Seebeck coefficient, V/K
ρ	electrical resistivity, Ω m

GALGOTIAS UNIVERSITY

JITENDRA MOHAN GIRI <jitendra.giri@galgotiasuniversity.edu.in>

Final Refereeing Decision IJEX_305421

2 messages

Inderscience Publishers <noreply@indersciencemail.com> Sat, Feb 20, 2021 at 9:32 PM
Reply-To: Inderscience Publishers <noreply@indersciencemail.com>
To: jitendra.giri@galgotiasuniversity.edu.in, pawan.kumar@galgotiasuniversity.edu.in, Editor <Ibrahim.Dincer@uoit.ca>

Dear JITENDRA MOHAN GIRI, Pawan Kumar Singh Nain,

Ref: Submission "Maximization of Energy and Exergy Efficiencies for a Sustainable Thermoelectric Cooling System by applying Genetic Algorithm"

Congratulations, your above mentioned submitted article has been refereed and accepted for publication in the International Journal of Exergy. The acceptance of your article for publication in the journal reflects the high status of your work by your fellow professionals in the field.

You need now to login at http://www.inderscience.com/login.php and go to http://www.inderscience.com/ospeers/admin/author/articlelist.php to find your submission and complete the following tasks:

1. Save the "Editor's post-review version" on your local disk so you can edit it. If the file is in PDF format and you cannot edit it, use instead your last MS Word revised version, making sure to include there all the review recommendations made during the review process. Rename the new file to "authorFinalVersion."

2. Open the "authorFinalVersion" file and remove your reply or any response to reviewers that you might have in the front of your article.

3. Restore the author's identification, such as names, email addresses, mailing addresses and biographical statements in the first page of your local file "authorFinalVersion."

4. IMPORTANT: The paper is accepted providing that you, the author, check, edit and correct the English language in the paper. Please proofread all the text and make sure to correct any grammar and spelling mistakes.

5. Save your changes in the file "authorFinalVersion" and use the "Browse" and "Upload" buttons to upload the file on our online system.

6. Click on "Update Metadata" to correct the title, abstract and keywords according the recommendations received from the Editor. You must make sure that the title, abstract and keywords are totally free of English Spelling and Grammar errors. Do not forget to click the "Update" button to save your changes.

7. Once you have updated the metadata, check the box "Yes."

8. Upload a zipped file with the Copyright Agreement forms signed by each author. We need a signed author agreement form for every author and every co-author. Please insert the full names of all authors, reflecting the name order given in the article.

9. To see a sample of real articles that have been published in the International Journal of Exergy visit http://www.inderscience.com/info/ingeneral/sample.php?jcode=ijex.

Finally click on the "Notify Editor" button to let the editor know that you have completed the six tasks.

Your continuing help and cooperation is most appreciated.

Best regards,

Dr. Ibrahim Dincer
Editor of International Journal of Exergy
Inderscience Publishers Ltd.
submissions@inderscience.com

Maximization of Energy and Exergy Efficiencies for a Sustainable Thermoelectric Cooling System by applying Genetic Algorithm

Jitendra Mohan Giri* and Pawan Kumar Singh Nain

School of Mechanical Engineering,
Galgotias University,
Greater Noida, Uttar Pradesh-201312, India
Email: jitendra.giri@galgotiasuniversity.edu.in
Email: pawan.kumar@galgotiasuniversity.edu.in
*Corresponding author

Abstract: The efficient thermal management of thermoelectric cooler (TEC) as a sustainable cooling technology is important. The energy loss, electrical power requirement, and irreversibility of the TEC system need to be minimized. Hence, the loss of energy and energy quality (exergy) are two significant points of concern. Thus, energy and exergy efficiency can be used as the key indicators to optimize TEC's performance. Through this work, authors separately optimized TEC energy efficiency (η_I) and exergy efficiency (η_{II}) considering thermoelectric elements geometry and electric current by using the genetic algorithm (GA). The effects of electrical contact resistance and thermal resistance are considered in the mathematical model of this work. Unlike previously reported works, the authors have used junction temperatures different from surface temperatures at the respective cold and hot sides of TEC. This study reveals that maximum energy and exergy efficiencies are obtainable at the same values of electric current, length, and cross-sectional area of thermoelectric elements. It is significant as these identical optimum design variables assert maximum η_I and η_{II}. At cold surface temperature (T_c) of 20°C, the maximum energy efficiency of 4.11 and the maximum exergy efficiency of 0.0715 are obtained. Exergy efficiency can be used as the basis to choose TEC since it assures better energy quality and connects with sustainable development. The genetic algorithm optimization result is validated through ANSYS® finite-element simulation. This study will help enhance actual TEC performance.

Keywords: thermoelectric cooler; energy efficiency; exergy efficiency; genetic algorithm; optimization; finite-element simulation

Reference to this paper should be made as follows: Giri, J.M., and Nain, P.K.S. (xxxx) 'Maximization of Energy and Exergy Efficiencies for a Sustainable Thermoelectric Cooling System by applying Genetic Algorithm', *Int. J. Exergy,* Vol. No., pp.

Biographical notes: Jitendra Mohan Giri received his B.E. degree in Mechanical Engineering from Dr. B.R. Ambedkar University, Agra, India, and M.Tech. from the Uttar Pradesh Technical University, Lucknow, India. He is pursuing Ph.D. from the Galgotias University, Greater Noida, India. He is presently working on the performance optimization of thermoelectric coolers.

Pawan Kumar Singh Nain is a Professor in the School of Mechanical

Author

Engineering at Galgotias University, Greater Noida, India. He is Gold Medalist in the undergraduate program in Mechanical Engineering at A.M.U. Aligarh, India. He received his M.E. degree from the Indian Institute of Technology (IIT) Roorkee and Ph.D. from the Indian Institute of Technology (IIT) Kanpur. He received British Telecom (U.K.) Fellowship for Ph.D. at IIT Kanpur. His area of interest is design and optimization. He has over 25 publications so far in the area of evolutionary algorithms, thermoelectric devices, and interdisciplinary research in optimization through the design of experiments.

1 Introduction

At present, more than three-fourths of refrigeration systems work on vapour compression and use refrigerants. These systems are one of the most important factors of stratospheric ozone depletion. The adverse environmental impacts of chloro-fluoro-carbons (CFCs), hydro-chloro-fluoro-carbons (HCFCs), and hydro-fluoro-carbons (HFCs) used in vapour compression-based cooling systems have forced the energy researchers to strongly explore renewable alternatives. A promising eco-friendly replacement for the cooling systems using refrigerants is thermoelectric cooler (TEC). A thermoelectric cooler is a solid-state and practically silent device. TEC is powered by the Peltier effect and achieved by supplying electric current through n-type and p-type thermoelectric material. TEC does not have moving components. Thermoelectric coolers are significant because of the need for steady, small size and environmental sustainability for many applications. Thermoelectric coolers are prominently used for cooling requirements of small volumes. These are preferred in various high technology applications such as electronics, space, medicine, telecommunications, and others. TECs are best suited to areas that are not accessible to compressors.

Notwithstanding, currently, thermoelectric coolers have low rate of cooling and energy conversion efficiency compared to other traditional cooling technologies that impeded their wide-spread usage (Hermes and Barbosa, 2012). Various models and hypotheses have been presented in the literature on this problem, and several solutions have been suggested (Abramzon, 2007; Astrain et al., 2003; Cheng and Lin, 2005; Fabián-Mijangos et al., 2017; Ferreira-Teixeira and Pereira, 2018; Ghoshal et al., 2002; Giri and Nain, 2019; Huang et al., 2013; Jeong, 2014; Lee, 2013; Lee and Kim, 2007; Manikandan et al., 2016; Miner et al., 1999; Nain et al., 2010; Pan et al., 2007; Seifert and Pluschke, 2014; Shen et al., 2020; Thiébaut et al., 2017; Völklein et al., 1999; Yamanashi, 1996; Yu and Wang, 2009; Zhang, 2010). A significant number of papers are concerned with the design and simulation of thermoelectric cooling or heat pumping systems. However, it is important to note that most of these optimization attempts were primarily made to improve rate of cooling or coefficient of performance (COP) of TEC. Energy has two faces: Exergy and Anergy. The expression "exergy" derives from the Greek terms ex and ergon, representing from and work (Dincer and Rosen, 2013). Exergy represents available part of energy. Anergy shows dispersed part of energy source or lost potential. Very few articles appear to deal with the exergy aspects of the thermoelectric cooling or heat pumping devices, two of such articles which are prominent (Kaushik et al., 2015) and (Nami et al., 2017). Kaushik et al. (2015) performed exergy analysis of reversible, endoreversible, exoreversible, and irreversible heat pump. Analytical expressions of thermodynamic models were derived. Exergy output

for the different temperature difference between hot and cold sides was observed. It was found that exergy output increases at a higher temperature difference. The increment in contact resistance reduces exergy output. Nami et al. (2017) reported a comparison of single-stage and two-stage thermoelectric devices for COP and exergetic efficiencies. It was established that a higher current is needed in a single-stage device for maximum values of energy efficiency and exergy efficiency. The research on exergy is focused on the quality of energy used to assess the energy process in compliance with ideal thermodynamic equality (Bejan, 2002; Dincer and Kanoglu, 2017). The exergy study is used to recognize exergy losses. It is used to understand irreversible energy conversion losses in the design of the system. To provide effective efficiency and meet several design requirements, computer-aided design, optimization, and analysis have been important parts for the design of thermoelectric cooling systems.

This work is a focussed effort on optimization of TEC to achieve maximum energy and exergy efficiencies. The TEC geometry and current can change the efficiencies, and optimum values can be obtained under given circumstances. In this article, the authors attempted to present an optimization method for the TEC design for improved results by considering three of the main parameters: namely electric current, length of thermoelectric elements, and cross-sectional area of thermoelectric elements. Thereafter, a three-dimensional TEC model is developed, and finite-element simulation is carried out following the optimized value of exergy efficiency to validate GA results.

2 System description

A thermoelectric cooler consists of several couples made out of n-type and p-type thermoelectric elements, as shown in Figure 1. These thermoelectric (TE) elements are tied together electrically by using highly conductive copper tabs. These elements are connected thermally parallel. This arrangement is sandwiched between two ceramic layers.

Figure 1 Schematic diagram of a Thermoelectric Cooler

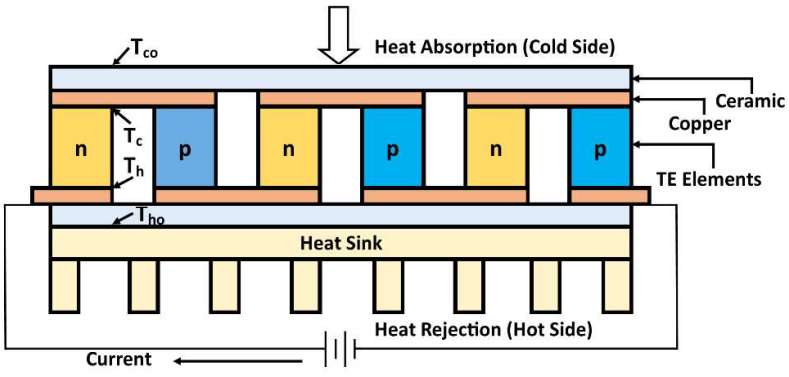

A thermoelectric cooling system is configured to transfer thermal energy from the source at temperature T_{co} to a sink at a higher temperature T_{ho}. The basic units of a TEC are thermocouples that possess temperatures T_c and T_h at cold and hot junctions respectively. Unlike previous works in the TEC system, the authors have used a model that appreciates the difference between T_{co} and T_c at the cold side and the difference between T_{ho} and T_h at the hot side. The material properties and heat balance equations are fundamentally established for thermocouple portions of TEC. In the present work, the authors have modelled TEC realistically considering copper and ceramic effects with cold and hot side temperatures of T_{co} and T_{ho} for GA based optimization and finite-element simulations. Electric power is provided as input to the TEC system, and the Peltier effect is at work according to the direction of electric current.

Thermoelectric coolers are inherently irreversible because the flow of heat and current is necessary during operation. These irreversibilities are the reason for the requirement of the performance optimization of thermoelectric coolers.

3 Theoretical model of an irreversible TEC system

The reversible cycle concept as explained by Sadi Carnot is well established and significant. Thermodynamically, a practical thermoelectric cooler can be modelled as an irreversible reversed heat engine. An irreversible thermoelectric cooler possesses both types of the irreversibilities, i.e., internal and external. The internal irreversibility is generated as TEC operates between cold and hot junctions of n-type and p-type thermoelectric elements at temperatures T_c and T_h, respectively. The external irreversibility is generated for temperature gap T_{co}-T_c carrying heat absorption rate, Q_c at the cold side and for temperature gap T_h-T_{ho} carrying heat rejection rate, Q_h at the hot side of the TEC system. In the present work, unlike previous papers, the authors have used temperature T_c different from T_{co} and temperature T_h different from T_{ho}.

At the cold side of the thermoelectric cooler, the heat energy balance may be expressed as:-

$$Q_c = Q_{Peltier} - Q_{conduction} - Q_{Joule} \quad (1)$$

At the hot side of the thermoelectric cooler, the heat energy balance may be expressed as:-

$$Q_h = Q_{Peltier} - Q_{conduction} + Q_{Joule} \quad (2)$$

The Peltier heat ($Q_{Peltier}$) at the cold and hot sides corresponds to $I\alpha T_c$ and $I\alpha T_h$ respectively. The irreversible heat transfer due to conduction ($Q_{conducion}$) at the cold side and hot side corresponds to $K(T_h\text{-}T_c)$. The irreversible Joule heat generation (Q_{Joule}) corresponds to ½ I^2R. In these expressions, I refers to supplied electric current (A), α is the Seebeck coefficient (V/K) and R represents the electrical resistance. T_c and T_h are the cold side and hot side temperatures (K) of n-type and p-type elements. If N represents the total number of thermoelectric couples used in the thermoelectric cooler, the heat energy balance equations become:

$$Q_c = 2N\left[I\alpha T_c - K(T_h - T_c) - \frac{1}{2}I^2(R)\right] \quad (3)$$

$$Q_h = 2\,N\left[I\,\alpha\,T_c - K(T_h - T_c) + \frac{1}{2}I^2(R)\right] \quad (4)$$

If k and r_c represent the thermal conductivity (W/mK) and the electrical contact resistance (Ωm^2), respectively. L and A represent the length (m) and cross-sectional area (m^2) of n-type and p-type thermoelectric elements, respectively. Equations (3) and (4) can be rearranged as:

$$Q_c = 2\,N\left[I\,\alpha\,T_c - \frac{k\,A\,(T_h - T_c)}{L} - \frac{1}{2}I^2\left(\frac{\rho L}{A} + 2\frac{r_c}{A}\right)\right] \quad (5)$$

$$Q_h = 2\,N\left[I\,\alpha\,T_h - \frac{k\,A\,(T_h - T_c)}{L} + \frac{1}{2}I^2\left(\frac{\rho L}{A} + 2\frac{r_c}{A}\right)\right] \quad (6)$$

The choice of the thermoelectric element's material directly affects TEC performance. Bismuth telluride (Bi_2Te_3) is the premium material used in thermoelectric coolers. The temperature-dependent properties of Bismuth telluride used in this study are calculated from the below-mentioned expressions as specified (Fraisse et al., 2013).

$$\alpha = (22224 + 930.6\,T_{ave} - 0.9905\,T_{ave}^2) \times 10^{-9} \quad (7)$$

$$\rho = (5112 + 163.4\,T_{ave} + 0.6279\,T_{ave}^2) \times 10^{-10} \quad (8)$$

$$k = (62605 - 277.7\,T_{ave} + 0.4131\,T_{ave}^2) \times 10^{-4} \quad (9)$$

$$Where, \quad Average\ Temperature, T_{ave} = 0.5.(T_c + T_h)$$

The irreversible heat flow rate with the heat source or TEC cold surface temperature (T_{co}) to the cold side temperature of n-type and p-type elements (T_c) is given by:

$$Q_c = U_c\,A_c(T_{co} - T_c) \quad (10)$$

Similarly, the irreversible heat flow rate with the hot side temperature of n-type and p-type elements (T_h) to the heat sink or TEC hot surface temperature (T_{ho}) is given by:

$$Q_h = U_h\,A_h(T_h - T_{ho}) \quad (11)$$

In the above expressions, U_c and U_h represent the overall heat transfer coefficients (W/m^2K) while A_c and A_h represent heat transfer surface areas (m^2) at the cold and hot surfaces of TEC.

Thermal conductance is reciprocal thermal resistance. The authors have used a thermal resistance model. They have incorporated thermal resistances of ceramic substrates, copper conductors, and heat sink at the hot side for realistic TEC model consideration. By using thermal resistance models, Equations (10) and (11) are restructured as:

$$T_h = Q_h(R_{hs} + R_{cr} + R_{cu}) + T_o \quad (12)$$

$$T_c = T_{co} - Q_c(R_{cr} + R_{cu}) \quad (13)$$

Where, R_{hs}, $R_{cr,}$ and R_{cu} are the thermal resistances ($^0C/W$) of the ceramic substrates, copper conductors and heat sink.

From the 'available work' or 'exergy' point of view, it is well established by the researchers that the exergy input to the thermoelectric cooling system is equal to the input electric

power (P), and it is 100% exergy. The concept of exergy needs the first law of thermodynamics as well as the second law of thermodynamics. In the thermoelectric cooling system, the temperature of the cold side of TEC (T_{co}) is less than the environment temperature (T_o). The temperature difference (T_o-T_{co}) leads to the absorption of heat from the refrigerated space.

The first law of thermodynamics can be applied to obtain:

$$Exergy\ Input = Input\ Electric\ Power\ (P) = Q_h - Q_c \tag{14}$$

Applying the second law of thermodynamics for irreversible TEC, we can write:

$$\frac{Q_c}{T_{co}} - \frac{Q_h}{T_{ho}} < 0 \tag{15}$$

The second law of thermodynamics can also be applied to obtain rate of entropy generation as:

$$Rate\ of\ Entropy\ Generation, S_{gen} = \left(\frac{Q_h}{T_{ho}} - \frac{Q_c}{T_{co}}\right) > 0 \tag{16}$$

If we combine the first law and second law of thermodynamics used for conservation of energy and non-conservation of entropy, exergy balance for a thermodynamic system can be obtained as:

$$Exergy\ Input = Exergy\ Output + Exergy\ Losses \tag{17}$$

$$Exergy\ Input = Exergy\ Output + (Exergy\ Waste\ Emission + Exergy\ Destruction) \tag{18}$$

The exergy output refers to the thermal exergy deposited at the cold side of the thermoelectric cooler. This exergy transfer accompanying heat transfer Q_c can be calculated by (Bejan, 2016; Çengel, Yunus A. Boles, Michael A. Kanoğlu, 2019; Moran et al., 2018):

$$Exergy\ Output = Q_c \left(\frac{T_o}{T_{co}} - 1\right) \tag{19}$$

Where T_o represents a typical environment or outside temperature.

Exergy Waste Emission or Exergy lost represents the exergy rejected at the hot side of the thermoelectric cooler (If present) and can be written as (Manikandan et al., 2016):

$$Exergy\ Lost = Q_h \left(1 - \frac{T_o}{T_{ho}}\right) \tag{20}$$

Substituting Equations (14), (19), and (20) into Equation (18), Irreversibility or exergy destruction in the process can be obtained as:

$$Irreversibility\ or\ Exergy\ Destruction = T_o \left(\frac{Q_h}{T_{ho}} - \frac{Q_c}{T_{co}}\right) = T_o\ S_{gen} \tag{21}$$

First law efficiency or energy efficiency of a thermoelectric cooler is obtained as:

First Law Efficiency or Energy Efficiency (η_I) $= \frac{Energy\ Output}{Energy\ Input} = \frac{Q_c}{P}$

$$= \frac{Q_c}{Q_h - Q_c} \tag{22}$$

The Second law efficiency or exergy efficiency is a measure of approach to reversibility or ideality. A key goal of exergy analysis is to identify this significant efficiency and actual values of exergy losses with the identification of possible reasons (Dincer, 2016).

$$\textit{Second Law Efficiency or Exergy Efficiency } (\eta_{II}) = \frac{Exergy\ Output}{Exergy\ Input} \tag{23}$$

Alternatively, this can be expressed as:

$$\eta_{II} = 1 - \frac{Exergy\ Losses}{Exergy\ Input} \tag{24}$$

The purpose of the thermoelectric cooler is to absorb heat from the space to be cooled. Thus, it helps in increasing exergy output while this heat absorption takes place. The exergy efficiency of a thermoelectric cooler can be understood as the ratio of minimum exergy or work requirement to the actual exergy input. For simplicity, the thermal reservoir at hot surface temperature T_{ho} is set to be the typical environment. Hence, T_{ho} is the outside temperature (T_o) for the thermoelectric cooler.

Hence,

$$Exergy\ Output = Q_c \left(\frac{T_{ho}}{T_{co}} - 1\right) \tag{25}$$

Second law efficiency or exergy efficiency of an irreversible thermoelectric cooler is obtained as:

$$\eta_{II} = \frac{Q_c \left(\frac{T_{ho}}{T_{co}} - 1\right)}{P} = 1 - \frac{T_{ho} S_{gen}}{P} \tag{26}$$

This establishes a relationship between first law efficiency (η_I) and second law efficiency (η_{II}) of the thermoelectric cooler:

$$\eta_{II} = \frac{\eta_I}{\frac{1}{\left(\frac{T_{ho}}{T_{co}} - 1\right)}} \tag{27}$$

The COP of the thermoelectric cooler is the ratio of useful energy to the required energy and is equal to energy efficiency as described in Equation (22). According to the reversed Carnot cycle phenomenon, $\frac{1}{\left(\frac{T_{ho}}{T_{co}} - 1\right)}$ represents the Carnot or reversible Coefficient of performance (COP), the highest theoretical COP of thermoelectric cooler working within temperature bounds T_{co} and T_{ho}. Hence, the second law efficiency of TEC can also be expressed as:

$$\eta_{II} = \frac{Actual\ COP}{Reversible\ COP}\ or\ \frac{Actual\ COP}{Maximum\ COP} \tag{28}$$

It is clear that Second law efficiency indicates the irreversibilities associated with the thermoelectric cooling system and can vary from 0 to 1.

4 Optimization model formulation and implementation of genetic algorithm

In this study, two objectives are optimized separately. The first optimization problem's objective is the First Law Efficiency (η_I), which is of significance to obtain higher energy efficiency in a restricted space. The second optimization problem's objective is the Second Law Efficiency (η_{II}), which is important to achieve a higher exergy efficiency. After modelling, we select the design variables to achieve optimum engineering goals. The geometry, material and operating conditions play a vital role in designing a TEC with higher performances. The restriction of space in designing TEC is a major constraint. At present, thermoelectric coolers are widely used in the high technology fields such as electronics, telecommunications, space, and others. Space restrictions are very prevalent in these fields and hence there are practical limits to the size of the thermoelectric cooler. Therefore, the space constraints of the thermoelectric elements are very relevant assumptions to consider. This study introduces a new approach by selecting three design variables, i.e., length of n-type and p-type TE elements, the cross-sectional area of n-type and p-type TE elements and the input electric current. For simplifying the complexity of calculation, some assumptions are made for this study.

- Heat transfer is assumed to take place along the length of TE elements.
- The thermoelectric elements have the same cross-section and length.
- Thomson effect is not considered.
- Steady-state condition is prevailing.

4.1 Optimization of energy efficiency or first law efficiency (η_I)

The first single-objective optimization problem for maximization of the energy efficiency or first law efficiency (η_I) of the thermoelectric cooler is formulated mathematically as:

$$\begin{cases} Maximize\ \eta_I \\ Subject\ to \\ I_{min} \le I \le I_{max} \\ L_{min} \le L \le L_{max} \\ A_{min} \le A \le A_{max} \end{cases} \tag{29}$$

Where, (I_{min}, I_{max}), (L_{min}, L_{max}) and (A_{min}, A_{max}) are the bounds of design variables I, L and A, respectively. The bounds of the design variables of this optimization study are listed in Table 1.

Table 1 Lower and upper bounds of design variables

Variable	*Description*	*Lower Bound*	*Upper Bound*
I	Input electric current, A	0.1	3.0
L	Length of n-type and p-type TE elements, mm	1.0	2.0
A	Cross-sectional area of n-type and p-type TE elements, mm^2	1.0	2.0

Besides, the total number of thermoelectric couples (N) depends on the cross-sectional area of TE elements and packaging density. Its value can be evaluated using this equation:

$$N = \frac{Available\ area\ (S)\ of\ TEC\ \times\ packaging\ density\ (PD)}{2 \times A} \tag{30}$$

The detailed specifications of the thermoelectric cooling system considered for this work are presented in Table 2.

Table 2 Specifications of the thermoelectric cooling system

Description	*Parameter*	*Value*
Available C.S. area of TEC	S	15 mm x 15 mm
Packaging density	PD	80%
Ambient temperature	T_o	25°C or 298.15 K
Cold surface temperature	T_{co}	20°C or 293.15 K
Electrical contact resistance	r_c	1 x 10^{-8} Ω m^2
Thermal resistance of heat sink	R_{hs}	0.10 ^{0}C/W
Ceramic thermal conductivity	k_{cr}	35.3 W/m°C
Copper thermal conductivity	k_{cu}	386 W/m-°C

The lower bound and upper bound of the number of thermoelectric couples is the dependent variable and become 45 and 90, respectively for the present work. The cold side and hot side ceramic substrates are 0.2 mm in thickness. The cold side and hot side copper tabs are considered 90% of the available cross-sectional area of TEC and 0.1 mm in thickness. The parameter values as described in Table 1 and Table 2 are based on information provided by TEC manufacturers on technical catalogues.

4.2 Optimization of exergy efficiency or second law efficiency (η_{II})

The second single-objective optimization problem for maximization of the exergy efficiency or second law efficiency (η_{II}) of the thermoelectric cooler is formulated mathematically as:

$$\begin{cases} & Maximize\ \eta_{II} \\ Subject\ to & \\ & I_{min} \le I \le I_{max} \\ & L_{min} \le L \le L_{max} \\ & A_{min} \le A \le A_{max} \end{cases} \tag{31}$$

The bounds of design variables and specifications of thermoelectric cooling system resulting in variations of output are identical to previous optimization problem of maximization of energy efficiency as discussed in section 4.1.

4.3 Implementation of Genetic Algorithm

In complex engineering applications, the implementation of stochastic algorithms has become popular and common. The stochastic algorithm, like genetic algorithm attempts to perform a global search within the search space of design variables. Because of the promising potential researchers are using stochastic methods to evaluate, predict, and optimize different systems.

Genetic algorithm (GA), which is used for this study, uses a population of individuals to search the design space. It is based on natural genetics. A population represents a set of solutions. Each individual of a population represents a candidate solution. The initial population is processed for fitness evaluation. Each individual of the population is assigned a fitness score based on the objective function. GA performs its evolution by undergoing processes inspired by evolutionary biology. New generations are created using selection, crossover, and mutation of solutions. In each generation, the individuals are evaluated for fitness scores. Individuals with the highest fitness are chosen to produce offspring for the new generation. GA tries the search process in whole design space and has the ability to concentrate on global optimum or near-global optimum location. After completion of certain generations, GA population finally converges towards the optimum solution.

In the literature, many coding schemes are available for genetic algorithm such as binary-coded GA, gray coded GA, integer genes, and real-coded GA (RGA). RGA is more popular than others because of its inherent potential to directly provide numeric value solutions with no need to code and decode the solutions. Many real-world applications have shown the advantage of RGA compared to others. The simulated binary crossover (SBX) operator performs excellently in optimization problems with continuous search space. The real-variable GA is implemented in this paper as created by Deb and Agarwal (1995). GA parameters settings used for this work are given in Table 3.

Table 3 GA parameters

Parameter	*Value*
Population Size	50
Generations limit	1000
Crossover probability	0.80
Mutation probability	0.25

The GA solution procedure adopted for this study has the major steps as described below:
Major Steps used for Genetic Algorithm Optimization Process
Input: TEC dataset and GA parameters
Output: Optimum solution as per the objective
Begin

a. Initialize the population
b. Guess the values of T_h and T_c
c. Compute the values of TE material properties and Q_c and Q_h using Equations (5-9).
d. Compute new values of T_h and T_c and replace old values with new values.
e. Repeat the process until the difference in new and old values of T_h and T_c becomes negligible.
f. Accept the individual (solution) of the population, if it satisfies the conditions at step-e mentioned above.
g. Evaluate the individual of the population for fitness values.
h. Take the next individual of the current population and repeat the process discussed above.
i. After the entire population is evaluated, a new population is formed by using selection, crossover, and mutation operators of genetic algorithm.
j. The entire process is repeated for a stipulated number of maximum generations.
k. The important statistics of generations are reported.

5 Results and discussion

In two single-objective optimization problems, the energy efficiency and the exergy efficiency of the irreversible thermoelectric cooler are maximized using genetic algorithm. Genetic algorithm based optimizations are coded in C language. In this study, the GA source code developed by Deb (2001) was employed. Multiple independent runs were performed for each optimization problem. Table 4 contains the best optimization results after 1000 generations for multiple runs of energy efficiency maximization and exergy efficiency maximization. These best results are repeatedly found over various runs.

The optimal values of design variables are identical for both the optimization problems as per simulation results. The optimum input current to obtain maximum energy and exergy efficiency are with the same values of 0.28A. This finding of results is a reliable match as reported by researchers (Kaushik et al., 2015; Manikandan et al., 2016). This study found that besides input current, the length and cross-sectional area of TE elements to obtain maximum energy and exergy efficiencies are also the same. The overall findings of this

study are superior to previous approaches because the previous studies reported similar values of one variable while other parameters were kept constant to obtain peak values of η_I and η_{II}. In the optimized solutions, the length of TE element is found as 2.0 mm which is the upper limit of the range. The other design variables (I and A) are unique and well between the bounds of given ranges. Depending on the optimal design values of three different variables, the corresponding temperature T_h is obtained as 25.11°C, and T_c is found as 19.97°C. The corresponding hot surface temperature (T_{ho}) is estimated as 25.09°C. The rate of cooling (Q_c) and the rate of heat rejection (Q_h) are achieved as 0.746 W and 0.927 W, respectively. Exergy parameters for optimized exergy efficiency are given in Table 5.

Table 4 Results of GA based optimization for maximization of Energy and Exergy Efficiencies

Case	η_I	η_{II}	*Optimal Values of Design Variables*			
			I	*L*	*A*	*N (Dependent)*
Optimization of Energy Efficiency	4.116	0.0715	0.28 A	2.0 mm	1.956 mm^2	45
Optimization of Exergy Efficiency	4.116	0.0715	0.28 A	2.0 mm	1.956 mm^2	45

Table 5 Exergy parameters for maximized exergy efficiency (η_{II})

Maximized Exergy Efficiency	*Exergy Input*	*Exergy Output*	*Exergy Destructed*	*Entropy Generation Rate*
7.15%	0.1874 W	0.0134 W	0.1740 W	0.5835×10^{-3} W/K

The heat rejection increases the rate of entropy generation (S_{gen}) and exergy destruction in the TEC system. The work provided to the TEC system includes exergy transfer towards the cold side and loss of available work due to the irreversibility of the system. Hence, the required work exceeds the threshold value. S_{gen} is minimized for maximum exergy efficiency. The exergy efficiency or second law efficiency is maximized and achieved as 7.15%.

6 Finite-element simulation with ANSYS®

The finite-element simulation is an effective computational method for approximate solutions to a number of complex real-world engineering problems with boundary conditions. It has become a key software for the analysis of real-world problems in the engineering domain. The authors have used finite-element simulation to validate GA result.

Since the maximum energy and exergy efficiency are obtained at the same amount of *I*, *L,* and *A*, any of the two maximization results can be tested. The authors have selected maximum exergy efficiency to be verified as it can be the preferred basis of TEC design because of environmental concerns. The ANSYS® is a multi-purpose analysis tool to generate the finite-element model and perform simulation for a wide range of engineering areas. ANSYS® is capable of providing coupled solutions to electric and thermal fields that are required for TEC simulation. Hence, the authors have used ANSYS® for finite-element simulation for this work. There are three major steps involved in the finite-element analysis of the thermoelectric cooling system using ANSYS® : (a) Finite-element model generation (b) Finding solution after specifying boundary conditions (c) Reviewing plots and results

A non-linear three-dimensional finite-element model has been set up. This finite-element model consists of a TEC structure with one pair of n-type and p-type thermoelectric elements following GA result. The authors have used a new approach for taking consideration of electrical contact resistances in both the junctions. A new geometric part at each end of each thermoelectric element is added to incorporate the effect of electrical contact resistances. These new parts are termed as 'Contact Resistance', and the complete TEC structure for finite-element simulation is shown in Figure 2. Each 'Contact Resistance' part has material properties pertinent to thermo-electric behaviour of electrical contact resistance.

Figure 2 TEC structure for finite-element simulation

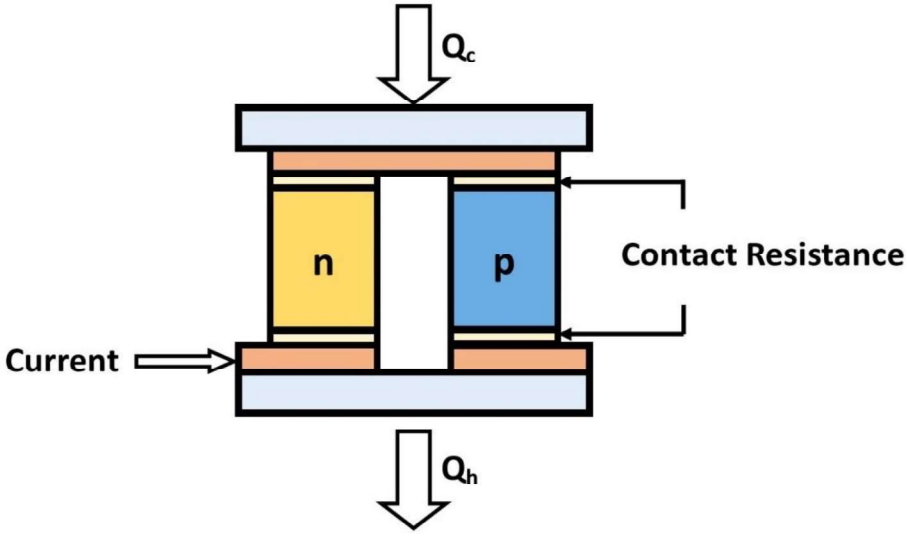

The input parameters for finite-element simulations to validate genetic algorithm result of maximum exergy efficiency of TEC are given in Table 6. Except for those for which the boundary conditions are specified in Table 6, a small convection loss of 0.000001 W/mK

is added to all surfaces of the adiabatic heat transfer models from the exposed surfaces of the thermoelectric cooling system.

Table 6 Input Parameters for Finite-element simulations to validate GA result of maximum exergy efficiency

Description	*Parameter*	*Value per pair of TE Elements*
Rate of Cooling	Q_c	0.0165 W
Current	I	0.28 A
Hot Side Temperature of TEC	T_{ho}	25.09 ℃

The steady-state finite-element TEC model for validating GA results has thermoelectric elements of length and cross-sectional area as reported in Table 4. The material properties of thermoelectric elements are temperature-dependent and computed using T_c and T_h values. The GA predictions for maximum exergy efficiency were tested. The mesh generated for this simulation, electric voltage distribution, and temperature distribution are shown in Figure 3.

Figure 3 (a) Mesh generation (b) Temperature distribution (c) Voltage distribution in the Finite-Element Model for Maximum Exergy Efficiency

(a) Mesh generation

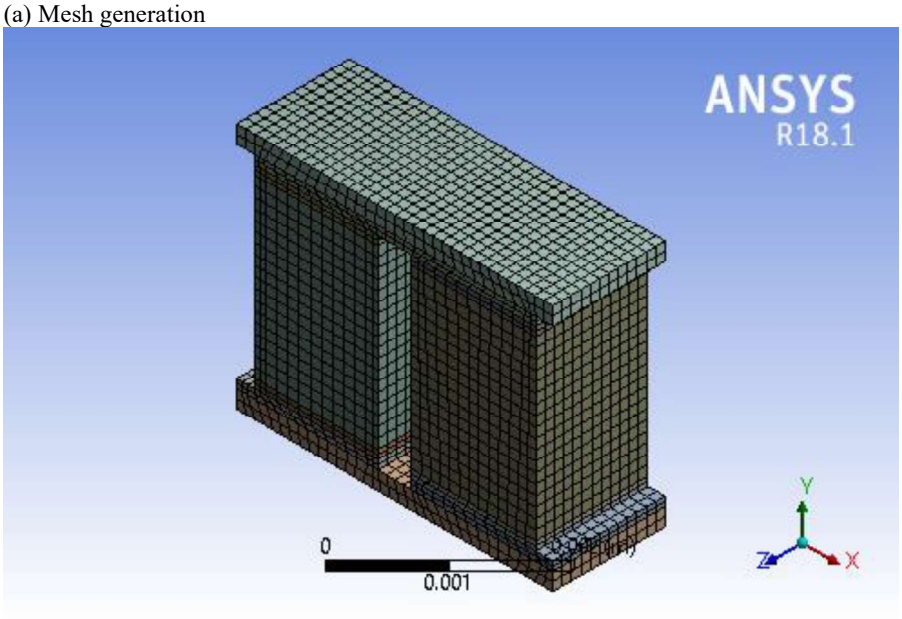

(b) Temperature distribution

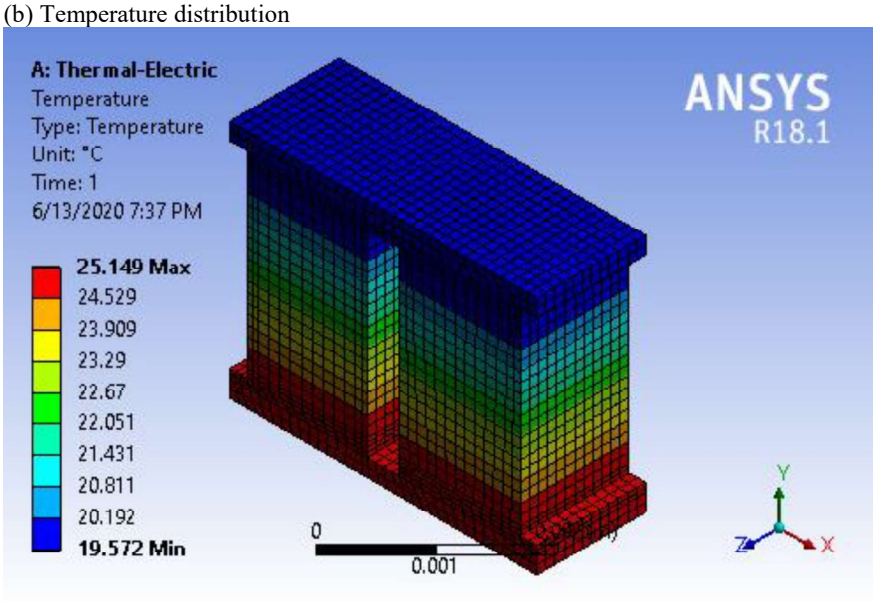

(c) Voltage distribution

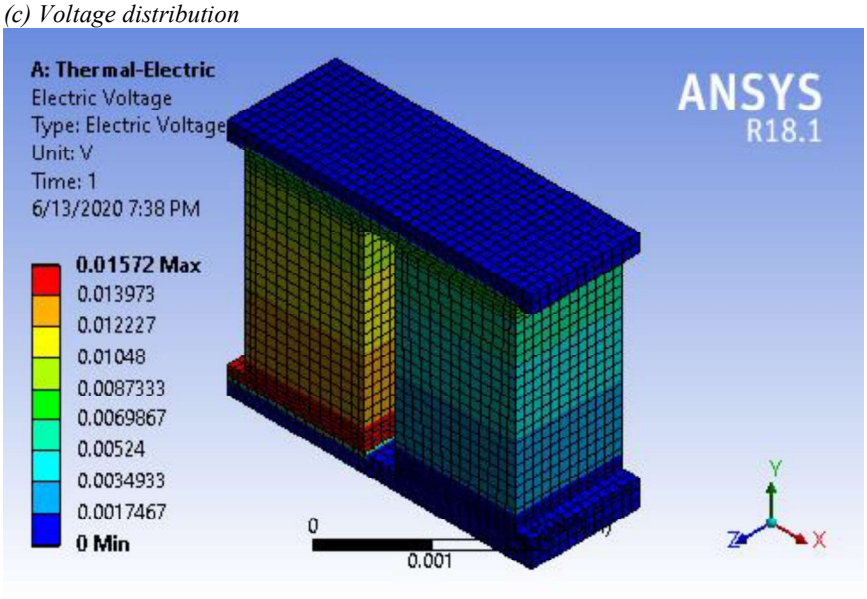

The result of the finite-element simulation is in strong alignment with those predicted by GA. This comparison of the results is shown in Table 7.

Table 7 Comparison of GA and *ANSYS*® results for maximum exergy efficiency

Description	*Parameter*	*GA*	*ANSYS*®	*Remarks*
Input Electric Power	P	0.004 W	0.004 W	Value for one
Rate of heat rejection	Q_h	0.021 W	0.021 W	pair of TE
Cold surface temperature	T_{co}	20 °C	19.61 °C	elements

As can be seen from the comparison presented in Table 7, the values of P and Q_h perfectly match while T_{co} slightly differs which is quite acceptable. The ANSYS® result strongly matches the GA result. The GA optimization result is verified by the ANSYS® thermal-electric module solutions.

7 Conclusion

The purpose of the first and second laws of thermodynamic analysis of this work is to find maximized energy efficiency (η_I) and exergy efficiency (η_{II}) of a TEC. This study introduces a new approach by selecting three design variables, i.e., length of n-type and p-type TE elements, the cross-sectional area of n-type and p-type TE elements, and the input electric current. The authors have used a thermal resistance model in both analytical and numerical models. The thermal resistances of ceramic substrates, copper conductors, and heat sink at the hot side have been incorporated for realistic TEC model consideration. Unlike previously reported works, the authors have used junction temperatures different from surface temperatures at the respective cold and hot sides of TEC.

Previous studies (Kaushik et al., 2015; Manikandan et al., 2016) indicate that η_I and η_{II} are maximum at the same current. This study has shown that the maximum values of η_I and η_{II} are obtained not only at the same current but the length and cross-sectional area of thermoelectric elements are also the same. In previous studies, the identical electric current for maximum η_I *and* η_{II} were recorded, while other parameters were kept constant. If we consider three performance indicators for thermoelectric coolers, i.e., cooling capacity, energy efficiency (η_I) and exergy efficiency (η_{II}), through this work it is clear that maximum η_{II} automatically assures maximum η_I.

For environmental consideration, the authors recommend the maximization of exergy efficiency as the basis of TEC design. The improvement in exergy efficiency is a reflection of the thermodynamic improvement of the thermoelectric cooling operation and high sustainable score. Exergy analysis includes all losses (irreversibilities) in the parts and complete thermoelectric cooling system. Irreversibilities can be minimized to get maximum exergy efficiency, which makes the TEC system more sustainable.

Since it is a numerical simulation, a different technique is required to validate the GA result. Hence, the authors have tried to validate the maximized exergy efficiency solution and tested with the finite-element TEC model. The genetic algorithm solution is validated

through finite-element simulation using ANSYS® thermal-electric module which is well in agreement with each other.

The dimensionless figure of merit (*ZT*) of thermoelectric materials plays an important role in characterizing the performance of TEC. It is important to develop more efficient thermoelectric materials with a focus on maximizing *ZT* value. When significant advances in the peak value of the dimensionless figure of merit of thermoelectric materials will be found, the exergy efficiency of TEC can be higher than the vapour compression refrigeration systems. Future research on sustainable TEC design should consider different thermoelectric materials at different temperatures range.

References

Abramzon, B. (2007) 'Numerical optimization of the thermoelectric cooling devices', *J. Electron. Packag. Trans. ASME,* Vol. 129, pp. 339–347. https://doi.org/10.1115/1.2753959

Astrain, D., Vián, J.G., Domínguez, M. (2003) 'Increase of COP in the thermoelectric refrigeration by the optimization of heat dissipation', *Appl. Therm. Eng.,* Vol. 23, pp. 2183–2200. https://doi.org/10.1016/S1359-4311(03)00202-3

Bejan, A. (2016) *Advanced Engineering Thermodynamics*, John Wiley & Sons, Singapore. https://doi.org/10.1002/9781119245964

Bejan, A. (2002) 'Fundamentals of exergy analysis, entropy generation minimization, and the generation of flow architecture', *Int. J. Energy Res.*, Vol. 26, pp. 0–43. https://doi.org/10.1002/er.804

Çengel, Yunus A. Boles, Michael A. Kanoğlu, M. (2019) *Thermodynamics: An Engineering Approach*, McGraw Hill, New York.

Cheng, Y.H., Lin, W.K. (2005) 'Geometric optimization of thermoelectric coolers in a confined volume using genetic algorithms', *Appl. Therm. Eng.,* Vol. 25, pp. 2983–2997. https://doi.org/10.1016/j.applthermaleng.2005.03.007

Deb, K., Agrawal, R.B. (1995) 'Simulated Binary Crossover for Continuous Search Space', *Complex Syst.* Vol. 9, pp. 115–148. https://doi.org/10.1.1.26.8485Cached

Dincer, I. (2016) 'Exergization', *Int. J. Energy Res.* Vol. 40, pp. 1887–1889. https://doi.org/10.1002/er.3606

Dincer, I., Kanoglu, M. (2017) *Refrigeration Systems and Applications*, John Wiley & Sons, Chichester

Dincer, I., Rosen, M.A. (2013) *Exergy* : *Energy, Environment and Sustainable Development,* Elsevier Science, Oxford, UK.

Fabián-Mijangos, A., Min, G., Alvarez-Quintana, J. (2017) 'Enhanced performance thermoelectric module having asymmetrical legs', *Energy Convers. Manag.* Vol. 148, pp. 1372–1381. https://doi.org/10.1016/j.enconman.2017.06.087

Ferreira-Teixeira, S., Pereira, A.M. (2018) 'Geometrical optimization of a thermoelectric device: Numerical simulations', *Energy Convers. Manag.,*Vol. 169, pp. 217-227. https://doi.org/10.1016/j.enconman.2018.05.030

Fraisse, G., Ramousse, J., Sgorlon, D., Goupil, C. (2013) 'Comparison of different modeling approaches for thermoelectric elements', Energy Convers. Manag. Vol. 65, pp. 351–356. https://doi.org/10.1016/j.enconman.2012.08.022

Ghoshal, U., Ghoshal, S., McDowell, C., Shi, L., Cordes, S., Farinelli, M. (2002)

'Enhanced thermoelectric cooling at cold junction interfaces', *Appl. Phys. Lett.* Vol. 80, pp. 3006–3008. https://doi.org/10.1063/1.1473233

Giri, J.M., Nain, P.K.S. (2019) 'Optimization of Refrigeration Rate for a Thermoelectric Cooler in Restricted Space using Stochastic Algorithms', *Int. J. Recent Technol. Eng.* Vol. 8, pp. 2306–2311. https://doi.org/10.35940/ijrte.b2701.078219

Hermes, C.J.L., Barbosa, J.R. (2012) 'Thermodynamic comparison of Peltier, Stirling, and vapor compression portable coolers', *Appl. Energy*, Vol. 91, pp. 51–58. https://doi.org/10.1016/j.apenergy.2011.08.043

Huang, Y.X., Wang, X.D., Cheng, C.H., Lin, D.T.W. (2013) 'Geometry optimization of thermoelectric coolers using simplified conjugate-gradient method', *Energy*, Vol. 59, pp. 689–697. https://doi.org/10.1016/j.energy.2013.06.069

Jeong, E.S. (2014) 'A new approach to optimize thermoelectric cooling modules', *Cryogenics*, Vol. 59, pp. 38–43. https://doi.org/10.1016/j.cryogenics.2013.12.003

Kaushik, S.C., Manikandan, S., Hans, R. (2015) 'Energy and exergy analysis of thermoelectric heat pump system', *Int. J. Heat Mass Transf.* Vol. 86, pp. 843–852. https://doi.org/10.1016/j.ijheatmasstransfer.2015.03.069

Lee, H.S. (2013) 'Optimal design of thermoelectric devices with dimensional analysis', *Appl. Energy*, Vol. 106, pp. 79–88. https://doi.org/10.1016/j.apenergy.2013.01.052

Lee, K.H., Kim, O.J. (2007) 'Analysis on the cooling performance of the thermoelectric micro-cooler', *Int. J. Heat Mass Transf.* Vol. 50, pp. 1982–1992. https://doi.org/10.1016/j.ijheatmasstransfer.2006.09.037

Manikandan, S., Kaushik, S.C., Anusuya, K. (2016) 'Thermodynamic modelling and analysis of thermoelectric cooling system', *International Conference on Energy Efficient Technologies for Sustainability, ICEETS 2016*. *Institute of Electrical and Electronics Engineers Inc.*, pp. 685–693. https://doi.org/10.1109/ICEETS.2016.7583838

Miner, A., Majumdar, A., Ghoshal, U. (1999) 'Thermo-electro-mechanical refrigeration based on transient thermoelectric effects', *International Conference on Thermoelectrics, ICT, Proceedings. IEEE*, pp. 27–30. https://doi.org/10.1109/ict.1999.843327

Moran, M.J., Shapiro, H.N., Boettner, D.D., Bailey, M.B. (2018) *Fundamentals of Engineering Thermodynamics*, John Wiley & Sons, Chichester.

Nain, P.K.S., Sharma, S., Giri, J.M. (2010) 'Non-dimensional multi-objective performance optimization of single stage thermoelectric cooler', *Lecture Notes in Computer Science (Including Subseries Lecture Notes in Artificial Intelligence and Lecture Notes in Bioinformatics).* pp. 404–413. https://doi.org/10.1007/978-3-642-17298-4_44

Nami, H., Nemati, A., Yari, M., Ranjbar, F. (2017) 'A comprehensive thermodynamic and exergoeconomic comparison between single- and two-stage thermoelectric cooler and heater', *Appl. Therm. Eng.* Vol. 124, pp. 756–766. https://doi.org/10.1016/j.applthermaleng.2017.06.100

Pan, Y., Lin, B., Chen, J. (2007) 'Performance analysis and parametric optimal design of an irreversible multi-couple thermoelectric refrigerator under various operating conditions', Appl. Energy 84, 882–892. https://doi.org/10.1016/j.apenergy.2007.02.008

Seifert, W., Pluschke, V. (2014) 'Maximum cooling power of a graded thermoelectric cooler', *Phys. Status Solidi Basic Res.*,Vol. 251, No.7, pp. 1416-1425. https://doi.org/10.1002/pssb.201451038

Shen, L., Zhang, W., Liu, G., Tu, Z., Lu, Q., Chen, H., Huang, Q. (2020) 'Performance enhancement investigation of thermoelectric cooler with segmented configuration', *Appl. Therm. Eng.* Vol. 168. https://doi.org/10.1016/j.applthermaleng.2019.114852

Thiébaut, E., Goupil, C., Pesty, F., D'Angelo, Y., Guegan, G., Lecoeur, P. (2017) 'Maximization of the Thermoelectric Cooling of a Graded Peltier Device by Analytical Heat-Equation Resolution', *Phys. Rev. Appl.* https://doi.org/10.1103/PhysRevApplied.8.064003

Völklein, F., Min, G., Rowe, D.M. (1999) 'Modelling of a microelectromechanical thermoelectric cooler', *Sensors Actuators, A: Physical, Vol.* 75, pp. 95–101. https://doi.org/10.1016/S0924-4247(99)00002-3

Yamanashi, M. (1996) 'A new approach to optimum design in thermoelectric cooling systems', *J. Appl. Phys.,* Vol. 80, pp. 5494–5502. https://doi.org/10.1063/1.362740

Yu, J., Wang, B. (2009) 'Enhancing the maximum coefficient of performance of thermoelectric cooling modules using internally cascaded thermoelectric couples', *Int. J. Refrig.* Vol. 32, pp. 32–39. https://doi.org/10.1016/j.ijrefrig.2008.08.006

Zhang, H.Y. (2010) 'A general approach in evaluating and optimizing thermoelectric coolers', *Int. J. Refrig.* Vol. 33, pp. 1187–1196. https://doi.org/10.1016/j.ijrefrig.2010.04.007

Optimization of Refrigeration Rate for a Thermoelectric Cooler in Restricted Space using Stochastic Algorithms

Jitendra Mohan Giri, Pawan Kumar Singh Nain

Abstract*: In the present study, a mathematical model of single stage thermoelectric cooler (TEC) is reported. This model is then employed to optimize the rate of refrigeration (ROR) which is one of the important performance measures of TEC. Two stochastic algorithms, namely, the genetic algorithm (GA) and simulated annealing (SA) are employed for optimizing the said performance of TEC for restricted space. The selected design variables are the geometric structural parameters of TEC elements and the input current. This study also includes the thermal resistance of hot side heat exchanger and electrical contact resistances into consideration. The results show that these design variables can be optimally set to maximize ROR within restricted space very significantly. The two algorithms for optimization attained almost the same values of design variables that lead to optimum ROR, though the GA could locate multi-modal optimum and hence can be used by the designer to choose among various options of design variables without compromising on the optimized value of ROR. .

***Index Terms*: Single-stage thermoelectric cooler, Rate of refrigeration, Genetic algorithm, Simulated annealing**

I. INTRODUCTION

Thermoelectric technology has endeavoured to pave the way for green energy devices. A thermoelectric cooler (TEC) fundamentally works on the Peltier effect, a well-known principle discovered by Jean Peltier in 1834. Thermoelectric coolers are hassle-free solid state devices with no moving components and no refrigerants. These devices produce no harmful chlorofluorocarbons (CFCs) compared to traditional refrigeration or cooling systems. In thermoelectric coolers, electric current flows through p-and n-type semiconductor elements and a temperature gradient is established. The small size thermoelectric coolers have applications in fields such as optical, laser, radio-electronic devices. Modular design, high reliability, low maintenance, and noiseless operation provide benefice for new horizons of TEC applications [1], [2], [3], [4]. Eco-friendliness of thermoelectric cooling makes these devices suitable for the cooling method of the future. However, thermoelectric coolers are limited in applications due to their low rate of refrigeration (*ROR*) and low coefficient of performance (*COP*) compared to compressor-based systems. In the past, some researchers have worked to synthesize newer semiconductor materials with a high figure of merit. But comparable refrigeration rate and coefficient of performance are still not achieved. Hence, it is a challenge to achieve the highest possible *ROR* and *COP* with the available semiconductor materials. Further, to increase market penetration of thermoelectric coolers, the main challenge is to upgrade its *ROR* and *COP* within available space.

The conversion of electrical energy into a temperature gradient depends on the figure of merit (*Z*), which is managed by the properties of thermoelectric materials and determined by α^2/RK; α represents Seebeck coefficient, R represents electric resistance and K represents overall thermal conductance. Numerous research is carried out to maximize the figure of merit of the thermoelectric materials which provide optimum cooling effects [5], [6], [7], [8].

The performance of thermoelectric coolers with different arrangements has been reported by the researchers. Martnez et al. [9] used the thermoelectric system for temperature control without the use of any external electrical power source. The heat generated in the internal source was transformed into the electricity and supplied for cooling of the device. It was highlighted that thermal resistance between the source of heat and environment can be lowered by 25-30%. Chang et al. [10] reported the performance of thermoelectric air cooling module employed in the electronic devices. The results show that at a specific heat load, the module reaches the best cooling performance at an optimum input current. Commercially available solid-state thermoelectric devices may be used for their electrical power generation capabilities when coupled to a thermometric refrigerator or heat pump. The DC current provided to run a thermoelectric refrigerator can also be generated from solar cells.

Many researchers have done experimental investigations of a TEC coupled with a solar cell. Dai et al. [11] investigated a thermoelectric refrigeration system driven by solar energy. The temperature in the refrigerator was successfully maintained between 5 to 10°C with a *COP* of 0.3. A solar driven thermoelectric cooling module with a waste heat refrigeration unit designed for green building application has been investigated by Cheng et al. [12]. It was found that the approach was able to produce a 16.2°C temperature difference between the ambient temperature and the air temperature in the model house. An analysis

Revised Manuscript Received on July 09, 2019.

Jitendra Mohan Giri, Research Scholar, School of Mechanical Engineering, Galgotias University, Greater Noida, India.
Pawan Kumar Singh Nain, Professor, School of Mechanical Engineering, Galgotias University, Greater Noida, India.

of TEC performance has been conducted for high power electronic packages such as processors by Zhang et al. [13]. The cooling configurations and optimum current resulted in substantial thermal enhancements.

Huang et al. [14] used the conjugate-gradient method for TEC geometry optimization at a fixed current and fixed temperature difference to achieve optimized cooling rate. The effects of applied current and temperature difference on the optimal geometry were discussed. A review of cooling parameters and related performance along with possible approaches to improve *COP* of TEC has been presented by Enescu and Virjoghe [15]. Lin and Yu [16] indicated that trapezoid-type two-stage Peltier couples can reduce thermal resistance followed by improved cooling capacity and *COP*. Nain et al. [17] optimize structural parameters to improve *ROR* and *COP* of a single-stage TEC.

The importance of the development of high performance and cost controlled cooling systems for small enclosures is significant. In this study, a mathematical model of single stage thermoelectric cooler is used for establishing the rate of refrigeration in terms of design variables and material properties. Then this *ROR* is optimized by two stochastic optimization techniques, namely, genetic algorithm (GA) and simulated annealing (SA) independently [18], [19], [20], [21] [22]. Genetic algorithm and simulated annealing are the stochastic algorithms that are able to search large regions of the solution's space without being trapped in local optima. The design variables that maximize *ROR* within considered available space are reported.

II. MATHEMATICAL MODELLING

The physical model of a single stage thermoelectric cooler is shown in Fig. 1. It includes one thermoelectric module, corresponding cold, and hot side material, and external hot side heat exchanger.

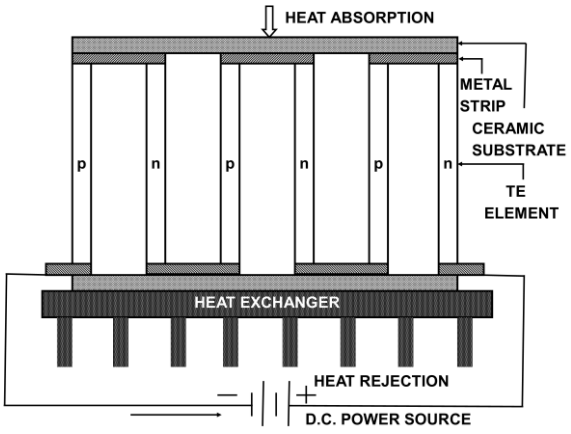

Fig. 1: Schematic Diagram Of A Single Stage Thermoelectric Cooler

The present analysis starts with the phenomenological relations described in the literature [23], [24]. The Peltier effect is the basis for thermoelectric cooling. As a result of DC current flow through a number of pairs of n- and p-type thermoelectric elements linked together electrically in series and thermally in parallel, a temperature difference is created. The thermal conduction from the hot side of the module to the cold side. The Joule heat resulting from the current flow in the thermoelectric materials will also be generated. Half the Joule heat thus generated will flow on each side of the module. An electrically insulated and thermally conductive material is in thermal contact with a heat source on the cold side of the junctions and with a heat sink on the hot side of the junctions. The electrically conductive material is alternately attached to the cold and hot side to form an electrical circuit inside the thermoelectric module as shown in Fig.1. The external hot side heat exchanger dissipates heat to the ambient environment.

The equations for heat balance at the two junctions of the module are:-

.

$$Q_c = 2N\left[I\alpha T_c - \frac{kA(T_h - T_c)}{L} - \frac{1}{2}I^2\left(\frac{\rho L}{A} + 2\frac{r_c}{A}\right)\right] \quad (1)$$

$$Q_h = 2N\left[I\alpha T_h - \frac{kA(T_h - T_c)}{L} + \frac{1}{2}I^2\left(\frac{\rho L}{A} + 2\frac{r_c}{A}\right)\right] \quad (2)$$

Where, Q_h is the rate of heat rejection from the hot junction and Q_c is the rate of heat absorption at the cold junction which is referred as the rate of refrigeration (*ROR*) in common usage. Thermoelectric material properties α, ρ, k and r_c are the Seebeck coefficient, electrical resistivity, thermal conductivity, and electrical contact resistance, respectively. T_h and T_c are the hot and cold junction temperatures and L and A are the length and cross-sectional area of thermoelectric elements, respectively. I is the input electric current and N is the number of thermoelectric couples in the module. Heat flows $kA(T_h - T_c)/L$ and $\frac{1}{2} I^2 (\rho L/A + 2r_c/A)$ refers to thermal conduction and Joule heat, respectively. $I\alpha T_h$ is the Peltier heat at the hot junction and $I\alpha T_c$ is the Peltier heat at the cold junction.

The material of the thermoelectric elements used in this study is bismuth telluride. The thermoelectric material properties are based on the average temperature (T_{ave}) of the cold and hot side temperatures. The equations for this temperature range are provided by Melcor [25] and described as follows:

$$\alpha = (22224 + 930.6\,T_{ave} - 0.9905\,T_{ave}^2) \times 10^{-9} \quad (3)$$

$$\rho = (5112 + 163.4\,T_{ave} + 0.6279\,T_{ave}^2) \times 10^{-10} \quad (4)$$

$$k = (62605 - 277.7\,T_{ave} + 0.4131\,T_{ave}^2) \times 10^{-4} \quad (5)$$

In this work, the thermal resistance of hot side heat exchanger is taken into account in order to discuss its effect on the hot junction temperature prediction and performance of the system in such a way that following equation is satisfied.

$$T_h = Q_h \times R_{th} + T_a \quad (6)$$

Where R_{th} is the thermal resistance of hot side heat exchanger and T_a is the ambient temperature.

III. NUMERICAL OPTIMIZATION OF SINGLE STAGE TEC

In order to analyze the performance of a single stage TEC, the rate of refrigeration of the system is examined. The thermoelectric cooler has to be designed as compact as possible because the space in electronic equipment is limited. In this study, the cross-sectional area of the thermoelectric cooler (S) is fixed as 25 mm^2. Further, there is also a restriction on the maximum length of elements which makes the total space restricted. The optimization process starts by selecting the length of elements (L), cross-sectional area of elements (A), a number of thermoelectric couples (N) in TEC and input current (I) to be the design variables. The objective is now to find the values of L, A, N and I for achieving the best performance, i.e., max *ROR* using equation (1) for the thermoelectric cooling system in restricted space.

The optimization of the rate of refrigeration of thermoelectric cooler is stated as the following single objective constrained optimization problem

$$\left.\begin{aligned} &\textit{Maximize} && ROR \\ &\textit{subject to} && \\ & && I_{min} \le I \le I_{max} \\ & && L_{min} \le L \le L_{max} \\ & && A_{min} \le A \le A_{max} \\ & && N_{min} \le N \le N_{max} \end{aligned}\right\} \quad (7)$$

The thermal resistance of hot side heat exchanger is fixed as 0.1°CW^{-1}. An increase in thermal resistance of hot side heat exchanger decreases the rate of refrigeration and increases the hot-side temperature. The other fixed design parameters are the electrical contact resistance as 1x10^{-8} Ω-m^2, cold junction temperature as 293.15 K and ambient temperature as 298.15 K. The packaging density is taken as 80% considering practical manufacturing limitation. The four design variables are allowed to vary within certain ranges as per real-world applications. The length and cross-sectional area of elements are in the range of 0.5-1.5 mm and 0.25-1.0 mm^2, respectively. The available cross-sectional area of TEC and the maximum length of elements makes the total space restricted as 25 mm^2 x 1.5 mm = 37.5 mm^3.

The number of thermocouples (N) is a dependent variable, as its value depends on the available cross-sectional area of thermoelectric cooler and the cross-sectional area of TE elements. The number of thermocouples is rounded down to the nearest integer which is obtained using equation (8).

$$N = \frac{S \times packaging\ density}{2 \times A} \quad (8)$$

The available TEC cross-sectional area of 25 mm^2 with 0.8 packaging density allows the number of thermocouples to vary from 10 to 40 in this work. The input current is allowed to vary in the range of 0.1-3.0 ampere. The hot side temperature (T_h) is initially fixed to some guessed value so that the material properties can be obtained using equations (3), (4) and (5). Employing equations (1), (2) and (6), the new value of T_h is calculated. This difference of guessed and the new value of T_h is used to modify the guess value of T_h iteratively, till the difference becomes negligible. In this work, we have separately applied genetic algorithm & simulated annealing as optimization tools for the same optimization problem.

IV. OPTIMIZATION RESULTS

(A) Optimization results using GA

The real-variable genetic algorithm employing SBX operator developed by Deb and Agarwal is used for single objective optimization [20]. The algorithm is coded in C language. GA requires a population of data points to be evaluated over multiple generations to reach an optimal solution. Table I shows GA parameters, applied in the single objective optimization of *ROR*. Since the genetic algorithm is a stochastic algorithm, therefore, the simulation was run five times and the best one is reported. The parameters values which are used in optimization by GA are reported in Table I.

Table I. Parameters Settings for GA

Population size	20
Crossover probability	0.80
Mutation probability	0.25
Termination Criteria	1000 generations
Number of runs	5

The search process is completed very quickly with GA. The optimization history for best run in terms of the optimized average *ROR* for the entire population with generation number is shown in Fig. 2. Under the set conditions GA has achieved the optimum *ROR* as 1.144869 W at a current (I) of 2.360 A, TE element length (L) of 0.542 mm, cross-sectional area of TE element (A) of 1.0 mm^2. The optimal value of the length of TE elements is 0.542 mm and it demonstrates that it is unique while maximizing *ROR* and does not hit any variable bound of the permitted range of 0.5-1.5 mm. The optimal value of the cross-sectional area of TE elements hit the upper variable bound of 1.0 mm^2 and hence, it signifies the importance of exploring the upper limit of the permitted range of cross-sectional area of TE element. The optimal number of thermoelectric couples (N) is 10.

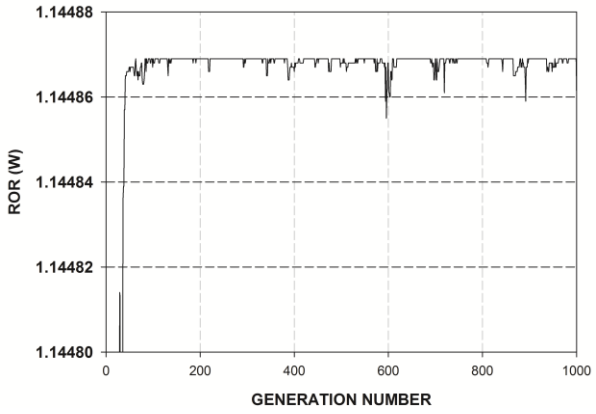

Fig. 2: GA Convergence Curve Of Optimized ROR

Additionally, in order to examine the possibility of multiple optima in the search space, this simulation was repeated many times with different settings. It was found that the present optimization problem is having three distinct optima with same values of *ROR*. Hence, it is a case of multimodal function optimization. The optimal parameters for these captured peaks are reported in Table II. These three captured peaks of the objective function are labeled as Optima-1, Optima-2, and Optima-3. If we observe all three optimum solution vectors reported in Table II, it is found that the optimal value of the length of TE elements '*L*' is 0.542 mm in all three cases.

Table II. GA optimization results

S. No.	I (A)	L (mm)	A (mm^2)	N	Optimized ROR (Watts)	Label
1	2.360	0.542	1.0	10	1.144869	Optima -1
2	1.180	0.542	0.5	20	1.144869	Optima -2
3	0.944	0.542	0.4	25	1.144869	Optima -3

(B) Optimization results using SA

These optimization results and searchability of GA is checked by applying another robust stochastic algorithm which is simulated annealing. Simulated annealing is a random search procedure for global optimization problems, and it resembles the annealing process to solve an optimization problem. The process uses the careful control of temperature and cooling rate that controls the search. The temperature parameter is high at the start and a number of iterations are executed before lowering the temperature at each instant till the convergence criteria is satisfied. The SA source code that works robustly for MATLAB® and able to handle non-linear constraints is developed by Xin-She Yang and used in this work [26]. The simulation was run with different settings of SA. Table III shows SA parameters with best-obtained performance, applied in optimizing *ROR*.

Table III. Parameters Settings for SA

Initial Temperature	1.0
Final Temperature	$1e^{-10}$
Cooling Factor	0.8
Boltzmann Constant	1
Number of iterations per temperature level	500

The Optimum *ROR* captured by SA is 1.144869 watts. The solution vector is identical to one obtained from GA and labeled as Optima-1 in Table II. This simulation was also carried out several times with different settings but SA is able to capture only single best peak as reported in Table IV. These identical results obtained from GA and SA doubly ensure the optimized value of ROR and corresponding optimal design parameters.

Table IV. SA optimization result

S. No.	I (A)	L (mm)	A (mm^2)	N	Optimized ROR (Watts)	Label
1	2.360	0.542	1.0	10	1.144869	Optima -1

The mathematical model of the present work has defined *ROR* as a function of *I*, *L*, *A*, and *N*. The variables *I*, *L* and *A* are the independent design variables whereas *N* is a dependent design variable because it is calculated by using the value of *A* and employing equation (8). We observe from Table II and Table IV that the optimal value of *L* is 0.542 mm in all the results discovered by GA and SA. Though *ROR* is a function of three independent variables namely *I*, *L* and *A*. If we fix *L* at 0.542 mm as found in all solutions of this optimization problem, it is possible to represent *ROR* with two remaining independent variables *I* and *A* in a 3D plot by using equation (1). Hence a 3D plot is drawn employing equation (1) with *L* fixed at 0.542 mm and shown in Fig. 3. The parameters *I*, *A* and *ROR* are shown on the X-axis, Y-axis, and Z-axis, respectively. Then, we have superimposed the three optima which were discovered by GA and reported in Table II. These are labeled as Optima-1, Optima-2, and Optima-3 in the same order as reported in Table II. If we refer to Table II and Table IV, we find that the Optima-1 is discovered by both, GA and SA while the Optima-2 and Optima-3 are discovered by GA only. Though the optimum *ROR* is 1.144869 W in all the solutions vectors, GA has discovered all three possible optima and hence, it is able to handle this multimodal optimization problem. SA was unable to find multiple optima though the simulation was run at repeated times with different settings. Hence, in the present multimodal problem, GA has partially outperformed SA.

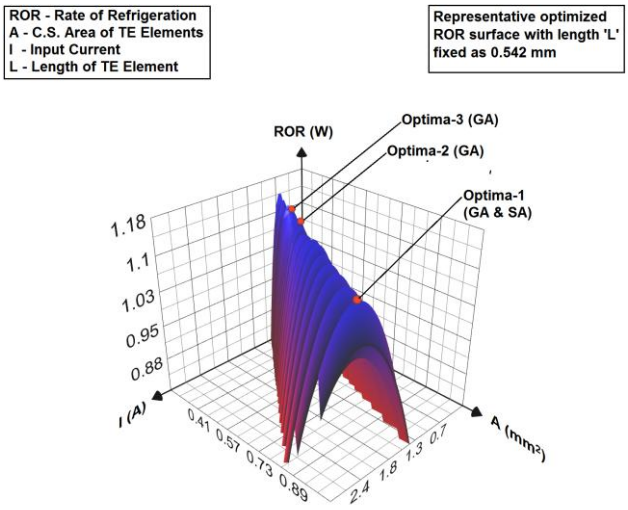

Fig. 3 Multiple optima labeled at the *ROR* surface with thermoelectric element length *L* = 0.542 mm

V. CONCLUSION

The importance of TECs is significant in the present scenario when the world is facing the challenge to provide devices which are ecologically green and the cost-effective. Thus, it is important to study these devices to derive their maximum performance within the technological limitation of manufacturing. This work attempted to find out the optimum design parameters to improve an important performance measure (*ROR*) of TEC using GA and SA. This work has demonstrated that the geometric structural parameters of the thermoelectric elements and the input current have an influence on the rate of refrigeration of TEC and can be suitably varied to enhance the performance of TEC. The *ROR* of thermoelectric cooler within the total restricted space of 37.5 mm^3 of TEC was successfully optimized in this work. The conspicuous observation of GA and SA results in present work is that GA search outperformed SA and located multiple optima. The combined selection of input current and the geometric structural parameters used as design variables in this work provides a guide to future research. The current optimization problem can also be attempted by using different optimization methods as Huang et al. have employed in their work [14]. Designers can handle space restriction for the case at hand and improve *ROR*.

REFERENCES

1. F. J. Disalvo, "Thermoelectric Cooling and Power Generation" in Science, 285 (5428), pp. 703–706, 1999.
2. C. B. Vining, "Semiconductors are cool" in Nature, 413 (6856), pp. 577–578, 2001.
3. D. Zhao and G. Tan, "A review of thermoelectric cooling: Materials, modeling and applications" in Applied Thermal Engineering, 66 (1-2), pp. 15–24, 2014.
4. M. Sajid, I. Hassan, and A. Rahman, "An overview of cooling of thermoelectric devices" in Renewable and Sustainable Energy Reviews, 78, pp. 15–22, 2017.
5. G. Mahan, B. Sales, and J. Sharp, "Thermoelectric Materials: New Approaches to an Old Problem" in Physics Today, 50 (3), pp. 42–47, 1997.
6. R. Venkatasubramanian, E. Siivola, T. Colpitts, and B. Oquinn, "Thin-film thermoelectric devices with high room-temperature figures of merit" in Nature, 413 (6856), pp. 597–602, 2001.
7. T. C. Harman, "Quantum Dot Superlattice Thermoelectric Materials and Devices" in Science, 297 (5590), pp. 2229–2232, 2002.
8. E. Thiébaut, C. Goupil, F. Pesty, Y. D'Angelo, G. Guegan, and P. Lecoeur, "Maximization of the Thermoelectric Cooling of a Graded Peltier Device by Analytical Heat-Equation Resolution" in Physical Review Applied, 8 (6), 2017.
9. Martínez, D. Astrain, and A. Rodríguez, "Experimental and analytical study on thermoelectric self cooling of devices" in Energy, 36 (8), pp. 5250–5260, 2011.
10. Y.-W. Chang, C.-C. Chang, M.-T. Ke, and S.-L. Chen, "Thermoelectric air-cooling module for electronic devices" in Applied Thermal Engineering, 29 (13), pp. 2731–2737, 2009.
11. Y. Dai, R. Wang, and L. Ni, "Experimental investigation on a thermoelectric refrigerator driven by solar cells" in Renewable Energy, 28 (6), pp. 949–959, 2003.
12. T.-C. Cheng, C.-H. Cheng, Z.-Z. Huang, and G.-C. Liao, "Development of an energy-saving module via combination of solar cells and thermoelectric coolers for green building applications" in Energy, 36 (1), pp. 133–140, 2011.
13. H. Zhang, Y. Mui, and M. Tarin, "Analysis of thermoelectric cooler performance for high power electronic packages" in Applied Thermal Engineering, 30 (6-7), pp. 561–568, 2010.
14. Y.-X. Huang, X.-D. Wang, C.-H. Cheng, and D. T.-W. Lin, "Geometry optimization of thermoelectric coolers using simplified conjugate-gradient method" in Energy, 59, pp. 689–697, 2013.
15. D. Enescu and E. O. Virjoghe, "A review on thermoelectric cooling parameters and performance" in Renewable and Sustainable Energy Reviews, 38, pp. 903–916, 2014.
16. S. Lin and J. Yu, "Optimization of a trapezoid-type two-stage Peltier couples for thermoelectric cooling applications" in International Journal of Refrigeration, 65, pp. 103–110, 2016.
17. P. K. S. Nain, J. M. Giri, S. Sharma, and K. Deb, "Multi-objective Performance Optimization of Thermo-Electric Coolers Using Dimensional Structural Parameters" in Swarm, Evolutionary, and Memetic Computing Lecture Notes in Computer Science, pp. 607–614, 2010.
18. L. Davis, Genetic algorithms and simulated annealing. London: Pitman, 1990.
19. D. E. Goldberg, Genetic algorithms in search, optimization, and machine learning. Boston: Addison-Wesley, 2012.
20. K. Deb, and R.B. Agrawal, "Simulated Binary Crossover for Continuous Search Space" in Complex Systems, 9 (2), pp. 115–148, 1994.
21. K. Deb, Optimization for engineering design: algorithms and examples. New Delhi: PHI Learning Private Limited, 2012.
22. G. C. Onwubolu and B. V. Babu, "New Optimization Techniques in Engineering" in Studies in Fuzziness and Soft Computing, 2004.
23. D. M. Rowe, CRC Handbook of Thermoelectrics. Boca Raton, FL: CRC Press, 2018.
24. H. J. Goldsmid, Introduction to thermoelectricity. Springer-Verlag Berlin And Hei, 2016.
25. "Melcor Thermoelectric Handbook," Laird Thermal Systems. [Online]. Available: https://www.lairdthermal.com/
26. "Xin-She Yang" Xin-She Yang - MATLAB Central. [Online]. Available:https://www.mathworks.com/matlabcentral/fileexchange/29739-simulated-annealing-for-constrained-optimization

AUTHORS PROFILE

Jitendra Mohan Giri is a research scholar in School of Mechanical Engineering at Galgotias University, Uttar Pradesh, India. He has graduated in Mechanical Engineering from Dr. B.R.Ambedkar University, Agra and post graduated from Uttar Pradesh Technical University, Lucknow. Currently, his research interest includes thermoelectric devices and optimization techniques. He has two international publications in Springer-Verlag. He is an Associate Member of the Institution of Engineers (India). He is working as an Assistant Professor in the Mechanical Engineering Department at Skyline Institute of Engineering & Technology, Greater Noida.

Thermal Engineering, Operations Research, Fluid Mechanics and Fluid Machinery are his subjects of interest.

Dr. P. K. S. Nain is a professor in School of Mechanical Engineering at Galgotias University, Uttar Pradesh, India. He is Gold Medalist in undergraduate program in Mechanical Engineering at A. M. U. Aligarh, India. He has received his M.E. from IIT Roorkee and Ph.D. from IIT Kanpur. He has received British Telecom (U.K.) Fellowship for Ph.D. at I.I.T. Kanpur. His area of interest is design and optimization. He has over 25 publications so far in the area of evolutionary algorithm, thermoelectric devices and interdisciplinary research in optimization through the design of experiments. He is a life member of ISTE and a teaching and research experience of 27 years.

Review of Recent Progresses in Thermoelectric Materials

Jitendra Mohan Giri and Pawan Kumar Singh Nain

Abstract Thermoelectric (TE) technology facilitates the direct conversion of heat into electricity and vice versa. Thermoelectric materials attract researchers since they facilitate a promising green energy solution in the form of solid-state cooling and power generation. However, the low energy conversion efficiency restricts the use of TE materials in real-world applications. Developing highly efficient thermoelectric materials is necessary to benefit the environment as well as the economy. The performance of a particular TE material is generally evaluated by the dimensionless figure of merit (*ZT*). Recent years have witnessed progress with new techniques in maximizing the *ZT* values of various thermoelectric materials. In this review, we summarize recent development in thermoelectric materials for a specific temperature range, which has been developed to improve their maximum *ZT* value up to 95% at the same temperature.

Keywords Thermoelectric materials · Thermoelectric performance · Dimensionless figure of merit · Seebeck coefficient

1 Introduction

The environmental issues resulting from unsustainable consumption of fossil fuels are well known. Thermoelectric (TE) devices are compact, noiseless, and environmentally friendly and exhibit a leading potential for sustainable development. The thermoelectric module is a p-type and n-type semiconductor element-based solid-state device that converts the thermal energy with temperature difference into electric power (known as Seebeck effect) and also capable of converting electrical energy into temperature gradient (known as Peltier effect). Based on the directions of energy

J. M. Giri (✉) · P. K. S. Nain
Galgotias University, Greater Noida 201312, India
e-mail: jitendra.giri@galgotiasuniversity.edu.in

P. K. S. Nain
e-mail: pawan.kumar@galgotiasuniversity.edu.in

B. P. Sharma et al. (eds.), *Advances in Engineering Materials*, Lecture Notes in Mechanical Engineering, https://doi.org/10.1007/978-981-33-6029-7_26

conversion, these devices are termed as thermoelectric coolers (TEC) and thermoelectric generator (TEG). Thermoelectric generators allow obtaining electricity from any heat source, which shows fantastic application potential. From micro-scale applications to large-scale applications, thermoelectric coolers offer a futuristic role in cooling systems as they work without any moving element involving working fluid.

2 Background

Thermoelectricity is based on two primary thermoelectric effects; the Seebeck effect and the Peltier effect. According to the Seebeck effect, an electromotive force emerges through the electrical circuit consisting of p-type and n-type semiconductor materials and connected in series when contacts are maintained at different temperatures. According to the Peltier effect, if the electric current passes through the circuit of p-type and n-type semiconductor materials, interconnected in series, heat flows from one side to the other side. So, one side of the thermoelectric module is cooled while the other side gets heated.

The performance of any thermoelectric material is generally recognized by the figure of merit (Z). Z depends on three essential material parameters: Seebeck coefficient (S), electrical conductivity (σ), and thermal conductivity (κ) and usually expressed in the dimensionless form at an absolute temperature (T). The dimensionless figure of merit (ZT) is defined as $ZT = S^2\sigma T/\kappa$. Alternatively, ZT is also defined as $(S^2/\rho\kappa)\,T$, where ρ is the electrical resistivity. A large power factor (S^2/ρ) is required to enhance thermoelectric performance. A good thermoelectric material should possess a large Seebeck coefficient (S), low thermal conductivity (σ), and high electrical conductivity (κ). The conversion efficiency of TE devices is directly related to the dimensionless figure of merit of their constituting materials. Thus, a high value of the figure of merit is highly desirable.

3 Recent Progresses to Enhance *ZT* of Thermoelectric Materials

In recent years, researchers applied new approaches and techniques in maximizing the ZT values of various thermoelectric materials. The available thermoelectric materials exhibit varying performance in the different temperature ranges. Improvement in each available thermoelectric material is a focused goal of researchers for a sustainable alternative of conventional energy converters. Earlier, the performance of the semiconductors used in TE applications was dependent on the available pure and perfect single crystals. However, these materials can be doped by adding small quantities of impurities. These impurities act as the electron donor for the parent materials. Most traditional semiconductors have cubic structures, whereas anisotropic crystals

are used for TE applications. The task of designing high-performance thermoelectric materials is to adjust the physical parameters of interconnected S, σ, and κ for a crystalline structure. Thermoelectric transport includes the flow of thermal energy and charge. The energy of phonons (vibrational waves of atoms) represents the thermal energy. Electron scattering on phonons creates electrical resistance. Through incorporating some new scattering mechanisms, nanostructures provide an opportunity to sever the connection between electric and thermal transport. The lattice thermal conductivity needs to be reduced for improvement in TE performance. Mass fluctuations increase through vacancies, and interstitial atoms result in higher phonon scattering that can lead to better TE performance. Sintering of bulk materials and melting production are the techniques used for research efforts to get improved TE materials. This work summarizes recent approaches to enhance the *ZT* of various thermoelectric materials. There is a wide variety of elements and compounds which can be categorized as thermoelectric materials. It is to be noted that every thermoelectric material exhibits different performance at different temperatures. Hence, it is not possible to recommend a single TE material that is suitable for all practical ranges of temperature in real-world applications. Thus in the present study, the authors have classified the TE materials based on their suitability for low-, medium-, and high-temperature applications.

3.1 Low-Temperature Thermoelectric Materials (300–500 K)

Bi_2Te_3 and its alloys with *ZT* values of around 0.9–1.0 are considered prominent TE materials at room temperature and widely used for practical thermoelectric applications [1, 2]. Hu et al. demonstrated that the porous structure affects thermoelectric performance [3]. As porosity increased, electrical and thermal conductivity decreased significantly. Reducing thermal conductivity compensates for the deterioration in electrical conductivity and improves the *ZT* value. A sample premixed with five wt percent NH_4HCO_3 was reported with 1.1 value of maximum *ZT* at temperature 343 K. This was around 20% better than that of the entirely dense sample with 0.92 value of *ZT*. Bi-containing Sb_2Te_3 and the related alloys with a high thermoelectric figure of merit can be futuristic options to use in thermoelectric devices. $Sb_{2-x}Bi_xTe_3$ samples were milled, pressed, and annealed under vacuum for 3 h at 250 °C by Adam et al. [4]. Bi was added to the binary Sb_2Te_3 system. An increased Seebeck coefficient and power factor were obtained for $Sb_{1.65}Bi_{0.35}Te_3$ with the reduced value of thermal conductivity. Subsequently, a high *ZT* of 1.14 at 400 K was achieved. The sample composition of $(Bi_2Te_3)_{0.15} + (Sb_2Te_3)_{0.85}$ was prepared to shift maximum *ZT* to the high-temperature zone by Madavali et al. [5]. The maximum *ZT* values of 1.3 and 1.07 were reported at 400 K and 300 K, respectively.

Tellurium is the prevailing thermoelectric material utilized in low to medium range of temperature. However, it contains an inferior thermoelectric efficiency with a low value of *ZT*. An enhancement in the performance of amorphous silicon has

been reported by Banerjee et al. [6]. They applied the method of arsenic ion implantation. The low-temperature dopant activation was done. It was observed that the *ZT* value of amorphous silicon (a-Si) thin films could be enhanced by seven orders at room temperature. Arsenic doping at low-temperature results in the enhancement of electrical conductivity. Empowering a-Si as a conspicuous TE material may be useful for sustainable energy applications at room temperature with maximum *ZT* up to 0.77. The magneto-thermoelectric figure of merit (*ZT*) in 3-D Dirac semimetal Cd_3As_2 crystal was reported by Wang et al. [7]. The magnetic field very effectively reduces electric conductivity and thermal conductivity. A maximum *ZT* value of 1.1 was obtained at 350 K temperature under 7 T of the magnetic field.

A hypothesis of thermoelectric transport properties in 2-D semiconducting quantum well structures is built up by Yelgel et al. [8]. Within the temperature range 50–600 K, computations are performed for n-type 0.1 wt% CuBr-doped $Bi_2Se_3/Bi_2Te_3/Bi_2Se_3$ and also for p-type 3 wt% Te-doped $Sb_2Te_3/Bi_2Te_3/Sb_2Te_3$ quantum well frameworks. It is discovered that diminishing the well thickness pronouncedly affects upgrading the *ZT* value. At 350 K temperature, the maximum *ZT* value of 0.97 is obtained for $Bi_2Se_3/Bi_2Te_3/Bi_2Se_3$. At 440 K temperature, the maximum *ZT* value of 1.945 is obtained for $Sb_2Te_3/Bi_2Te_3/Sb_2Te_3$. $CaMnO_3$ has a generally high Seebeck coefficient; however, the electrical conductivity (σ) is quite low (within the temperature range 300–1000 K). Hence, an un-doped material brings a low power factor ($S^2\sigma$). The bismuth doping of $Ca_{1-x}Bi_xMnO_3$ has been reported by Paengson et al. [9]. With x range of 0-0.05, TE materials were setup. The solid-state reaction and hot pressing techniques were used. Bi doping increased carrier concentration for all samples with different x. The electrical resistivity diminished with expanding bismuth content. The maximum *ZT* value of 0.065 at 473 K was found for $Ca_{0.97}Bi_{0.03}MnO_3$. It is worth mentioning that the *ZT* value was increased by 95% at the same temperature compared to $CaMnO_3$. Bi_2Te_3 and the family of similar compounds potentially satisfy the thermoelectric efficiency levels at low temperatures. However, the dimensionless figure of merit values decreases severely at a temperature over 450 K. The bulk $Bi_{1.9}Lu_{0.1}Te_3$ samples with diverse micro-grained particles were fabricated using cold isolated pressing (CIP) with annealing at high temperature and secondly by spark plasma sintering (at 653 and 683 K) by Yaprintsev et al. [10]. The maximum *ZT* ~ 0.9 for 450–500 K range of temperature range is obtained.

The summary of recent *ZT* improvements of thermoelectric materials at low temperatures discussed in this study is presented in Table 1.

3.2 Medium-Temperature Thermoelectric Materials (500–900 K)

CuAgSe exhibits excellent potential due to its fantastic carrier mobility. It also has low thermal conductivity. To prepare monodisperse CuAgSe nanocrystals, a scalable

Table 1 Summary of recent *ZT* improvements of TE materials at low temperatures

Researchers	Year	Thermoelectric material	Method for properties enhancement	Impact on *ZT* performance
Hu et al.	2020	$Bi_{0.4}Sb_{1.6}Te_3$	Pre-mixing with NH_4HCO_3	• Max. Dimensionless figure of merit (ZT_{max}) of 1.11 at 343 K • 20% increment in ZT_{max} as compared with fully dense material
Adam et al.	2020	Sb_2Te_3	Bi-containing	ZT_{max} value of 1.14 at 400 K for Sb_2Te_3
Madavali et al.	2018	$(Bi_2Te_3)_x + (Sb_2Te_3)_{1-x}$	Increasing Sb_2Te_3 content	• ZT_{max} value of 1.3 at 400 K • ZT_{max} value of 1.07 at 300 K
Banerjee et al.	2018	Amorphous silicon	Arsenic doping	*ZT* around ~0.64 ± 0.13 at room temperature
Wang et al.	2018	Cd_3As_2	Enhancement by the magnetic field	ZT_{max} value of 1.1 at 350 K
Yelgel and Srivastava	2014	$Bi_2Se_3/Bi_2Te_3/Bi_2Se_3$ and $Sb_2Te_3/Bi_2Te_3/Sb_2Te_3$	By varying the well thickness+	$ZT_{max} = 0.97$ at 350 K for $Bi_2Se_3/Bi_2Te_3/Bi_2Se_3$ and $ZT_{max} = 1.945$ at 440 K for $Sb_2Te_3/Bi_2Te_3/Sb_2Te_3$
Paengson et al.	2017	$CaMnO_3$	Bi doping and hot pressing of $CaMnO_3$	• ZT_{max} value of 0.065 at 473 K for $Ca_{0.97}Bi_{0.03}MnO_3$ • 95% increment in ZT_{max} as compared with un-doped material
Yaprintsev et al.	2017	$Bi_{1.9}Lu_{0.1}Te_3$	Fabrication by cold isostatic pressing and SPS	ZT_{max} value ~0.9 for 450–500 K

colloidal synthesis has been reported by Zuo et al. [11]. The gathered powder test was cleaned by a non-sulfur substance of $NaNH_2$. It was done to expel the organic ligands from the surface. After that, annealing process was also done. A 0.68 value of maximum *ZT* at 566 K was obtained. The obtained material shows the potential of TE applications for mid-range temperatures. The material before annealing exhibits a temperature- controlled transition from n-type toward p-type. This makes it suitable for thermal control transistor applications. $CoSb_3$ skutterudite is considered potential TE material for power generation. La Filler atoms are used to minimize lattice thermal conductivity for the skutterudite to get better TE performance [12, 13]. Bashir et al. reported a high *ZT* value of 1.15 at 692 K with La and In as the $In_{0.3}La_{0.5}Co_4Sb_{12}$ skutterudite [14]. BiCuSeO contains low thermal conductivity and an average power

factor. BiCuSO was doped with Pb and effectively synthesized by high pressure by Zhu et al. [15]. BiCuSeO doped with Pb increases the carrier concentration. This Pb doping improves the power factor. The thermal conductivity is smothered by Pb doping. At 700 K temperature, the maximum *ZT* of 0.14 is achieved. Synthesization with feasible high-pressure and high-temperature techniques can increase the TE performance of Cu_2Se bulk materials. At 723 K, a high *ZT* value of 1.19 was reported for Cu_2Se synthesized at 3 GPa by Xue et al. [16]. Recently, GeTe and its derivatives have gained considerable attention as promising thermoelectric materials. Perumal et al. [17] reported a maximum *ZT* value of 2.1 for In and Bi co-doped GeTe at 723 K.

The synthesization of a group of TiNiSn-based alloys has been performed by Chen et al. [18]. It was done by way of an easy solid-state reaction followed by the SPS method. The amount and mixture of the heterogeneous phase were precisely managed, which results in a successful decrement of thermal conductivity (up to 2.3–3.0 $Wm^{-1}K^{-1}$). Besides, TE figure of merit was enhanced up to 0.49 at 750 K temperature. Silicon–germanium-based alloys are appealing. For radioisotope thermoelectric power generation at an excessive temperature (more than 1000 °C), they offer a good choice of TE material. On the other side, mesostructured $In_{0.25}Co_4Sb_{12}$ and $In_{0.25}Yb_{0.05}Co_4Sb_{12}$ samples have been synthesized by Benyahia et al. [19]. The samples were fabricated through melting and annealing. Then, the ball-milling procedure was applied to minimize size and sintered through the SPS method. With a mean grain size of 400 nm, a maximum dimensionless figure of merit of 1.4 at 750 K temperature is obtained. It was achieved in the BM $In_{0.25}Co_4Sb_{12}$ + 0% CeO_2. TiNiSn-based half-Heusler (HH) alloys are widely studied. These thermoelectric materials show a high-temperature stabilization. However, the thermal conductivity is constantly enormously high, and hence, further *ZT* enhancement is difficult. SiC nanoparticles were brought into the matrix of $Pb_{0.98}Na_{0.02}Te$ doped with SrTe by Ai et al. [20]. The increased Seebeck coefficient and decreased electrical conductivity resulted in a remarkable peak *ZT* of 1.73 at 750 K.

Copper selenide is a promising thermoelectric material because of its fantastic electrical properties. A hydrothermal technique to incorporate astounding β-$Cu_2Se_{1-x}I_x$ nanopowder with a cost-effective minimum consumption of energy is reported by Wang et al. [21]. The nanopowder with different levels of doped iodine was used. Utilizing this straightforward and modest methodology, an improved *ZT* of 1.13 is obtained at a temperature of 773 K in iodine-doped Cu_2Se ($x = 0.03$) pellets after hot squeezing. Recently, the synthesis of p-type SiGe with boron using varied proportion is reported by Murugasami et al. [22]. The material was sintered through the spark plasma sintering technique. Doped with $B_{1.5}$ at.% synthesized SiGe alloy exhibits the enhanced *ZT* of 0.525 at 800 °C temperature. A considerable improvement of approximately 9.38% is obtained. Recently, the enhancement of skutterudite performance is reported by Yang et al. [23]. Tellurium-doped skutterudite has been shown to have promising TE properties using nano-micro-level pores. Cobalt, antimony, and tellurium powders were utterly blended with a nominal composition of $Co_4Sb_{11.5}Te_{0.5}$. Then, the material was stacked into carbon cauldrons and kept inside quartz tubes below vacuum for heating. The acquired ingots were ground into powders utilizing two successive methods, first by a mortar and then

by ball milling below vacuum. The two powders (without ball milling and with ball milling) with different proportions were blended, and after that, sintered using spark plasma sintering technique. The annealing process below vacuum was also done on the obtained bulk material. The authors reported that annealed nanoparticles carry some randomly allotted nanopores with a range of sizes from 200 nm to 2 μm. The development of these nanosized pores is due to strain during sintering. The thermal conductivity drops drastically which is a desired effect. A 1.2 value of the maximum dimensionless figure of merit is obtained for the annealed material at a temperature of 800 K. A significant increment of approx. 35% was reported. The thermoelectric properties of n-type-doped Mg_2 $(Si_{0.4}Sn_{0.6})_{1-y}$ Bi_y solid solutions are investigated theoretically by Yelgel [24]. From 300 to 800 K temperature range, the selected y range is 0.005–0.06 for doping Bi with available experimental data. It was found that an appropriate y can increase *ZT*. The maximum *ZT* is obtained with y = 0.03 at 800 K and values 1.82.

The graphene nanoplate incorporated into Cu_2Se samples has been fabricated by Li et al. [25]. The ball-milling technique was applied. Then, sintering through the SPS method was done. The homogeneous dispersion of the carbon phase reduced the Cu_2Se particles to form an excellent dense construction. Maximum *ZT* reached a high 1.7 value at 873 K. This gives an appropriate technique to use carbon engineering to maximize TE performance for Cu_2Se and family compounds. The deliberate actuated dislocations and vacancies are compelling in diminishing the thermal conductivity of polycrystalline SnS, as reported by Asfandiyar et al. [26]. Low thermal conductivity and high electrical conductivity $Sn_{0.99}Ag_{0.005}S$ sample were obtained at 877 K. Ag doping brings high power factor, and an enhanced *ZT* of 1.1 at 877 K was recorded for $Sn_{0.99}Ag_{0.005}S$. N-type half-Heusler NbCoSn performs well in TE performance, but p-type performs poorly. Replacing Sc at Nb site may change the n-type NbCoSn to a p-type semiconductor as reported by Yan et al. [27] by changing the Fermi level, indicating that Sc is a suitable p-type dopant. ZT_{max} value of 0.13 at 879 K has been reported.

The summary of recent *ZT* improvements of thermoelectric materials at medium temperatures discussed in this study is presented in Table 2.

3.3 High-Temperature Thermoelectric Materials (>900 K)

Lead selenide (PbSe) displays a temperature-dependent Seebeck coefficient, low thermal conductivity, and low electrical resistivity. Further, it has resolved the issue that emerges to get both n- and p-type legs. A simultaneous advancement of thermal and electrical properties of p-type PbSe has been reported by Zhao et al. [28]. The density hypothesis for estimations of valence band energy levels was used. Between lead selenide and nanostructures of $CdS_{1-x}Se_x/ZnS_{1-x}Se_x$, appropriate valence band alignments were introduced. A highly enhanced dimensionless figure of merit of 1.6 at 923 K was attained at $Pb_{0.98}Na_{0.02}Se + 3\%Cds$. Due to its high TE efficiency, Si-Ge alloys are considered valuable TE materials operating at high temperatures. The effect

Table 2 Summary of recent *ZT* improvements of TE materials at medium temperatures

Researchers	Year	Thermoelectric material	Method for properties enhancement	Impact on *ZT* performance
Zuo et al.	2018	CuAgSe	Colloidal synthesis of monodisperse CuAgSe NCs	ZT_{max} value of 0.68 at 566 K
Bashir et al.	2018	$CoSb_3$	La and In filling	ZT_{max} value of 1.15 at 692 K
Zhu et al.	2018	BiCuSO	Doping with Pb	ZT_{max} value of 0.14 at 700 K
Xue et al.	2019	Cu_2Se	Synthesis with high pressure	ZT_{max} value of 1.1 at 723 K
Perumal et al.	2019	GeTe	In and Bi doping	ZT_{max} value of 2.1 at 723 K
Chen et al.	2017	TiNiSn-based half-Heusler (HH) alloys	Synthesis with solid-state reaction	ZT_{max} value of 0.49 at 750 K
Benyahia et al.	2018	$In_{0.25}Co_4Sb_{12}$	Synthesis by a melting–annealing–ball-milling–SPS method	ZT_{max} value of 1.4 at 750 K
Ai et al.	2020	PbTe	SiC dispersing and SrTe doping	ZT_{max} value of 1.73 at 750 K for $Pb_{0.98}Na_{0.02}Te$/4 mol%SrTe composite
Wang et al.	2019	Cu_2Se	Synthesis of Cu_2Se alloys doped with iodine	ZT_{max} value of 1.13 at 773 K for $Cu_2Se_{1-x}I_x$ ($x = 0.03$)
Murugasami et al.	2019	SiGe	Synthesis of SiGe alloys doped with Boron	ZT_{max} value of 0.525 at 800 °C for doped with $B_{1.5}$
Yang et al.	2019	Te-doped skutterudite ($Co_4Sb_{11.5}Te_{0.5}$)	Nanomicroporous structure in $Co_4Sb_{11.5}Te_{0.5}$ materials via annealing the nano-$Co_4Sb_{11.5}Te_{0.5}$/$Co_4Sb_{11.5}Te_{0.5}$ composites	• Max. Dimensionless figure of merit (ZT_{max}) of 1.2 at 800 K for annealed sample (N10-A100) • 33.7% increment in ZT_{max} as compared with dense material (N0)
Yelgel	2016	$Mg_2Si_{0.4}Sn_{0.6}$	Mg_2 $(Si_{0.4}Sn_{0.6})_{1-y}$ Bi solid solutions	ZT_{max} value of 1.82 at 800 K
Li et al.	2018	Cu_2Se	By graphene nanoplate incorporation	ZT_{max} value of 1.7 at 873 K
Asfandiyar et al.	2020	SnS	Intentional-induced dislocations and vacancies and Ag doping	ZT_{max} value of 1.1 at 877 K for $Sn_{0.99}Ag_{0.005}S$
Yan et al.	2020	NbCoSn	Sc substitution at the Nb site	ZT_{max} value of 0.13 at 879 K

Table 3 Summary of recent *ZT* improvements of TE materials at high temperatures

Researchers	Year	Thermoelectric material	Method for properties enhancement	Impact on *ZT* performance
Zhao et al.	2013	PbSe	Integration of band structure with hierarchical structuring	ZT_{max} value of 1.6 at 923 K
Muthusamy et al.	2020	Si–Ge–Au	Boron doping	ZT_{max} value of 1.63 at 973 K
He et al.	2014	Cu_2S	Cu deficiency	ZT_{max} value of 1.7 at 1000 K
Fu et al.	2015	FeNbSb	Hf doping	ZT_{max} value of 1.5 at 1200 K
Wille et al.	2019	$Yb_{14}ZnSb_{11}$	Containing RE	ZT_{max} value of 0.7 at 1275 K

on thermoelectric properties of B-doped Si-Ge-Au nanocomposites was investigated, taken as $Si_{65-x}Ge_{31}Au_4B_x$ by Muthusamy et al. [29]. At 973 K, a maximum *ZT* value of 1.63 was reported at $x = 3$. The phonon-liquid electron-crystal concept for copper sulfide with reduced thermal conductivity and higher thermoelectric performance has been proposed by He et al. [30]. A high *ZT* value of 1.7 was reported at 1000 K by using copper deficiency as $Cu_{2-x}S$ with $x = 0.03$.

Half-Heusler compounds are increasingly attracting attention because of their strong mechanical and electrical properties at high temperatures. At 1200 K, through heavier Hf doping the p-type FeNbSb heavy-band half-Heusler alloys with 1.5 value of high *ZT* was reported by Fu et al. [31]. $Yb_{14}ZnSb_{11}$ is considered for intermediate valence interest. With rare earth (RE) solution as $Yb_{14-x}RE_xZnSb_{11}$ was investigated by Wille et al. [32]. The dimensionless figure of merit was reported as high as 0.7 at 1275 K with $x = 0.5$.

The summary of recent *ZT* improvements of thermoelectric materials at high temperatures discussed in this study is presented in Table 3.

4 Conclusion

Exploring advancement in thermoelectric materials for sustainable energy solutions is the contemporary area of interest. The *ZT* value of thermoelectric materials should be enhanced for a broad range of potential applications of thermoelectric devices. From this study, it can be highlighted that:

- In the recent past, material researchers are successfully applying new approaches to upgrade the performance of available materials for a particular temperature range.

- A promising new approach is to create nanolevel and macro-level pores in tellurium doped skutterudite to enhance *ZT* by approximately 35%.
- Another interesting approach is introducing a facile method for colloidal synthesis of copper-silver selenide. With ZT_{max} value of 0.68 at temperature 566 K, this resulted as a promising candidate for TE research in the intermediate temperature range.

The significant outcomes of researchers will boost the applicability of TE devices contribution to the present world's green energy solutions. For greater commercialization of thermoelectric applications, improved materials with high values of *ZT* are required at prevailing operating temperatures. This will boost the manufacture of better performing TE modules. These advancements in *ZT* values could close the gap in performance between conventional bismuth-tellurium-based materials and newer materials. The costs to invent newer thermoelectric materials are quite different from the production cost of those materials. The costs of candidate materials, costs to process those materials into TE elements, and cost to compensate the material loss are significant for the real commercial applications of newly researched materials. The non-availability of the requisite raw materials might result in holding the production of TE devices. More extensive work on that would be useful.

References

1. Witting, I. T., Chasapis, T. C., Ricci, F., Peters, M., Heinz, N. A., Hautier, G., & Snyder, G. J. (2019). The thermoelectric properties of bismuth telluride. *Advanced Electronic Materials, 5*, 1800904. https://doi.org/10.1002/aelm.201800904.
2. Goldsmid, H. J. (2014). Bismuth telluride and its alloys as materials for thermoelectric generation. https://doi.org/10.3390/ma7042577.
3. Hu, X., Hu, J., Fan, X., Feng, B., Pan, Z., Liu, P., Zhang, Y., Li, R., He, Z., Li, G., & Li, Y. (2020). Artificial porous structure: An effective method to improve thermoelectric performance of Bi_2Te_3 based alloys. *Journal of Solid State Chemistry, 282*. https://doi.org/10.1016/j.jssc.2019.121060.
4. Adam, A. M., El-Khouly, A., Novitskii, A. P., Ibrahim, E. M. M., Kalugina, A. V., Pankratova, D. S., Taranova, A. I., Sakr, A. A., Trukhanov, A. V., Salem, M. M., & Khovaylo, V. (2020). Enhanced thermoelectric figure of merit in Bi-containing Sb_2Te_3 bulk crystalline alloys. *Journal of Physics and Chemistry of Solids, 138*, 109262. https://doi.org/10.1016/j.jpcs.2019.109262.
5. Madavali, B., Kim, H. S., Lee, C. H., Kim, D.-S., & Hong, S. J. (2019). High thermoelectric figure of merit in p-type $(Bi_2Te_3)_x-(Sb_2Te_3)_{1-x}$ alloys made from element-mechanical alloying and spark plasma sintering. *Journal of Electronic Materials, 48*, 416–424. https://doi.org/10.1007/s11664-018-6706-7.
6. Banerjee, D., Vallin, Ö., Samani, K. M., Majee, S., Zhang, S. L., Liu, J., & Zhang, Z. B.: Elevated thermoelectric figure of merit of n-type amorphous silicon by efficient electrical doping process. *Nano Energy, 44*, 89–94.
7. Wang, H., Luo, X., Chen, W., Wang, N., Lei, B., Meng, F., Shang, C., Ma, L., Wu, T., Dai, X., Wang, Z., & Chen, X. (2018). Magnetic-field enhanced high-thermoelectric performance in topological Dirac semimetal Cd_3As_2 crystal. *Science Bulletin, 63*, 411–418.

8. Yelgel, Ö. C., & Srivastava, G. P. (2014) Thermoelectric properties of $Bi_2Se_3/Bi_2Te_3/Bi_2Se_3$ and $Sb_2Te_3/Bi_2Te_3/Sb_2Te_3$ quantum well systems. *Philosophical Magazine, 94*, 2072–2099. https://doi.org/10.1080/14786435.2014.903340.
9. Paengson, S., Pilasuta, P., Singsoog, K., Namhongsa, W., Impho, W., & Seetawan, T. (2017). Improvement in thermoelectric properties of $CaMnO_3$ by Bi doping and hot pressing. In: *Materials today: Proceedings* (pp. 6289–6295). https://doi.org/10.1016/j.matpr.2017.06.129.
10. Yaprintsev, M., Lyubushkin, R., Soklakova, O., & Ivanov, O. (2018). Microstructure and thermoelectric properties of $Bi_{1.9}Lu_{0.1}Te_3$ compound. *Rare Metals, 37*, 642–649.
11. Zuo, Y., Liu, Y., He, Q. P., Song, J. M., Niu, H. L., & Mao, C. J. (2018). CuAgSe nanocrystals: Colloidal synthesis, characterization and their thermoelectric performance. *Journal of Materials Science, 53*, 14998–15008. http://doi.org/10.1007/s10853-018-2676-7.
12. Bao, S., Yang, J., Zhu, W., Fan, X., Duan, X., & Peng, J. (2006). Preparation and thermoelectric properties of La filled skutterudites by mechanical alloying and hot pressing. *Materials Letters, 60*, 2029–2032. https://doi.org/10.1016/j.matlet.2005.12.074.
13. Liu, K., Dong, X., & Jiuxing, Z. (2006). The effects of La on thermoelectric properties of $La_xCo_4Sb_{12}$ prepared by MA-SPS. *Materials Chemistry and Physics, 96*, 371–375.
14. Bashir, M. B. A., Said, S. M., Sabri, M. F. M., Miyazaki, Y., Shnawah, D. A., Shimada, M., Salleh, M. F. M., Mahmood, M. S., Salih, E. Y., Fitriani, F., & Elsheikh, M. H. (2018). Infilled $La_{0.5}Co_4Sb_{12}$ Skutterudite system with high thermoelectric figure of merit. *Journal of Electronic Materials, 47*, 2429–2438.
15. Zhu, H., Su, T., Li, H., Hu, Q., Li, S., & Hu, M. (2018). Thermoelectric properties of BiCuSO doped with Pb. *Solid State Communications.* https://doi.org/10.1016/j.ssc.2018.04.013.
16. Xue, L., Zhang, Z., Shen, W., Ma, H., Zhang, Y., Fang, C., Jia, X. (2019). Thermoelectric performance of Cu_2Se bulk materials by high-temperature and high-pressure synthesis. *Journal of Materiomics, 5*, 103–110. http://doi.org/10.1016/j.jmat.2018.12.002.
17. Perumal, S., Samanta, M., Ghosh, T., Shenoy, U. S., Bohra, A. K., Bhattacharya, S., Singh, A., Waghmare, U. V., & Biswas, K. (2019). Realization of high thermoelectric figure of merit in gete by complementary co-doping of Bi and In. *Joule, 3*, 2565–2580. https://doi.org/10.1016/j.joule.2019.08.017.
18. Chen, J. L., Liu, C., Miao, L., Gao, J., Zheng, Y. Y., Wang, X., Lu, J., & Shu, M. (2018). Improved thermoelectric performance achieved by regulating heterogeneous phase in half-heusler TiNiSn-based materials. *Journal of Electronic Materials* (2018).
19. Benyahia, M., Ohorodniichuk, V., Leroy, E., Dauscher, A., Lenoir, B., & Alleno, E. (2018). High thermoelectric figure of merit in mesostructured $In_{0.25}Co_4Sb_{12}$ n-type skutterudite. *Journal of Alloys and Compounds.* http://doi.org/10.1016/j.jallcom.2017.11.195.
20. Ai, X., Hou, D., Liu, X., Gu, S., Wang, L., & Jiang, W. (2020). Enhanced thermoelectric performance of PbTe-based nanocomposites through element doping and SiC nanoparticles dispersion. *Scripta Materialia, 179*, 86–91.
21. Wang, J., Liu, B., Miao, N., Zhou, J., & Sun, Z. (2019). I-doped Cu_2Se nanocrystals for high-performance thermoelectric applications. *Journal of Alloys and Compounds* (2019). https://doi.org/10.1016/j.jallcom.2018.08.291.
22. Murugasami, R., Vivekanandhan, P., Kumaran, S., Suresh Kumar, R., & John Tharakan, T. (2019). Simultaneous enhancement in thermoelectric performance and mechanical stability of p-type SiGe alloy doped with Boron prepared by mechanical alloying and spark plasma sintering. *Journal of Alloys and Compounds* (2019). https://doi.org/10.1016/j.jallcom.2018.09.029.
23. Yang, H., Wen, P., Zhou, X., Li, Y., Duan, B., Zhai, P., & Zhang, Q. (2019). Enhanced thermoelectric performance of Te-doped skutterudite with nano-micro-porous architecture. *Scripta Materialia.* http://doi.org/10.1016/j.scriptamat.2018.09.015.
24. Yelgel, Ö. C. (2016). Theoretical study of thermoelectric properties of n-type doped $Mg_2Si_{0.4}Sn_{0.6}$ solid solutions. *Philosophical Magazine.* https://doi.org/10.1080/14786435.2016.1143128.
25. Li, M., Kazi Nazrul Islam, S. M., Dou, S., & Wang, X. (2018). Significantly enhanced figure-of-merit in graphene nanoplate incorporated Cu_2Se fabricated by spark plasma sintering. *Journal of Alloys and Compounds* (2018). https://doi.org/10.1016/j.jallcom.2018.07.353.

26. Asfandiyar, Cai, B., Zhao, L. D., & Li, J. F. (2020). High thermoelectric figure of merit ZT > 1 in SnS polycrystals. *Journal of Materiomics, 6*, 77–85.
27. Yan, R., Xie, W., Balke, B., Chen, G., & Weidenkaff, A. (2020) Realizing p-type NbCoSn half-Heusler compounds with enhanced thermoelectric performance via Sc substitution. *Science and Technology of Advanced Materials, 21*, 122–130.
28. Zhao, L. D., Hao, S., Lo, S. H., Wu, C. I., Zhou, X., Lee, Y., Li, H., Biswas, K., Hogan, T. P., Uher, C., Wolverton, C., Dravid, V. P., & Kanatzidis, M. G.: High thermoelectric performance via hierarchical compositionally alloyed nanostructures. *Journal of the American Chemical Society*. https://doi.org/10.1021/ja403134b.
29. Muthusamy, O., Ghodke, S., Singh, S., Delime-Codrin, K., Nishino, S., Adachi, M., Yamamoto, Y., Matsunami, M., Harish, S., Shimomura, M., & Takeuchi, T.: Enhancement of the thermoelectric performance of Si-Ge nanocomposites containing a small amount of Au and optimization of boron doping. *Journal of Electronic Materials, 49*, 2813–2824. https://doi.org/10.1007/s11664-019-07857-5.
30. He, Y., Day, T., Zhang, T., Liu, H., Shi, X., Chen, L., & Snyder, G. J. (2014). High thermoelectric performance in non-toxic earth-abundant copper sulfide. *Advanced Materials, 26*, 3974–3978. https://doi.org/10.1002/adma.201400515.
31. Fu, C., Bai, S., Liu, Y., Tang, Y., Chen, L., Zhao, X., & Zhu, T.: Realizing high figure of merit in heavy-band p-type half-Heusler thermoelectric materials. *Nature Communications, 6*, 1–7. https://doi.org/10.1038/ncomms9144.
32. Kunz Wille, E., Grewal, N., Bux, S., & Kauzlarich, S.: Seebeck and figure of merit enhancement by rare earth doping in $Yb_{14-x}RE_xZnSb_{11}$ (x = 0.5). *Materials, 12*, 731. https://doi.org/10.3390/ma12050731.